GIS Based Methodologies of Seismic Hazard and Risk Analysis for Bangladesh

Jiban Kumar Sarker

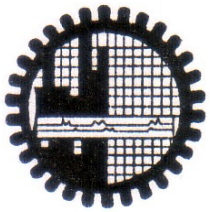

DEPARTMENT OF CIVIL ENGINEERING
BANGLADESH UNIVERSITY OF ENGINEERING AND TECHNOLOGY
DHAKA-1000

GIS Based Methodologies of Seismic Hazard and Risk Analysis for Bangladesh

by

Jiban Kumar Sarker

A Thesis in Partial Fulfillment of the Requirement for the Degree of

DOCTOR OF PHILOSOPHY

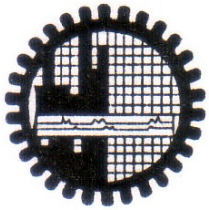

DEPARTMENT OF CIVIL ENGINEERING

BANGLADESH UNIVERSITY OF ENGINEERING AND TECHNOLOGY, DHAKA-1000.

2011

CANDIDATES DECLARATION

It is hereby declared that this thesis or any part of it has not been submitted elsewhere for the award of any degree or diploma.

_____

Jiban Kumar Sarker

Affectionately dedicated

To

My Parents, Wife and Children

TABLE OF CONTENTS

LIST OF FIGURES

LIST OF TABLES

ACKNOWLEDGEMENT

The author wishes to express his profound gratitude and indebtedness to his Supervisors Professor Dr. M A Ansary and Co-supervisors Professor Dr. A M M Safiullah for their unfailing guidance continuous supervision, invaluable suggestions, helpful criticisms and encouragement given throughout the course of this research work. Without their unstinted help in both academic and personal concerns throughout the years of author's graduate studies at the Bangladesh university of engineering and Technology (BUET) Dhaka, this dissertation work could not have been completed.

Author is also very grateful to Professor Dr. Md. Mujibur Rahman , Professor Dr Syed Fakrul Ameen and Professor Dr. Abu Siddique for their valuable suggestions, guidance and encouragement. Fervent debt of deep gratitude, sincere thanks, and extreme respects are due to them for their valuable help throughout the study. The author is also grateful to Professor Dr. Kenji Ishihara for his comments on this study as an external examiner. A note of appreciation and regards is extended for his valuable suggestions, encouragement and interest in this study.

The author express his gratefulness to the Head of the Civil Engineering Department, BUET, Dhaka, for providing laboratory facilities and co-operation during the period of the research. Sincere gratitude is due to the BUET, Dhaka, and Bangladesh Water Development Board (BWDB), for providing financial support and rendering an excellent learning environment. The author expresses sincere thanks to Professor Dr. Tammeed Al Hussaini, Associate Professor Dr. Ashutosh Sutradhar and Associate professor Dr. Md Jahangir Professor Dr. Tammeed Al Hussaini for helping in this study. The author expresses thanks to Md Shamsur Rahman for providing necessary help needed for conducting research. The author expresses sincere thanks to M. Zaman (former Director General of BWDB) for his valuable help and encouragement for this study.

A very special debt of deep gratitude is offered to his parents and all members of his family. The author dedicates this piece of work to his loving parents and all family members, religions, and this work related future researcher, who are always a constant source of inspiration throughout his whole life.

NOTATIONS

a_c	critical acceleration to begin the process of slope failure
D	epicentral distance in km
D_b	total number of damaged household of type *b*
DR	damage ratio
g	acceleration due to gravity
$H(\omega)$	the linear transfer function
h	depth of focus
I	seismic intensity
M	earthquake magnitude
Ms	surface-wave magnitude
MM_{IF}	combined hazard
MMI_{GS}	ground shaking hazard
MMI_{FR}	surface fault rupture hazard
MMI_{LIQ}	liquefaction hazard
PGA	peak ground acceleration
PGV	peak ground velocity
PGD	peal ground displacement
P	probability
P_L	liquefaction potential index
R	hypocentral distance
r_d	stress reduction factor
$S_s(\omega)$	the spectral amplitude at the ground surface level
$S_r(\omega)$	the spectral amplitude at the bedrock level
V_s	shear wave velocity
Y	ground motion intensity
y	ground motion index (PGA)
ω	the circular frequency in rad/sec
σ_o	total overburden pressure
σ'_o	effective overburden pressure
τ_{av}	average equivalent uniform shear stress
τ_{max}	maximum shear stress
α_{Smax}	estimated peak surface acceleration (in percentage of g)
γ	unit weight of the soil
θ	the slope angle
σ	standard deviation
φ	pipeline diameter

ABSTRACT

A geographic information system (GIS) provides the ideal environment for conducting a comprehensive regional seismic hazard and risk analysis. GIS has the ability to store, manipulate, analyse and display the large amount of required spatial and tabular data. The system can typically be linked to external computational programs, high level database management systems, and knowledge-based expert systems. The objective of this research is the development of a methodology using geographic information system technology to conduct a regional multi-hazard seismic risk analysis. The term multi-hazard refers to the consideration of ground shaking and secondary site effects of soil amplification, liquefaction, landslide, and surface fault rupture. The methodology involves a modular framework that allows new models and data base information to be included as the technology advances.

This thesis describes in detail the current GIS and the various steps in a regional seismic hazard and risk analysis. An overview of the different models for estimating the effects of local site conditions is presented. This research includes the development and example illustration of a GIS-based methodology for quantifying and combining the hazards associated with these secondary site effects. The methodology to combine the various hazards is based on a weighted average approach that utilises the knowledge of local experts. This thesis also covers the estimation of regional earthquake damage and loss, including the development of a methodology for compiling a comprehensive inventory of structures in a large region.

An attempt is also made to investigate and distinguish the PGA/intensity values of a region due to liquefaction, land slide and fault rupture. To generate artificial earthquake a locally built SHAKE table with two chambers has been used. The left chamber and the right chamber have been used to investigate the primary effect and the secondary effects of an earthquake respectively. By analyzing the data of ground motion obtained from the two chambers, quantification of secondary site effects of fault rupture, liquefaction, and landslide have been made possible.

This thesis also covers the development of acceleration based attenuation relation for Bangladesh. Due to lack of sufficient recorded strong ground motion data, intensity data have been used to develop an attenuation relation by regressing 40 past

earthquake records from eight events. This relation shows that Joyner and Boore's acceleration attenuation model may be adequate to predict the dissipation of acceleration with distance for Bangladesh and its surrounding region.

A substantial part of this thesis is devoted to a case study that illustrates the ideas and methodologies developed in this research. The case study shows possible damage and loss within Sylhet City corporation area for a scenario event having the same magnitude and location of 1918 Srimangal earthquake with magnitude 7.6. The various seismic hazards such as liquefaction, landslide and amplification have been quantified and integrated, and a structural inventory of nearly 3040 buildings, 106 km gas lines and about 118 km of water supply lines have been compiled. Economic loss estimation has been estimated using the damages expected to be suffered due to the scenario event. Among total buildings, 59% is expected to be damaged. In case of lifeline, total number of damage points is 204 for water pipes and total number of damage points is 981 for gas pipes.

A GIS model has been developed which can be used for estimating regional seismic hazard including secondary site effects for a large region. Numerous maps and tables of inventory data and results have been included in this thesis to help prove the effectiveness of the GIS.

CHAPTER 1

INTRODUCTION

1.1 Background and Present State of the Problem

Earthquake is a natural phenomenon that occur in certain parts of the World creating most deadly natural disasters that destroys infrastructure, houses, loss of human life and human habitat. Even a relatively moderate earthquake can lead to a very large number of deaths. Although earthquakes may affect rural as well as urban areas, it is the urban areas that are most affected due to earthquakes. There are records of whole cities being destroyed by earthquakes.

Bangladesh is vulnerable to earthquake. A series of recent tremors that shook parts of the country including the capital Dhaka indicates that Bangladesh sits on a earthquake zone. So far, all the recent major earthquakes have mostly occurred away from major cities, and have affected sparsely populated areas. Therefore the human casualty and economic losses are very limited.

The 1993 Killari and 2001 Gujarat earthquakes in India, 2003 Bam earthquake in Iran and 2004 Sumatra earthquake, 2005 Kashmir Earthquake in Pakistan and India and the recent 2010 Haiti earthquake have amply demonstrated that inappropriate construction technology may lead to high casualty levels even for a moderate earthquake. According to a report published by United Nations IDNDR-RADIUS Initiatives, Dhaka and Tehran are the cities with the highest relative earthquake disaster risk (Cardona et al., 1999). Dhaka, the capital of Bangladesh is the center for economy, commerce, politics and society, with a large population of more or less 12 million. Once a earthquake of large magnitude occur in this sub-continent major cities of Bangladesh such as Dhaka, Chittagong, Sylhet, Mymensigh, Bogra, Rangpur will suffer immense losses of life and property. This will have very severe long term consequences for the entire country.

A good background of historical earthquake information is essential to evaluate the seismicity. Information on earthquake events in and around Bangladesh is available for

the last 200 years. The earthquake records suggest more than 100 moderate to large earthquakes occurred within Bangladesh since 1900, out of which more than 65 events occurred after 1960. More than 125 earthquakes occurred in and around Bangladesh since the beginning of the new millennium of which about 27 events of magnitudes ranging between 4 and 5 have occurred inside Bangladesh. Fifteen new epicenters have been identified inside Bangladesh since January 2001. This clearly indicates an increase in frequency of earthquakes in Bangladesh. The 1869 Cachar earthquake, 1885 Bengal earthquake, 1897 Great Indian earthquake, 1918 Srimangal earthquake, 1930 Dhubri earthquake and 1950 Assam earthquake are likely to recur any time and may cause devastation for the cities in Bangladesh.

The 2001 Gujarat earthquake in India and 2005 Kashmir earthquake in Pakistan and India revealed the vulnerability of "non-earthquake-proof" cities and villages in South-Asia. In 1897, an earthquake of magnitude 8.7 (recently modified by Ambraseys (2000) to be 8.0) caused serious damages to buildings in the northeastern part of India (including Bangladesh) and 1542 people were killed. Recently, Bilham et al. (2001) pointed out that there is high possibility that a large earthquake will occur around the Himalayan region based on the difference between energy accumulation in this region and historical earthquake occurrence. Figure 1.1 shows the estimated slip potential along the Himalaya. A recent study by OIC (2009) identified five earthquake sources for Bangladesh as shown in Figure 1.2. Figure 1.3 shows the major seismic sources in and around Bangladesh. The major past earthquakes that affected Bangladesh is presented in Table 1.1. The current population around this region is at least 50 times greater than the population of 1897 and cities like Chittagong, Dhaka, Kathmandu, Guwahati have population exceeding several millions. It is a cause for great concern that the next great earthquake may occur in this region at any time. Although Bangladesh is located in this region of significant seismic activity, the low incidence of severe earthquakes during this century has led to a situation where most of the population and policy makers don't perceive seismic risk to be important. However, due to increasing number of buildings, bridges and industrial structures being built during the last two decades, proper assessment of hazard due to earthquake is essential.

Considering the seismicity of Bangladesh, disaster mitigation work should be immediately undertaken. The first step in disaster mitigation is to recognize the existence of earthquake hazard. The next step is to quantify the risk and to minimize its effect. The total elimination of risk may be difficult and impractical. Moreover in developing countries like Bangladesh, economic considerations sometimes take precedence over safety and reliability considerations in engineering design.

Every damaging earthquake reaffirms the importance of seismic hazard and risk analysis for estimating the consequences of an earthquake. Hazard means the probability of occurrence of a potentially damaging phenomenon within a given time period and area. Risk means expected losses (such as lives, injury, property damage etc.) due to a particular hazard for a given area and reference period. Based on mathematical calculations, risk is the product of hazard and vulnerability.

Although some progress in the area of seismic prediction has been made, time, magnitude or location of an earthquakes cannot be accurately predicted. Even if an accurate prediction were possible, the earthquake occurrence and consequent damage potential could not be prevented. Seismic hazard and risk can not be eliminated, but it can be effectively analyzed and possibly reduced by combining the available regional geologic and geographic information with recent technological developments.

A comprehensive regional hazard and risk analysis is a fairly standard procedure that requires combining the effects of many factors. Each of these factors usually involves the modeling and analysis of both spatial and tabular data. The amount of requisite information can often be overwhelming, even for a small region. Recent advances in geographic information system (GIS) technology have created new opportunities for managing the large amount of data, for interfacing with external analysis programs, and for presenting the results in a manner that may be useful for disaster planning, hazard and risk mitigation, and rehabilitation strategy comparison.

Table 1.1 Some historical earthquakes with magnitude, intensities, epicentral distance and focal depth

Name of past Earthquake	Fault	Magnitude	EMS Intensity	Distance (Km)	Focal Depth (Km)
1869 Cachar Earthquake	Plate Boundary 2	7.5	VIII	92	56
1885 Bengal Earthquake	Modhupur	7.0	V	234	72
1897 Great Indian Earthquake	Dauki	8.1	IX	151	60
1918 Srimangal Earthquake	Plate Boundary 2	7.6	IX	71	14

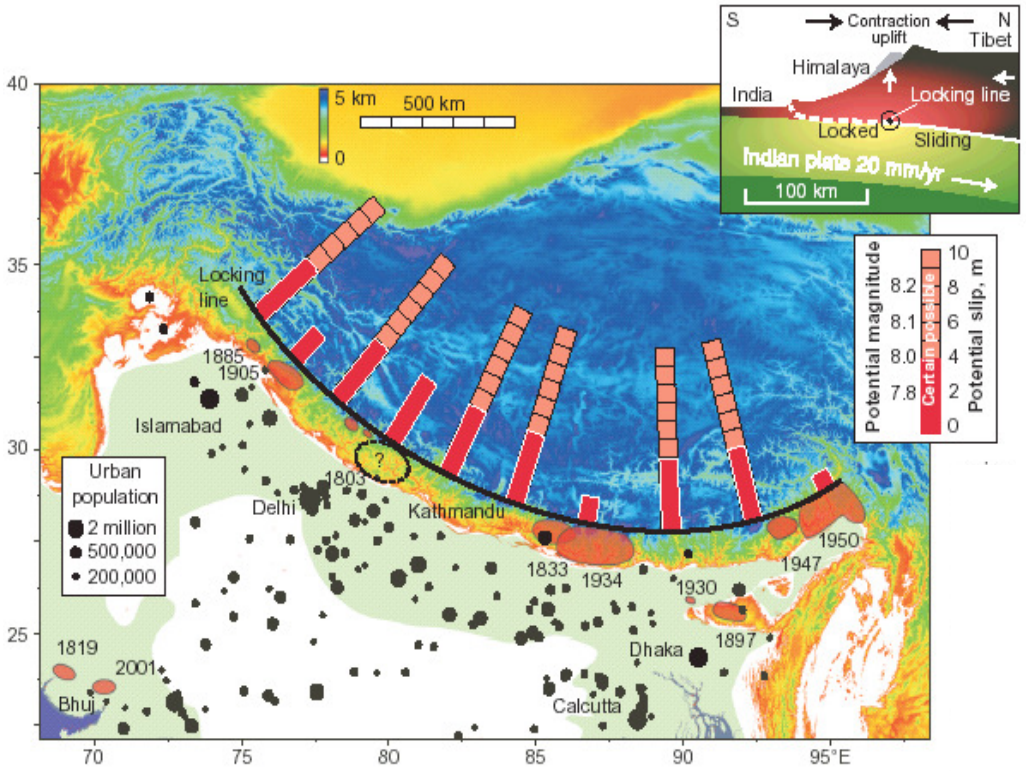

Figure 1.1 Estimated slip potential along the Himalaya (after Bilham et al., 2001)

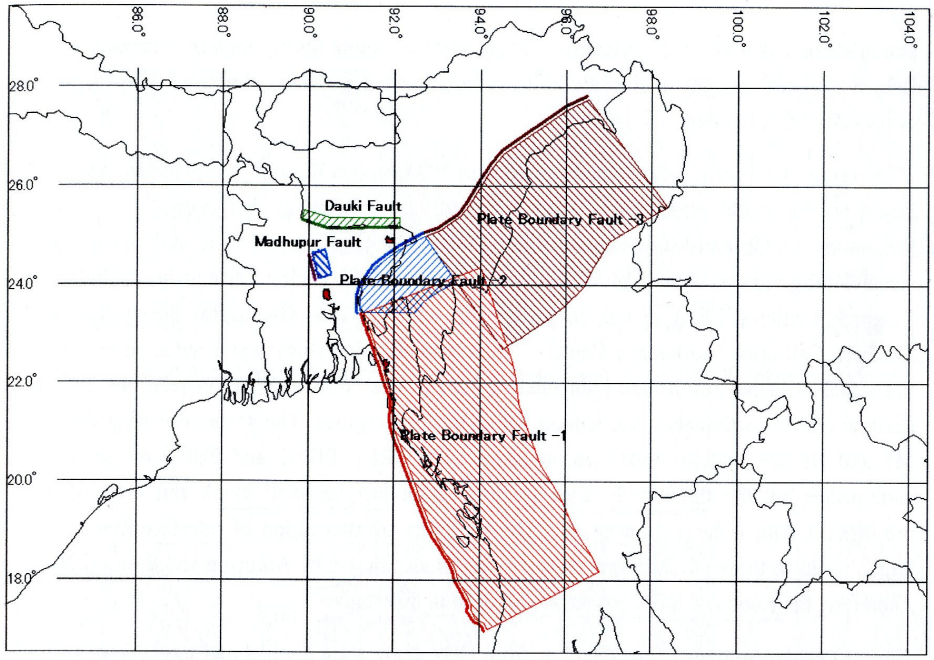

Figure 1.2 Scenario Earthquake Fault Model (OIC, 2009)

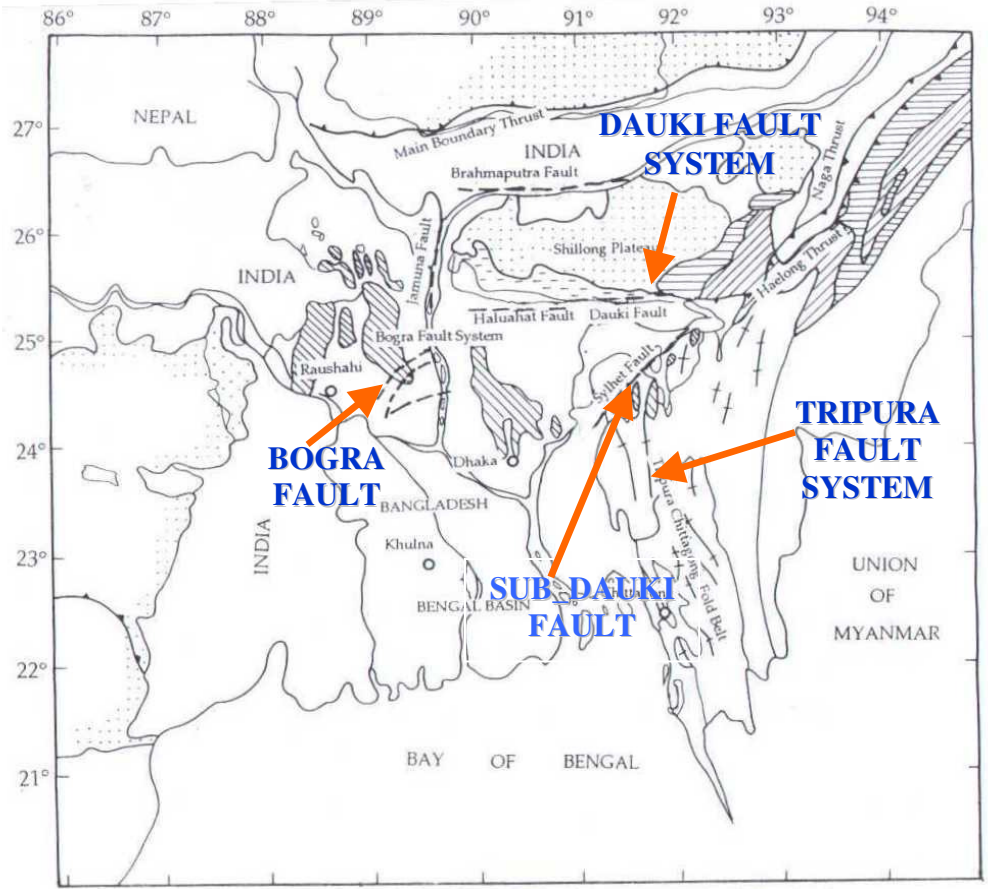

Figure 1.3 Major seismic sources in and around Bangladesh (Bolt , 1987).

A geographic information system can be used to integrate the various steps in a regional seismic hazard and risk analysis in a modular framework. The system is independent of analysis scale and geographic location, allowing analysis at any level and in any area where the necessary information is available. Seismic hazard due to local site effects such as amplification, liquefaction, landslide, and fault rupture can be estimated by combining the available soil parameter data with the current hazard models or by making use of existing maps showing estimated levels of these collateral hazards. Regional structural inventories, often stored in external database management systems, are combined with the seismic hazards to produce damage and loss distributions for the region analyzed.

Most of the previous works for regional seismic hazard and risk analysis has been limited to methods usually considering only one type of seismic hazard and often applied to a small region or to a specific type of facility. Rentzis, et al. (1992) used a GIS to estimate damage and loss distributions due to ground shaking alone in a 50-year exposure period for residential and commercial buildings in Palo Alto, California. Borcherdt et al. (1991) developed a GIS-based methodology for identifying special study zones for strong ground shaking in the San Francisco Bay region based on regional surface geology and an intensity attenuation relationship for a repeat of the 1906 San Francisco Earthquake. Kim, et al.(1992) developed a GIS-based regional risk analysis program to interactively study the vulnerability of bridges in a regional highway network. Very few of these studies, however, have considered combination of the effects of the various seismic hazards such as ground shaking, soil amplification, liquefaction, landslide, and fault rupture. Currently, there is no existing methodology for Bangladesh for integrating all of the separate modules for comprehensive regional seismic hazard and risk analysis. Due to recent improvements in the availability and quality of GIS technology, tabular database software, as well as computer hardware, a significant amount of current research has been devoted to incorporating GIS technology in seismic hazard and risk analysis.

1.2 Objectives

The objectives of this research are as follows:

- Development of a methodology for evaluating seismic hazard, which will be based on factors such as ground shaking, soil amplification, liquefaction, landslide and fault rupture.
- Factors involve in risk assessment will be identified and building inventory of sample area of different cities will be developed. This may be included in local Building Code.
- Maps representing regional geologic and geographic information will be overlaid and their attributes will be combined to produce maps of regional seismic hazards.
- These hazard maps will then be overlaid and combined with building inventory maps to produce maps predicting regional damage distributions. Combining the maps of damage distributions with a map of population distributions for the area results in final regional estimates of the direct loss, indirect loss, and casualties.

The GIS-based seismic hazard and risk will be useful to engineers, planners, emergency personnel, government officials, and anyone else who may be concerned with the potential consequences of seismic activity in a given region.

The results of a regional seismic hazard and risk analysis will be presented in the form of micro zone maps. Micro zone maps will be used for estimating potential damage and loss to existing facilities as well as for planning location and construction of future facilities. Micro zone maps will be helpful for the decision-makers who are involved in hazard and risk mitigation planning.

1.3 Scope

This research focuses on the development of a methodology for using geographic information system technology to integrate the various components necessary for a multi –hazard seismic risk analysis. In this thesis, the seismic risk analysis includes consideration of primary hazards due to ground shaking and to local site effects such as soil amplification, liquefaction, landslide, and surface fault rupture. Secondary hazards such as tsunami, conflagration, and inundation are not considered. The analysis incorporates structural inventories, motion-damage relationships, and loss modeling for

estimating regional damage and loss distributions. Only those damages and losses associated with the primary hazards listed above are considered.

The integrated GIS-based analysis methodology for Bangladesh presented in this thesis is designed for seismic hazard and risk analysis on regional level. The analysis results are intended to give general estimates of damage and loss distributions and to indicate areas that require further detailed investigation. These results are not intended to predict the expected damage and loss at a specific site or for a specific facility. For this reason, the models chosen to be included in the GIS- based analysis are fairly simplified and suitable for use with regional spatially-distributed data, which can often be incomplete in the amount and type of available information. The flexible frame work of this GIS-based methodology will allow the analysis system to be updated and expanded with new models and database information. Figure 1.4 presents the flowchart for this study.

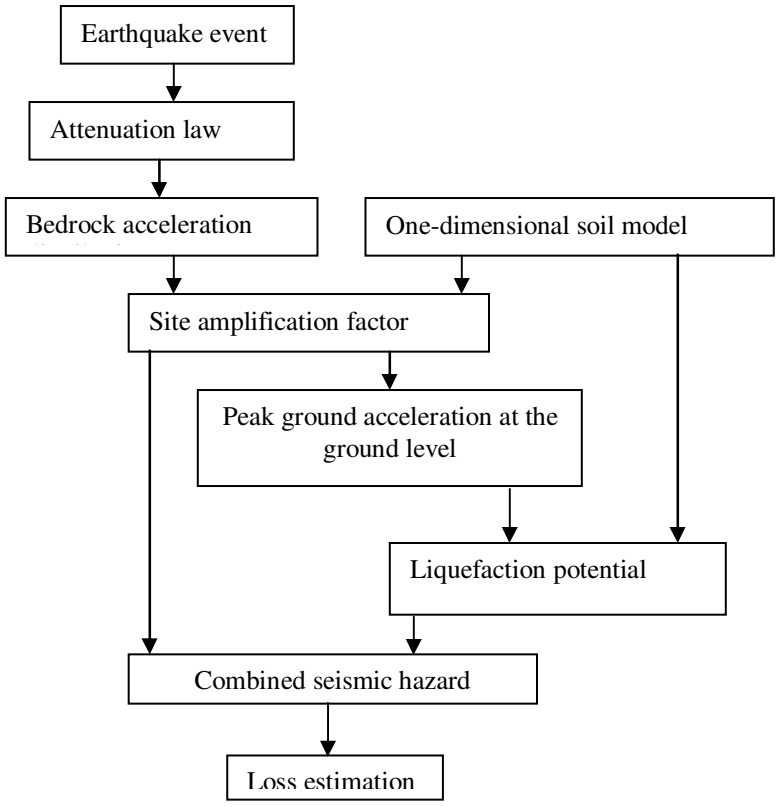

Figure 1.4 Flow chart for this study

1.4 Outline of the study

This study presents a methodology for using geographic information system to conduct a regional multi-hazard seismic risk analysis. The thesis consists of six chapters.

Chapter 1 provides background and present state of the problem, objectives and scope of the thesis.

Chapter 2 reviews the existing literature on seismic environment. Earthquake hazard, site amplification, soil liquefaction, landslide potential is described. Descriptions of the various types of damage, the motion-damage relationships and attenuation of earthquake ground motion are also included here.

Chapter 3 gives a description of a geographic information system (GIS). Spatial data structures and the functional elements of an integrated GIS are discussed. Analysis and Modelling capabilities of additional applications of GIS Technology to Regional Seismic Hazard and Risk Analysis and Methodology of Regional Seismic Hazard and Risk analysis are also discussed. GIS-based methodologies for combining site attributes through a weighted – average approach are presented in this chapter.

Chapter 4 deals with the Strong motion monitoring system in Bangladesh and Development of an Acceleration Based Attenuation relation for Bangladesh. Basic data collection is discussed here. Using multiple regression an acceleration based attenuation relation is also developed.

Chapter 5 presents a case study of 'GIS Based Methodologies for Seismic Hazard and Risk Analysis for Bangladesh'. A regional multi-hazard seismic risk analysis performed for Sylhet City, located in the north-east part of Bangladesh. A detailed description of the GIS-based analysis methodology is presented. A discussion of the sources of regional, geographic, and structural inventory information, as well as the problems associated with incomplete information is also given. Results and seismic microzonation maps for various stages of the analysis process are presented for illustration of the methodology. Finally, conclusions and recommendations are presented in chapter 6.

CHAPTER 2

LITERATURE REVIEW

2.1 General

2.1.1 Overview

It is well understood that earthquake damage to life and property results primarily from strong-ground shaking and shaking-induced hazards such as liquefaction, landslide, and surface fault rupture. Severe earthquakes of the last decade in Japan, Mexico, Armenia, and the United States have reemphasized the importance of local geologic site conditions in estimating the regional damage and consequent losses due to future major earthquakes (King, et al. 1993a). Evidence obtained from the 1989 Loma Prieta Earthquake indicated a strong influence of geotechnical status on the observed damage and casualties. The majority of the deaths and damage resulted from large number of failures that occurred due to liquefaction, soil amplification, and landslide (Clough, et al, 1993) which were related to geotechnical factors.

Seismic zonation maps for strong-ground shaking, liquefaction, landslide, and surface fault rupture can play a significant role in planning mitigating effects of earthquakes in urban areas. As discussed earlier, a geographic information system provides an ideal environment for compiling and integrating regional databases of spatial geologic and geotechnical information for purposes of seismic zonation. One of the main goals of this research is the development and illustration of a methodology for implementing and combining the seismic hazard models for each of the local site effects as part of a GIS-based multi-hazard regional seismic risk analysis. This chapter discusses in detail the different hazard models and Chapter 3 discusses their integration in the GIS environment. The various models for soil amplification are described in Section 2.1.2. Section 2.1.3 gives an overview of the models that are currently available for quantitative estimation of the secondary seismic effects of liquefaction, landslide, and surface fault rupture. The

GIS-based methodology for integrating the seismic hazards associated with these secondary effects is presented in Section 3.4, Chapter 3.

2.1.2 Soil Amplification

Soil amplification due to earthquake motion is one of the most difficult site effects to model. The difficulties result from (a) the lack of sufficient data on local soil parameters; (b) the lack of sufficient strong ground motion data at locations with different surface soil types; (c) the lack of sufficient strong ground motion data from vertical array measurements; (d) the inability to accurately quantify the non-linear behavior of soils when subjected to dynamic forces (Kiremidijian, et al., 1991).

The effect of local geology on the characteristics of earthquake ground motion has been a much researched subject dating back to observations made after the 1906 San Francisco Earthquake. Numerous methodologies have been proposed for estimating the surface ground motion from the motion at the bedrock level for different the geologic characteristics and local soil conditions. Current methods for estimating ground motion due to site amplification can generally be divided into three types: (a) empirical multiplication factors; (b) theoretical transfer function models and (c) dynamic non-linear models. The remainder of Section 2.1.2 contains a detailed description of these three types of soil amplification methods.

2.1.2.1 Empirical Multiplication Factors

Often the simplest method of quantifying the effect of local soil conditions on the amplification of earthquake ground motion is the use of empirical multiplication factors. This method involves multiplying a selected ground motion parameter such as peak ground acceleration (PGA) or peak ground velocity (PGV) at the bedrock level by an empirically-derived factor to estimate the ground motion parameter at the surface. These factors are often functions of the severity of shaking at the bedrock level and the properties of local soil condition such as shear wave velocity and thickness of soil deposits. Aki (1988) conducted an in-depth review of local site effects on strong ground motion and concluded, “The most realistic approach to the microzonation is then to

determine empirical site-amplification factors for as many sites as possible by the regression analysis of earthquake data, and correlate them with various geotechnical parameters of the site which are relatively easier to measure."

Several multiplication factors have been developed for various regions based on statistical analysis of observed strong ground motion data. Kiremidjian, et al. (1991) developed simple site-dependent PGA and PGV amplification factors for the San Francisco Bay Area based on an analysis of 52 rock and soil site recordings from the 1989 Loma Prieta Earthquake. These factors are a function of the input PGA or PGV, the depth to bedrock and average shear wave velocity of the soil deposit. Section 3.3.3 illustrates the implementation of this model in a GIS environment. Borcherdt (1992), Idriss (1990), Seed, et al. (1976) and Trifunac (1976) are a few of the many researchers who have analyzed strong ground motion data to develop ratios of peak ground motion values for different soil conditions.

Modifying only the peak ground motion values such as PGA and PGV is often not a suitable means of representing the soil amplification effects of local site conditions because the frequency contents of both the input bedrock motion and the soil deposit are not considered in the analysis. PGA values are usually amplified by high frequency motions, PGV values tend to be amplified by medium frequency motions, and low frequency motions usually amplify PGD values. For this reason a great deal of past research has focused on the effect of local soil conditions on amplification of ground motion spectra such as spectral acceleration (S_a), spectral velocity (S_v), and spectral displacement (S_d). Spectral amplification is often measured for peak values, values at certain frequencies or periods, average values, and the entire spectra.

Mohraz (1976) studied the earthquake response spectra on different geologic conditions recorded from several earthquakes. Borcherdt (1990) thoroughly analyzed earthquake response spectra from the 1989 Loma Prieta Earthquake recorded at various geologic conditions in the San Fancisco Bay area. These studies and others such as Trifunac (1976) and Seed, et al. (1976) have shown that soil amplification is frequency-dependent with a cross-over period at approximately 0.2 seconds. Above this period the ground

motion is amplified by the local site conditions and below it the ground motion is attenuated by the local site conditions. Observations such as these have led to a review of the methods of site characterization used in several structural design codes for new buildings. It is the accepted practice to classify soil sites as one of three or four broad types and then use a corresponding site-factor in the calculation of the applied lateral force to the structure. It is anticipated that the next generation of structural design codes will employ a more frequency-dependent site classification with some consideration of the fundamental site period (Whitman, 1992).

2.1.2.2 Theoretical Transfer Function Models

Earthquake motions at the surface of horizontally stratified soil can be treated as filtering of horizontal shear waves going through successive reflections and refractions in the soil deposit (Newmark and Rosenblueth, 1971). Linear wave propagation theory has become one of the most widely used techniques for assessing the effects of local soil conditions on the amplitude and frequency contents of seismic motions in soil deposits (Kausel an Roesset, 1984). This method involves idealizing the soil deposit as horizontally layered strata overlying rock with incident vertically propagating horizontal shear waves. The dynamic equations of motion are solved in the frequency domain with the soil deposit acting as a linear filter having a transfer function that depends on the viscoelastic material properties of the soil. Non-linearities in the soil material are typically modeled by iterative use of the linear solution, adjusting the material properties at each step to be compatible with the computed level of strain.

The linear transfer function model for soil amplification has been the subject of earthquake engineering research since the early 1950's when the work of Thomson (1950) and Kanai (1957) first suggested the methodology. Numerous linear transfer functions with varying degrees of complexity and required soil properties have been proposed for modifying different spectral ordinates. The general form of the equation for a spectrum at the ground surface level is typically given as:

$$S_s(\omega)=H(\omega)S_r(\omega) \quad (2.1)$$

where

$S_s(\omega)$ = the spectral amplitude at the ground surface level

$S_r(\omega)$ = the spectral amplitude at the bedrock level

$H(\omega)$ = the linear transfer function

ω = the circular frequency in rad/sec

Most of these transfer functions have been theoretically derived and then verified with empirical data from either strong ground motion or microtremor recordings, although there has been much disagreement about the applicability microtremor results because the material properties of the soil often remain in the linear range at these low levels of strain. A brief overview of the most commonly used linear transfer functions is given below. The various iterative methods for including the effects of non-linear soil material properties will not be discussed in this section, but Section 2.1.2.3 will include a brief treatment of non-linear soil behavior.

One of the first transfer functions developed for modeling spectral ratios is the Haskell-Thomson (Thomson, 1950) propagation matrix for a vertically traveling shear wave. This matrix relates the shear stress and displacement at the top of a soil layer to the stress and displacement at the bottom of the layer using parameters such as the frequency of the incoming shear wave, the soil layer thickness, and the shear wave velocity and damping in the layer (Seale and Archuleta, 1989). Newmark and Rosenblueth (1971) developed a linear transfer function for the ratio of psuedovelocity spectra between two layers based on the work of Kanai (1957). Their ratio is a function of density of the material in each layer, the shear wave velocity in each layer, the predominant period of the soil site, and the predominant period of the incoming seismic waves.

Ohsaki (1982) also formalized a linear transfer function that uses the average shear wave velocity, depth, and damping coefficient in each layer to represent the spectral amplification of ground motion in a soil deposit. Tsai and Housner (1970) and Faccioli (1976) developed frequency-based soil amplification methodologies that use similar soil parameters but consider a more rigorous modal-superposition analysis.

The most commonly used transfer function model is included in the computer program SHAKE developed by Schnabel, et al. (1972). SHAKE discretizes the soil profile into several layers and uses an iterative technique to represent the non-linear behavior of the soil by adjusting the material properties at each iteration step. The required input information includes shear modulus vs. shear strain and damping coefficient vs. shear strain curves, the depth, shear wave velocity, and unit weight of each soil layer, the location of the water table, and the time history input at the base of the soil profile.
To determine soil amplification, the SHAKE program is used in this thesis and detail of this program explained in Section 2.1.2.4

Although the transfer function method of soil amplification is an improvement over the peak value multiplication factor method in its representation of the frequency contents of the earthquake motion and soil profile, there are a few criticisms of this technique (Ho, et al. 1991). The assumption of horizontal stratigraphy and vertically incident seismic waves may not adequately represent the true conditions. Equivalent linear models that employ iterative techniques can often over-simplify the actual non-linear behavior of the soil material. The simple transfer function models often capture the soil amplification effects only at the predominant period of the soil profile as illustrated for the Ohsaki (1982) model in Figure 2.1, and can often over-estimate the effects of resonance. Despite these draw backs, transfer function methods are typically utilized in a regional multi-hazard seismic risk because they are able to give an adequate representation of soil amplification over a large region with a reasonable level of input and analysis effort.

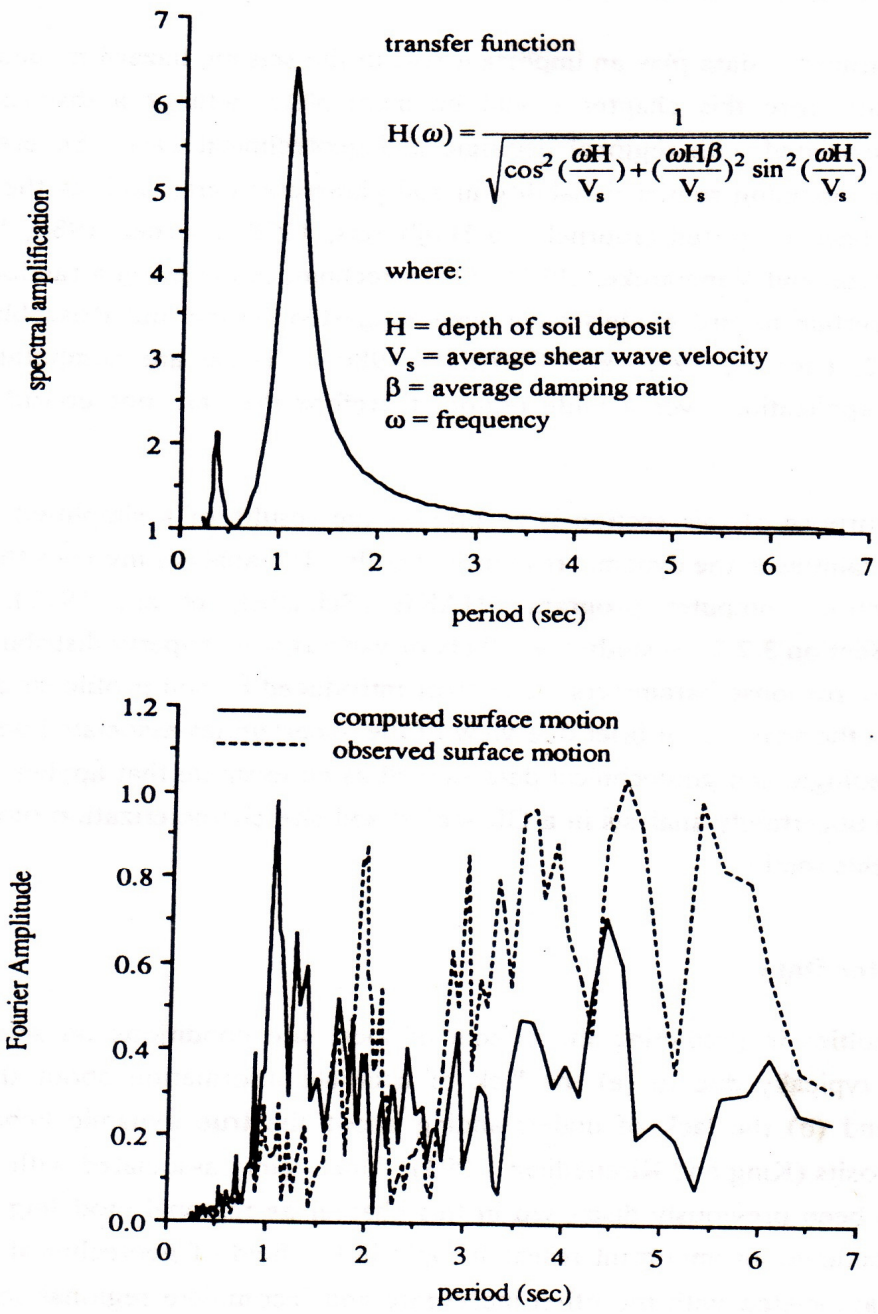

Figure 2.1 Illustration of the Ohsaki (1982) model for soil amplification, continued.

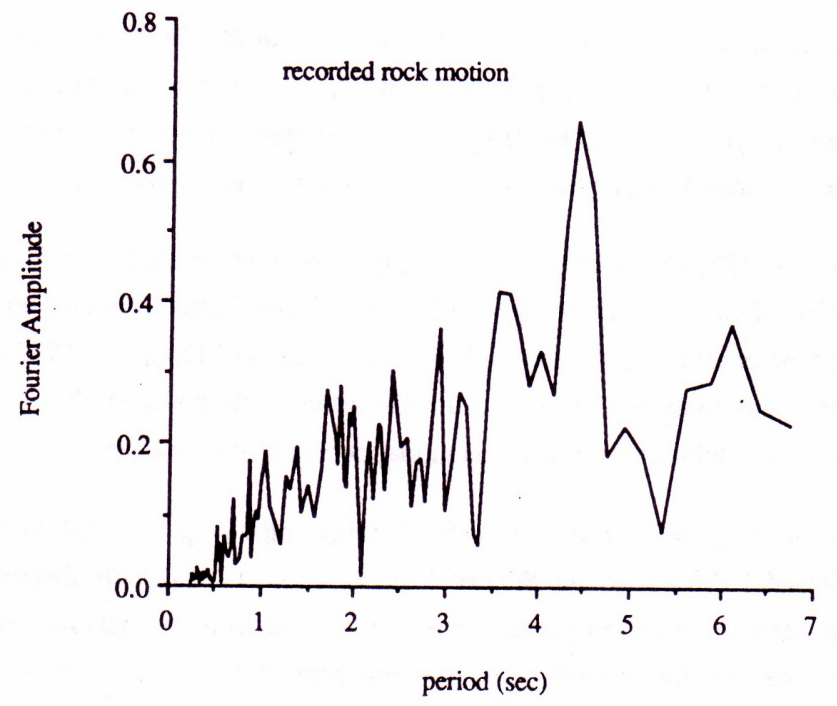

Figure 2.1(Contd.) Illustration of the Ohsaki (1982) model for soil amplification

2.1.2.3 Dynamic Non-Linear Models

The third type of method for estimating soil amplification involves the use of dynamic-non-linear models. These models are similar to the two previously discussed methods in that they idealize the soil profile as a system of horizontal layers with a vertically incident seismic motion at the base. However, the non-linear models are typically much more computationally intensive because they solve the dynamic equations of motion with time-step integration. The non-linear behavior of the soil material is usually modeled by hysteretic stress vs. strain and damping vs. strain relationships, and soil properties are updated at each time step to be compatible with the calculated level of strain. Although these models give the most accurate representation of the non-linear effects of soil on seismic motion, they typically require excessive computer time and very detailed site-specific soil parameter information, often rendering them impractical for soil

amplification analysis on regional basis. A brief overview of a few of the more commonly used dynamic non-linear models is included below for completeness.

Several dynamic non-linear models for characterizing the seismic response of a soil profile have been proposed in recent years, typically varying in the time-step integration technique and the hysteretic models used for representing non-linear soil material properties. Martin and Seed (1978) developed the computer program MASH that uses the cubic inertia time-step integration method for faster convergence and the Davidenkov stress-strain model for non-linear soil behavior and compare the results of their model using three different iteration techniques with the observed surface motion. Pyke (1979) compares several relationships for modeling the non-linear stress-strain behavior of soil including the Davidenkov model that gives shear strain in terms of shear stress. Ishihara and Towhata (1980) compare surface motions computed with the Ramberg-Osgood non-linear soil model and the SHAKE equivalent-linear analysis program with recorded ground motions at several study sites. They conclude that the non-linear model more accurately represents the true dynamic behavior of the soil profiles.

2.1.2.4 The Computer Program SHAKE

Background

Several methods for evaluating the effect of local soil conditions on ground response during earthquakes are presently available. Most of these methods are based on the assumption that the main responses in a soil deposit are caused by the upward propagation of shear waves from the underlying rock formation. Analytical procedures based on this concept incorporating non-linear soil behaviour, have been shown to give results in good agreement with field observations in a number of cases. Accordingly they are finding increasing use in earthquake engineering for predicting responses within soil deposits and the characteristics of ground surface motions.

The analytical procedure generally involves the following steps:

- Determination of the characteristics of the motions likely to develop in the rock formation underlying the site, and selection of an accelerogram with these characteristics for use in the analysis. The maximum acceleration, predominant period, and effective duration are the most important parameters of an earthquake motion. Empirical relationships between these parameters and the distance from the causative fault to the site have been established for different magnitude earthquakes. A design motion with the desired characteristics can be selected from the database of strong motion accelerograms.

- Determination of the dynamic properties of the soil deposit: Average relationships between the dynamic shear moduli and damping ratios of soils, as functions of shear strain and static properties, have been established for various soil types. Thus a relatively simple testing program to obtain the static properties for use in these relationships will often serve to establish the dynamic properties with a sufficient degree of accuracy. However, more elaborate dynamic testing procedures are required for special problems and for cases involving soil types for which empirical relationships with static properties have not been established.

- Computation of the response of the soil deposit to the base rock motions. A one dimensional method of analysis can be used if the soil structure is essentially horizontal. Programs developed for performing this analysis are in general based on either the solution to the wave equation or on a lumped mass simulation. More irregular soil deposits may require a finite element analysis.

Features of the Program

The program can compute the responses for a design motion given anywhere in the system. Thus accelerograms obtained from instruments on soil deposits can be used to generate new rock motions which, in turn, can be used as design motion for other soil deposits as shown in Figure 2.2 (after Schnable et al., 1972). The program also incorporates non-linear soil behaviour, the effect of the elasticity of the base rock and systems with variable damping.

Program Theory

The theory considers the responses associated with vertical propagation of shear waves through the linear visco-elastic system shown in Figure 2.3. The system consists of N horizontal layers which extend to infinity in the horizontal direction and has a half space as the bottom layer. Each layer is homogeneous and isotropic, and is characterized by the thickness, h, mass density, ρ, shear modulus, G, and damping factor, β.

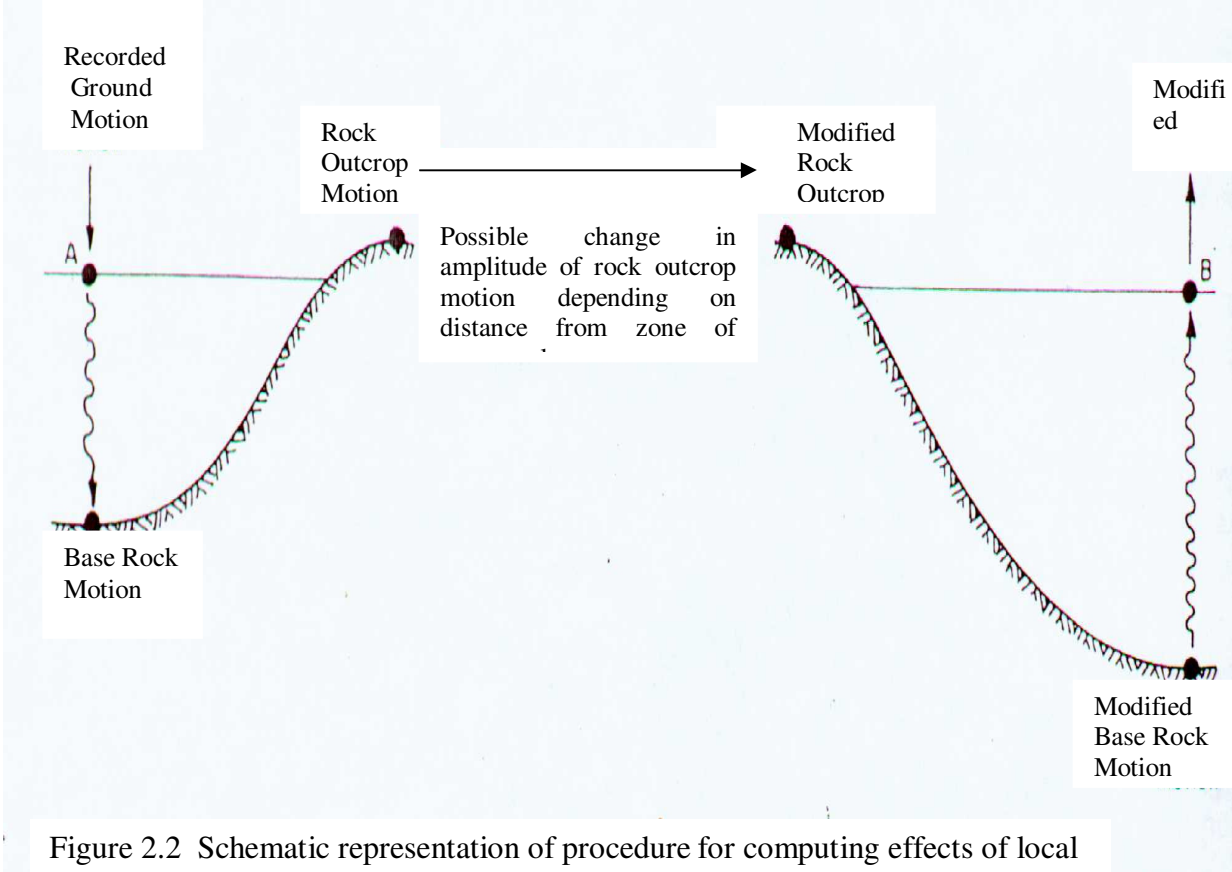

Figure 2.2 Schematic representation of procedure for computing effects of local soil conditions on ground motions (after Schnabel et al., 1972)

Description of Program SHAKE

Program SHAKE computes the responses in a system of homogeneous, visco-elastic layers of infinite horizontal extent subjected to vertically travelling shear waves. The system is shown in Figure 2.3. The program is based on the continuous solution to the wave- equation adapted for use with transient motions through the fast Fourier transform algorithm. The nonlinearity of the shear modulus and damping is accounted for by the

use of equivalent linear soil properties using an iterative procedure to obtain values for modulus and damping compatible with the effective strains in each layer.

The following assumptions are implied in the analysis:

- The soil system extends infinitely in the horizontal direction. Each layer in the system is completely defined by its value of shear modulus, critical damping ratio, density, and thickness. These values are independent of frequency.
- The responses in the system are caused by the upward propagation of shear waves from the underlying rock formation.
- The shear waves are given as acceleration values of equally spaced time intervals. Cyclic repetition of the acceleration time history is implied in the solution.
- The strain dependence of modulus and damping is accounted for by an equivalent linear procedure based on an average effective strain level computed for each layer.

The program is able to handle systems with variation in both moduli and damping, and takes into account the effect of the elastic base. The motion used as a basis for the analysis, the object motion, can be given in any one layer in the system and new motions can be computed in any other layer.

The set of operations can be performed by the program:

- Read the input motion, find the maximum acceleration, scale the values up or down, and compute the predominant period.
- Read data for the soil deposit and compute the fundamental period of the deposit.
- Compute the maximum stresses and strains in the middle of each sub-layer and
- Obtain new values for modulus and damping compatible with a specified percentage of the maximum strain.
- Compute new motions at the top of any sub-layer inside the system or outcropping from the system.

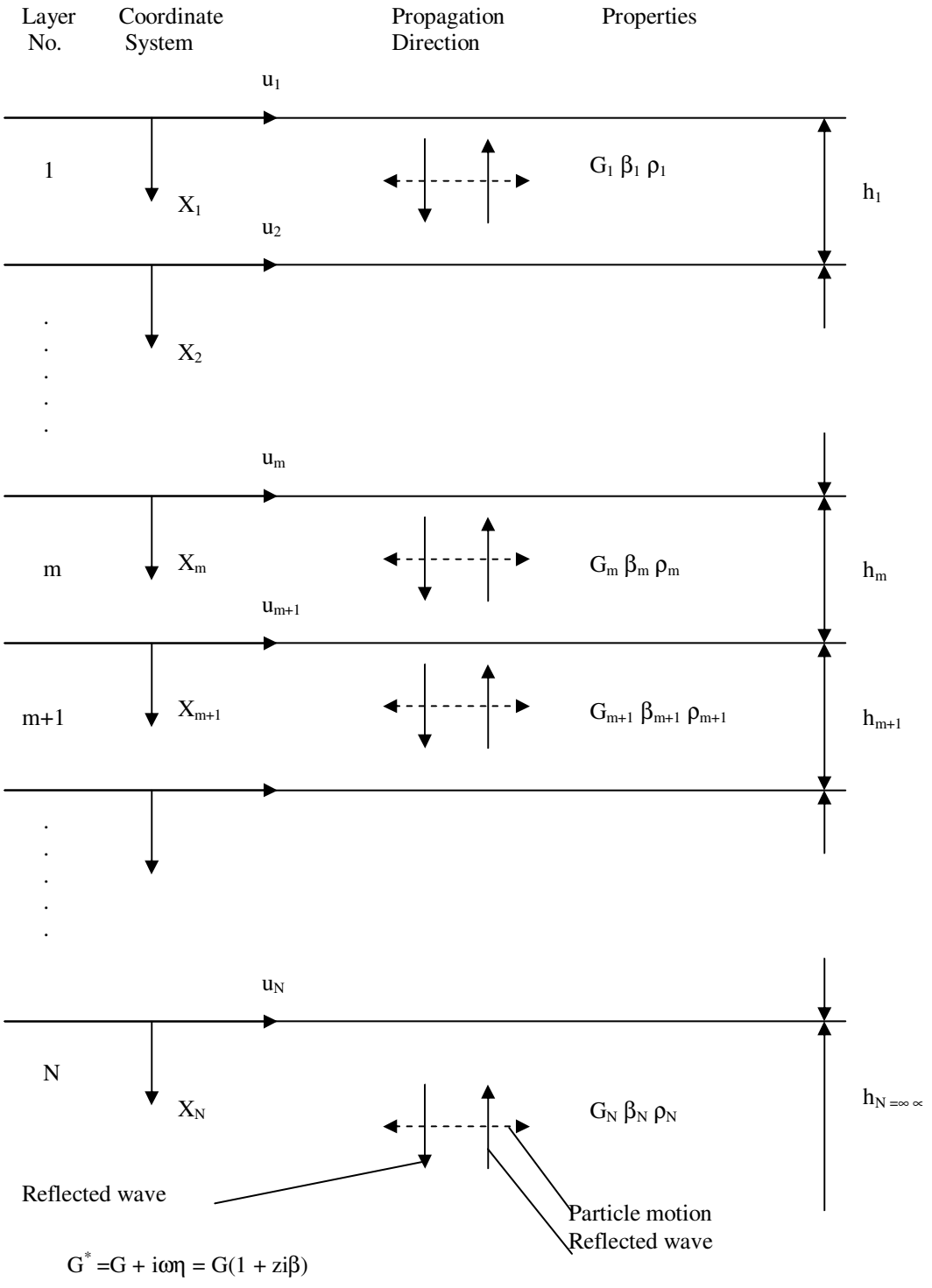

Figure 2.3 One-dimensional wave propagation system (after Schnabel et al., 1972)

2.1.3 Secondary Seismic Effects

Unlike the local site effect of soil amplification described above, the secondary seismic effects of liquefaction, landslide, and surface fault rupture have very few quantitative models associated with them. Microzone maps of hazard potential have been developed for these three effects for several regions. The hazard potential maps typically either give a “yes” or “no” estimation of occurrence for an assumed scenario earthquake, or they give a “”high , “moderate”, “low”, or “very low” estimation of occurrence based on a given set of probability thresholds. The probabilities are typically associated only with the occurrence of ground shaking levels and do not include the occurrence of the site effects.

Very few probabilistic models for liquefaction, landslide, and surface fault rupture have been developed (Kiremidjian, 1992). For this reason, one of the most common methods for estimating these site effects in a regional multi-hazard seismic risk analysis is to just increase the level of estimated surface ground motion in areas where these effects are likely to occur. The definition of “likely to occur” is often very subjective and varies from study to study. Damage from the three effects, and in some cases ground shaking as well, is typically summed in a conservative manner. The remainder of Section 2.1.3 is devoted to an overview of the quantitative models that are available for estimating the secondary seismic effects of liquefaction, landslide, and surface fault rupture. A less conservative methodology for integrating these effects in the GIS environment is presented in Section 3.4, along with an illustrative example of the methodology.

2.1.3.1 Liquefaction

General concepts

One of the most dramatic causes of damages to structure during an earthquake has been due to the development of liquefaction in saturated sand and silt deposits, manifested either by the formation of boils and mud-spouts at the ground surface, by seepage of water through ground cracks or in some cases by the development of quicksand-like conditions over substantial areas. Where latter phenomenon occurs, buildings may sink

substantially into the ground or tilt excessively, light-weight structures may float upwards to the ground surface and foundations may displace laterally causing structural failures.

The basic cause of liquefaction of sands has been understood, in a qualitative way, for many years. If a saturated sand is subjected to ground vibrations, it tends to compact and decrease in volume; if drainage is unable to occur, the tendency to decrease in volume results in an increase in pore water pressure, and subsequently if the pore water pressure builds up to the point at which it is equal to the overburden pressure, the effective stress becomes zero, the sand loses its strength completely, it develops a liquefied state.

In more quantitative terms, it is now generally believed that the basic cause of liquefaction in saturated cohesion less soils during earthquakes is the buildup of excess hydrostatic pressure due to the application of cyclic shear stresses induced by the ground motions. These stresses are generally considered to be due primarily to upward propagation of shear waves in a soil deposit, although other forms of wave motions are also expected to occur. Thus, soil elements can be considered to undergo a series of cyclic stress conditions as illustrated in Figure 2.4, the stress series being somewhat random in pattern but nevertheless cyclic in nature.

The phenomena of liquefaction is generally associated with cohesionless soils. It results from the seismic shaking that is of a sufficient intensity and duration. It occurs most commonly in loose, saturated granular soils that are uniformly graded and that contain few fines. Although sands are especially susceptible, liquefaction is also known to develop in some silts and gravels. Two necessary conditions for liquefaction to occur are the presence of soils of sufficiently low density that will tend to undergo volume reduction upon shaking, and a state of full or near full saturation. Under these conditions, cohesionless soils will tend to densify when subjected to cyclic shear stresses from ground vibrations but will be temporarily prevented from doing so at depth due to restricted drainage. As a result, excess pore pressure accumulate, effective stresses decrease and soils loose strength and may become liquefied (Seed and Iddris, 1982). The damaging effects of soil liquefaction have been well recognized since the Niigata and Alaska Earthquakes of the early 1960s. The types of failures associated with liquefaction

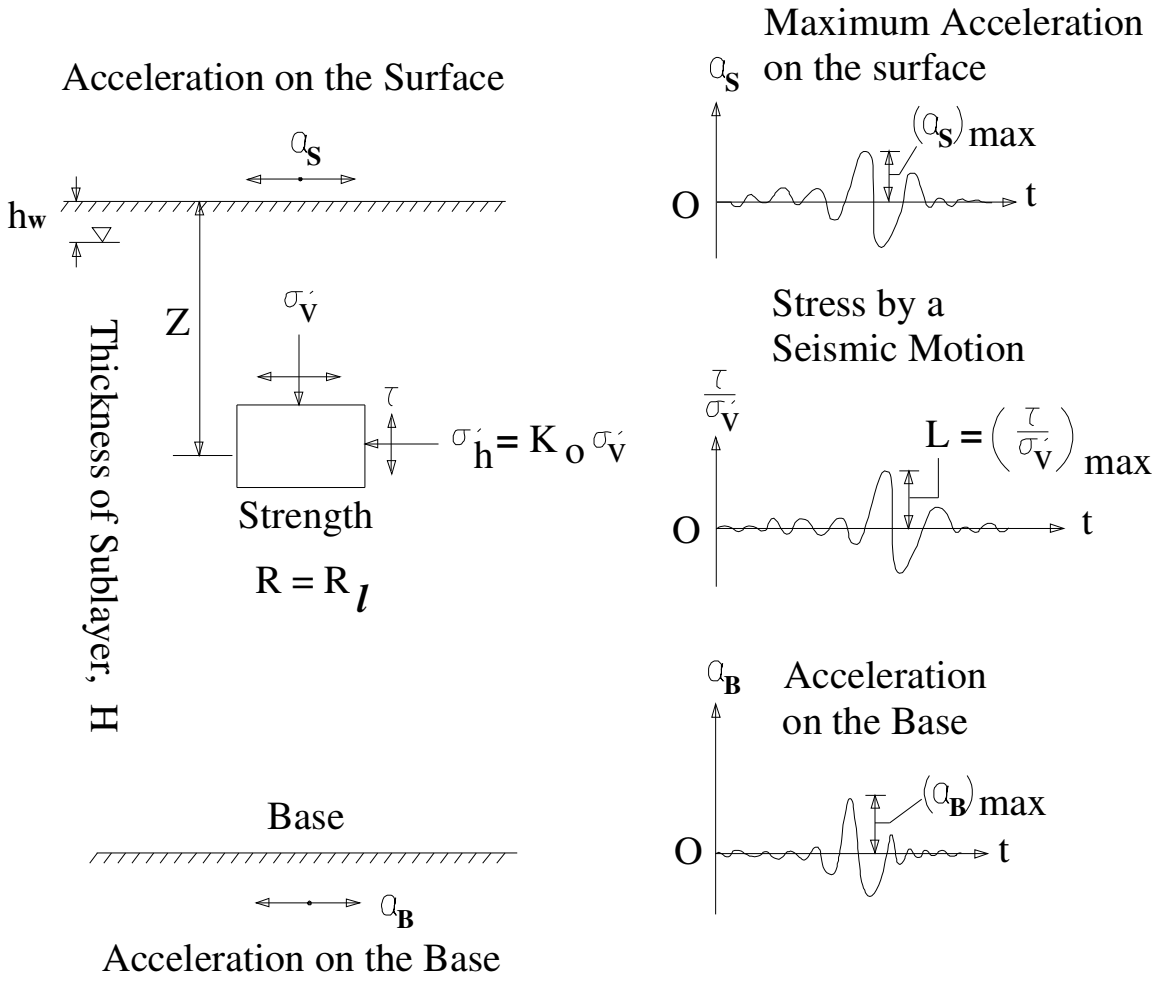

Figure 2.4 Cyclic shear stresses on a soil element during ground shaking (after Iwasaki et al., 1982)

include: (a) sinking or overturning of structures; (b) excessive differential settlement of structures; (c) sand boils; and (d) surface lateral spreading. There are several factors that influence liquefaction such as the geologic history of the deposit, the depth of the ground water table, the grain size distribution, the density of the soil, and the ground slope, often requiring expert evaluation (Juang and Elton, 1991). This detailed investigation is necessary for a site-specific soil liquefaction assessment, but more simplified models are required for quantitative analysis on a regional basis.

Because the capacity of soils to bear foundation loads is directly related to their strength, liquefaction poses a serious hazard to constructed structures and must be assessed in seismic areas when susceptible deposits exist. It should be noted that liquefaction here in refers to loss of strength and stiffness due to cyclic pore pressure-generation mechanism described in this article, and not due to strength loss and stiffness changes that occur in sensitive soils upon monotonic shearing or remolding. This later mechanism presents a danger in its own right but is not normally seismically related.

Liquefaction phenomena have been recorded and developed in many parts of the world where ground shaking is frequent and soils consist of loose fine sand under water table. Bangladesh including Dhaka is largely an alluvial plain consisting of loose fine sand and silt deposits. The ground water table is shallow in most places, specially, along the river flood plains. Although the older alluvium consisting of mainly silty clay with deeper ground water table is less susceptible to liquefaction, the recent deposits consisting of loose fine sand with shallower water table along the river flood plains may liquefy during a severe earthquake.

Not all granular soils are prone to liquefaction. As a general rule of thumb, cohesionless deposits with depth-corrected standard penetration values $(N_1)_{60}$ >30, depth –corrected normalised cone penetration resistance values q_{av} >175, or stress-corrected shear wave velocity V_{s1}>230 m/s (755 ft/s) are considered of sufficient density to pose little risk of liquefying. The potential for fine-grained soils to liquefy can be evaluated with reference to the Modified Chinese Criteria (Finn et al., 1994) shown in Fig. 2.5. According to these criteria, soils may liquefy if the clay fraction is less than 15% (using the Chinese

definition of clay size as less than 0.005 mm), the liquid limit is less than 35%, and the water content is larger than 0.9 times the liquid limit. These criteria are somewhat controversial and they do not represent a consensus among practicing engineers (NCEER, 1997). Establishing more precise and reliable measures for identifying which finer-grained soils are potentially susceptible to liquefaction is an area of on going research (Seed et al., 2001). For example, Andrews and Martin (2000) have reevaluated a large number of field liquefaction case histories and have proposed an adaptation of the Modified Chinese Criteria for U.S. use (Table 2.1).

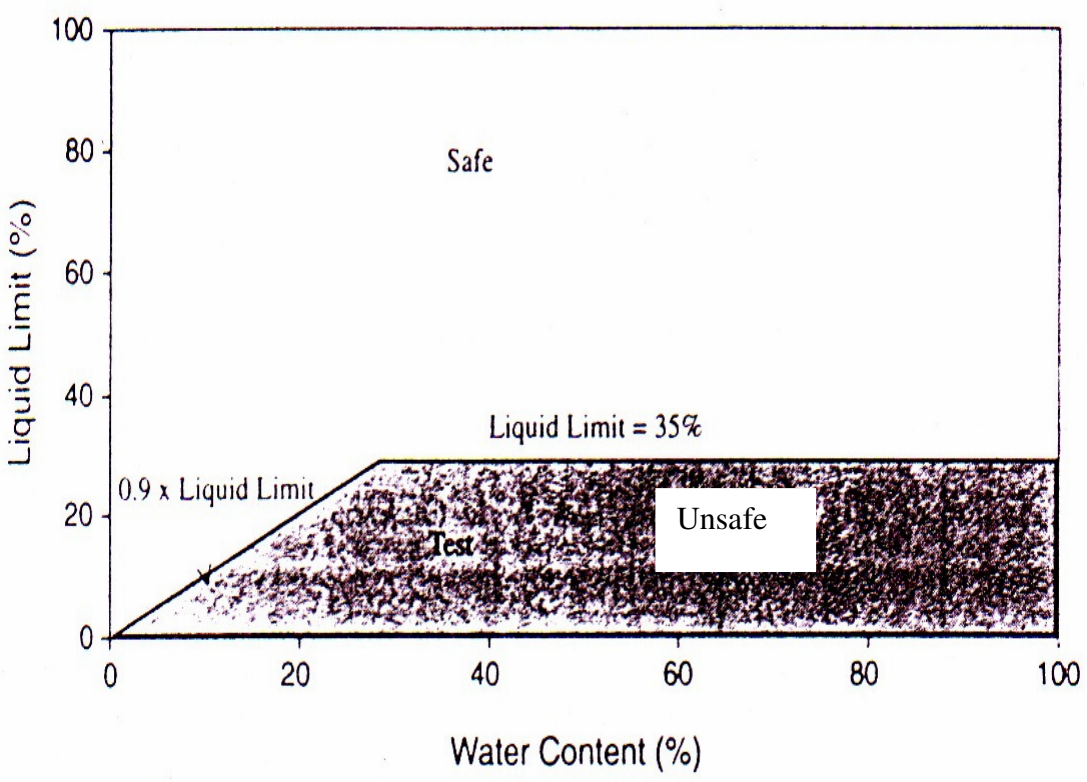

Figure 2.5 Modified Chinese Criteria for liquefaction assessment of fine-grained soils. (after Finn et al., 1994)

Table 2.1 Liquefaction criteria for fine-grained soils. (After Andrews and Martin, 2000).

Clay content (%)	Liquid limit <32	Liquid limit ≥ 32
< 10	Susceptible	May be susceptible (conduct additional testing)
≥ 10	May be susceptible (conduct additional testing)	Not susceptible

Evaluation of the liquefaction resistance of soils deposits has evolved over the years into a commonly accepted, simplified empirical procedure, originally developed by Seed and Idriss (1971). This simplified procedure represents the standard of practice in North America and many other countries. It is reviewed periodically by groups of experts who make recommendations for changes according to data collected from new earthquakes and new developments in liquefaction hazard assessment. The latest consensus statement is contained in a 1996 NCEER workshop report (NCEER, 1997; Youd and Idriss, 2001), upon which much of the following discussion is based.

Assessment of Soil Liquefaction

Regional liquefaction hazard mapping is typically done using either a geologic or a geotechnical technique (Juang and Elton, 1991). Table 2.2 and Table 2.3 show the most well known geologic techniques developed by Youd and Perkins (1978) and Ishihara and Yasuda (1991). It gives a qualitative estimate ranging from “very high” to “very low” or “likely” to “not likely” indicate the likelihood of liquefaction in various soil deposits under seismic loading. During the past 25 years, several geotechnical techniques for analyzing soil liquefaction have been proposed, resulting from the need for a more quantitative estimate of regional liquefaction hazard. Most of these techniques involve the comparison of the cyclic stress ratio generated by an earthquake with the cyclic stress ratio which would be required to liquefy the soil (Youd, 1991).

Table 2.2. Estimated Liquefaction susceptibility of geologic sediments during strong ground shaking (after Youd and Perkins, 1978).

TYPE OF DEPOSIT	GENERAL DISTRIBUTION OF COHESION-LESS SEDIMENTS IN DEPOSITS	LIKELIHOOD THAT COHESIONLESS SEDIMENTS, WHEN SATURATED, WOULD BE SUSCEPTIBLE TO LIQUEFACTION (BY AGE OF DEPOSIT)			
		<500 YR	HOLOCENE	PLEIS-TOCENE	PRE-PLEIS-TOCENE
(a) CONTINENTAL DEPOSITS					
River channel	Locally variable	Very high	High	Low	Very Low
Flood plain	Locally variable	High	Moderate	Low	Very Low
Alluvial fan and plain	Widespread	Moderate	Low	Low	Very Low
Marine terraces and plains	Widespread	---	Low	Very Low	Very Low
Delta and fan-delta	Widespread	High	Moderate	Low	Very Low
Lacustrine and playa	Variable	High	Moderate	Low	Very Low
Colluvium	Variable	High	Moderate	Low	Very Low
Talus	Widespread	Low	Low	Very Low	Very Low
Dunes	Widespread	High	Moderate	Low	Very Low
Loess	Variable	High	High	High	Unknown
Glacial till	Variable	Low	Low	Very Low	Very Low
Tuff	Rare	Low	Low	Very Low	Very Low
Tephra	Widespread	High	High	Unknown	Unknown
Residual soils	Rare	Low	Low	Very Low	Very Low
Sebka	Locally variable	High	Moderate	Low	Very Low
(b) COASTAL ZONE					
Delta	Widespread	Very high	High	Low	Very Low
Esturine	Locally variable	High	Moderate	Low	Very Low
Beach - High Wave	Widespread	Moderate	Low	Very Low	Very Low
Beach - Low Wave	Widespread	High	Moderate	Low	Very Low
Lagoonal	Locally variable	High	Moderate	Low	Very Low
Fore shore	Locally variable	High	Moderate	Low	Very Low
(c) ARTIFICIAL					
Uncompacted Fill	Variable	Very high	---	---	---
Compacted Fill	Variable	Low	---	---	---

Table 2.3. A renewed Microzoning Procedure Based on Geomorphological Conditions (Ishihara and Yasuda,1991)

Geomorphological condition		Liquefaction potential
Classification	Specific conditions	
Valley plain	Valley plain consisted of gravel or cobble	Liquefaction not likely
	Valley plain consisted of sandy soil	Liquefaction possible
Alluvial fan	Vertical gradient is more than 0.5%	Liquefaction not likely
	Vertical gradient is less than 0.5%	Liquefaction possible
Natural levee	Top of natural levee	Liquefaction possible
	Edge of natural levee	Liquefaction likely
Back marsh		Liquefaction possible
Abandoned river channel	Indistinct	Liquefaction likely
	Distinct	
Former pond		Liquefaction likely
Marsh and swamp		Liquefaction possible
Dry river bed	Dry river bed consisting of gravel	Liquefaction not likely
	Dry river bed consisting of sandy soil	Liquefaction likely
Delta		Liquefaction possible
Bar	Sand bar	Liquefaction possible
	Gravel bar	Liquefaction not likely
Sand dune	Top of dune	Liquefaction not likely
	Lower slope of dune	Liquefaction likely
Beach	Beach	Liquefaction not likely
	Artificial beach	Liquefaction likely
Inter levee lowland		Liquefaction likely
Reclaimed land by drainage		Liquefaction possible
Reclaimed land /filled land		Liquefaction likely
Spring		Liquefaction likely
Fill	Fill on boundary zone between sand dune and lowland	Liquefaction likely
	Fill adjoining cliff	Liquefaction likely
	Fill on marsh or swamp	Liquefaction likely
	Fill on reclaimed land by drainage	Liquefaction likely
	Other type of fill	Liquefaction possible

Liquefaction Potential Based on N-Values

A simple method suggested by Seed et al. (1983) was used here to evaluate a liquefaction resistance factor, F_L. In this method required parameters are SPT N-values, grain-size distribution curves of soils, overburden pressure, and estimated peak surface acceleration. The assessment of the liquefaction resistance factor at any depth by this method involves comparison of the predicted cyclic stress ratio (τ/σ'_o) that would be induced by a given design earthquake (L) with the cyclic stress ratio required to induce liquefaction (R). For this method, F_L is calculated for a given depth by the following formula. Liquefaction is judged to occur at that depth if F_L is less than 1.0.

$$F_L = R / L \qquad (2.2)$$

The shear stresses developed at any point in a soil deposit during an earthquake appear to be due primarily to the vertical propagation of shear waves in the deposit. If the soil column above a soil element at depth 'h' behaved as a rigid body, the maximum shear stresses on the soil element would be

$$(\tau_{max})_r = (\gamma h)/g \,.\alpha_{Smax} = \sigma_o/g \,.\, \alpha_{Smax} \qquad (2.3)$$

where

σ_o = total overburden pressure

α_{Smax} = estimated peak surface acceleration (in percentage of g)

γ = unit weight of the soil

g = acceleration due to gravity ;

Because the soil column behaves as a deformable body, the actual shear stress at depth h, $(\tau_{max})_d$, as determined by the ground response analysis will be less than $(\tau_{max})_r$ and might be expressed by

$$(\tau_{max})_d = r_d \ (\tau_{max})r \qquad (2.4)$$

where

r_d = a stress reduction factor with a value less than 1 given by (1- 0.015z) in which z = depth of ground surface in meters.

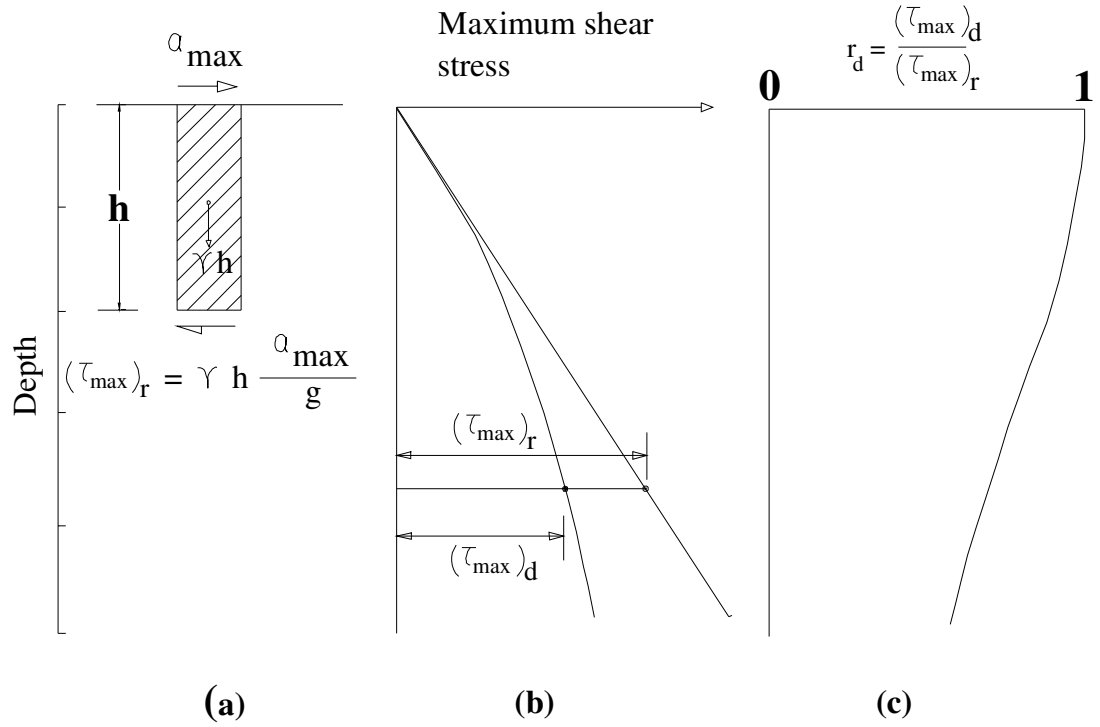

Figure 2.6 Procedure for determining maximum shear stress (after Seed et al., 1983)

Computations of the value of r_d for a wide variety of earthquake motions and soil conditions having sand in the upper 50 ft. have shown that r_d generally falls within the range of values shown in Figure 2.7. It may be seen that in the upper 30 or 40 ft., the scatter of the results is not so great and, for any of the deposits, the error involved in using the average values shown by the dashed line would generally be less than about 5%. Thus to a depth of about 40 ft., a reasonably accurate assessment of the maximum shear stress developed during an earthquake can be made for the relationship given in equation (2.2) by using values of r_d to be taken from the dashed line in Figure 2.7.

The actual time history of shear stress at any depth in a soil deposit during an earthquake will have an irregular form such as that shown in Fig. 2.8. From such relationships it is necessary to determine the equivalent uniform average shear stress. By appropriate weighting of the individual stress cycles, based on laboratory test data, this determination

can readily be made. However, after making these determinations for a number of different cases it has been found that with a reasonable degree of accuracy, the average equivalent uniform shear stress, τ_{av}, is about 65% of the maximum shear stress, τ_{max} . Combining this result with the above expression for τ_{max}, the average cyclic stress ratio (τ_{av}/σ'_o) induced by an earthquake is given by the expression (Seed et al., 1983):

$$L = \tau_{av}/\sigma'_o = 0.65(\alpha_{Smax}/g)(\sigma_o/\sigma'_o)\, r_d \qquad (2.5)$$

in which

σ'_o = effective overburden pressure

The cyclic stress ratio required to cause liquefaction has been evaluated using empirical relationship between cyclic stress ratio and N values. This curve is presented in Figure 2.9. Since the standard penetration resistance, N, measured in the field actually reflects the influence of the soil properties, test procedure (hammer energy) and the effective confining pressure, it has been found desirable to eliminate the influence of confining pressure by using a normalized penetration resistance $(N_1)_{60}$ or N_1, where N_1 is the measured penetration resistance of the soil under an effective overburden pressure of 1 ton per sq.ft. So, before using the graph in Figure 2.9, normalization to the field SPT-N value is needed as follows:

$$N_1 = C_N N \qquad (2.6)$$

Where

N_1 = modified N values

C_N = a correction factor

The correction factor, C_N was provided by and presented here as Fig. 2.10

The severity of foundation damage caused by soil liquefaction depends to a great extent on the severity of liquefaction, which can not be evaluated solely by the F_L. Generally speaking, liquefaction under the following conditions tends to be severe if:

- The liquefied layer is thick
- the liquefied layer is shallow

- The F_L of the liquefied layer is far less than 1.0.

In order to take care the above effect, the Japanese bridge code recommended a modification to the procedure suggested by Seed et al. (1983). In this modification, the factor of safety value, F_L against resistance to liquefaction have been computed for all the bore holes and these values have been subsequently been converted into liquefaction potential index (P_L). The P_L is given by the following equation (Iwasaki et al., 1982).

$$P_L = \int_0^{20} F(z)\, w(z)\, dz \qquad (2.7)$$

Where

$F(z) = (1-F_L)$ for $F_L \leq 1.0$

$F(z) = 0$ for $F_L > 1.0$

$W(z) = (10 - 0.5\,Z)$ for $z \leq 20$ m

$W(z) = 0$ for $z > 20$ m

$P > 15$ very high possibility of liquefaction

$15 > P_L > 5$ high possibility of liquefaction

$5 > P_L > 0$ low possibility of liquefaction

$PL = 0$ very low possibility of liquefaction

The value of liquefaction potential, P_L indicates that a soil mass is susceptible to liquefaction if $P_L > 0$. If the value of P_L is large, the soil is very susceptible for liquefaction.

2.1.3.2 Landslide

The effects of earthquake-induced landslide have received much less research attention than the seismic effects of soil amplification and liquefaction discussed in the previous sections. Landslide hazard is typically very difficult to quantify because landslides come in many forms and are caused by a variety of processes. The local site factors that affect landslides generally include slope stability, geology, slope angle, hydrological conditions, vegetation, land use, and severity of the earthquake. Most of these factors are necessary for the investigation of an individual slope, but for seismically-induced landslide analysis

on a broad regional basis, the factors are typically limited to slope angle, geology, location of previous landslides, magnitude of the seismic event, and distance from the source (Hansen and Franks, 1991).

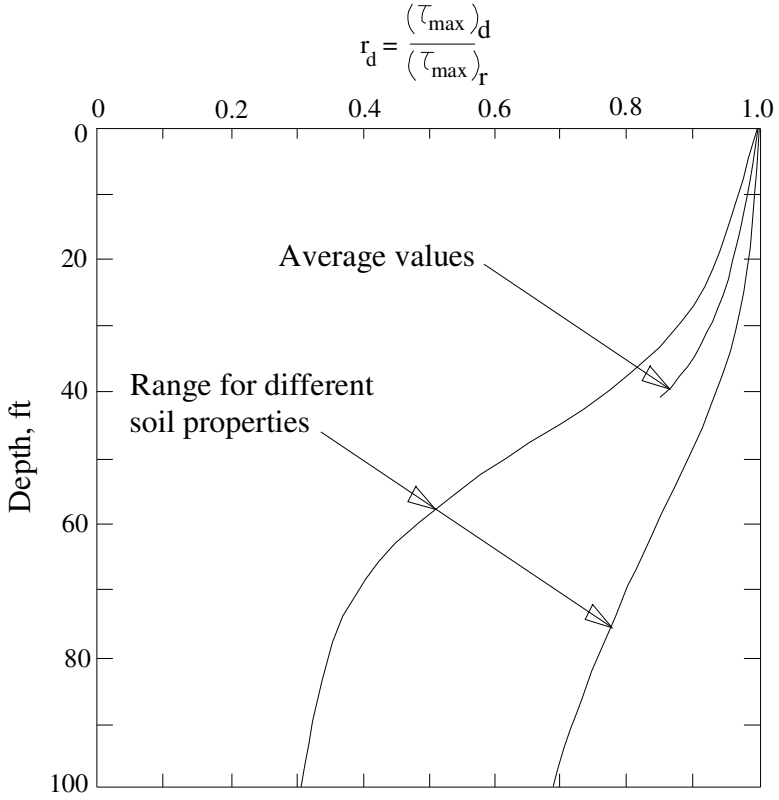

Figure 2.7 Range of values of r_d for different soil profiles (after Seed et al.,

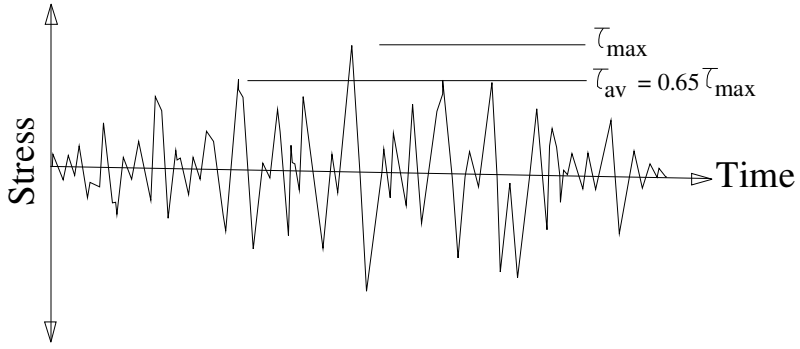

Figure 2.8 Time history of shear stresses during earthquake (after Seed et al., 1983)

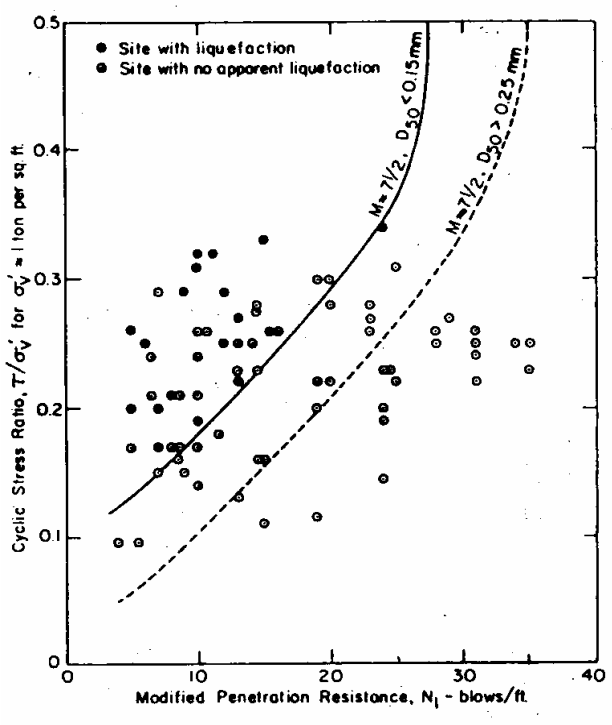

Figure 2.9 Correlation between field liquefaction behavior of silty sands under level ground conditions and standard penetration resistance (after Seed et al., 1983)

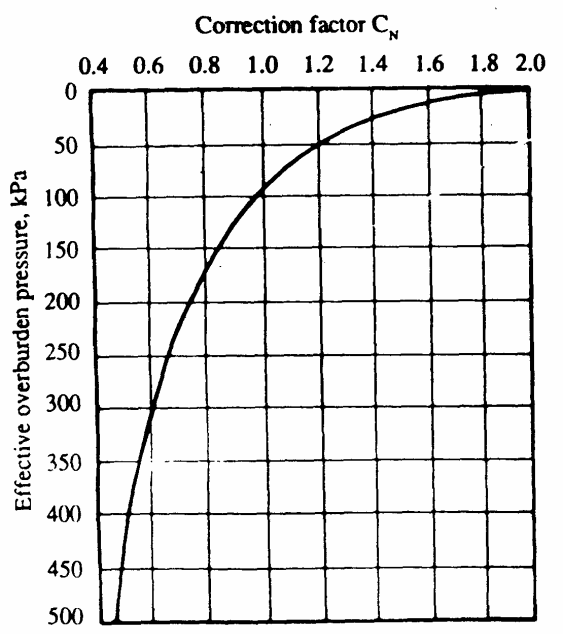

Figure 2.10 Recommended curve for determination of C_N (after 1991)

As with liquefaction, regional landslide hazard has traditionally been analyzed in a qualitative manner utilizing expert opinion, although recently more quantitative geotechnical methods have been proposed. The qualitative methods typically produce microzone maps indicating the relative susceptibility of various regions to landslides with no investigation into the possible triggering mechanisms for the land movement. The maps often result from an expert analysis of regional factors such as previous landslide locations, geologic deposits, and topography.

The complicated nature of the landslide process has made regional estimates of this local site effect very difficult to define quantitatively. Most of the recent research in this field has focused on determining the critical level of a given ground motion parameter that will trigger landslides in various geologic deposits. Wieczorek, et al. (1985) model a landslide as a translational failure on an infinite slope with a depth of 3 meters. They define three classes of geological units, assign shear parameters for each class, and then perform stability analyses using dry and saturated conditions to obtain the static factor of safety (FS) for each class. Based on the static FS, the critical acceleration to begin the process of slope failure, a_c, is computed as:

$$a_c = (FS - 1)g \sin\theta. \qquad (2.8)$$

Where:

θ = the slope angle

FS = the factor of safety determined from a static slope stability analysis

g = the acceleration of gravity

Several recorded strong ground motions were analyzed to develop average curves of induced landslide displacement versus a_c. The critical levels of displacement to produce structural damage are identified, such as 100 mm for cohesive slides (Wilson and keefer, 1985). The a_c values that correspond to these assumed critical displacement values are determined from the displacement vs. acceleration curves. These a_c values are compared to the regional estimates of surface peak ground acceleration to give a prediction for the occurrence of damaging earthquake-induced landslides in the area.

2.1.3.3 Surface Fault Rupture

The final local site effect to be considered is differential ground displacement due to surface fault rupture. Several empirical relationships have been developed for various faulting mechanisms that relate earthquake magnitude to length of fault rupture and length of fault rupture of horizontal ground displacement.

Slemons (1977) and Bonilla et al. (1984) have determined statistical relations between these parameters for worldwide and regional data sets, aggregated and segregated by type of faulting (normal, reverse, strike-slip). Bonilla et al.'s worldwide results for all types of faults are:

$$Ms = 6.04 + 0.708 \log_{10} L \qquad s = 0.306 \tag{2.9}$$

$$\log_{10} L = -2.77 + 0.619\, Ms \qquad s = 0.286 \tag{2.10}$$

$$Ms = 6.95 + 0.723 \log_{10} d \qquad s = 0.323 \tag{2.11}$$

$$\log_{10} d = -3.58 + 0.550 Ms \qquad s = 0.282 \tag{2.12}$$

Which indicates for example that, for Ms = 7, the average fault rupture length is about 36 km (and the average displacement is about 1.86) and s indicates standard deviation. Recently other resaerchers extensively dealing regarding the earthquake faults but very few methods for estimating differential ground displacement hazard have been proposed. Kiremidjian (1984) formalized a methodology for determining probabilities of horizontal ground displacement at specific locations on a fault of finite length. This method is applied in the San Francisco Bay Area and includes a procedure for estimating stresses and strains induced in a pipe crossing the fault. The Applied Technology Council (ATC-13, 1985) defines two different zone widths around an active fault. For various magnitude earthquakes, differential fault displacements are estimated with corresponding expected damage factors for both subsurface and surface structures.

For a probabilistic seismic hazard and risk analysis in an area with well understood faulting mechanisms, the differential ground displacement model proposed by Kiremidjian (1984) is ideal for estimating fault rupture hazard. However, for a deterministic seismic hazard and risk analysis on a regional basis, the simplified

procedure of defining specific buffer zones around an active fault and then estimating the corresponding differential displacement for the given faulting mechanism and various earthquake magnitudes (Applied Technology Council, ATC-13, 1985) is often adequate. This methodology may be too conservative in that the buffer zone is typically defined for the entire length of the active fault when in reality only a portion of the fault will rupture in an earthquake. For a scenario earthquake of given size and location, this methodology and the corresponding estimated damage factors for subsurface and surface structures provide and effective means of quantifying the local site effects of fault rupturing.

The seismic hazard associated with surface fault rupture is typically limited to a narrowly banded region, therefore this local site effect has received much less attention than liquefaction or landslide in earthquake engineering research. Public ordinances, such as the Alquist-Priolo Special Studies Zone Act of 1972 that restricts new construction with 50 feet of an active geologic fault in California, have reduced the regional risk associated with surface faulting. Most of the research in fault rupture hazard has been concerned with the risk to extended lifeline structures, such as highways, buried pipelines, bridges, tunnels, and canals, that unfortunately must sometimes cross active fault zones.

2.2 Seismic Damage Estimation of Gas pipeline and Water pipeline

Quantitative studies on seismic damage for Gas supply pipelines in Bangladesh are not available. Although the strength of the pipeline materials is not particularly different from that of the pipeline materials in other countries, it is considered that the construction quality of the joints always leads to problems. Damage of Gas pipeline system and water supply system of Bangladesh can be analysed based on some recent damage functions developed for different Gas line systems during Chi-Chi (or called Ji-Ji) earthquake in Taiwan (2002).

After the 1999, Ji-Ji Earthquake, more comprehensive pipe damage data were collected in Taichung City and a more detailed analysis was made to examine the relationships between earthquake forces and the resulting damage (Chen et al, 2002).

In order to perform analysis, the study area is divided into 1 km* 1km grid with pipelines enclosed in the grid, and the damage locations. For each group of pipelines, the damage ratio (DR) that is also denoted as the repair rate (RR) was calculated by dividing the numbers of damage by the total length of Gas pipelines in each grid.

Pipeline is divided into two groups according to their diameters, namely pipelines as with diameters 25 mm and 50 mm are classified as small pipelines in this study. The pipeline with diameters 75 mm, 100mm and 150mm is classified as medium pipelines in this study. The total length of the pipelines 106.4365 Km with 70.4257 Km in the small category pipeline and 36.0108 Km in the medium category pipeline.

During Ji-Ji earthquake, the time of histories of ground accelerations indicated that the component in the east-west direction was the largest. The peak ground acceleration (PGA) values at the center of each grid were calculated using linear interpolation. The resulting RR and PGA pairs were then grouped into 5-8 intervals to arrive at representative RR and PGA values for each interval. The intervals were used in the following regression analysis. The results were shown in Figure 2.11. It can be seen that the regression lines for three different diameters followed a general trend, which was similar to that, obtained in the Northridge earthquake by Toprak (1998).

The peak ground acceleration (PGA) is an acceleration that occurs on ground surface level due to hard bed rock shaking. The value of PGA for a specific location is the combination of magnitude of the earthquake; various soil properties like liquefaction, land sliding; fault line; distance from epicenter etc. The value of PGA expressed in g (gravitational acceleration) and the unit is cm/sec^2 or m/sec^2.

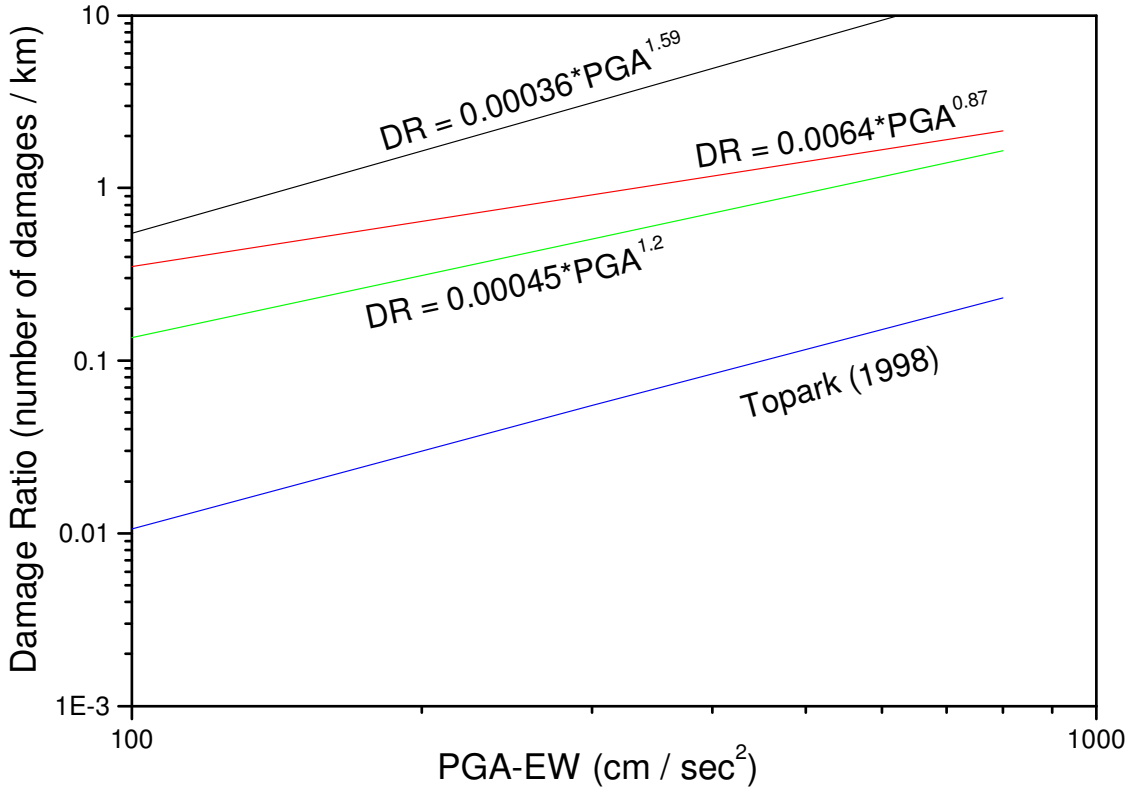

Figure 2.11 The correlation between Damage Ratio and PGA values for Pipeline diameters (after Cheng et al., 2002)

However, the analysis of Toprak was made on Mild steel pipes of Gas distribution systems. Still, the RR of the natural gas pipelines (mostly steel pipes and PE pipes) of Taichung City was higher than those of Toprak's analysis. For the three groups of pipelines analyzed in this study, empirical damage Relations with respect to PGA is as follows:

$$DR = 0.00036 * PGA^{1.59} \quad \text{for } \varphi \leq 65 \text{ mm} \tag{2.13a}$$

$$DR = 0.0064 * PGA^{0.87} \quad \text{for, } 65 \text{ mm} < \varphi < 150 \text{ mm} \tag{2.13b}$$

$$DR = 0.00054 * PGA^{1.2} \quad \text{for, } \varphi \geq 165 \text{ mm} \tag{2.13c}$$

Where φ is the pipeline diameter, PGA is peak ground acceleration (cm/s^2).

Damage data analysis of water pipelines:

Similarly, a damage analysis of water pipelines was conducted on Wufeng Shiang, a village located at the southern end of Taichung County. The results were as follows;

$$DR = 49.90 * PGA^{0.39} \quad \text{for } 20 \leq \varphi \leq 50 \text{ mm} \tag{2.14a}$$

$$DR = 3.97 * PGA^{4.54} \quad \text{for } 65 \leq \varphi \leq 600 \text{ mm} \tag{2.14b}$$

Where φ is the pipeline diameter, PGA is peak ground acceleration (cm/s^2).

2.3 Earthquake Damage and Loss Estimation

2.3.1 Structural Inventories

The development of a complete and detailed inventory of structures is typically the most crucial, time consuming, and expensive component of a regional seismic risk analysis. The accuracy of the final regional estimates of damage and loss is highly dependent upon the accuracy of the underlying structural inventory developed for the area. Although the accumulation of inventory data on a structure-by-structure basis would produce the most accurate inventory, this method is neither practical nor feasible for a regional study. The most widely used methods typically involve a consolidation of the information contained in various existing structural inventory databases. Vasudevan, et al. (1992) developed a methodology for compiling an integrated inventory of buildings and Rentzis, et al. (1992) applied this methodology to the development of a building inventory based primarily on the Tax Assessor's database for the city of Palo Alto, California. French, et al. (1991) presents a thorough discussion of building inventory development, including an overview of existing data sources and schemes for classifying buildings. Emmi and Horton (1993) developed an inventory of residential and commercial buildings in Salt Lake Country, Utah for use in an earthquake property damage and casualty risk analysis. The Applied Technology Council (ATC-25, 1991) compiled an inventory of all major lifelines in the United States from information in various government databases.

These and other regional earthquake damage and loss studies have typically involved structural inventory development for one specific type of facility, such as residential and commercial buildings, water systems, highway bridges, government buildings, and emergency facilities. One of the major components of the work presented in this thesis is a methodology for compiling a complete and detailed structural inventory for all facility types, particularly for a regional damage and loss assessment utilizing geographic information system technology. Structural inventory development typically involves four major parts: (a) identification of required inventory information or database attributes; (b) acquisition and review of available data sources; (c) development of engineering classification schemes; and (d) integration and compilation of the complete inventory. The remainder of Section 2.4.1 discusses these four issues and an example illustration of this methodology for regional structural inventory development is presented in Chapter 5.

2.3.1.1 Required Inventory Information

The information to be included in a structural inventory often depends upon the classes of facilities under consideration and the type of analysis being conducted. For the most general regional seismic hazard and risk analysis, information about the location, use, and structural properties of each facility is typically desired. Several studies have discussed characteristics of structural inventories in detail (Applied Technology Council, ATC-13, 1985, Rentzis, et al, 1992, Vasudevan, et al., 1992, and French, et al. 1991), therefore only a brief overview of the desired inventory information is given in this section. Even for a small region, the databases of structural inventory information can quickly become very large, resulting in excessive computer storage and inefficient analyses. For this reason, the number of included data attributes should be kept to a minimum through the use of several inter-related database tables in the inventory compilation methodology.

The data attributes most commonly required for a structural inventory include:

a) **Location Attributes**. Information such as street address, longitude and latitude, and Post Code number, used in determining the ground shaking and other local site effects to which the structure may be subjected.

b) **Use Attributes**. Information such as a use code or social function class (Applied Technology Council, ATC-13, 1985), used in determining losses (replacement or repair cost, loss of business use, casualties, and other socio-economic effects).

c) **Structural Property Attributes.** Information such as construction material, type of framing system, age, height, square footage, length, and present condition, used to determine the engineering classification (Applied Technology Council, ATC-13, 1985) or indicated the expected structural damage for a given shaking parameter.

The available databases for compiling an inventory of structures can often be incomplete, out-dated, inaccurate, or available only in paper format. The compilation of a complete and accurate structural inventory typically requires the integration of several existing databases of information from various public and private sources. Missing attributes are often inferred from known data by use of expert opinion or fuzzy logic. Recent advances in computer software technology, namely geographic information systems, relational database management systems, and expert systems have increased the efficiency and accuracy of structural inventory development. Section 2.3.1.2 describes the various available databases and Section 2.3.1.3 discusses the inference of missing attributes, primarily the assignment of earthquake engineering and social function classifications. Finally the integration and consolidation of information for a complete and accurate inventory of structures, including the use of geographic information system technology, is addressed in Section 2.3.1.4.

2.3.1.2 Sources of Inventory Data

There are numerous available databases for inventory development that vary greatly in completeness, accuracy, and type of included information. The use of these databases can result in large reductions in the time and cost associated with developing a complete inventory of structures for a region. The databases most commonly used as sources of inventory data include: (a) Central Government Databases; (b) Local Government Databases; and (d) Private Sector Databases. Only a brief overview of these four sources of inventory data is given below, as several studies have provided detailed reviews of the various available databases, including their data attributes, area of coverage, accuracy, completeness, cost to obtain, media format, and frequency of update (see Applied Technology Council, ATC-13, 1985, French et al. 1991, Vasudevan, et al. 1992, and Rentzis, et al. 1992).

a) **Central Government Database.** Two Common sources of data are the Survey of Bangladesh (SoB) and BBS. Currently CDMP (2009) maintains numerous databases of information for various facilities and various business sectors on the national, state, and local levels. The BBS has databases of population, housing, economics, and linear features for various geographical areas.

b) **Local Government Databases.** These are often the most commonly used and include such sources as City corporation/pourasabha Tax Assessor's file, the various databases maintained by Ward level offices, the public utilities databases of lines and other equipment, the county and city building permit files, and other databases containing regional information about facilities such as police stations, hospitals, fire stations, and emergency broadcast stations.

c) **Private Sector Databases.** Several private companies and agencies have compiled databases of information on various facilities for specific purposes. Examples of these include the Insurance Services Office's files of large buildings for fire risk assessment, the Real Estate Multiple Listing of property currently for sale, the private utilities databases of lines and other equipment, and several databases developed from satellite imagery processing.

2.3.1.3 Classification and Inference Schemes

Prior to the development of an inventory of structures, two classification systems are typically required. One system classifies each structure according to its structural response to earthquake excitation for purposes of regional damage estimation. The second system classifies each structure according to its use and provides for the regional estimation of monetary and non-monetary losses. Almost every study of regional damage and loss assessment has developed definitions for these two classification systems. The most widely used are the Earthquake Engineering Facility Classification and the Social Function Classification developed by the Applied Technology Council (ATC-13, 1985) for all facility types in California. Although these definitions are for a specific region, they are very comprehensive and can easily be modified for use in other regions as illustrated in the case study presented in Chapter 5.

The use of existing databases for inventory development typically requires the application of expert systems or fuzzy logic for inferring missing data attributes and for assigning the two classifications discussed above. These classification and inference rules are highly dependent upon the content and format of the inventory data sources and the expert knowledge about the history and current state of structural development in the study region. Rules for inferring missing data attributes and assigning classifications are often based either upon statistical relationships developed in nearby regions or upon the opinions of experts in the area. The use of secondary data sources with broad regional averages is another means of inferring database information. Occasionally there is not enough known information to make an exact data inference, therefore a rule may assign probabilities or weights to inferred data. Examples of three basic types of classification and inference rules are listed below. The case study presented in Chapter 5 illustrates the use of similar rules in the development of a regional inventory of structures.

(a) Example rule for inferring missing data attributes:
IF (Code number = 1001 and material = wood)

THEN (date built = 1970)

(b) Example rule for assigning earthquake engineering classification:

IF (use = residential and data built < 1950 and number of stories = 1)

THEN (engineering class = unreinforced masonry)

(c) Example rule for assigning social function classification:

IF (date built > 1980 and number of stories = 2 and material = light metal)

THEN (social function class = 50% light industrial and 50% heavy industrial)

2.3.1.4 Inventory Compilation Methodology

The previous sections of this chapter have given a brief overview of the various aspects of regional inventory development including the required information, the sources of data, and the classification and inference schemes. This section describes a methodology for integrating and combining the various available data sources in order to develop a complete regional inventory of structures. Integrations methodologies have been developed for building inventories by French, et al (1991), Vasudevan, et al. (1992), and Rentzis, et al. (1992), and for lifelines by the Applied Technology Council (ATC-25, 1991). Very few studies have considered the development of a complete and accurate inventory of all facilities for a regional earthquake damage and loss estimation (Applied Technology Council, ATC-13, 1985, Massachusetts Civil Defence Agency, 1991).

The methodology for compiling a regional inventory of all facilities depends upon the contents and format of the available sources of data. It is assumed that the inventory is for a large region in which several electronic databases of various structural information already exist, therefore the use of field survey techniques is considered only as a last resort for certain facility types. Several inter-related database tables of facility characteristics are used to describe the regional exposure to earthquake damage and losses. The use of inter-related tables helps to reduce the large amount of required data storage by eliminating repeated attributes through the use of relational identification numbers or indexed values.

Figure 2.12 shows a simplified example subset of database tables in a final inventory of structures. A more though example of the integration methodology as well as the use of

the inventory in a regional earthquake loss estimation is illustrated in the case study presented in Chapter 5. The basic steps in compiling a regional structural inventory, such as that shown in Figure 2.12, include:

(1) Determine the data attributes to be included in each table and the interaction among the various database tables in the final structural inventory.

(2) Determine the use or social function classification to be used in the inventory.

(3) Determine the structural or earthquake engineering classification to be used in the inventory.

(4) For each major social function class defined in Step (2), identify and acquire the first and second level sources (based on completeness and accuracy) of available database information.

(5) Analyze the available database information in each source and consult local experts to define heuristic rules for inferring minor social function classifications, earthquake engineering classifications, and missing data attributes.

(6) Apply the rules defined in Step (5) for each first level source identified in Step (4) to fill in the final inventory tables defined in Step (1).

(7) Apply the rules defined in Step (5) for each second level source identified in Step (4) to check the accuracy of the information contained in the final inventory tables for each major social function class. This check is typically done by one of the following three methods:

(a) Geographic Location: A geographic information system allows several sets of database information to be mapped and overlaid for identification of data discrepancies. A GIS can also be used for address matching and for the application of inference rules that may involve spatial instead of tabular data manipulations.

(b) Regional Averages. Existing databases of broad regional averages can be used to identify areas that appear to be missing or over-estimating data.

(c) Expert Opinion. Local experts familiar with the history and current state structural development in the region can help to identify possible data errors.

(8) Determine if the desired level of accuracy and completeness has been achieved for the final inventory of structures. If not, identify those major social function classes requiring further inventory development and either repeat steps (4) through (7) with alternative existing databases (third and fourth level sources), or utilize field survey techniques to compile the final inventory.

2.3.2 Damage Distributions

Methods for estimating regional distributions of earthquake damage to buildings, bridges, dams, utility systems, and other man-made structures have been the subject of extensive research over the past several decades (Rojahn, 1993). Reitherman (1985) provides a detailed review of over thirty earthquake damage estimation methods. Damage assessment for a region typically depend upon three factors: (a) the level of seismic hazard in the region, including the effects of local site conditions; (2) the distribution of facilities in the region, according to earthquake engineering class; and (3) the definition of functions that relate the expected levels of damage for the various earthquake engineering classes to the estimated levels of seismic hazard. The estimation of regional seismic hazard, including local site effects, was discussed in Section 2.2, and the previous section of this chapter covered earthquake engineering classification and the development of an inventory for describing the regional distribution of facilities. The purpose of Section 2.4.2 is to provides an overview of the procedure for estimating regional damage distributions in the GIS environment. There are several definitions for damage and also several relationships for estimating damage due to given levels of seismic hazard for various facility types, therefore a brief overview of these two topics is also included in this section.

2.3.2.1 Definitions of Damage

There are several parameters used to express earthquake damage and terms such as "damage ratio", "damage factor", and "damage index" have different meanings to different authors. Regional damage can be given, for example, in percent financial loss or percent of structures damages to a certain degree. Damage to a given structure can be described in terms of damage to the individual elements, often based on dynamic response measures. The term "damage index" is typically taken to mean the characterization of individual element (local) or entire structure (global) damage based on response parameters such as ductility ration, inter-story drift, and dissipated energy (see Park and Ang, 1985 and Chung, Meyer, and Shinozuka, 1987). These indices are generally too structure specific to be considered for regional damage description, therefore they will not be discussed in the remainder of this thesis. The term "damage ratio" is typically defined as (Applied Technology Council, ATC-13, 1985):

$$\text{Damage Ratio (DR)} = \frac{number\ of\ structures\ damaged}{total\ number\ of\ structures} \tag{2.15}$$

The level of damage required for a building to be considered "damages" is often ambiguous, and this type of ration can typically be derived from other estimates of regional damage, therefore this damage measure will not be further discussed.

The most widely used measure of earthquake damage is an expression of damage in terms of percent financial loss that can be applied to all types of structures (Rojahn, 1993). This measure is typically given the name "damage factor" and is defined as (Applied Technology Council, ATC-13, 1985):

$$\text{Damage Factor (DF)} = \frac{dollar\ loss}{replacement\ cost} \tag{2.16}$$

The definition of damage will be used throughout this thesis. The methodology for applying GIS technology to regional damage estimation, however, is intended to be general, allowing the use of any damage definition.

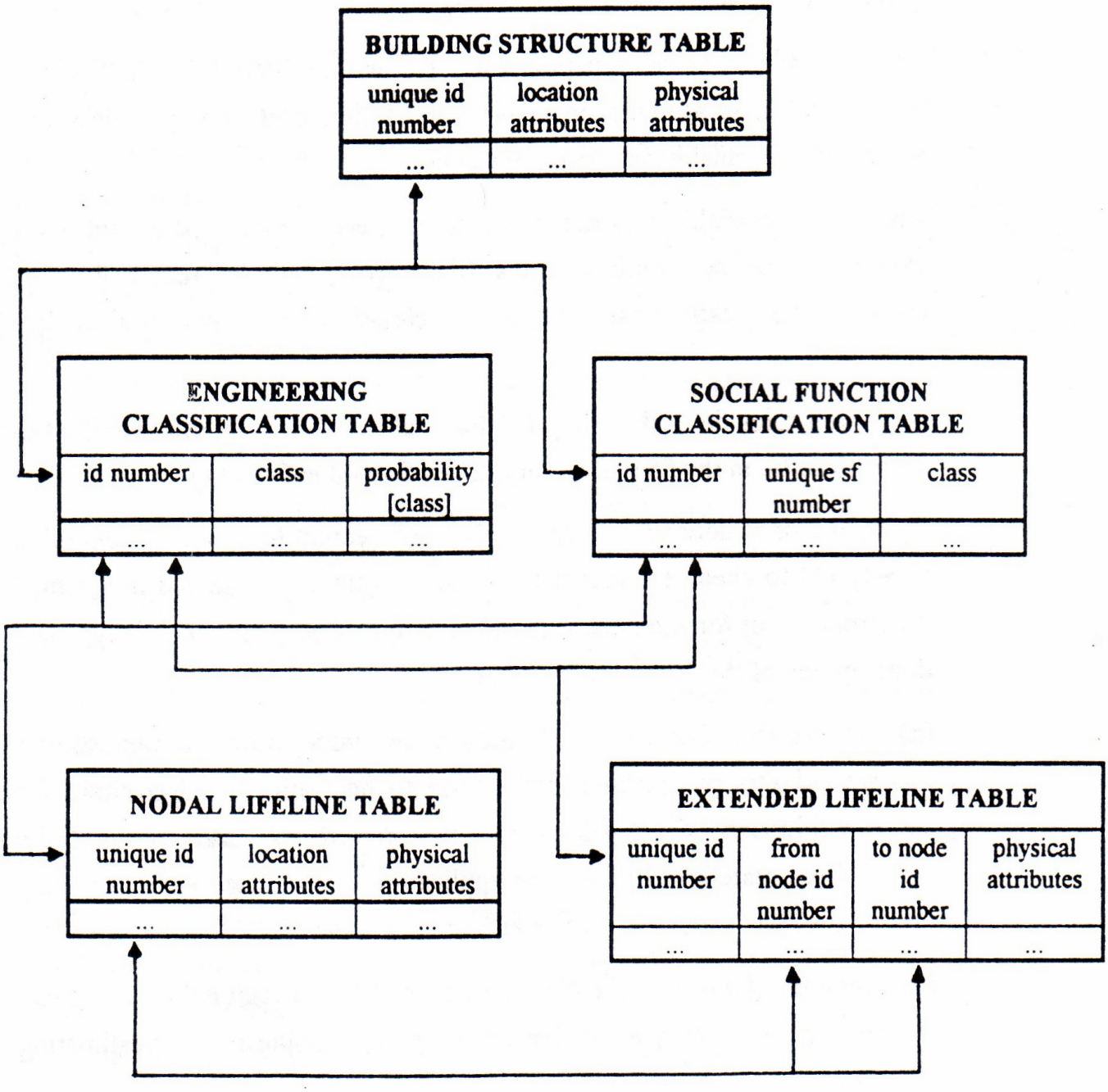

Figure 2.12 Example inter-related database tables in a structural inventory (from Applied Technology Council, ATC- 36).

2.3.2.2 Motion-Damage Relationships

Motion-damage relationships are used to estimate earthquake damage for each facility type due to various levels of ground shaking. These relationships, also known as vulnerability functions, are typically expressed in terms of (Kiremidjian, 1992).

(1) Damage-Loss Curves. These relationships, shown in Figure 2.13, were developed by Algermissen and Steinbrugge (1994) for use by the Insurance Services Office. They estimate mean damage ratios (number of damages buildings divided by the total number of buildings in a region) as a function of ground shaking intensity for various building types.

(2) Fragility Curves. These curves (Kircher and McCann, 1983) describe the probability that a specified damage level will be exceeded for a given intensity of ground motion. The curves are typically developed for all facility types in the general form:

a. $p\{D \leq d|Y\} = 1 - F_{D|Y}(d|Y)$ (2.17)

where:

D, d = damage level

Y = ground motion intensity

An example of these curves is shown in Figure 2.14.

(3) Damage Probability Matrices (DPM). These matrices, first introduced by Martel (1964) and later modified by Whitman (1973), describe the probability that a structure is in a specified damage state given the level of ground shaking intensity. In ATC-13 (Applied Technology Council, 1985), they are derived from the probability distribution of damage given ground shaking intensity, $f_{D/Y}(d/Y)$, where D, d, and Y are defined as in equation 2.17, illustrating the analyst rating the analytical relationship between DPMs and fragility curves. A Beta distribution is frequently used to describe to uncertainty in damage for a given ground shaking intensity. An example of one of the 78 DPMs developed by the Applied Technology Council (ATC-13, 1985) for facilities in California is shown in Table 2.4.

(4) Expected Damage Factor Curves. These curves are just another representation of the relationship between damage and ground shaking intensity that can be used to drive DPMs and fragility curves. There is no difference in the information that is conveyed or can be obtained through the use of fragility curves, DPMs, and expected damage curves. Provided that the parameters (λ,v) of the Beta distribution $f_{D/Y}$ (d/Y) are known, the expected value and standard deviation of damage (in this case, damage factor or percent financial loss) for each level of ground shaking intensity can be computed as follows:

$$E[D/Y] = 100\frac{\lambda}{\lambda + v} \quad \text{in \%} \tag{2.18}$$

$$\sigma_{D/Y} = 100\frac{\sqrt{\lambda v}}{(\lambda + v)\sqrt{(\lambda + v + 1)}} \quad \text{in \%} \tag{2.19}$$

An example curve, corresponding to the DPM illustrated in Table 2.4, is shown in Figure 2.15.

For the illustration of regional damage estimation in the GIS environment, the motion-damage relationships will be described in terms of expected damage factor curves, the amplest of the four representations discussed above, although the methodology is intended to be general enough to allow extension to more complex motion-damage relationships. As briefly discussed in Chapter 3, the regional seismic hazard in this thesis is quantified in terms of the Modifies Mercalli Internsity (MMI) scale. Although this subjective scale has many drawbacks, it has traditionally been used in the motion-damage relationships of most major earthquake loss studies (Rojahn, 1993). Current research is focusing on the development of vulnerability functions based on other less subjective ground motion parameters.

Table 2.4 Damage probability matrix for low-rise wood-frame buildings (after ATC-13, 1985)

Damage State	Damage State	MMI VI	MMI VII	MMI VIII	MMI IX	MMI X	MMI XI	MMI XII
1	0	3.7	-	-	-	-	-	-
2	0-1	68.5	26.8	1.6	-	-	-	-
3	1-10	27.8	73.2	94.9	62.4	11.5	1.8	-
4	10-30	-	-	3.5	37.6	76.0	75.1	24.8
5	30-60	-	-	-	-	12.5	23.1	73.5
6	60-100	-	-	-	-	-	-	1.7
7	100	-	-	-	-	-	-	-

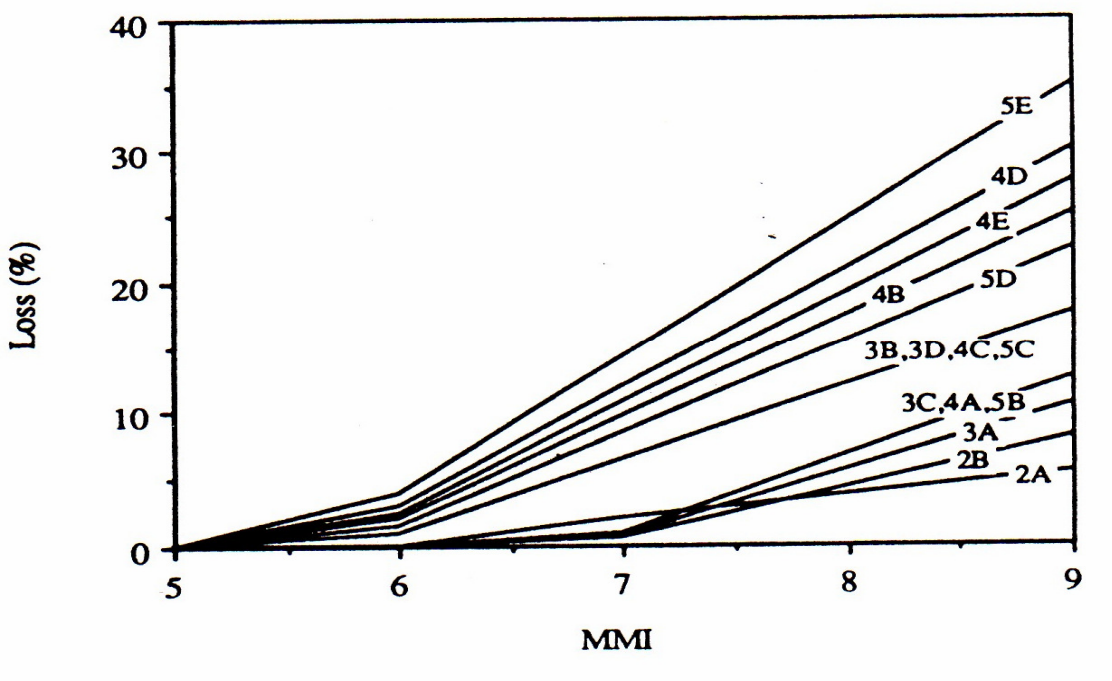

Figure 2.13 Example damage-loss curves for different building construction classes(from Algermissen and Steinbrugge, 1984)

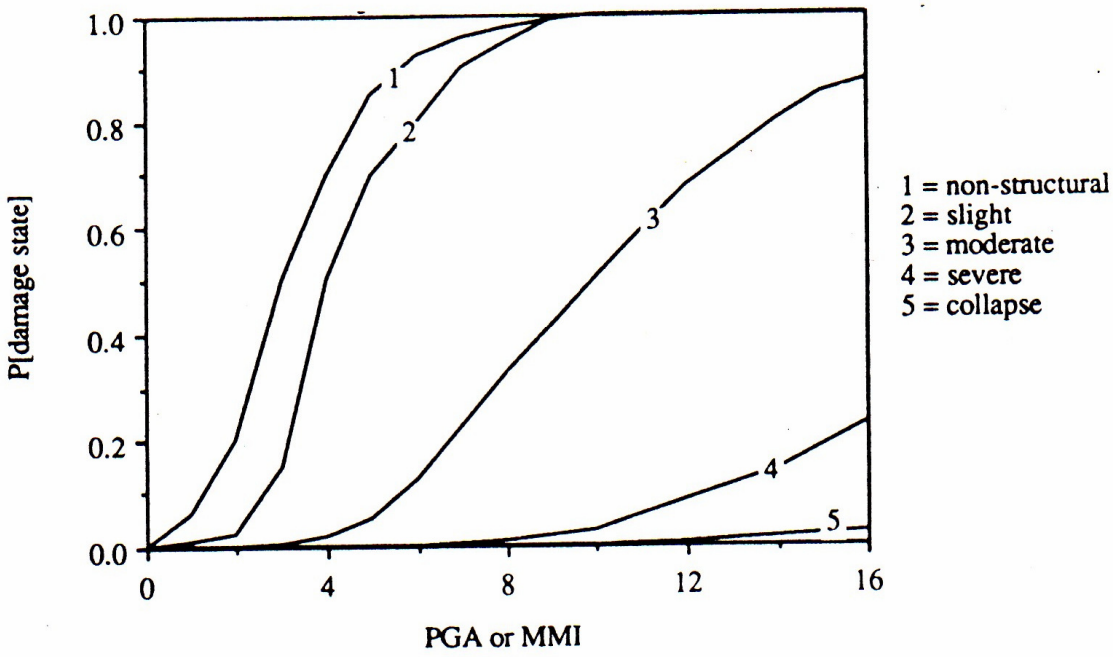

Figure 2.14 Example Fragility curves (from Kircher and McCann, 1983)

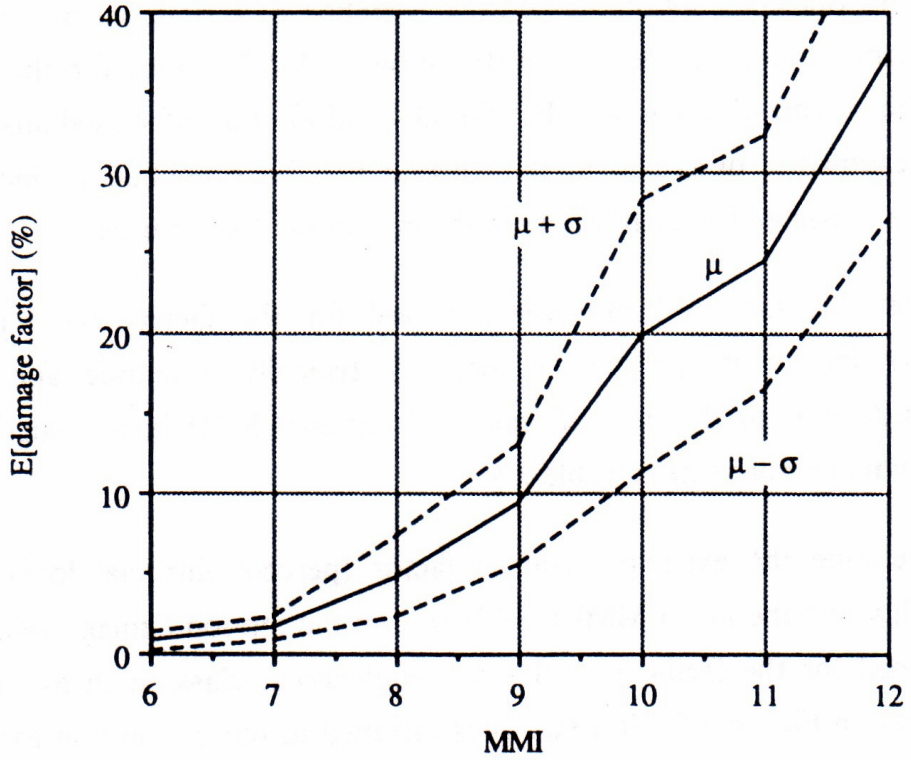

Figure 2.15 Expected damage factor with standard deviation as a function of MMI for low-rise wood-frame buildings (from Applied Technology Council, ATC- 36).

2.3.2.3 Fragility Curves for Bangladesh

Fragility curves are used in the FEMA/NIBS methodology to estimate damage to buildings resulting from ground shaking (Whitman et al, 1997). The fragility curves predict the probability of reaching or exceeding specific damage states for a given level of peak earthquake response. The probability of being in a particular state of damage, the input used to predict the building related losses, is calculated as the differences between fragility curves.

Building fragility curves are log-normal functions that describes the probability of reaching or exceeding structural and non-structural damage states, given deterministic estimates of spectral responses, for example spectral displacement. These curves take into account the variability and uncertainty associated with capacity curves properties, damage states and ground shaking.

Fragility curves are used for estimation of damages of buildings in particular area. A number of fragility curves exist for Indian Buildings prepared by Arya (2000) and for Nepalese buildings prepared by Bothara et al. (2000). There also exist a number of fragility curves for different types of structure and for different earthquake intensities (Kircher et al., 1997; Fah et al, 2001; Yamazaki and Murao, 2000; Yamaguchi and Yamazaki, 2000; Bommer et al., 2002), but the Indian and Nepalese curves may be the most suitable for Bangladeshi structures, until Bangladeshi researchers develop their own fragility curves. In this study, fragility curves for the buildings in Dhaka were prepared by calibrating the existing fragility curves for Indian buildings prepared by Arya (2000) and for Nepalese buildings prepared by Bothara et al. (2000). Neither Arya (2000) nor Bothara et al (2000) mentioned the types of damages (i.e., collapsed or heavily or moderately damaged) to be estimated using those fragility curves. Segawa et al. (2002) used those curves after some calibration and quoted those curves to be developed for heavily damaged structures. Figure 2.16 shows the fragility curves modified from Arya (2000) and Bothara et al. (2000).

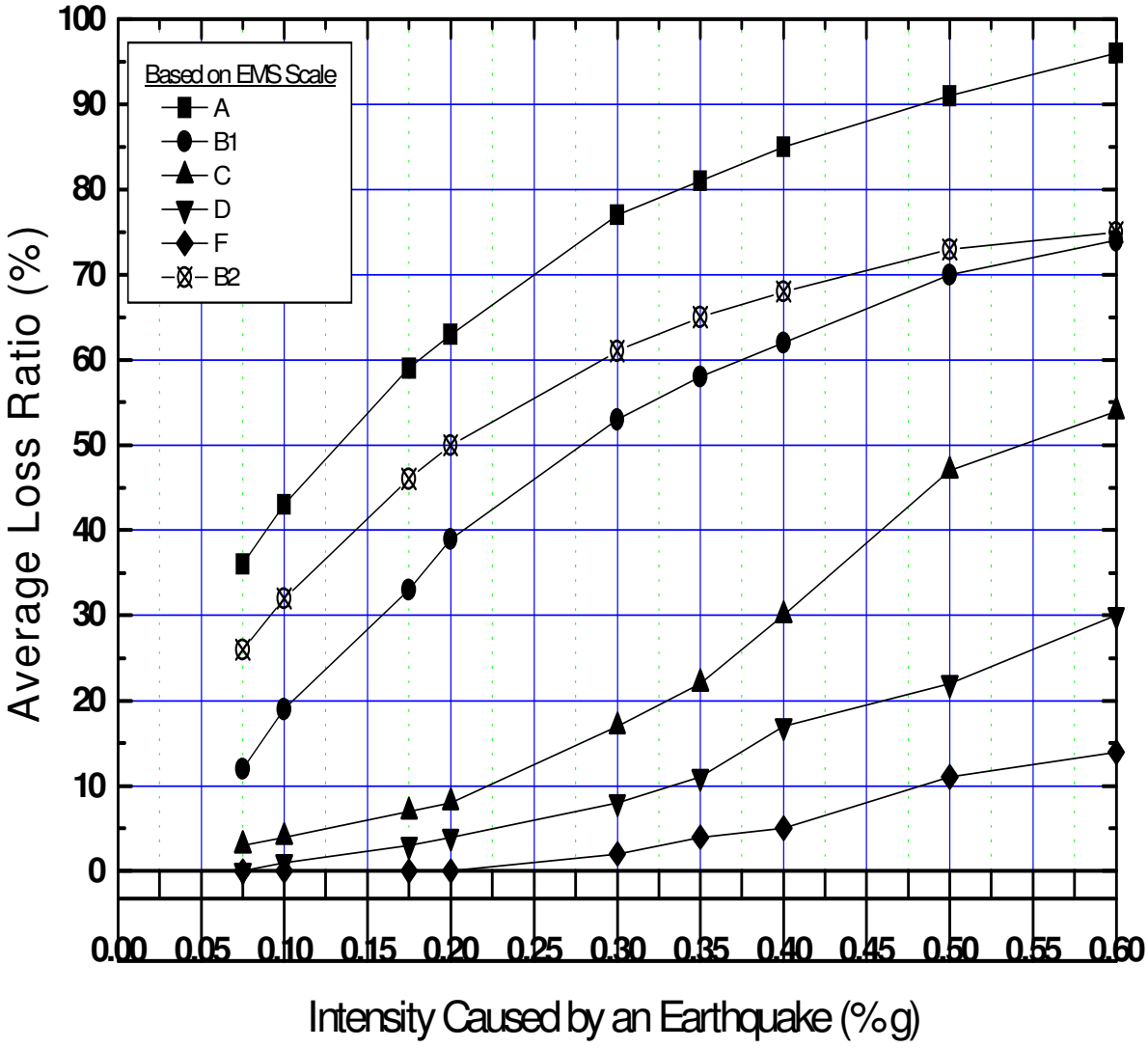

Figure 2.16 Vulnerability functions based on peak ground acceleration (after Arya, 2000)

2.3.3 Morbidity Model

In order to assess the human casualty levels due to the earthquake, the estimates of average fatality and injury levels have been used. These figures have been derived by using a mortality prediction model for different categories of structures. This prediction model is based on investigation of casualty due to several major earthquakes that have occurred during last century (Coburn et al., 1992). The total number of people that may be killed due to damage of each building type can be represented by:

$$Ksb = Db*[M1b * M2b * M3b * M4b] \quad (2.20)$$

where Db is the total number of damaged household of type b, M1 is the occupant density and M2 to M4 are conditional probability factors to modify the potential casualty figures. The factor M1 represents the population per household.

The factor M1 represents the population per household. M2 is the occupancy of buildings at the time of earthquake. The occupancy cycle proposed by Coburn and Spence (1992) was presented in Figure 2.17 for residential and business structures. Depending on the time of the earthquake, the occupancy rate can been found from this figure.

M3 is the proportion of occupants who are trapped by collapse of buildings. This depends on the type of building. M4 is the proportion of occupants who are either killed or injured in the earthquake. It was observed that collapsed multi-storied masonry and reinforced concrete buildings lead to death of a large number of trapped occupants, while collapsed masonry buildings lead to death of relatively small number of trapped occupants.

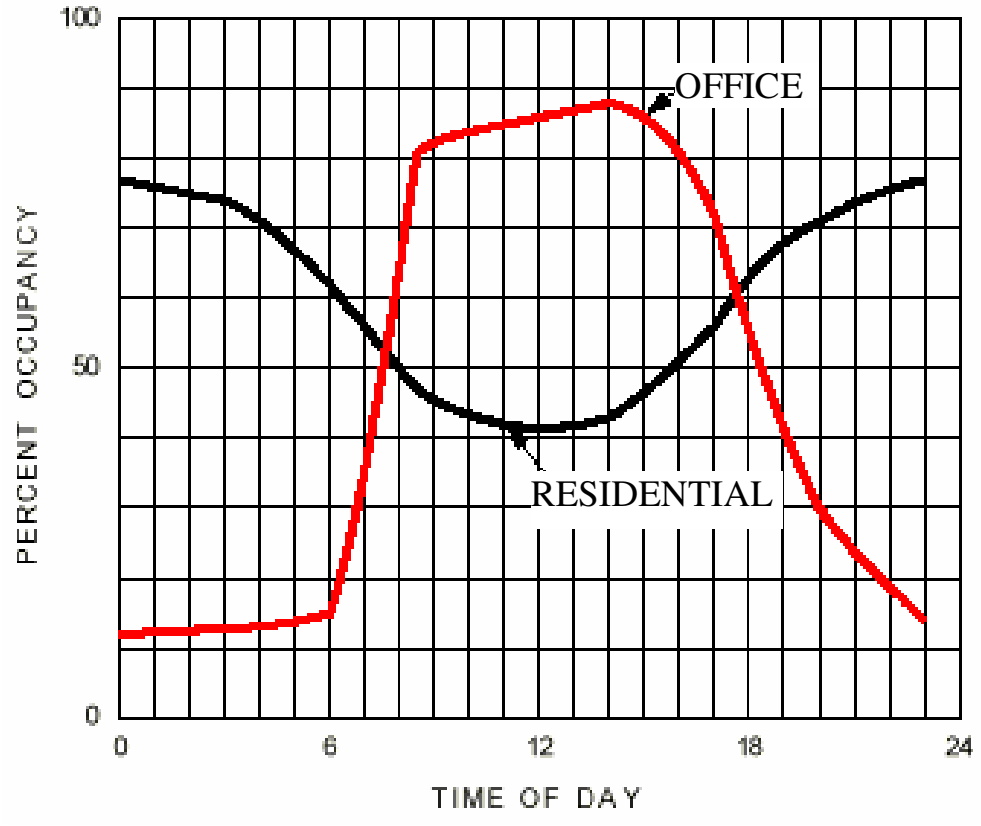

Figure 2.17 Building occupancy at the time of earthquake (Coburn et al., 1992)

2.3.4 Loss Distributions

Direct monetary losses due to earthquake damage in major metropolitan areas can run into the billion of dollars (Kiremidjian, 1992). For example, the 1989 Loma Prieta Earthquake is estimated to have caused a direct monetary loss of 5.9 billion dollars, with another 15% to 25% of this total due to indirect losses (ABAG, 1991). Steinberg, et al. (1981) estimate $62.2 billion (1980) dollars in direct property losses for the Los Angeles, California metropolitan area due to a magnitude 7.5 earthquake on the Newport-Inglewood Fault. The figures for non-monetary losses, such as casualties and homelessness, can be just as devastating. Since the beginning of this century, major earthquakes in the seismic regions of world have caused more than 1.25 million fatalities (Agbabian and Chilingarian, 1991). For example, the 1995 Kobe Earthquake, Japan

caused more than 6,000 casualties and left over 500,000 people homeless. Total loss was US $100 Billion.

Loss statistics such as these emphasize the importance seismic hazard and risk analysis for estimating earthquake losses for purposes such as emergency planning and hazard mitigation. Research on the topic of earthquake loss estimation has typically paralleled that of regional damage estimation, as losses are typically considered to be functions of damage. However, earthquake loss studies have often received more attention in the earthquake engineering community, typically because estimates of dollar loss and casualties are more easily understood than measures such as damage factors and damage ratios. Over the last century, the rate of fatalities per severe earthquake has not decreased despite our advances in technology, indicating the on-going need for research in the area of earthquake loss mitigation.

The estimation of regional damage distributions for an integrated inventory of structures was covered in the previous sections of this chapter. The purpose of Section 2.3.4 is to provide an overview of the procedures for using the estimated regional damage and corresponding structural inventory to predict both monetary and non-monetary loss distributions, particularly through the use of GIS technology. Chapter 5 presents a case study of a GIS-based regional earthquake loss analysis, illustrating the various methodologies that have been covered in this thesis, from estimating the levels of seismic hazard to forecasting the final losses.

2.4.4.1 Monetary Losses

Monetary losses resulting from an earthquake are typically due to: (1) direct structural damage, such as failed beams, excessive deflections, and differential settlement to man-made facilities; and (2) indirect effects, such as damage to non-structural elements and contents, clean-up and financing of repairs, and loss of facility use (down time). The Applied Technology Council (ATC-13, 1985) provides a good overview of the different types of monetary losses, as well as the widely-used methodologies for estimating them, therefore only a brief discussion of the two types of monetary losses listed above will be presented here.

Although there are several methods for estimating losses due to direct structural damage, most are computed as a function of the replacement cost of the facility and the estimated damage to the facility. For purposes of illustrating the application of GIS technology to regional loss estimation, a simple formula for computing the direct losses to a facility will be used and is given as:

$$E[\text{Loss}] = E[DF] \times (\text{replacement cost}) \quad (2.21)$$

where:

E[DF] = the expected damage factor estimated for the facility, defined in Section 2.4.2.1 as the ratio of the dollar loss to the replacement cost of the facility.

Replacement cost for a facility is typically computed as the product of the area or length of the replacement cost per unit area or length for the given facility type. Replacement costs are generally dependent upon the use or social function class of the facility and often vary for different study locations. Local experts in construction practices are often consulted to help develop tables of replacement costs for various facility classifications.
Indirect monetary losses are much more difficult to quantify than losses due to direct structural damage. Often the contents and non-structural components of facility are assigned a monetary value that is a given percentage of the total value of the facility based on the social function class of the facility. The damage factor for the contents and components is either assumed to be the same as that of the facility, or it is calculated through the use of one of the previously discussed motion-damage relationships developed specifically for contents and components. Monetary loss is then computed as the product of the damage factor and the replacement cost. Although this is an important and often sizable loss, the estimation is considered to be beyond the scope of this thesis and it will not be further discussed.

Other indirect monetary losses are typically due to clean-up, financing of repairs, and loss of business use. These socio-economic effects of earthquake damage are the subject of much current research in the economic community. Models for post-earthquake clean-up and financing have not been developed, but several methods for estimating loss of

business use, or down time, have been suggested (Applied Technology Council, ATC-13, 1985 and ATC-25, 1991 and Massachussetts Civil Defense Agency, 1989). Loss of business use for a facility is typically a function of two factors: (a) the social function class of the facility and (b) the damage factor computed for the facility due to the given earthquake event. Down time is then estimated based on opinions of experts in the field and expressed in one of the following two ways that can easily be derived from each other:

(1) The required time (in days) after the earthquake to restore the facility to a given level of service, typically defined as a percentage of the full functionality of the facility.

(2) The level of service (percentage of full functionality) of the facility at a given time after the earthquake.

Table 2.5 and Figure 2.18 illustrate the two representations of the down time discussed above for a facility use type defined by the Applied Technology Council (ATC-13, 1985). The extension from an estimation of down time to a monetary loss is a very complicated process that depends on numerous socio-economic factors currently under study. The interaction of various facilities in a region, such as the effect of the loss of lifeline use on the loss of business use in building served by those lines, is also assumed to be too complicated to be included in this thesis. For the purpose of illustrating regional earthquake loss estimation in the GIS environment, only those losses associated with direct structural damage and loss of business use will be considered. As previously discussed, GIS technology allows new models to be tested and compared and then added to the regional damage and loss analysis.

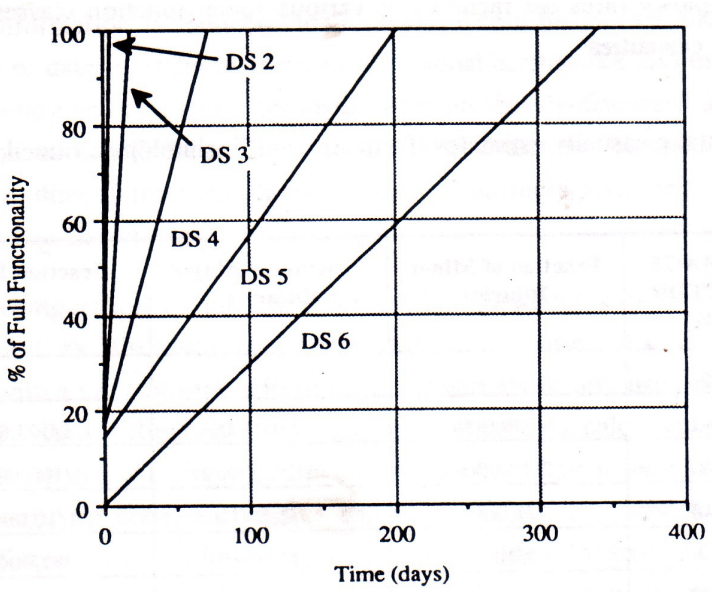

Figure 2.18 Percentage of functionality as a function of time following an earthquake for use class retail store (from Applied Technology Council, ATC-36)

2.3.4.2 Non-Monetary Losses

Non-monetary earthquake losses typically include fatalities, injuries, unemployment and homelessness. Earthquake-induced casualties have traditionally been a common research topic in the earthquake engineering community, although very few general quantitative models have been proposed. Casualty statistics from earthquakes occurring in the United States are typically very limited, and those from foreign occupancy. Earthquake casualty models are often developed from expert opinion, such as the model suggested by the Applied Technology Council (ATC-13, 1985). Although this model was developed for the state of California and has been criticized for being overly simplifies, it does provide a methodology for computing fatalities and injuries on a regional basis. Table 2.5 illustrates the model by providing estimates of deaths and injuries as a function of damage factor. This table is typically used in conjunction with a table of day and night occupancy rates for facilities of various social function classes to predict earthquake-induced casualties.

Table 2.5 Earthquake casualty estimates (from Applied Technology Council, ATC – 13, 1985).

DAMAGE STATE	DAMAGE FACTOR(%)	Fraction of minor injuries	Fraction of major injuries	Fraction Dead
1	0	0	0	0
2	0 – 1	3/100,000	1/250,000	1/1,00,000
3	1 – 10	3/10,000	1/25,000	1/100,000
4	10-30	3/1,1000	1/2,500	1/10,000
5	30 – 60	3/100	1/250	1/1,000
6	60 – 100	3/10	1/25	1/100
7	100	2/5	2/5	1/5

Models for the other non-monetary earthquake losses, such as homelessness and unemployment, have not been fully developed as these effects as these effects depend on several factors that are typically difficult to quantify. Casualties will be the only non-monetary earthquake loss treated in this thesis, but future inclusion of other socio-economic models in the GIS-based regional analysis is anticipated. The final section of Chapter 4 presents a brief illustration of the application of GIS technology for estimating regional earthquake losses due to direct structural damage, loss of business use, and casualties. The case study in Chapter 5 provides a detailed illustration of regional earthquake damage and loss evaluation in the GIS environment.

2.4 Attenuation of earthquake ground motion

Attenuation equations are basically intended to predict or estimate the ground motion intensity at a place where the ground motion is not recorded. It is widely accepted that the felt intensity of the ground motion is a convolution of effects due to the source, path, and local site. Models to predict the ground motion at a given site can be classified into the analytical and empirical types.

Analytical Models

The study of attenuation of ground motion has been exclusively mainly due to the large uncertainties involved in the convolution. However, as methods for direct analytical computation are developed in conjunction with the availability of powerful yet affordable computers, more and more researchers are using analytical techniques.

To models the release of energy from the earthquake source a realistic model of the rupture process must be determined. The rupture is assumed to start at the hypocenter and travels through the affected fault. An assumption on the velocity of the rupture and amount of slip for each point in the fault surface must be made. Current seismic inversion methods estimate the slip amount and direction from recorded ground motion away from the fault (Kanamori, 1971; Wald and Somerville, 1994). Various models have been proposed to represent the fault rupture process. The fault is normally assumed as finite and is divided into smaller segments with each segment assigned a slip amount and direction. The slip can be modeled as uniform (Haskell, 1964), non-uniform (Papageorgiu and Aki, 1983) and the rupture velocity can be modelled as random in time and space to produce an incoherent source model (Koyama, 1985).

The amplification of ground motion from base rock to surface can be computed by theoretical wave propagation techniques, e.g., the one-dimensional shear-wave theory, if the stratification of soil layer at the site is known or assumed.

Advantages and disadvantages of analytical methods

Analytical methods are useful because present knowledge about the characteristics of the source, path, and site can be incorporated in the analysis and the resulting ground motion is site- and source-specific. However, there are still a significant amount of uncertainties in the modeling of the source, path, and site effects. This is compounded by the fact that it is impractical if not impossible to physically verify these assumptions. For recent events, there are methods to estimate these parameters since reliable records exist. However, most events in the past do not and it becomes difficult to estimate the source parameters.

Since analytical methods use a large number of parameters, it becomes more difficult to use directly in seismic hazard analysis since it is hard to describe how these parameters will behave in future earthquakes. Generally, if the fault-rupture process is known or can be assumed, it is much better to use analytical methods to describe the ground motion expected at the site. However, if the fault-rupture process is unknown (i.e., for future events), empirical methods may be more practical.

Empirical models

The parameters most often used to describe the attenuation of ground motion are the magnitude and source-to-site distance (Joyner and Boore, 1981; Campbell, 1985). Regression from observations is performed to estimate coefficients that represent the source and path effects. In the past, regression were performed separately for each ground condition to account for the site amplification effects (PWRI), while it is now common to use dummy variables to determine the effect of amplification of soil sites. However, researcher have used several definitions of the magnitude, distance, and even the ground motion intensity considered, making comparison of results more difficult (Boore and Joyner, 1981; Ambraseys, 1990; Kawashima et al., 1983; Ansary et al, 1994).

The magnitude scale used is more dependent on the convenience/availability of the data although conversions from one magnitude scale to another has been done (Fukushima and Tanaka, 1990; Ambraseys, 1990) to be able to use more data in the regression. The effect on the regression seems to be minimal as long as only one magnitude scale is used throughout the analysis. Currently, the preferred magnitude scale is the moment magnitude, MW, because it is directly related to the size of the activated fault and it is the only magnitude scale not affected by saturation. However, available information about past earthquakes may not be enough to estimate the moment magnitude of these events.
The definition of source-to-site distance has a much more profound effect on the regression, especially at close distances. The definitions of distance used are the epicentral distance, hypocentral distance, closest distance to the surface projection of the fault, closest distance to the fault plane, distance to the center of energy release, distance to the center of activated fault. For large events involving large dimensions of the

activated fault, the location of where the strong motion is released may be very far from the hypocenter. For sites near the fault the use of improper distance may lead to large errors in the regressions analysis. Ohno et al. (1993) have shown that by adjusting the distance based on the fault parameters, the attenuation in the near field can be described by the attenuation in the far-field.

Attenuation at near field

Mainly due to the lack of adequate data, attenuation equations have been limited to the far field region. As strong motion data are gathered near the fault region, new attenuation studies are performed. Campbell (1981) used a weighted regression methodology to reduce the bias caused by the fact that the near source data was recorded from a small number of events and to include important data from other regions.

In Japan, earthquakes are mostly from subduction zones and a large number of epicenters are in the sea. Consequently, near field records are quite few. Fukushima and Tanaka (1990) supplemented the Japanese data with data from Campbell (1981) in order to have enough data in the near field.

Regression model based on physical considerations

Joyner and Boore (1981) introduced the used of an attenuation model that has a physical basis. It is based on the theoretical attenuation of body waves traveling through an elastic medium. The attenuation model considers geometric spreading and anelastic attenuation. This basic model has been used by several researchers (e.g., Fukushima and Tanaka (1990), Ambraseys and Bommer (1991), Ohno et al (1993), Yamazaki (1993)).

Two-stage regression

Joyner and Boore (1981) also introduced a two-stage regression procedure to separate the determination of the magnitude dependence from the distance dependence. Fukushima and Tanaka (1990) showed that due to the correlation between magnitude and distance of the data set, a systematic error is introduced in the regression procedure. They showed that using two-stage regression can effectively eliminate the systematic errors. This is

done by using dummy variables for each earthquake in the first stage regression to determine the distance dependence. The resulting event terms are then used in the second stage regression to determine the magnitude dependence. Joyner and Boore (1981) used weights in the second stage regression; events with only one record are given zero weights; while others a weight of 1. Fukushima and Tanaka (1990) used the number of records for each event as the weight. Masuda and Ohtake (1992) showed that the correct weighting matrix should be non-diagonal since event terms are mutually correlated as a consequence of the fact that they were all determined from the first stage. They suggested that the inverse of the variance-covariance matrix of the event terms be used as the weighting matrix. Joyner and Boore (1993) derived the correct weighting matrix. They proposed that the inherent variablity of the event terms be included in the weighting matrix.

Random effects model

In their analysis of the attenuation data of Joyner and Boore (1981), Brillinger and Preisler (1985) suggested that the two-stage regression method proposed by Joyner and Boore (1981) is similar to the random effect model where the earthquake-to-earthquake component of the residual (and variance) is separated from the record-to-record component of the residual (and variance). The regression can then solved by the maximum likelihood method.

Abrahamson and Youngs (1992) showed that the algorithm presented by Brillinger and Preisler (1985) will give incorrect results if the initial estimate of the solution is far from the best solution. They presented a more stable algorithm although less efficient than the algorithm of Brillinger and Preisler (1985).

Joyner and Boore (1993) examined the maximum likelihood analysis for the regression of the attenuation model. They compared the results of using one-stage and two-stage regression using maximum likelihood methods. They found that both one-stage and two-stage regression give the same results although the two-stage regression method is computationally more efficient.

Attenuation of response spectrum ordinates

Peak ground motion indices alone are not enough to adequately describe the damage potential of the ground motion. The response spectrum is one of the standard methods to describe the frequency contents of the ground motion. It is also useful in the model superposition method to estimate the peak response of a multi-degree-of-freedom structure.

There are basically three methods for the empirical prediction of the response spectra (Dunbar and Charlwood, 1991: 1) scaling amplification factors by peak ground motions (Newmark and Hall, 1982); 2) computing spectra directly by attenuation relationships (Campbell, 1985; Joyner and Boore, 1988); and 3) using records of past earthquakes to obtain a statistical estimate of a response spectrum (e.g., Guzman and Jennings, 1976; Tsai et al., 1990).

The attenuation of the response spectra of strong motion from subduction zone earthquake has recently been studies by Crouse et al. (1988).

2.5 Summary

This chapter covers several topics concerning local site conditions; therefore a summary section is included to highlight the main points.

Section 2.1.2 covered the various methods for soil amplification, including empirical multiplication factors, theoretical transfer functions, and dynamic non-linear models.

Section 2.1.3 discussed the secondary seismic effects, namely liquefaction, landslide, and surface fault rupture. An overview of each secondary effect was given, including a description of currently available techniques for modeling the associated hazards. Section 2.2 and 2.3 covered the currently available techniques for the estimation of damage and loss. Section 2.4 covered the various methods for the attenuation of earthquake ground motion.

The extension from seismic hazard to integration of different seismic hazards, as well as a general overview of Geographic Information Systems (GIS) and strong motion

monitoring system in Bangladesh and development of acceleration based attenuation relation, are the subjects of Chapter 3 and Chapter 4.

From the literature review it can be learnt that seismic hazard due to local site effects such as soil amplification, liquefaction, landslide, and fault rupture can be estimated by combining the available soil parameter data with the current hazard models or by making use of existing maps showing estimated levels of these collateral hazards. Very few of the researchers have considered combination of the effects of the various seismic hazards such as ground shaking, soil amplification, liquefaction, landslide, and fault rupture. Regional structural inventories are combined with the seismic hazards to produce damage and loss distributions for the region analyzed. This study will focus on the development of a methodology to integrate the various components necessary for regional multi-hazard seismic risk analysis.

CHAPTER 3

GEOGRAPHIC INFORMATION SYSTEM AND METHODOLOGY OF REGIONAL SEISMIC HAZARD AND RISK ANALYSIS

3.1 Geographic Information System

There are many definitions for a geographic information system (GIS) and there seems to be confusion as to what are the necessary components and capabilities of a true GIS. The most widely used definition in the literature for a GIS is given by The Federal Interagency Coordinating Committee (1988) as "A system of computer hardware, software, and procedures designed to support the capture, management, manipulation, analysis, modeling and display of spatially referenced data for solving complex planning and management problems." Figure 3.1a is adapted from Frost, et al. (1992) and shows how different information systems work together to function as a fully-integrated GIS. Modern geographic information system has evolved from thematic cartography due to the combination of increased computational capabilities, refined analytical techniques, and a renewed interest in environmental/social responsibility. Throughout this evolution the primary goal has been to take raw data and transform it, through overlays and other analytical operations, into new information that can support the decision making process (Parent & Church, 1987). The remainder of GIS in this chapter gives a detailed overview of geographic information system , including the various components and their utility in a GIS-based regional multi-hazard seismic risk analysis.

3.1.1 Data Types and Database Management

Data associated with a geographic information system can be divided into two general categories: graphic data and non-graphic data (Antenucci, et al., 1991). Graphic data are digital representation of map features, usually depicted as point, line, area, and annotation features. The graphic features can be stores in either vector or raster format.

Vector data are represented by coordinates of point and line locations with rules for computing new coordinate locations and connecting the points as line or area features. Raster data are depicted by a uniform grid of cells or pixels. Most modern geographic

information systems can handle both vector and raster representations of graphic data, but the vector format is generally preferred due to its efficiency in data storage and manipulation and its more attractive graphical display.

Non-graphic data are the attributes associated with the graphic data. They are stored in alphanumeric format and are representations of the characteristics, qualities, and relationships of map features and geographic locations. Figure 3.1b illustrates the relationship in a GIS between graphic and non-graphic data. Non-graphic or tabular data can be stored in the given database within a GIS, although these databases are often limited in their ability to store very large amounts of data and in their functional capabilities. As shown in Figure 3.2, most modern GIS programs have the ability to link both graphic and non-graphic data to tables of attribute information in an external high-level database management program.

The available coordinate systems in a GIS for storing, analyzing, and displaying graphic data are the Cartesian system and the geographic longitude/latitude system (Antenucci, et al., 1991). Coordinates are usually expressed in one of the numerous possible map projections that transform positions on the curved surface of the earth onto a flat map surface. A few of the commonly used projections are the State Plane Coordinate System, the Universal Transverse Mercator, the Albers Equal-Area Conic, and the Lambert Conformal Conic (ESRI, 1992). Most GIS programs have the ability to easily convert data from one projection to another without significant loss of accuracy.

The acquisition and input of data is typically the most costly and time-consuming part of implementing a GIS-based analysis (Ripple, 1989). Graphic data can be entered into a GIS through digitizing or photo-quality scanning an existing map. These two methods are the most time-consuming but they allow the user to have the most control and understanding of the accuracy and quality of the spatial data. Depending on the sophistication of the GIS, graphic data can also be entered in one of several digital file formats. A digital exchange file output from a computer-aided drafting system or a different geographic information system can be converted to a GIS map, although information such as line connectivity is often lost in the exchange due to the difference in

system data structures. Standardized digital files such as the USGS Digital Line Graph (DLG) files and the U.S. Census Bureau TIGER/Line files can be converted to maps in most GIS programs. Although these conversions are often "black-box" functions, the quality of the files is generally high, producing very accurate maps.

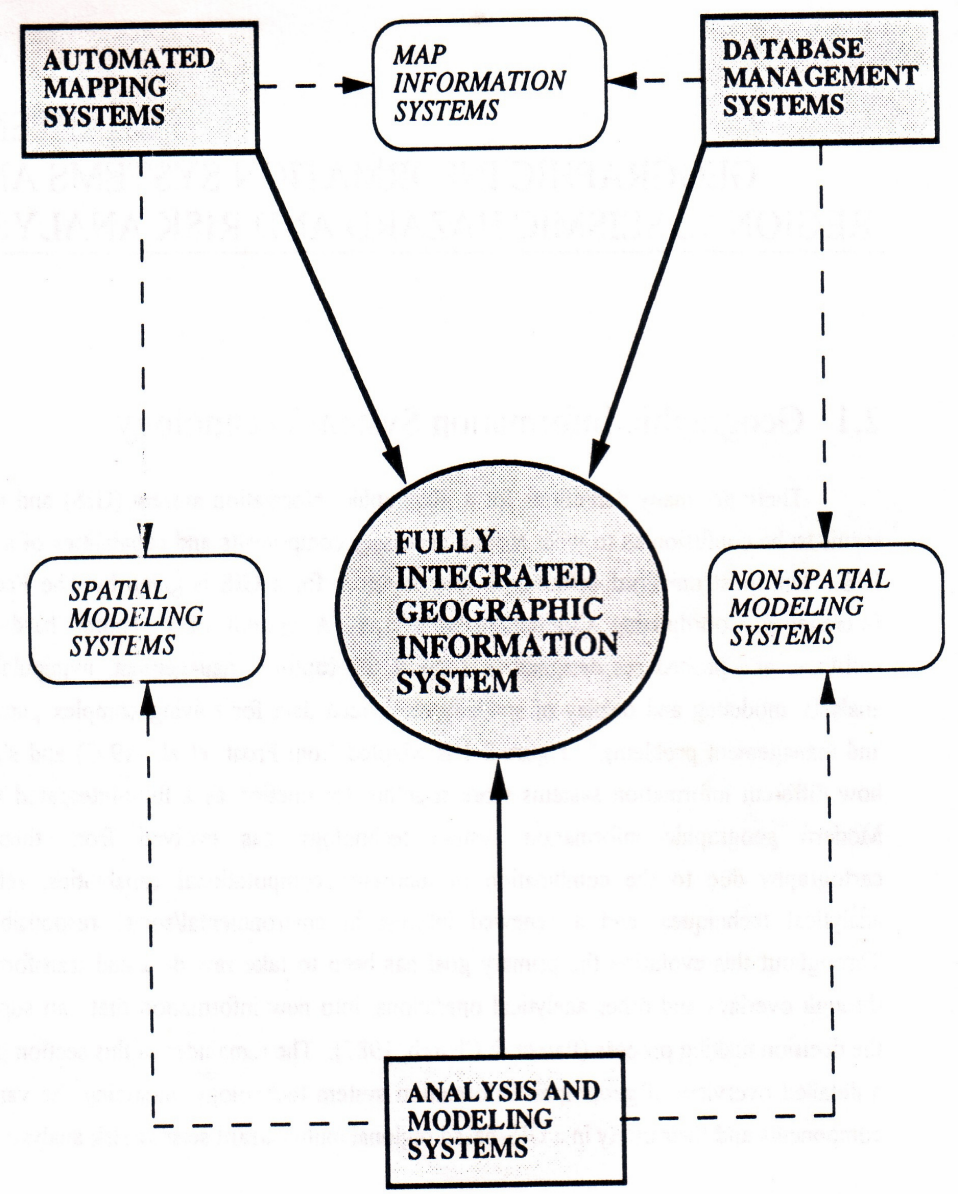

Figure 3.1a The information systems composing a fully-integrated geographic information system (after Frost, et al., 1992).

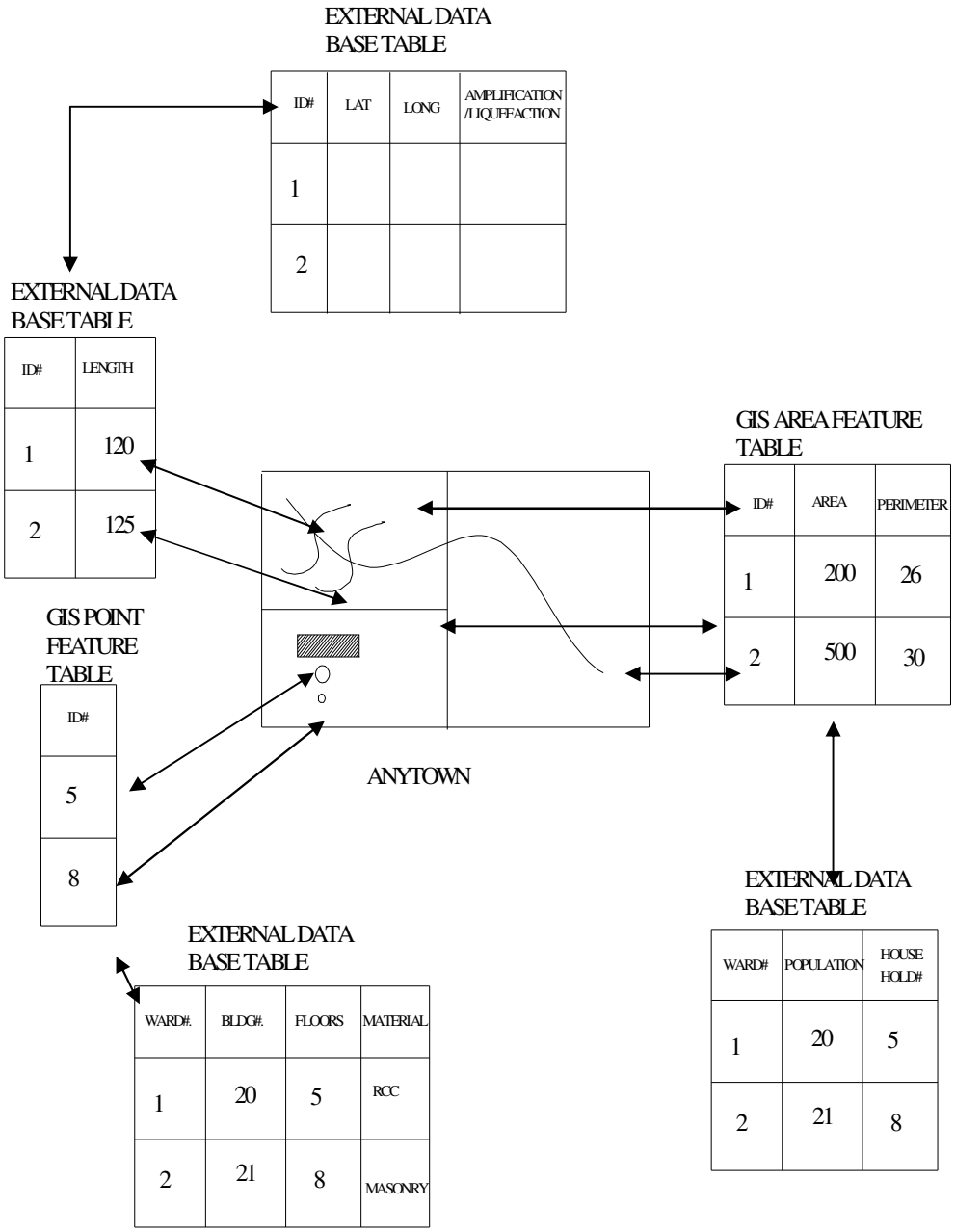

Figure 3.1b Illustration of data linkage in GIS environmrnt

Non-graphic data associated with digitized or scanned graphic data must usually be entered by hand, requiring the attribute data to be assigned to each individual feature. This is generally a very time-intensive procedure, but again it allows the user to have control and understanding of the accuracy and make-up of the feature attribute tables. The several possible digital file formats for conversion to a GIS map usually contain the relevant attribute information for the graphic data. Depending on the quality and source require extensive database manipulations to be useful. As explained above, attribute data can also be stored in external database management systems and linked to the graphic data, requiring no exchange or conversion of information. If necessary, tabular data can be added to the GIS database by defining the table structure and then entering the data.

3.1.2 Analysis and Modeling Capabilities

One of the most important features of a geographic information system is the manipulation and analysis of both spatial (graphic) and tabular (non-graphic) data (Smith, et al., 1987). The procedures for data analysis typically found in most GIS programs include:

(a) Map overlay procedures, including arithmetic, weighted average, comparison, and correlation functions.
(b) Spatial connectivity procedures, including proximity functions, optimum route selection, and network analysis.
(c) Spatial neighborhood statistics, such as slope, aspect ratio, profile, and clustering.
(d) Measurements of line and arc lengths, of point-to-point distances, of polygon perimeters, areas, and volumes.
(e) Statistical analysis, including histograms or frequency counts, regressions, correlations, and cross-tabulation.
(f) Report generation, including maps, charts, graphs, tables, and other user-defined information.

Depending on the level of sophistication of a GIS, numerous application-specific analysis functions may exist. These include procedures such as kriging of geotechnical data, air pollution dispersion, ground water flow, and highway traffic routing. Most systems include some sort of built-in programming capability usually in the form of a software-specific macro language. This allows the user to develop a set of functions or analysis procedures that can be stored in a user-defined library. Often, the GIS macro language is very simplified and is not able to handle very simplified and is not able to handle very high level computational features such as recursion, numerous simulations, subscripted variables, and subroutines. For this reason, most GIS programs have the ability to communicate with external analysis and modeling programs. A system can typically output data in various formats to be used in various external programs such as spreadsheets, word processing, graphics, and other user-specified executable programs. The results of an external analysis can then be used by the GIS as both graphic and non-graphic data for further manipulation and analysis, or for final report and map generation. Recently, the idea of using knowledge-based engineering techniques in a GIS environment has emerged. This requires thee coupling of GIS software with an expert system, a computer program that performs an analysis of a given situation and determines an answer or predicted outcome based on known information and rules. Applications such as site selection of critical facilities, resource allocation studies, and retrofit of bridges and other structures have been shown to operate very effectively in the GIS-expert system analysis environment. Boyle and Dong (1991) describe the use of a GIS, and expert system, and a database management system in the commercial product IRAS (Insurance/Investment Risk Assessment System) to estimate the seismic hazard of particular locations. Jensen and Christensen (1986) use a knowledge-based GIS technique to select solid and hazardous waste disposal sites and Usery, et al. (1988) use a similar knowledge-based GIS procedure to perform engineering geologic mapping. Several other studies in this area are currently in progress, including many applications in the social sciences.

3.1.3 GIS Software and Computer Hardware

There are hundreds of commercially available GIS software packages. They vary greatly in characteristics such as analysis capabilities, transportability of data, user-friendliness, storage capacity, graphic display, communication with other software, computer hardware requirements, speed, and price. GIS technology is a rapidly changing field. New and improved software is continuously being developed to meet the increasing popularity and use of geographic information systems in public agencies, private companies, educational programs, and several other areas. Kurt, et al. (1992) compare several commercially available GIS software packages developed for the microcomputer. They analyze thematic mapping and data queries, speed, compatibility with existing database information, conversion of maps between software, and the performance of a case study in each GIS.

Often the selection of a GIS package depends on the available computer hardware. Most of the currently available GIS software is designed for the microcomputer, as this type of computer has been the most popular in recent years. These packages are typically very user-friendly and relatively inexpensive, but are often lacking in computational speed, storage, and data exchange via the Windows™ environment, therefore these drawbacks should become irrelevant in the near future. The high performance workstation environment has recently become popular due to large cost reductions and the interest in file sharing among multiple users. A few of the more common GIS software packages are designed for the workstation environment. They typically require more time to learn and can be quite expensive, but are usually superior in analysis capabilities, data storage, speed, interfacing with external software, and macro language programming.

The GIS software package selected for this research is Mapinfo 7.0 developed by the Mapinfo Corporation, USA. It is designed for the workstation environment and is the most commonly used commercially available GIS software. Although this software is used in the case study presented in Chapter 5, the information and methodologies presented in this thesis are general and can be implemented in any geographic information system with the necessary data manipulation and analysis capabilities.

3.2 Regional Seismic Hazard and Risk Analysis

The goal of a regional seismic hazard and risk analysis is to quantify the potential damages and losses in a region due to future earthquakes. This analysis requires the synthesis of several types of information, as depicted in Figures 3.2 and 3.3. This section gives a broad overview of the classic approach to regional seismic hazard and risk analysis and Section 3.3 describes how the analysis is conducted in the geographic information system environment. The basic steps in a regional seismic hazard and risk analysis procedure typically include:

(a) Identification of earthquake sources.
(b) Modeling the occurrences of earthquakes on these sources.
(c) Estimating the attenuation of earthquake motions between the sources and the region.
(d) Evaluating the local site effects of soil amplification, liquefaction, landslide, and surface fault rupture.
(e) Estimating the damages to the regional inventories.
(f) Estimating the expected losses in the region.

The above steps are based on Lutz and Kiremidjian (1993) and are illustrated in Figure 3.4. A brief overview of these steps is given below with a more detailed description of steps (d), (e), and (f) given in later chapters of this thesis.

3.2.1 Identification of Seismic Sources

The first step in a regional seismic hazard and risk analysis is the identification of the potential seismic sources that can affect the region. Seismic sources are geographical features with homogenous seismicity (Vasudevan, et al., 1992). They can be modeled as point, line, and area sources (Lutz and Kiremidjian, 1993). Point sources repeatedly generate earthquakes from exactly the same point and are quite rare. Line sources are used to represent earthquake faults that generate earthquakes with epicenters following a linear trend. Regions with high seismicity that is not atributable to a well-defined source are typically modeled as area sources.

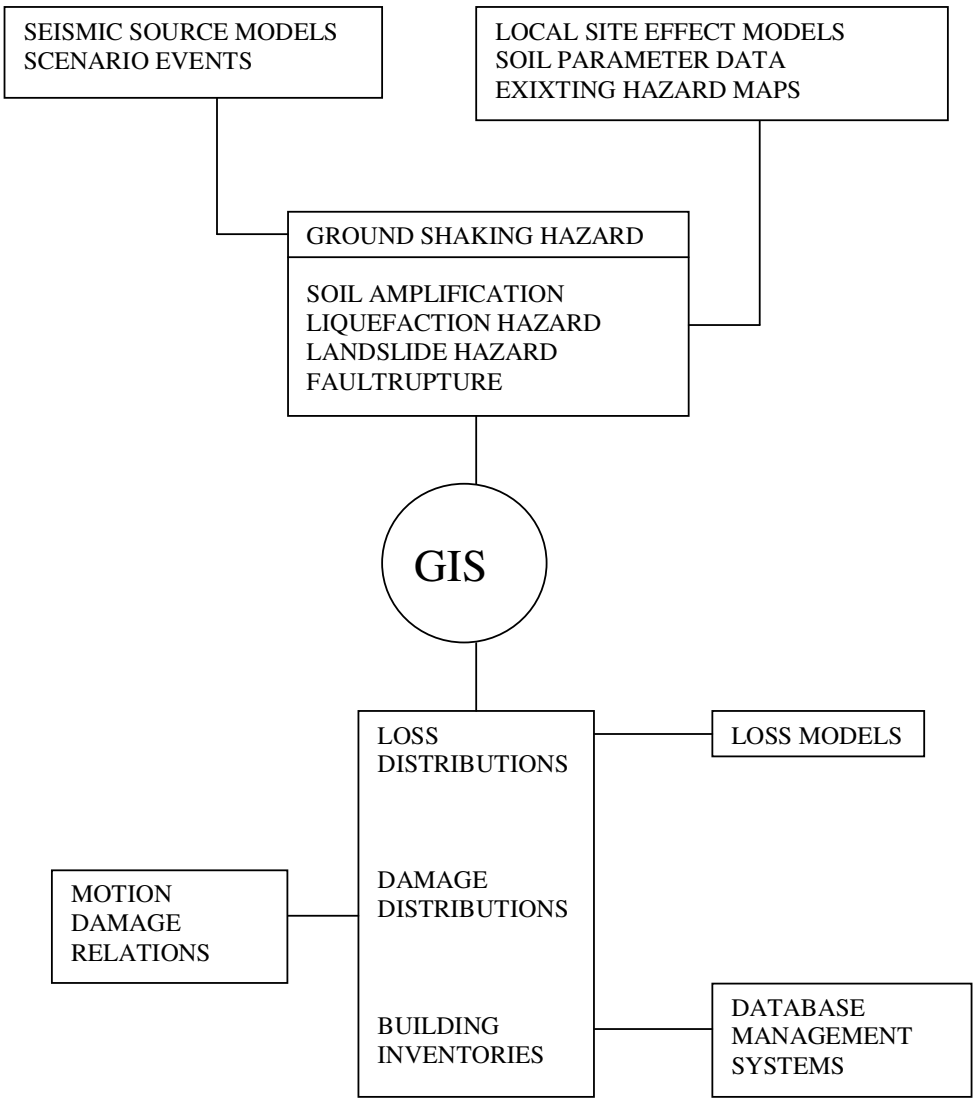

Figure 3.2 The role of geographic information systems in regional seismic hazard and risk analysis

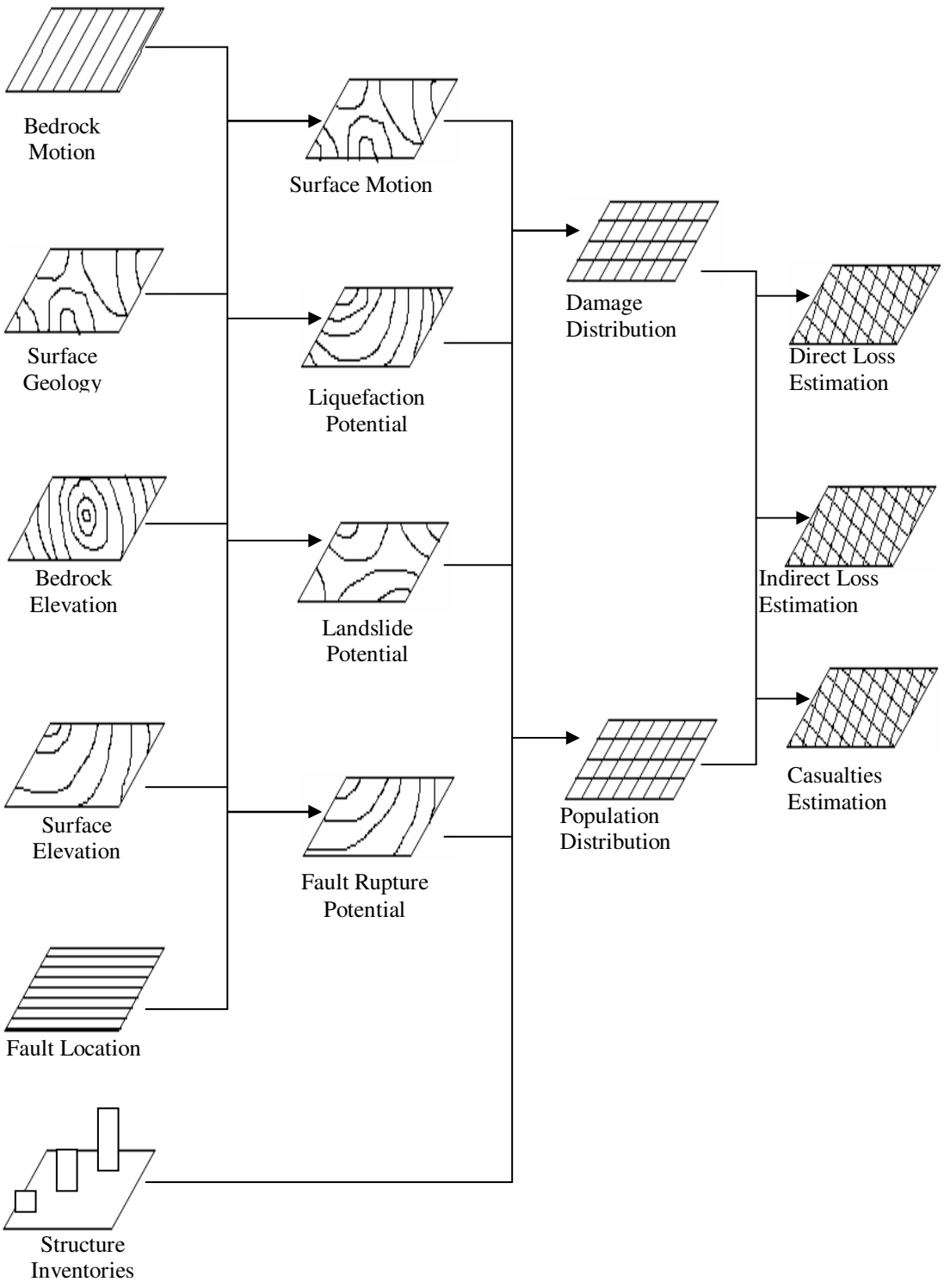

Figure 3.3 The mapping process for regional multi-hazard seismic risk analysis through GIS

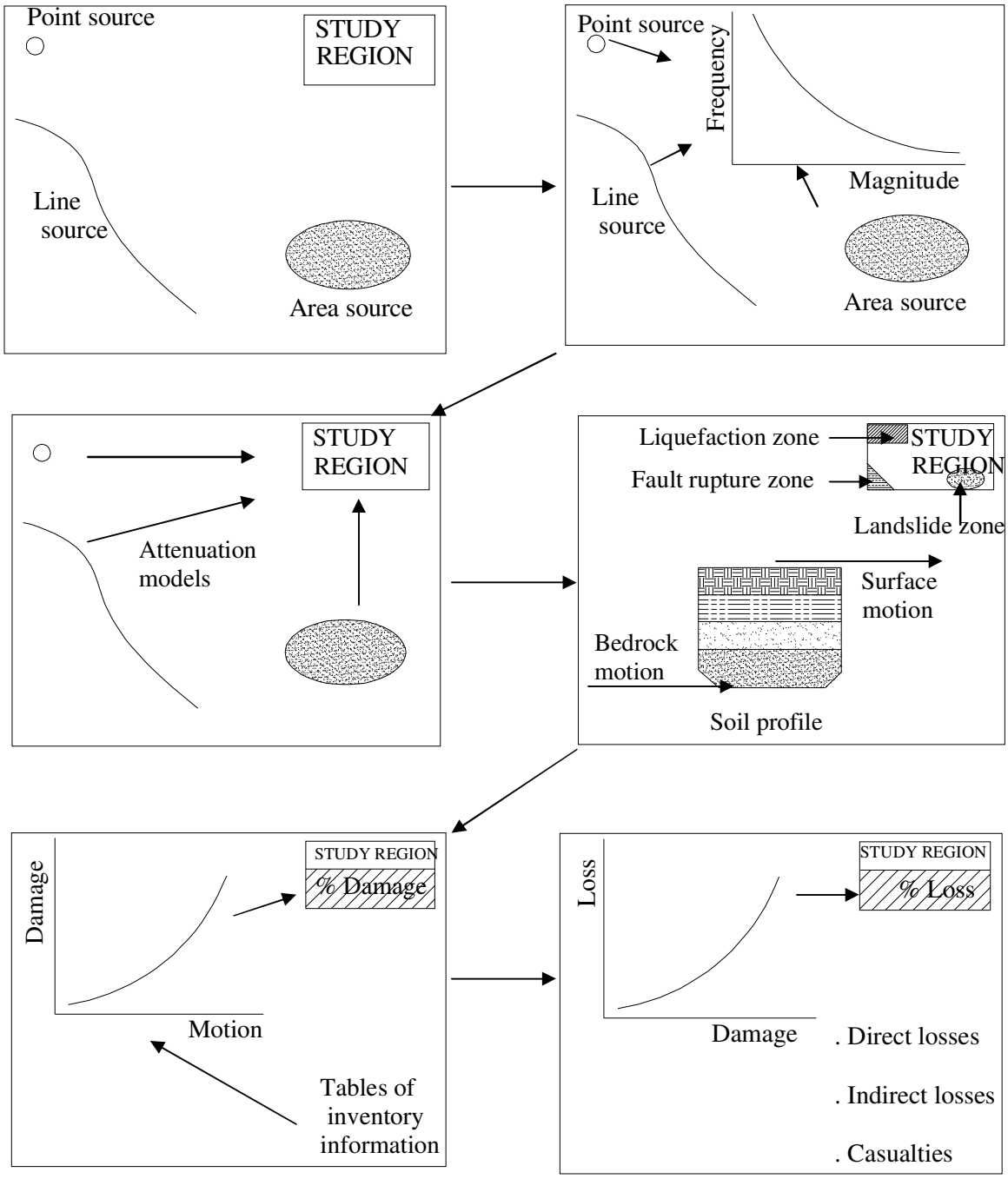

Figure 3.4 The basic steps in a regional seismic hazard and risk analysis.

3.2.2 Modeling of Earthquake Occurrences

The modeling of earthquake occurrences on each seismic source is the second step in the analysis. There are several occurrence models that have been proposed and a complete review is provided by Anagnos and Kiremidjian (1984). The major classes of models include the Poisson models, the time-predictable models, and the slip-predictable models. These three major classes of models, as well as the deterministic scenario analysis method, are briefly discussed below. Other recently developed models include the random slip rate model (Suzuki and Kiremidjian, 1988) and the spatially and temporally dependent model (Lutz and Kiremidjian, 1993).

Poisson models are the simplest class of earthquake occurrence models and assume that earthquakes occur randomly in time, space, and magnitude. The rate of earthquake occurrences is assumed to be uniform and is estimated from empirical data using the Guttenberg-Richter magnitude-frequency equation. These models are memory-less and give a constant probability of an earthquake in the time period (t, t +Δt) given that there was no earthquake in the time period (0,t). Poisson models are typically applied to regions with frequent, small magnitude earthquakes without spatial or temporal dependence.

Time-predictable models assume that earthquakes have a one-step temporal dependence (Anagnos and Kiremidjian, 1984). These models estimate the time of occurrence of the next earthquake given the size (seismic displacement) of the previous earthquake. A maximum stress release threshold and a constant stress accumulation rate are assumed. Knowing the amount of stress released by a given earthquake, the rate at which the stress will accumulate, and the maximum amount of stress the seismic source can accommodate, the time, but not size, of the next earthquake can be predicted. These models have been applied primarily to regions along plate boundaries.

Slip-predictable models also assume that earthquakes have a one-step temporal dependence (Kiremidjian and Anagnos, 1984). These models estimate the size of the next earthquake occurrence given the elapsed time since the previous earthquake. A minimum

stress release threshold and a constant stress accumulation rate (as in the time-predictable model) are assumed. It is also assumed that when an earthquake occurs, all of the accumulated energy is released down to the minimum level. Knowing the time since the previous earthquake occurrence, the rate at which the stress will accumulate, and the minimum amount of stress to remain on the seismic source, the size, but not the time, of the next earthquake can be predicted. These models have been applied to the Middle American Trench in Mexico.

Two other recently developed models include the random slip rate model and the time and space dependent model. The random slip rate model (Suzuki and Kiremidjian, 1988) assumes a non-uniform stress accumulation rate and inhomogeneous properties for the fault. The slip rate for each earthquake on the fault is assumed to be random with the rate between events assumed to be constant. The time and space dependent model (Lutz and Kiremidjian, 1993) utilized a generalized semi-Markov process for simulating fault behavior through time. The fault is discretized into short cells and the amount of slip accumulated on each cell and the amount of slip release on each cell due to earthquake occurrences is traced through time. The model can simulate the sized and locations of earthquakes occurring along the fault for the time period of interest.

A deterministic scenario analysis can also be used in this step to model the occurrence of an earthquake. In this method the location, size, and time of occurrence of a future earthquake is assumed. The earthquake scenario can be a repeat of a previous seismic event in the area, but most often it is the maximum earthquake that the given seismic source is capable of generating, according to experts in the field. This method is often used by the insurance industry to make probable maximum loss (PML) estimates for their insured properties.

With the exception of the time and space dependent model, the earthquake occurrence models discussed in this section are simplified representations of the actual behavior of large, rare earthquakes. The Poison model is typically applied to regions with small magnitude earthquakes without time and space dependence. The time-predictable, slip-predictable, and random slip rate models are adequate for seismic sources exhibiting

temporal, but not spatial, dependence. The emphasis of the work presented in this thesis is on regional seismic hazard and risk analysis for predicting damages and losses over a large area. For this reason, the deterministics scenario event occurrence model will be used to illustrate the GIS-based analysis methodology. This is the simplest model, as it requires little computation and is not region-specific, but as previously discussed, the analysis methodology is intended to be general, allowing more sophisticated models to be included instead.

3.2.3 Determination of Regional Bedrock Motion

After selecting one of the probabilistic occurrence models discussed above or assuming a deterministic seismic event scenario, the next step in the regional seismic hazard and risk analysis is to determine the bedrock motion in the region. The most common method involves the use of an empirical attenuation relationship. These relationships express a given ground motion parameter in a region as a function of the size and location of an earthquake event. Numerous relationships have been developed in the past, typically by applying statistical regression analyses to recorded data. Campbell (1985) provides an excellent summary of attenuation relationship development. Often these relationships are developed with different functional forms and site conditions. These biases coupled with the scarcity of data for large magnitude events at short distances have recently led to investigations into more theoretical methods for predicting bedrock motion. Geophysical models based on seismic source mechanisms and wave-propagation theory have been proposed, but these models often require extensive source and site geology data and are more computationally intensive.

3.2.4 Modeling Local Site Effects

Local geologic deposits are well known for their capabilities to modify the characteristics of seismic motions and influence the amount of damage to man-made facilities (Borcherdt, 1990). The local site effects are defined as soil amplification, local site effect considered in a regional seismic hazard and risk analysis. There are several given an input bedrock motion and a characterization of the local soil conditions. These based on recorded data to highly complex procedures that modify an entire earthquake time history

based on non-linear dynamic soil response. Aki (1988) provides a good overview of the different types of soil amplification models.

The secondary local site effects of liquefaction, landslide, and surface fault rupture are typically more difficult to quantify and model than soil amplification. These effects are often summarized in the form of microzone maps that give a hazard potential in the form of a "yes" of "no" prediction of occurrence based on numerous assumptions. Kiremidijn (1992) describes the currently available hazard models for estimating the effects of soil amplification, surface fault rupture and earthquake-induced liquefaction and landslide, and the need for a methodology that can accurately combine the seismic hazards due to these local site effects in a region.

The development of a methodology for combining the regional seismic hazards due to soil amplification, liquefaction, landslide, and surface fault rupture is one of the major components of the work presented in this thesis. This chapter gives a thorough discussion of this development in the GIS environment, and Chapter 2 gives a more detailed description of the effects of local soil conditions on earthquake ground motion and the hazard associated with fault rupture and earthquake-induced liquefaction and landslide.

3.2.5 Estimating Regional Damage Distributions

Once the seismic hazard due to ground shaking and local site effects has been adequately characterized, the next step in a regional seismic hazard and risk analysis is the estimation of damages to structural facilities in a region and well-defined relationships between earthquake motion (including local site effects) and both structural and non-structural facility damage. The development of an accurate and complete structural inventory for a region is often the most time-consuming, expensive, and important step in regional damage estimation. Most of the previous work in this area has focused on developing regional inventories for a specific type of facility, such as buildings (Vaseduvan, et al., 1992) and lifelines (Applied Technology Council, ATC-25, 1991).

One of the major components of the work presented in this thesis is the development of a methodology for integrating and compiling an accurate and complete inventory of all

structural facilities in a region. This methodology and its implementation in the GIS-based analysis process is thoroughly discussed in Section 2.3. A detailed overview of the various descriptions of damage and of the currently available relationships between earthquake motion and facility damage is also presented in Section 2.3.

3.2.6 Estimating Regional Loss Distributions

The final step in a regional seismic hazard and risk analysis is the estimation of regional losses based on the damage distributions predicted in the previous step. Several types of loss can be identified, typically divided into monetary and non-monetary loss. Monetary loss for a facility depends on the physical characteristics and use of the facility. This loss is often identifies as resulting from (a) structural damage; (b) non-structural damage to contents and architectural components; (c) loss of business revenue; (d) relocation of occupants, contents, or function; (e) clean-up and security; and (f) financing of repairs (Kiremidjian, 1992). Non-monetary loss due to seismic activity typically depends on the characteristics of the regional population and can include effects such as fatalities, injuries, unemployment, and homelessness.

The description given above does not include the secondary losses associated with fire-following earthquake, tsunami, and inundation due to dam failure. These losses can often surpass the primary monetary and non-monetary losses, but are considered to be beyond the scope of this thesis. The typical regional seismic hazard and risk analysis is limited to monetary loss due only to structural damage and to non-monetary loss due only to casualties. Geographic information system technology provides an excellent environment for analyzing and combing the various regional loss estimates due to a given seismic occurrence. Methods for estimating the loss types discussed in the previous paragraph in the GIS-based regional seismic hazard and risk analysis will be described in Section 2.3.

3.3 Application of GIS to regional Seismic Hazard and Risk Analysis

Section 3.1 of this chapter gave a detailed description of geographic information system and Section 3.2 presented a broad overview of regional seismic hazard and risk analysis. This section explains how these two topics fit together, that is the use of GIS technology

for conducting a regional seismic hazard and risk analysis. The development of a GIS-based analysis methodology is the main focus of the research presented in this thesis.

3.3.1 Overview

Figure 3.5 presents a detailed flowchart of the steps involved in a GIS-based regional seismic hazard and risk analysis. The circles represent methodology steps, the squares represent database information, and the triangles represent intermediate and final results. The general procedure illustrated in Figure 3.5 will be described below. A more detailed discussion for the areas of new development will be presented later in this chapter. As discussed in Chapter 1, the regional analysis presented here is somewhat simplified, but capable of being modified and updated in the future. A few important features such as conflagration loss and building-lifeline interaction analysis are omitted in order to focus on the development of the overall GIS-based analysis methodology and the new improvements in areas such as local site effect hazard and structural inventory compilation. Chapter 5 presents a case study that illustrates the application of this methodology to study region in Mymensingh Town, Sylhet City and Dhaka City.

3.3.2 Seismic Event Characterization

As shown in Figure 3.5, the first intermediate result in the regional analysis is the characterization of a seismic event. This typically requires a map of the region that identifies the potential seismic sources. A source is selected and an occurrence model is applied either by implementing the model within the GIS or by linking it as an external executable program. An alternate a scenario earthquake occurring on a given source. Database tables of seismic activity in the region are often used to aid in the occurrence modeling procedure and in the assumption of historical scenario earthquake.

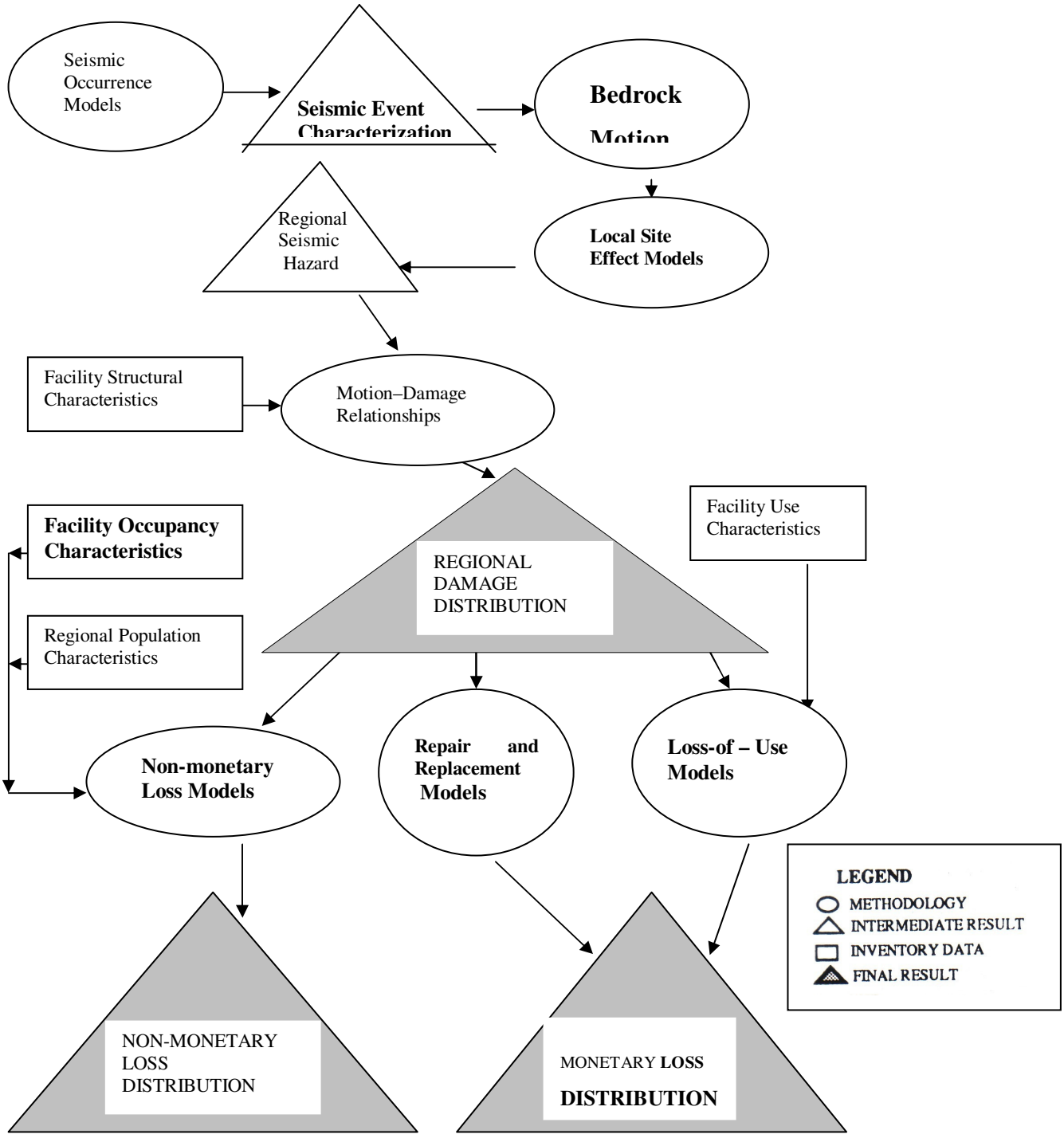

Figure 3.5 Flowchart showing the basic procedure for a GIS-based regional multi-hazard seismic risk analysis

3.3.3 GIS-Based Regional Estimation of Surface Ground Motion

The spatial database structure of a geographic information system is ideal for estimating the effects of soil amplification of earthquake ground motion over a large region. Three different types of soil amplification models were previously discussed in this section. The non-linear time-step integration methods are considered impractical for regional application and will not be further discussed in this thesis. The linear transfer function models are typically the most widely used and give an adequate level of accuracy on a regional basis. The peak value multiplication factors are often the simplest and most efficient soil amplification models to apply over a large region, but they typically fail to capture non-linear soil behavior and the frequency contents of the ground motion and the soil profile.

A map showing the regional distribution of seismic motion at the bedrock level is estimated by applying an attenuation model with an assumed occurrence model or scenario event. The seismic motion can be in the form of a peak value for use in the multiplication factor models or in a spectral form for use in the transfer function models. Regional maps of the soil parameter data required for input to the assumed soil amplification model are then overlaid on the bedrock motion map to estimate the surface ground shaking in the region. An example application of GIS to regional soil amplification model are then overlaid on the bedrock motion map to estimate the surface ground shaking in the region.

An application of GIS to regional soil amplification, utilizing the peak value multiplication factors developed by Kiremidjian, et al. (1991). He Illustrates a GIS-based analysis for estimating surface peak ground acceleration (PGA) values for a region. Regional bedrock PGA values are estimated using the Joyner and Boore (1988) attenuation function with a given magnitude of an event occuring on the region. Regional soil amplification factors are calculated using an empirical function developed by Kiremidjian, et al. (1991) based on 52 recorded motions from the 1989 Loma Prieta Earthquake. The PGA amplification is assumed to be a function of the depth to bedrock

at the site, the average shear wave velocity of the soil in the top 30 meters, and the input PGA at the bedrock level.

In this thesis regional bedrock PGA values are estimated using the McGuire (1978) attenuation function with 7.6 (for Sylhet City) and 8.7 (for Mymensingh Town) magnitude of an event occurring on the region. Regional soil amplification factors are determined using the most commonly used transfer function model SHAKE developed by Schnabel, et al. (1972). The PGA amplification is assumed to be a function of the depth to bedrock at the site, the average shear wave velocity of the soil in the top 30 meters, unit weight of soil, damping and the input PGA at the bedrock level.

The regional depth to bedrock values are determined from bore log data. The shear wave velocity are calculated from the empirical relation developed by Tamura and Yamazaki (2002). A map of regional bedrock PGA values was developed by applying McGuire (1978) attenuation model.

The Tamura and Yamazaki (2002) empirical relation of shear wave velocity is given by:

$$V_s=105.8\ N^{0.187}D^{0.179} \qquad (3.1)$$

Where:

V_s = Shear wave velocity (m/s) ;

N = Corrected SPT blow count (N-value)

D = Depth (m)

The Mc Guire (1978) attenuation function is given by:

$$y=0.0306e^{0.89M}r^{-1.17}e^{-0.2S} \qquad (3.2)$$

where :

S=0 for rock and S=1 for alluvium

y = PGA;

M = magnitude (7.6 in this example);

r = hypocentral distance;

The regional bedrock PGA is multiplied by the soil amplification factors obtained from SHAKE analysis. Figure 3.6 shows the final map giving regional estimates of surface PGA values (A_s) produced by combining the spatial soil parameter data. The example described in this section is included in this thesis only for purposes of illustrating the use of GIS in a regional soil amplification study. It shows the application of an amplification function over a large area, with regions of mapped values representing the variables in the equation. Rather than predicting site specific surface ground motions, the results are intended to give relative levels of surface PGA values for broad regions and to indicate areas requiring further detailed investigation.

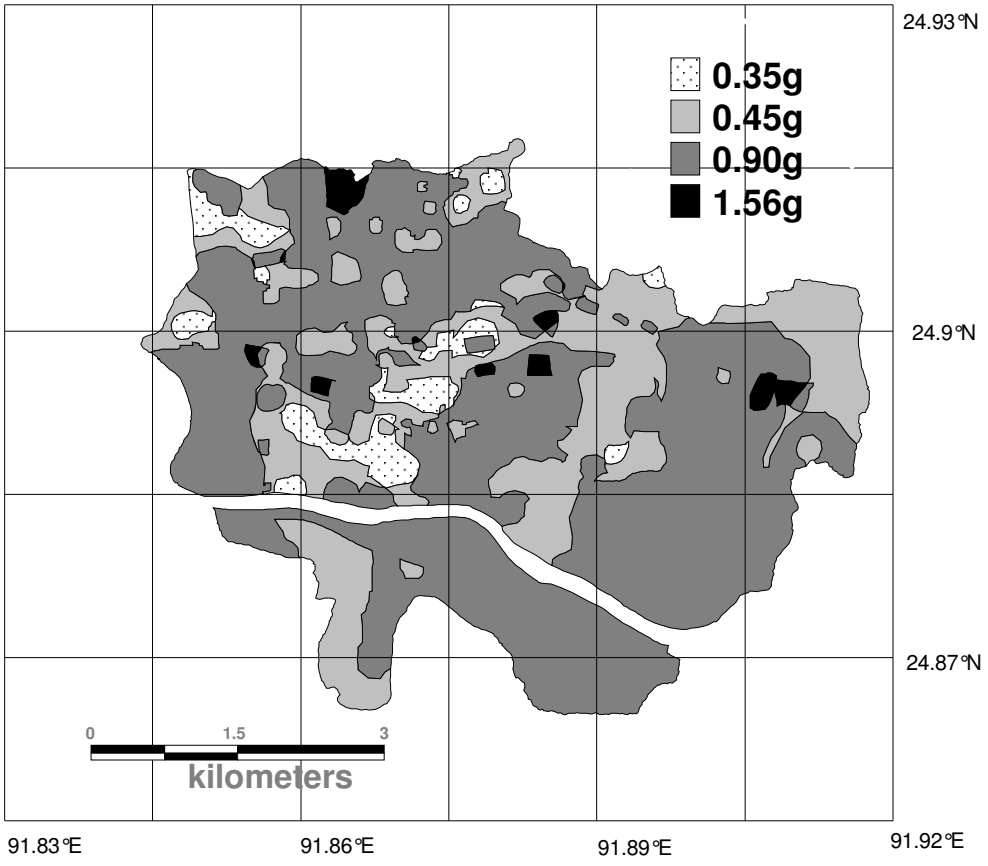

Figure 3.6. Map showing regional distribution of combined seismic peak ground acceleration in Sylhet

3.3.4 Regional Seismic Hazard Estimation

The second intermediate result shown in Figure 3.5 is the estimation of seismic hazard in the region. This procedure typically requires several geologic and geographic maps of the region. The bedrock motion in the region resulting from the seismic event must first be determined. This is often done by applying one of the attenuation functions within the GIS or again by linking the function as an external executable program. The GIS-based procedure for estimating regional bedrock motion is straight-forward and will not be discussed further, except with respect to the case study presented in Chapter 5.

Quantifying and combining the seismic hazard due to local site effects (soil amplification, liquefaction, landslide, and fault rupture) is one of the main areas of new development presented in this thesis. The procedure involves developing models for each of the effects, assembling the necessary geologic and geographic maps and databases, applying the models either within the GIS or as linked external programs, and then overlaying and combining the resulting hazard maps. The development of this hazard analysis methodology is more thoroughly discussed later in this chapter.

3.3.5 Regional Damage Distribution

The first final result obtained in the analysis procedure illustrated in Figure 3.5 is a regional damage distribution for the study area. Damage forecasting typically requires a detailed and accurate structural inventory for the region, a quantification of the regional seismic hazard, and equations relating damage to hazard for each facility type. The spatial database structure of a GIS environment is ideal for this procedure. Structural inventory information can be stored in tables within the GIS database or in tables in an externally linked database management program. Relationships to estimate facility damage are typically applied within the GIS, but can also be used through external program links. The general procedure involves combining maps of seismic hazard with maps of facility locations according to set motion-damage relationships producing maps of regional damage distribution. The resulting maps are useful for purposes such as resource allocation and rehabilitation prioritization. The development of a methodology for compiling an accurate and complete structural inventory is one of the major

components of this research, therefore damage forecasting in a GIS-based environment will be described in detail in Section 3.3.5.1.

3.3.5.1 Application of GIS Technology to Regional Damage Forecasting

The spatial data storage and analysis capabilities of a geographic information system make it an ideal environment for conducting a regional damage estimation. In Section 3.4 of this chapter the integration of various seismic hazards in the GIS environment is discussed, producing the final distribution of MMI values for the example regions shown in Figure 3.22 (m). For the illustration of a GIS-based analysis, the regional damage estimation described in this section will be simplified to include the following two steps, repeated for each facility in the inventory of structures:

(1) Determine the level of seismic hazard for the facility by mapping it according to its geographic location, typically longitude and latitude coordinates, to the map of estimated regional MMI levels, such as that shown in Figure 3.22(m).

(2) Determine the expected damage factor (percent financial loss) for the facility and the given MMI level based on the motion-damage relationship defined for the facility's earthquake engineering class, such as the curve shown in Figure 2.17 or fragility curves for Bangladesh. If a facility is assigned to more than one earthquake engineering classification in a probabilistic manner, then the expected damage for the facility is estimated by combining the expected damage computed for each class in a weighted average approach based upon the given probabilities.

As an example, consider a structure classified as low-rise masonry building, located in the area designated as "A" in Figure 3.22(m). The final MMI level for this region was computed in Section 3.4.2 to 11. Using the expected damage factor curve-for low-rise masonry buildings given in Figure2.17, the expected damage factor is estimated to be 75%. Modern GIS technology provides a means for the efficient repetition of this computation for all facilities in a region. As previously discussed, the results, such as the 75% expected damage factor computed above, are not to be used for site-specific analysis. The damage estimates are based on several simplifying assumptions and are

intended to give regional distributions of expected damage for a given earthquake occurrence model. The microzone mapping capabilities of the GIS can be used to illustrate these distributions in a format that can be very useful for hazard mitigation and emergency planning purposes.

3.3.6 Monetary and Non-Monetary Loss Estimation

Recent seismic events have demonstrated that the monetary loss resulting from earthquake damage to major metropolitan areas can run into the billions of dollars (Kiremidjian, 1992). World-wide statistics of annual fatalities due to earthquakes can be just as alarming. As shown in Figure 3.5, the final and most important result of a regional seismic hazard and risk analysis is the estimation of monetary and non-monetary loss distributions. As with damage forecasting, the GIS environment is ideal for estimating loss distributions. The procedure typically involves combining maps of damage distributions with maps and database tables of regional facility and population inventories according to relationship defining loss as a function of damage. The resulting microzone maps of regional loss distribution help to illustrate areas requiring further study for possible earthquake loss mitigation strategies. New improvements to loss estimation and a detailed description of the GIS-based analysis methodology are discussed further in Section 3.3.6.1.

3.3.6.1 Application of GIS to Regional Loss Forecasting

The spatial distribution of earthquake losses in a region is often used for purposes such as resource allocation, disaster planning, and various social and economic studies.

Geographic information systems provide a powerful tool for storing and manipulating the large amount of data typically required for a regional earthquake loss estimation. Several types of monetary and non monetary losses were previously discussed in Section 2.3.3, but for illustration of the GIS-based earthquake loss evaluation methodology, only those losses due to direct structural damage, loss of business use, and casualties will be considered in this thesis.

The computation of monetary losses due to direct structural damage is quite straight – forward as discussed in Section 2.3.4.1. Equation 2.21 is typically used in conjunction with a table of replacement costs for various facility use types to compute the loss for each facility. Regional losses can be estimated by calculating the loss for each individual facility and then aggregating the results on a given basis, such as by Census tract, city block, zip code, earthquake engineering class, or social function class. For example, in Section 3.3.5.1, a low-rise masonry building located in the area designated as "A" in Figure 3.22(m) was estimated to have a damage factor of 75%. Assuming that this building is used as a single family dwelling with an estimated replacement cost of Tk1000 / square foot, for a 2000 square foot building, the predicted monetary loss would be Tk 20,00,000.

As discussed in Section 2.3.4.1, loss of business use is typically computed for each facility as a function of the damage factor due to the earthquake event and the social function class of the facility. Unless a model for extending down time to monetary loss or a model for studying the effects of the facility interaction is included in the GIS-based analysis, the only regional aggregation of results for loss of business use is typically the average of the values for the different facility use types to be used for comparative purposes. As an example, if the low-rise masonry building discussed in the previous paragraph were a retail trade store instead of a single family dwelling, the loss of business would be computed from Table 2.5 and Figure 2.17 and a damage factor of 75% as:

Time to restore 30% functionality:	100 days
Time to restore 60% functionality:	205 days
Time to restore100% functionality:	340 days
Functionality at 30-days:	10%

The final regional earthquake loss estimation to be illustrated is the death and injury loss. The prediction of casualties is typically computed in a two-step process for each facility in a region. First the day and night occupancy values are estimated for the facility based on the square footage and social function class of the facility. Next, the death and injury

rates for a given damage factor (Table 2.5) are used with the occupancy values to predict the fraction of dead and injured persons in the facility.

Similar to monetary losses due to direct structural damage, regional casualties can also be aggregated on several levels, such as by area or facility type and use. For example, the day occupancy of the example 2000 square feet low-rise masonry building would be 4 persons. Table 2.5 estimates rate of 1 in 25 major injuries and 1 in 100 deaths for a facility with a damage factor of 75%. Using these values with the 4 person daytime occupancy results in 0.16 major injuries and 0.04 deaths in the buildings due to the assumed earthquake event. These casualty estimates are meaningless when reported for only one structure. Typically, these estimates are made for each structure in a region and then a summary value of deaths and injuries for the whole region is reported.

As indicated in Section 3.3.6.1, the resulting values such as Tk 20 Million, 100 days, 75% and 0.16 major injuries are not intended to be used for a site-specific analysis of one facility. the models from which this values are computed are simplified in order to be applicable to regional damage and loss estimation on a broad scale. Values are computed for one facility to illustrate the effectiveness of GIS for storing, manipulating, and displaying the spatial data involved in a regional seismic hazard and risk analysis. Section 2.3.1 has described structural inventory development and provided an overview of regional earthquake damage and loss estimation. Chapter 5 illustrates these concepts as well as those of the previous two chapters through a case study of a GIS-based multihazard regional seismic risk assessment in Sylhet City (Chapter 5) and Mymensingh Twon (Annexure-A).

3.4 Hazard Integration in the GIS Environment

One of the major objectives of the work presented in this thesis is the development and illustration of a GIS-based methodology for integrating the seismic hazards associated with the local site effects of soil amplification, liquefaction, landslide, and surface fault rupture. The local site effects and the various models for representing the hazard associated with each effect have been discussed in the previous chapter. When observing earthquake damage it is almost impossible to determine how much of the damage can be

separately attributed to each local site effect, therefore the final regional seismic hazard distribution is based on a weighted average combination of the hazard associated with each effect. The basic steps in the hazard integration methodology are presented below followed by an example that illustrates the methodology for a hypothetical region.

3.4.1 Integration Methodology

The regional seismic hazard integration methodology presented here is intended to be general enough so as to allow the application of more or less sophisticated models depending on the availability of information in the desired analysis region. Every analysis region is different, therefore the quantification of the secondary site effects and the weighting scheme for combining the various seismic hazards is heuristic, based on judgment and expert opinion about the influence of local site conditions information. Section 3.4.2 illustrates a simplified example of seismic hazard integration for a hypothetical regions. The basic steps in the methodology are listed below and illustrated in Figure 3.7.

1) A map showing the distribution of the bedrock-level ground shaking in the region is developed. The shaking can be described in terms of peak ground motion values, spectral values, or intensities. Sections 3.2.2 and 3.2.3 discussed the modeling of earthquake occurrences and bedrock-level shaking.

2) A map showing the distribution of the surface-level ground shaking in the region is developed. This shaking is described in the same manner as the bedrock-level ground shaking in Step (1). The various methods for soil amplification were discussed in Section 2.1.2.

3) Maps showing the distribution of hazards due to secondary site effects in the region are developed. Various models for these effects (surface fault rupture, liquefaction, and landslide) were described in Section 2.1.3.

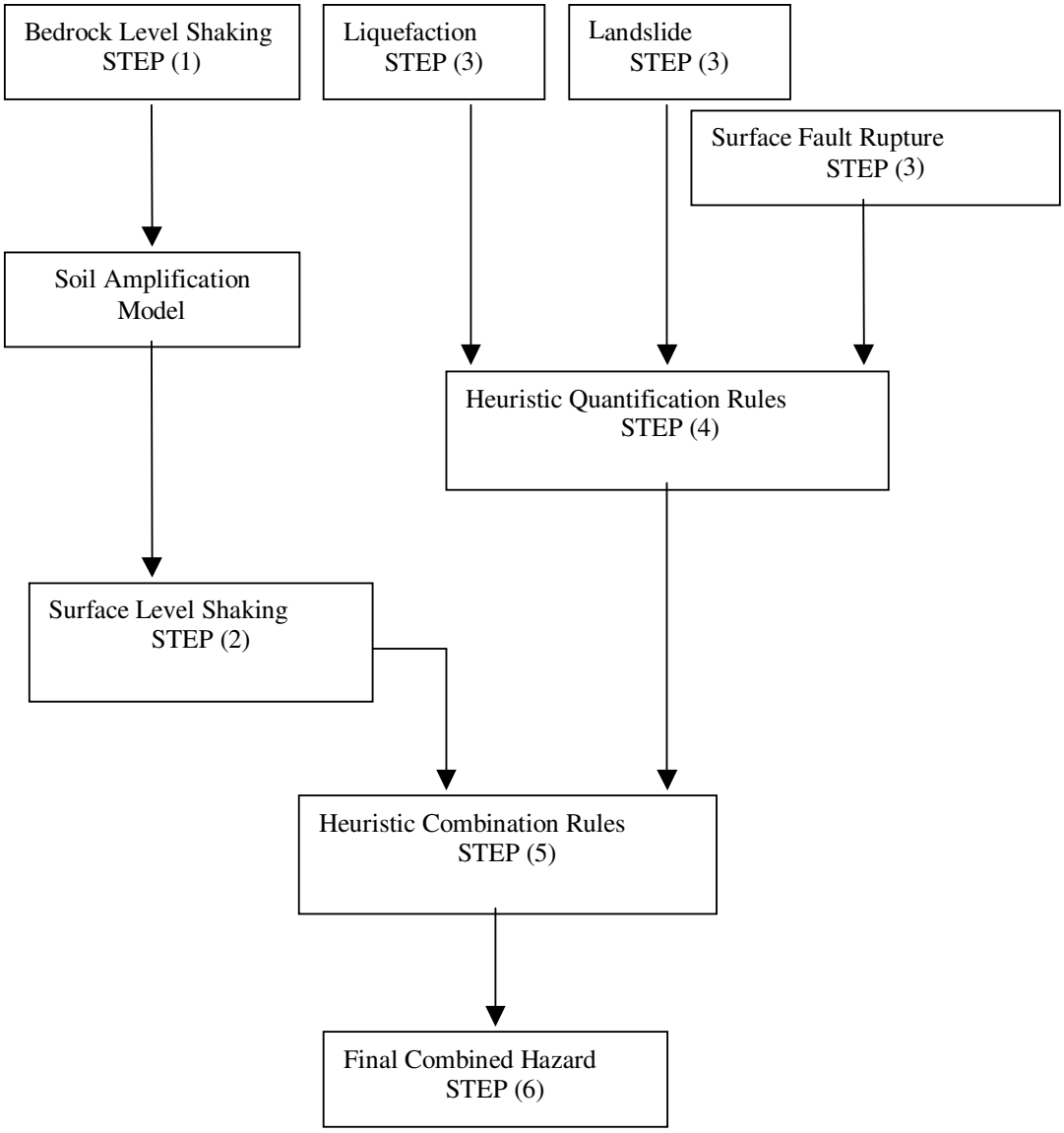

Figure 3.7 Steps for seismic hazard integration.

4) Rules are defines to quantify the regional hazard distributions developed in Step (3). To do this laboratory investigation was performed using an indigenous SHAKE TABLE for a particular soil. In general these rules are based on expert opinion about the local geology and the history of the severity of secondary seismic effects in the region. The rules should quantify the hazards in a consistent manner that allows them to be combined as described in Step (5).

5) Rules are defined to combine the seismic hazards of surface ground shaking and the local site effects of surface fault rupture, liquefaction, and landslide. The hazard combination rules are in the form of weighted averages with the weights determined by local expert opinion. The weights depend on knowledge about the behavior of the local geology and the relative accuracy associated with each hazard. The increased hazard due to two or more effects occurring simultaneously is also considered in these rules.

6) A final map showing the distribution of combined hazard in the region is developed by over-laying the maps developed in Steps (2) and (3) according to the heuristic rules defined in Steps (4) and (5).

3.4.2 Laboratory investigation for the quantification of secondary site effects

An attempt was taken to investigate and distinguish the PGA/intensity values of a region due to liquefaction, land slide and fault rupture. To generate artificial earthquake a locally built SHAKE Table (Figure 3.8a) was used which is a four-wheeler table. Each wheel is similar to rail wheel and the table is situated on the two parallel rails which is similar to railway track. A motor was set below the table and was used to create an artificial earthquake by applying vibration on the SHAKE Table. To create an artificial earthquake environment in the laboratory the 'power on' switch of the motor is operated. The wheels of the SHAKE Table start to vibrate over the rails with the same frequency (approximately 2 Hz) as applied by the motor. Figure 3.8b represents a SHAKE table used in the Bangladesh University of Engineering & Technology, Dhaka-1000. Two Chambers of equal size (1.2m×1.2m×1.0m) was made on the SHAKE Table. The left

chamber was filled with sand and compacted manually. Density of this sand was 1580 kg/m^3 and grain size distribution of the soil used was shown in Figure 3.9 .The left side chamber was used to investigate the primary effect of earthquake. On the other hand for the investigation of seismic hazard due to secondary effect the right side chamber was used. Strong motion accelerographs (SMA) were installed over the chambers to record the value of peak ground acceleration (PGA) as shown in Figure 3.8. Another SMA at the base of the soil (that is at the top of the SHAKE Table) is installed to record the acceleration. The acceleration of the right chamber on the SHAKE Table was expected to be different for different hazards. Sample preparation and output of different conditions are explained below.

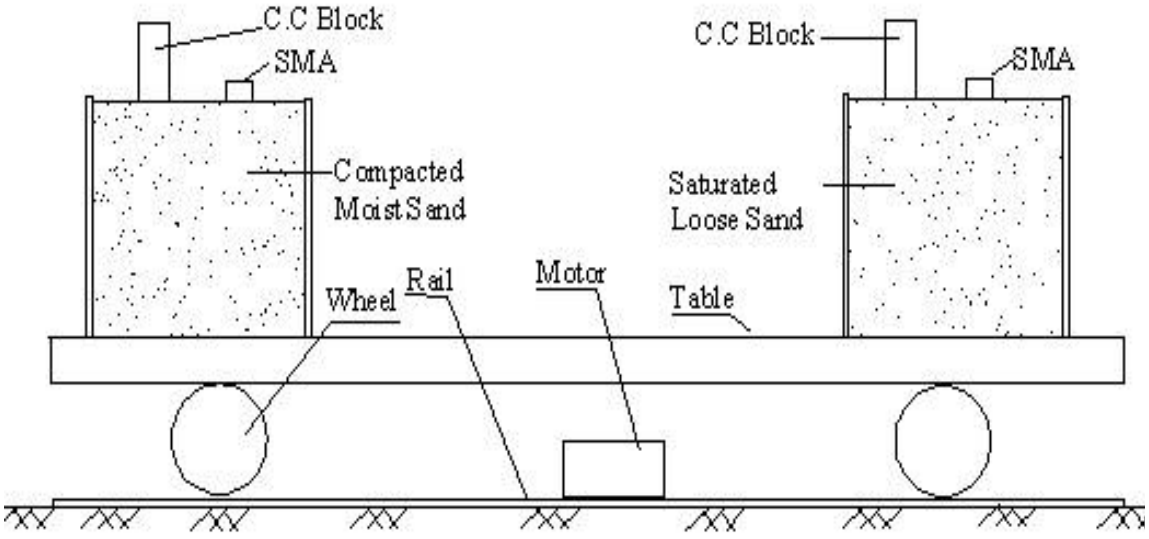

Figure 3.8a Schematic diagram of SHAKE table and investigation of liquefaction hazard

Figure 3.8b Indigenous of SHAKE table used in the BUET laboratory.

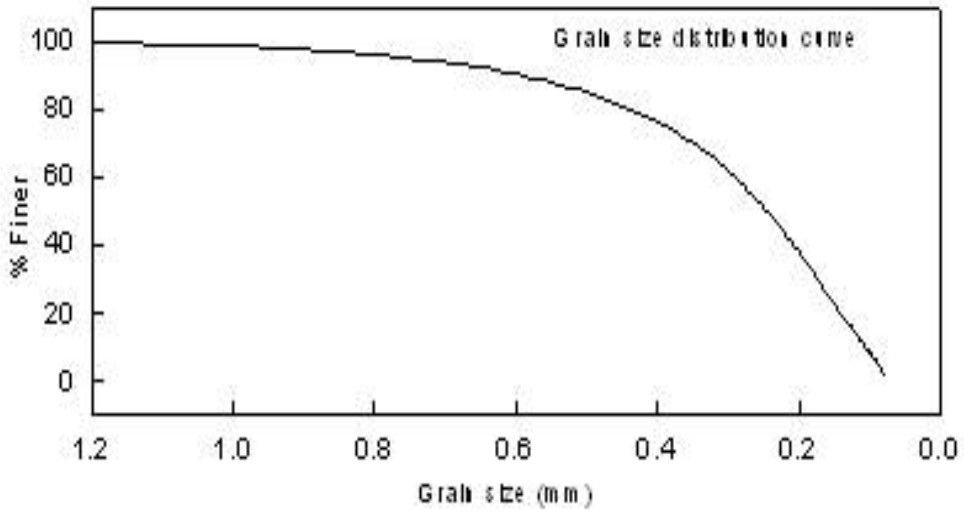

Figure 3.9 Grain size distribution curve for the soil used in the laboratory

3.4.2.1 Investigation of liquefaction

For the investigation of liquefaction, a saturated loose sample was prepared in the right chamber (see Figure 3.8) according to sedimentation method (Ishihara, 1993). Initially a depth of water of approximately 10 cm was maintained at the bottom of the chamber. Approximately from 10 cm high above the water surface dry sand was dropped into the water through a perforated cylindrical container (Figure 3.10) and diameter of each perforation was 1 ~ 2mm. As the thickness of sand layer gradually increases, the depth of water above the sand layer of about 10 cm is maintained by applying water into the chamber and dropping height of about 10 cm of dry sand through the cylindrical container is maintained carefully. Density of this saturated sand was 1345 kg/m^3. To investigate the liquefaction, a cement concrete block with a base pressure 1064 kg/m^2 was placed over the surface of the soil of the right chamber. Due to shaking, the soil in the right chamber liquefied but the left chamber did not. The arrangement and result of this experiment is shown in Figure 3.11. Figures 3.12 and 3.13 show that resultant horizontal acceleration due to liquefaction is 182 cm/s^2 and resultant horizontal acceleration due to ground shaking is 74 cm/s^2 . The corresponding values of MMI are 7.5 (MMI_{LIQ}) and 6.2 (MMI_{GS}). Trifunac and Brady (1975) relationship for converting PGA to MMI was used here. From this result, it can be seen

$MMI_{LIQ} - MMI_{GS} = 1.3$ i.e difference >1.

Therefore the following heuristic rule is used to quantify the seismic hazard due to liquefaction for regions with liquefiable soils:

$$MMI_{LIQ} = MMI_{GS} + 2 \quad (3.3)$$

Figure 3.10 Sample Preparation

Figure 3.11 Steps of liquefaction phenomena observed

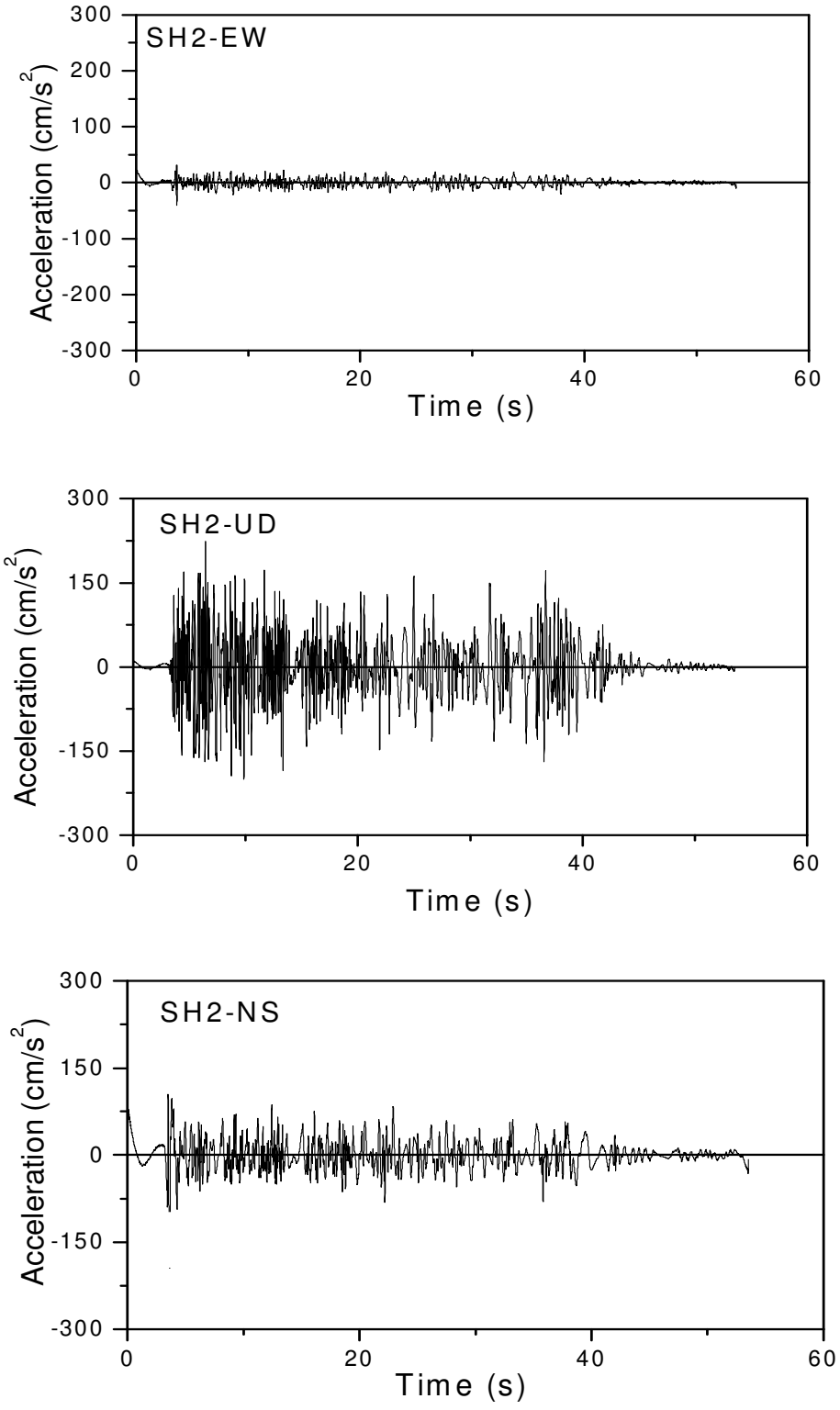

Figure 3.12 E-W, U-D and N-S acceleration due to ground shaking (Result from left chamber)

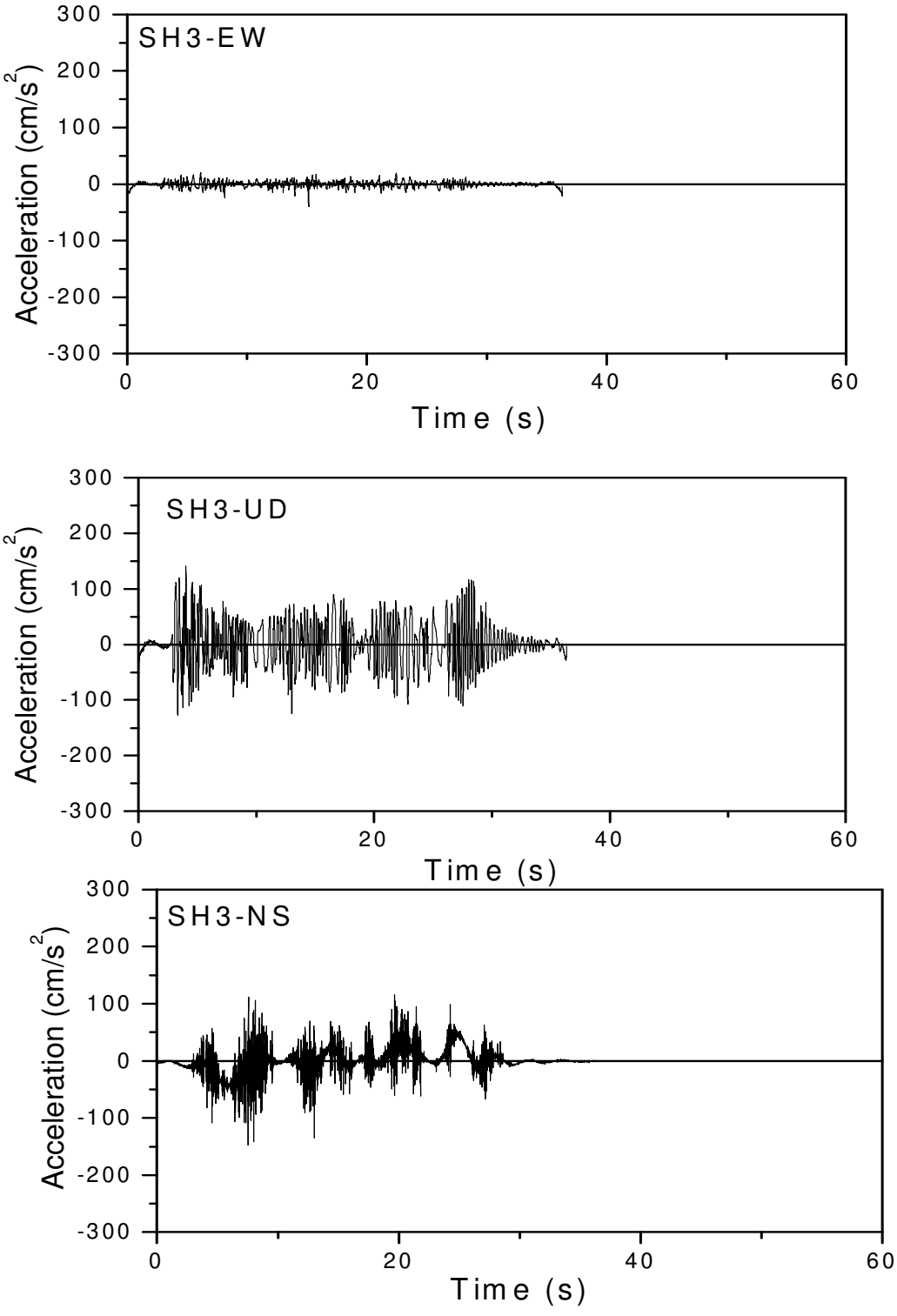

Figure 3.13 E-W, U-D and N-S acceleration due to liquefaction

3.4.2.2 Investigation of landslide

A model embankment was constructed in the right chamber of the SHAKE Table. The soil of the embankment was compacted manually. Density of the compacted soil was 1570 kg/m^3 and water content was 2.8 %. The angle of the sloping face of the embankment was approximately 46º. The slope angle of hills of our country varies from 0º to 90º. That is why an average slope angle (approximately 46 degree) was considered. The test arrangements and results are shown in Figures 3.14 to 3.17.

The resultant horizontal acceleration due to land slide is 170 cm/s^2 and the resultant horizontal acceleration due to ground shaking is 74 cm/s^2 as can be seen in Figure 11. The corresponding values of MMI are 7.4 (MMI_{LAN}) and 6.2 (MMI_{GS}). From this result it can be seen that

$MI_{LAN} - MMI_{GS} = 1.2$ i.e difference >1.

Therefore to quantify the seismic hazard due to landslide (MMI_{LAN}), the following heuristic rule may be assumed for regions with high possibility of land slide:

$$MMI_{LAN} = MMI_{GS} + 2 \quad (3.4)$$

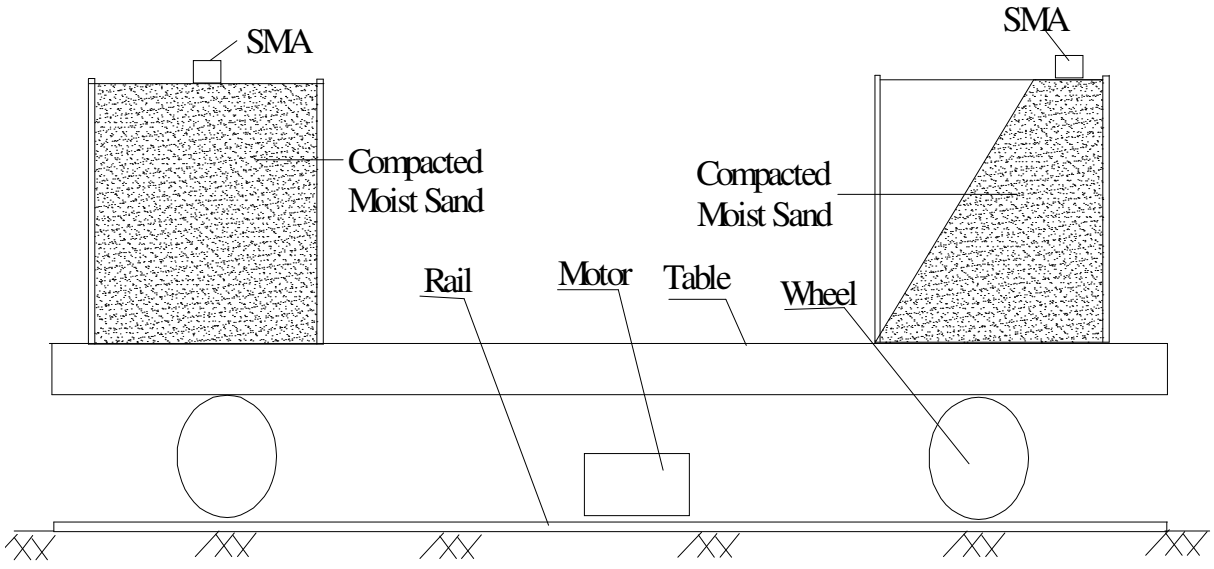

Figure 3.14 Schematic diagram of SHAKE table and investigation of landslide

Figure 3.15 Before land sliding

Figure 3.16 After land sliding

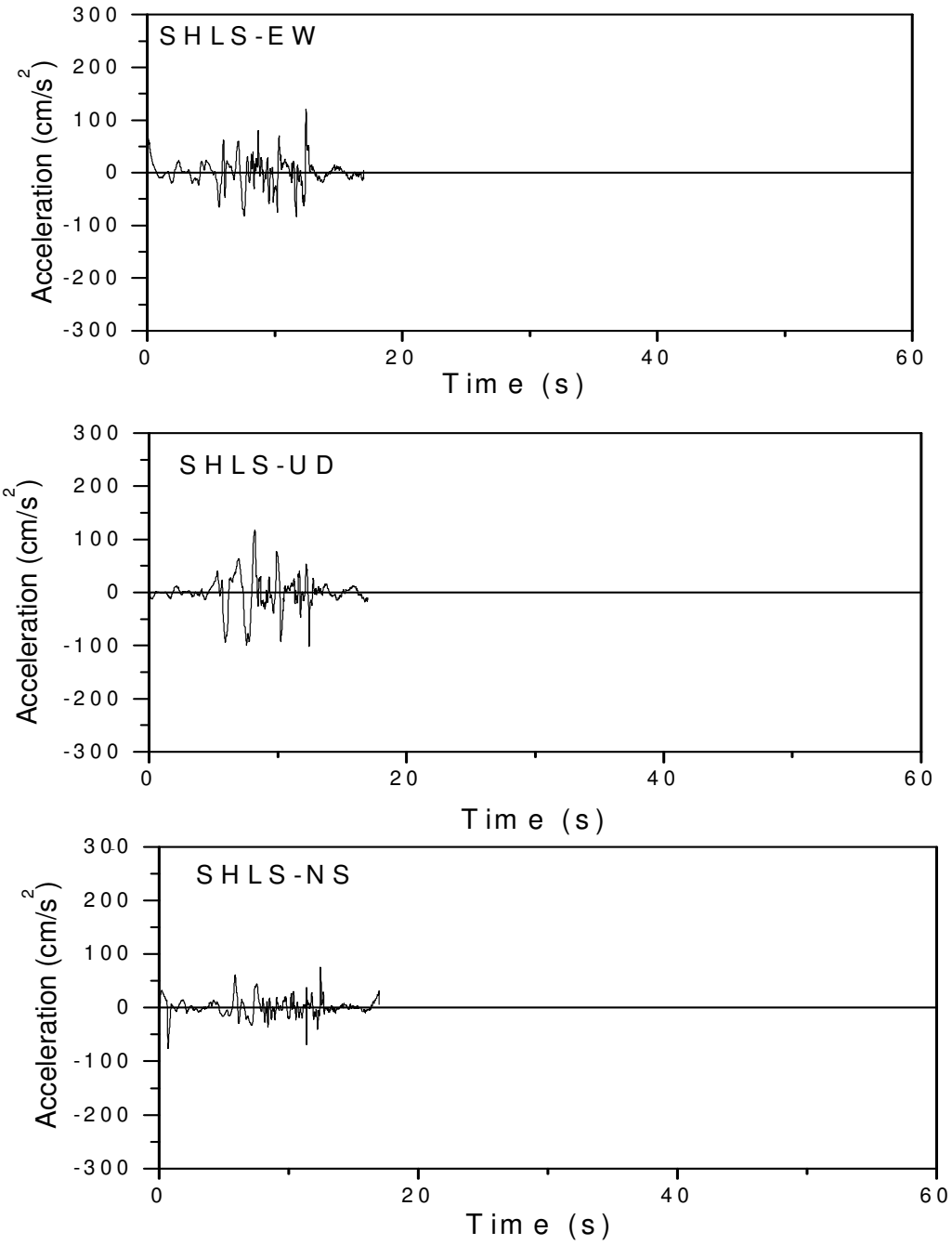

Figure 3.17 E-W, U-D and N-S acceleration due to landsliding

3.4.2.3 Investigation of fault rupture

An artificial fault was incorporated inside the right chamber of the SHAKE Table(Figure 3.17). The chamber was divided into two parts. In the right chamber a four-wheeler table of size 0.60 m ×1.10 m x 0.08 m high was placed at the bottom of the chamber as shown in Figure 3.17. At the top of the table two planks (thickness 2 cm) of 15 cm high was placed vertically widthwise across this table. Over these two vertical planks a wooden plank of size 0.60m ×1.10m was placed horizontally. The remaining half was initially empty. Moist sample was spread inside the chamber and compacted manually layer-by-layer and finally the compacted sample was prepared. Density of the sample was 1570 kg/m^3 and water content is 2.7 %. An SMA was placed over the sample. When an artificial earthquake was applied, the two vertical planks were displaced and the top wooden plank subducted. Vertical subduction at the surface was approximately 12 cm. The result obtained is shown in Figures 3.18 and 3.21.

The resultant horizontal acceleration due to fault rupture is 225 cm/s^2 and resultant horizontal acceleration due to ground shaking is 74 cm/s^2. The corresponding values of MMI are 7.75 (MMI_{FR}) and 6.2 (MMI_{GS}) as can be seen from Figure 15. From this result it can be seen that

$MMI_{FR} - MMI_{GS} = 1.55$ i.e difference >1.

Therefore to quantify the seismic hazard due to surface fault rupture (MMI_F), the following heuristic rule may be assumed for regions with high possibility of surface fault rupture i.e. at buffer zone:

$$MMI_{FR} = MMI_{GS} + 2 \quad (3.5)$$

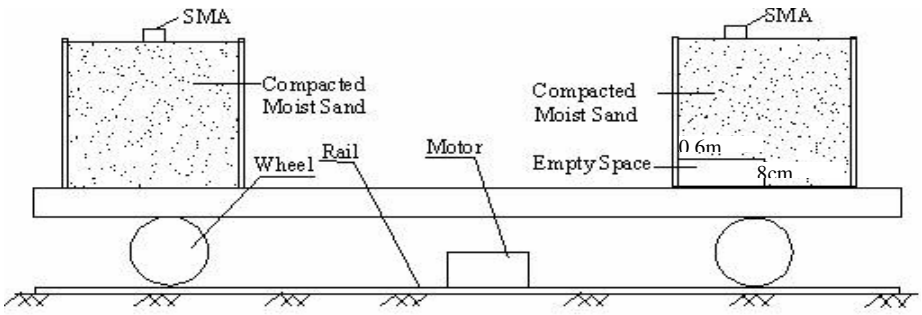

Figure 3.18 Schematic diagram of SHAKE table and investigation of surface fault rupture hazard

Figure 3.19 Before surface fault rupture occurs

Figure 3.20 After surface fault rupture occurs

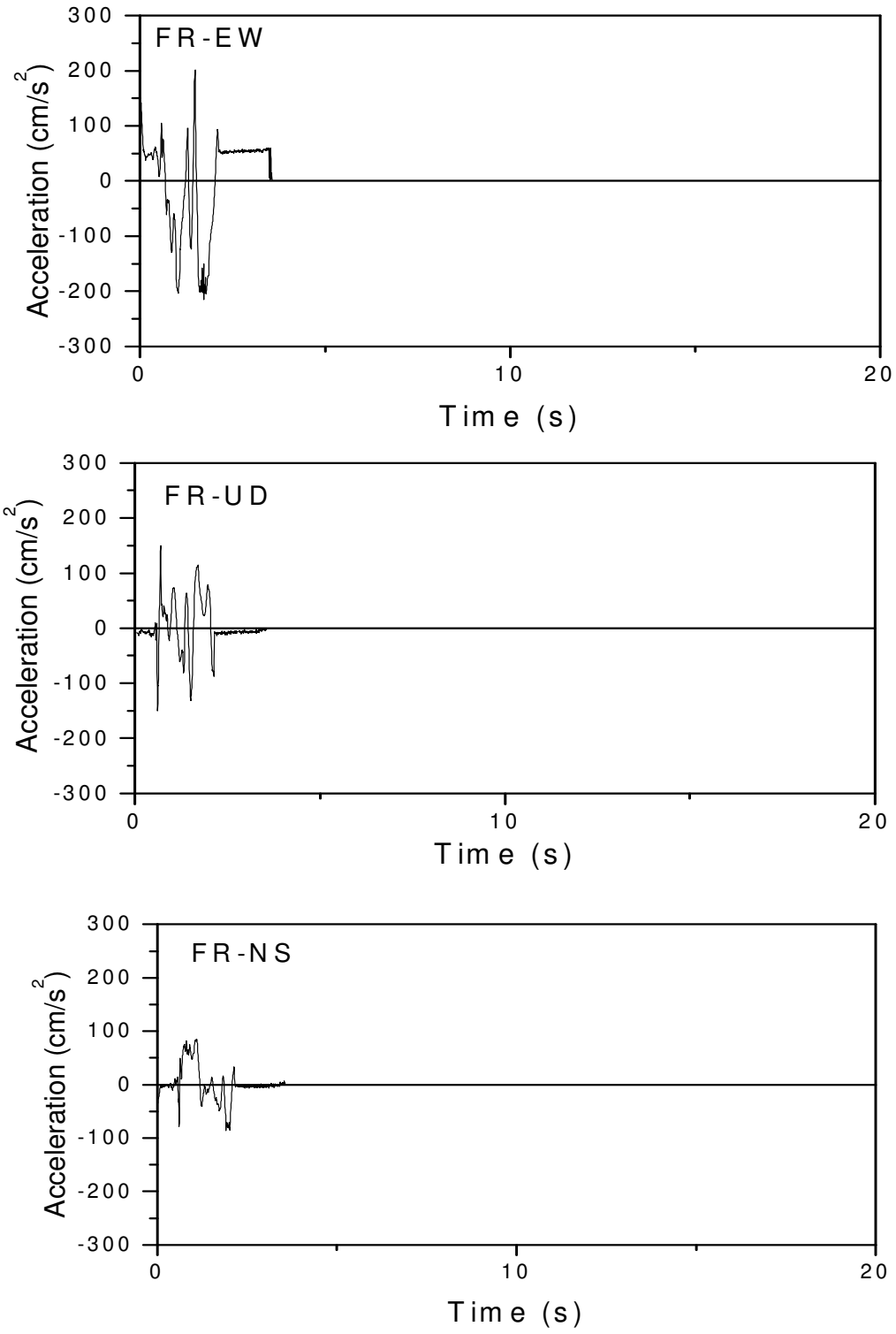

Figure 3.21 E-W, U-D and N-S acceleration due to fault rupture

3.4.3 Example Application

The hypothetical example presented in this section contains many simplifications to help illustrate the GIS-based seismic hazard integration methodology described in the previous section. The simplifications and assumptions correspond to the actual geologic and geotechnical information that is typically available for a comprehensive seismic hazard analysis conducted for a regional such as a city or country. The case study presented in Chapter 5 discusses the currently available regional hazard information and provides a more realistic example of the integration methodology. The simplified example of hazard combination for a hypothetical region is outlined below. The example maps and corresponding descriptions of the integration process are presented together for clarity.

Following steps for a simplified example of hazard integration for a hypothetical region is shown in Figure 3.22.

(a) Figure 3.22(a) shows the assumed fault map of the area. The analysis region is indicated by the small square.

(b) Figure 3.22(b) shows the regional distribution of bed-rock level shaking. For simplicity, the ground shaking parameter is assumed to be PGA. The values are computed by assuming a scenario event on the fault shown in Figure 3.22(a) and then applying an attenuation relationship to the region.

(c) Figure 3.22(c) shows the regional distribution of assumed PGA amplification factors based on the local geologic conditions in the area. The most commonly used transfer function model is included in the computer program SHAKE developed by Schnabel et al. (1972) can be used to determine amplification factor.

(d) Figure 3.22(d) shows the regional distribution of surface-level PGA values. This map is produced by over-laying the PGA amplification factor map shown in Figure 3.22(c) on the map of bedrock-level PGA values shown in Figure 3.22(b).

(e) It is assumed that the final combined seismic hazard will be quantified interms of Modified Mercalli Intensity (MMI). There are several relationships for converting PGA to MMI. The equation used here was developed by Trifunac and Brady (1975) and is given as:

$$\log(PGA) = 0.014 + 0.3\ (MMI) \quad (3.6)$$

Figure 3.22(e) shows the regional distribution of ground shaking hazard (MMI_{GS}). This map is developed by applying equation (3.6) to the map of surface level PGA values shown in Figure 3.22(d). The MMI scale is subjective and assigned as integer values, therefore the values in Figure 3.21(e) are rounded to the nearest 0.5.

(f) Figure 3.22(f) shows the buffer zones of 100 and 200 meters around the assumed fault rupture for the scenario event. The definition of these buffer zones is an example of the heuristics rules necessary to determine areas of surface fault rupture hazard.

(g) To quantify the seismic hazard due to surface fault rupture hazard, based on the laboratory investigation results the following heuristic rules are assumed for this example:

For regions in the 100 meter buffer zone:

$$MMI_{FR} = MMI_{GS} + 2 \quad (3.7)$$

For regions in the 200 meter buffer zone:

$$MMI_{FR} = MMI_{GS} + 1 \quad (3.6)$$

Otherwise:

$$MMI_{FR} = 0 \quad (3.8)$$

Figure 3.22(g) shows the regional distribution of surface fault rupture hazard (MMI_{FR}). This map is developed by over-laying Figure 3.22(f) on the map of ground shaking hazard (MMI_{GS}) shown in Figure 3.22(e) according to equation (3.7) through (3.8).

(h) Figure 3.22(h) shows the assumed regional distribution of critical surface PGA values (A_{crit}) required to induce liquefaction based on geotechnical investigations.

(i) Figure 3.22(i) shows the regional distribution of liquefiable soils. This map is produced by over-laying Figure 3.22(h) on the map of surface level PGA values shown in Figure 3.22(d). Areas with liquefiable soils ($A_{crit} \leq$ the surface level PGA) are shown in black.

(j) The following example heuristic rules are used to quantify the seismic hazard due to liquefaction:

For regions with liquefiable soils:

$$MMI_{LIQ} = MMI_{GS} + 2 \quad (3.9)$$

Otherwise:

$$MMI_{LIQ} = 0 \quad (3.10)$$

Figure 3.22(j) shows the regional distribution of liquefaction hazard (MMI_{LIQ}). This map is developed by over-laying Figure 3.22(i) on the map of ground shaking hazard (MMI_{GS}) shown in Figure 3.22(e) according to equations (3.9) and (3.10).

(k) Figure 3.22(k) shows the assumed qualitative description of landslide hazard in the region. Areas are designated as having “high”, “moderate”, “low”, or “very low” landslide potential.

(l) To quantify the seismic hazard due to landslide (MMI_{LAN}), based on the laboratory investigation results the following heuristic rules are assumed for this example:

For region designated as “high”:

$$MMI_{LAN} = MMI_{GS} + 2 \quad (3.11)$$

For region designated as “moderate”:

$$MMI_{LAN} = MMI_{GS} + 1 \quad (3.12)$$

Otherwise:

$$MMI_{LAN} = 0 \quad (3.13)$$

Figure 3.22(l) shows the regional distribution of landslide hazard (MMI_{LAN}). This map is developed by overlaying Figure 3.22(k) on the map of ground shaking

hazard (MMI_{GS}) shown in Figure 3.22(e) according to equations (3.11) through (3.13).

(m) The rules for combining the various hazards are based on expert opinion about the relative accuracy of the hazard information and the behavior of local geology. For this example, it is assumed that the ground-shaking hazard is the most accurate, followed by liquefaction, surface fault rupture, and landslide.

Also different types of structures, such as above ground and buried structures behaves differently when subjected to local site effects. Therefore in this hypothetical example, only seismic hazard to surface structures is considered.

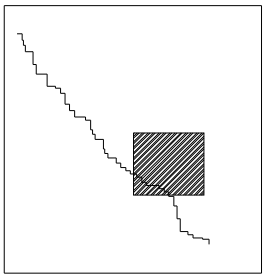

(a) Assumed fault map

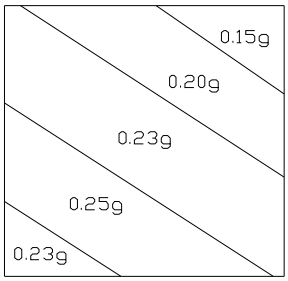

(b) Regional distribution of bed rock level PGA

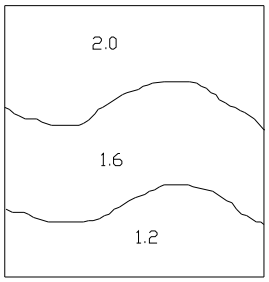

(c) Regional distribution of assumed PGA amplification factors

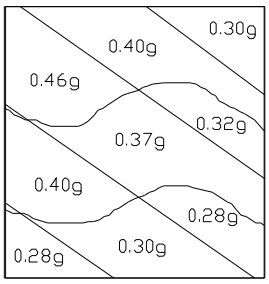

(d) Regional distribution of surface level PGA

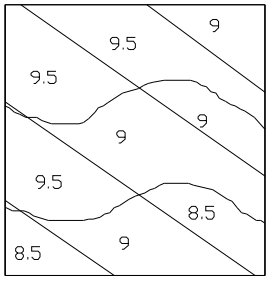

(e) Regional distribution of ground shaking hazard

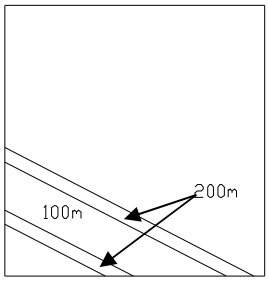

(f) Buffer zones for fault rupture hazard

Figure 3.22 Example of hazard integration for a hypothetical region

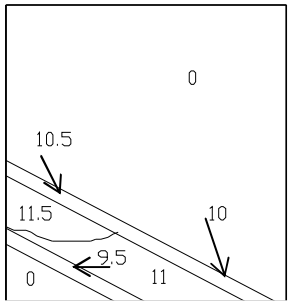

(g) Regional distribution of surface fault rupture hazard

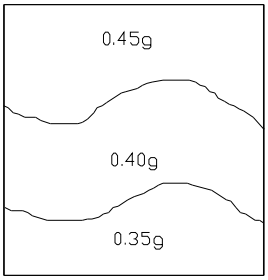

(h) Regional distribution of critical surface PGA values to induce liquefaction

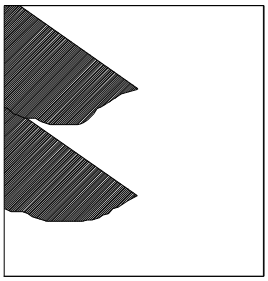

(i) Regional distribution of liquefiable soils

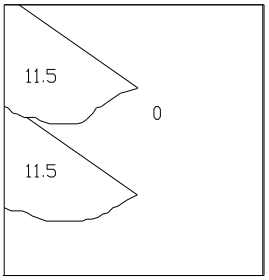

(j) Regional distribution of liquefaction hazard

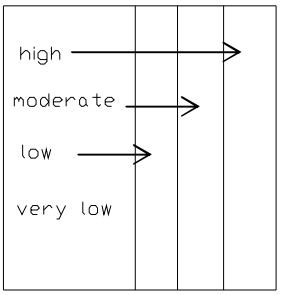

(k) Qualitative description of land slide hazard

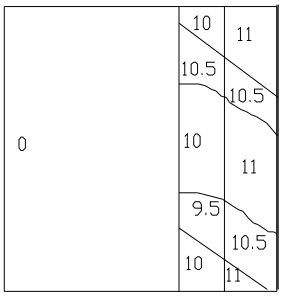

(l) Regional distribution of landslide hazard

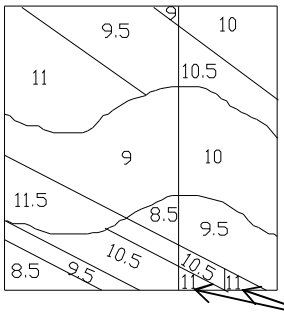

(m) Regional distribution of final combined hazard

Figure 3.22 (Contd.) Example of hazard integration for a hypothetical region

Typically there are up to four hazards to be combined, ground shaking plus one or more of the secondary site effect hazards. For this example, the eight possible combinations and their assumed weights are shown in Tables 3.1 and 3.2. The final combined hazard (MMI_C) is computed as a weighted sum of the various hazards. The weights in each rule must sum to 1.0. The additive factor in rules (b) through (h) in Table 3.1 is to account for the increase in hazard due to two or more hazards occurring.

Figure 3.21(m) shows the regional distribution of the final combined hazard (MMI_C) for this hypothetical example. This map is developed by over-laying the regional maps for each hazard shown in Figures 3.21(e), 3.21(g), 3.21(j) and 3.21(l) according to the rules listed in Table 3.1. The final values are rounded to the nearest 0.5 to account for the subjectivity of the MMI scale.

Geological formation of Bangladesh is very complex. Geological map of Bangladesh prepared by Geological Survey of Bangladesh (GSB) consists of geological units and geological profile throughout the country. From the study of geology, geotechnical properties of soil and considering the location of hillock areas Bangladesh has been divided into two areas to simplify the study of seismic hazard (Figure 3.23). Area 1 is basically area of low liquefaction potential zone; on the other hand area 2 is the area of without hillock areas and high liquefaction potential. The heuristic rules for hazard integration for these two areas of Bangladesh have been shown in Tables 3.1 and 3.2.

The numerical computations carried out in the GIS during this hazard integration can be illustrated by considering the small area indicated by “A” (in the Area 1 of Bangladesh) on Figure 3.22(m). This area has a final combined seismic hazard of $MMI_C = 11$, computed as follows:

$MMI_{GS} = 9$	(see Figure 3.22 (e))
$MMI_{FR} = 11$	(see Figure 3.22(g))
$MMI_{LIQ} = 0$	(see Figure 3.22(j))
$MMI_{LAN} = 10$	(see Figure 3.22(I))

Rule (g) from Table 1 applies for this area and is given as:

$MMI_C = 0.40MMI_{GS} + 0.30MMI_{FR} + 0.30\ MMI_{LAN} + 1.0$

which results in:

$MMI_C = 0.40 \times 9 + 0.30 \times 11 + 0.30 \times 10 + 1.0 = 10.89 \approx 11$

The example presented here is only hypothetical and cannot be compared to empirical data. The intent is to illustrate the general methodology for a GIS-based integration of the seismic hazards associated with local site effects. Several simplifying assumptions were made, but the integration process can easily be extended to include more analytical hazard models, different heuristic region-specific combination rules, and empirical data verification.

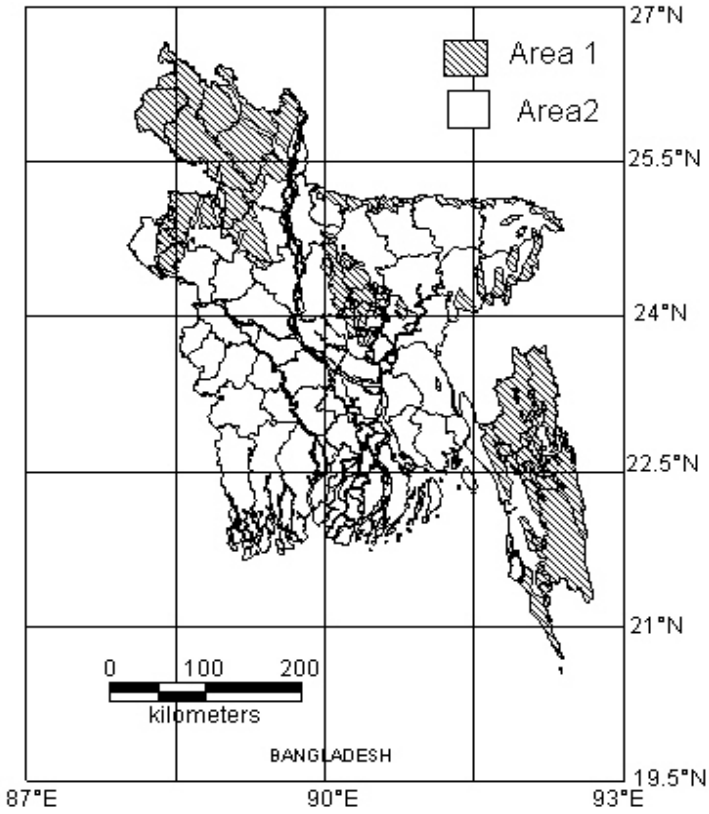

Figure 3.23 Zonation of Bangladesh on the basis of geological units (after Alam et al. 1990)

Table 3.1 Example heuristic rules for seismic hazard integration (FOR AREA 1)

RULE	POSSIBLE HAZARDS	WEIGHTING SCHEME FOR FINAL COMBINED HAZARD
(a)	ground shaking	$MMI_C = MMI_{GS}$
(b)	ground shaking + liquefaction	$MMI_C = 0.55MMI_{GS} + 0.45MMI_{LIQ} + 0.5$
(c)	ground shaking + fault rupture	$MMI_C = 0.55MMI_{GS} + 0.45MMI_{FR} + 0.5$
(d)	ground shaking + landslide	$MMI_C = 0.60MMI_{GS} + 0.40MMI_{LAN} + 0.5$
(e)	ground shaking + liquefaction + fault rupture	$MMI_C = 0.40MMI_{GS} + 0.25MMI_{LIQ} + 0.35MMI_{FR} + 1.0$
(f)	ground shaking + liquefaction + landslide	$MMI_C = 0.40MMI_{GS} + 0.30MMI_{LIQ} + 0.30MMI_{LAN} + 1.5$
(g)	ground shaking + fault rupture + landslide	$MMI_C = 0.40MMI_{GS} + 0.30MMI_{FR} + 0.30MMI_{LAN} + 1.0$
(h)	ground shaking + liquefaction + fault rupture + landslide	$MMI_C = 0.30MMI_{GS} + 0.20MMI_{LIQ} + 0.25MMI_{FR} + 0.25MMI_{LAN} + 1.5$

NOTES:

MMI_C must be less than or equal to 12.

MMI_{GS} = ground shaking hazard from Figure 3.22(e).

MMI_{FR} = surface fault rupture hazard from Figure 3.22 (g).

MMI_{LIQ} = liquefaction hazard from Figure 3.22(j).

MMI_{LAN} = landslide hazard from Figure 3.22(l).

Table 3.2 Example heuristic rules for seismic hazard integration (FOR AREA 2)

RULE	POSSIBLE HAZARDS	WEIGHTING SCHEME FOR FINAL COMBINED HAZARD
(a)	ground shaking	$MMI_C = MMI_{GS}$
(b)	ground shaking + liquefaction	$MMI_C = 0.55MMI_{GS} + 0.45MMI_{LIQ} + 0.5$
(c)	ground shaking + fault rupture	$MMI_C = 0.60MMI_{GS} + 0.40MMI_{FR} + 0.5$
(d)	ground shaking + liquefaction + fault rupture	$MMI_C = 0.40MMI_{GS} + 0.35MMI_{LIQ} + 0.25MMI_{FR} + 1.0$

NOTES:

MMI_C must be less than or equal to 12.

MMI_{GS} = ground shaking hazard from Figure 3.22(c)

MMI_{FR} = surface fault rupture hazard from Figure 3.22(g)

MMI_{LIQ} = liquefaction hazard from Figure 3.22(j)

3.5 Summary

A detailed description of geographic information system was presented in this Chapter. Graphic and non-graphic and data types and non-graphic data and the database management capabilities of a GIS were discussed in Section 3.1.

Section 3.2 presented the sequence of regional seismic hazard and risk analysis. Section 3.3 discussed the application of GIS to regional seismic hazard and risk analysis.

A GIS-based seismic hazard integration methodology was described in section 3.4.The general steps for combining the hazard associated with ground shaking, liquefaction, landslide, and surface fault rupture in a heuristic weighted average approach were identified. A hypothetical example was included to illustrate the integration methodology.

In section 3.4.2 an attempt was made to investigate and distinguish the PGA/intensity values of a region due to liquefaction, land slide and fault rupture. To generate artificial earthquake a locally built SHAKE Table was used which is a four-wheeler table. Two Chambers of equal size (1.2m×1.2m×1.0m) was made on the SHAKE Table. The left chamber was filled with sand and compacted manually. The left side chamber was used to investigate the primary effect of earthquake. By analyzing the data of ground motion obtained from the two chambers, quantification of secondary site effects of fault rupture, liquefaction, and landslide were made possible. In this research secondary site effects were studied in the laboratory for a particular soil. Based on these results and using some simplifying assumptions relation between the primary effects and secondary effects were developed. By using different types of soil the simplifying assumption for the relation between the primary site effect and secondary effects may be improved.

CHAPTER 4

STRONG MOTION MONITORING SYSTEMS IN BANGLADESH AND DEVELOPMENT OF ACCELERATION BASED ATTENUATION RELATION

4.1 General

Earthquake is one of the most feared natural disasters, which can cause incalculable destruction of properties and human lives. An examination of the historical catalogue of Bangladesh and its surrounding region reveal that several earthquakes of large magnitude with epicenters within this region have occurred in the past. The 1897 Great Indian earthquake with a magnitude of 8.7 (Oldham, 1899) is one of the strongest earthquakes in the world, had its epicenter only 230 km from Dhaka. While the earthquake affected almost whole of Bangladesh, damages were very severe particularly in Sylhet, Rangpur and Mymensingh. In the city of Dhaka most of the brick masonry buildings either collapsed or were severely damaged. The low incidence of severe earthquakes during this century has led to a situation where most of the population and policy makers do not perceive seismic risk to be important. The rapid urbanisation, development of critical engineering works, industrialisation of cities with modern types of buildings and the concentration of populations living or settling in hazardous areas are matters of growing concern, as these are likely to contribute to heavier loss of life and increase considerably the costs of disaster damage. In recognition of the threat to the major investment at risk in this part of the world from strong earthquakes, government of the respective countries should multiply and join their efforts to continue the study and analysis of the seismicity of the region in order to reduce the earthquake risk. The first step in mitigating the risk of the community from earthquake hazard is an assessment of the hazard itself.

Macroseismic earthquake data of the large historical earthquakes are important for seismic hazard analysis. The relationship between magnitude, epicentral distance and peak ground acceleration of these earthquakes constitute the basic parameter needed for assessing seismic hazard at a given site. The purpose of this study is to present a predicting model for acceleration-attenuation for earthquakes in Bangladesh and its neighboring region.

4.2 Objectives

During the last two centuries, Bangladesh and its neighbouring region have experienced several large earthquakes. The peak ground acceleration of these earthquakes has been estimated using different existing attenuation law. But for earthquake hazard analysis, unified acceleration attenuation relationship for Bangladesh is required. The major objectives of this chapter are as follows:

a) To compile a strong motion data base of Bangladesh.

b) To develop acceleration based attenuation relationship for Bangladesh and its surrounding region.

4.3 Earthquake monitoring system in Bangladesh

In July 2003, seven digital accelerometers were deployed for the first time in Bangladesh funded by Jamuna Bridge Authority (JMBA). Two were located in East and West end of the bridge and four were located in LGED offices in Natore, Bogra, Mymensingh and Gazipur and the last one in BUET. In April 2005, thirty-four analog SMAs obtained from USGS were deployed in free-field (on ground) at different PWD offices all over Bangladesh. Also in March 2010, another twenty five digital accelerometer were deployed in PWD offices all over Bangladesh. These accelerometers give data in North-South, East-West and Up-Down direction. The initial goal of the project is to develop an earthquake time history database for different soil condition and different earthquakes of Bangladesh. After compilation of a number of earthquakes, this database will be used to develop attenuation law for Bangladesh.

4.3.1 Earthquake records

From April 2005 to November 2010, these SMAs / free field stations recorded the following earthquakes:

- May 30, 2006 : Bay of Bengal Earthquake
- August 05, 2006 : Jessore Earthquake
- November 03, 2006 : Myanmar-India Earthquake
- November 10, 2006 : Bangladesh-India Earthquake
- July 28, 2007: India-Myanmar Earthquake

- November 07, 2007: Bangladesh-Myanmar Earthquake (1)
- March 20, 2008: Modhupur Earthquake
- July 05, 2008: Rajshahi Earthquake
- July 27, 2008: Haluahhat Earthquake
- August 23, 2008: Bangladesh-Myanmar Earthquake (2)
- January 06, 2009: Tangail Earthquake
- September 21, 2009: Bhutan Earthquake
- September 10, 2010: Chandpur Earthquake
- September 11, 2010: Bangladesh - India Earthquake (Meghalay)

As a result of continuous monitoring in the last five years of the monitoring phase, fourteen earthquakes have been detected at the SMA site. At first on May 30, 2006, a small earthquake was recorded at 19:43:51 hrs BST, (13:43:51 hrs GMT, May 30, 2006) at the Chittagong site and Name of Earthquake Bay of Bengal earthquake. Its Magnitude was 4.7 and depth was 29 km.This is,the first earthquake recorded by the stations since their installation. Epicentre of this earthquake lies close to the SMA site. Last on September 21, 2009 the free-field stations recorded Bhutan Earthquake. Panchagarh, Dinajpur, Lalmonirhat, Rangpur and Airport Hazi-camp at 14:40:45 hrs BST (08:40:45 hrs GMT, September 21, 2009). Its Magnitude was 5.5 and depth was 16 km. Maximum acceleration of this earthquake in Dinajpur was -48.0967 cm/sec.^{2} and it was in East-West direction. Figure 4.1 shows SMA and Earthquake locations. Figure 4.2 and 4.3 shows free fiend stations and its output respectively. Summary of recorded earthquake events with different accelerometer are shown in Table 4.1 and Table 4.2. Acceleration of previous earthquakes which were not recorded directly in Bangladesh is shown in Table 4.3. Trifunac and Brady (1975) relationship for converting PGA to MMI was used to convert MMI to peak ground acceleration. and are shown in Table 4.4. Using data from Table 4.2, the data obtained from SMAs were plotted(Figure 4.4). Although, the higher PGAs were obtained for higher magnitudes but due to lack of enough data, no proper attenuation reltionship can be developed.

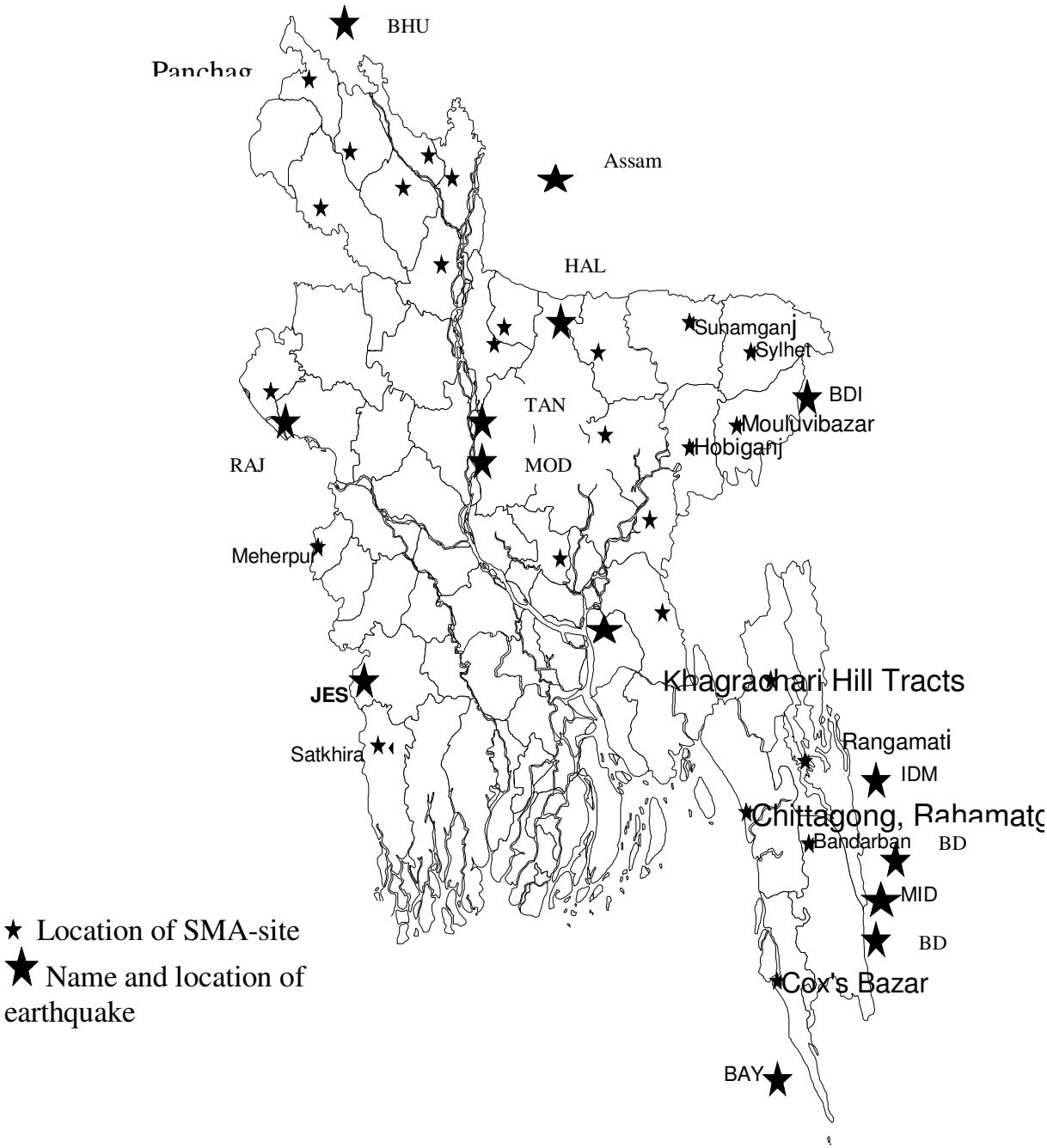

Figure 4.1 SMA locations and locations of recent earthquake in and around Bangladesh

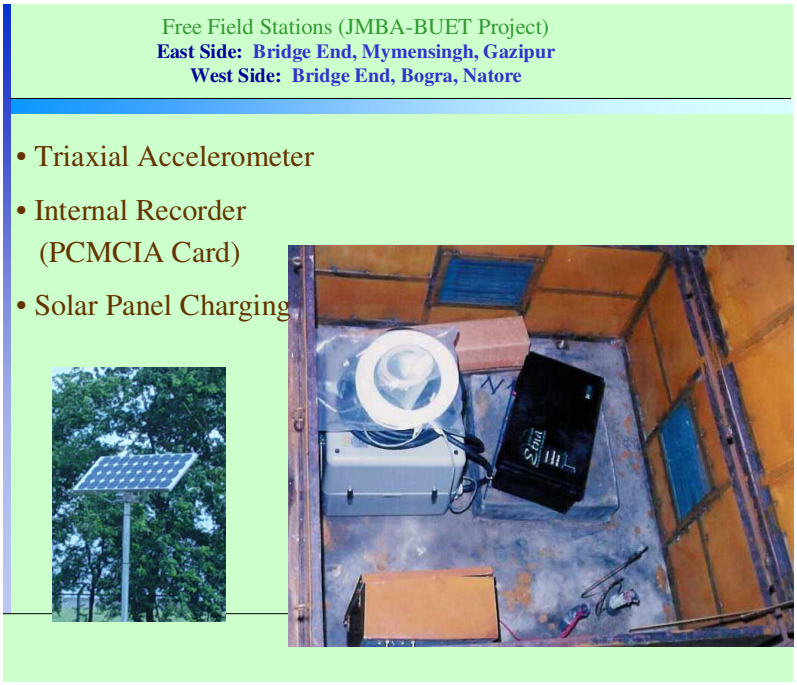

Figure 4.2 Free Field Station

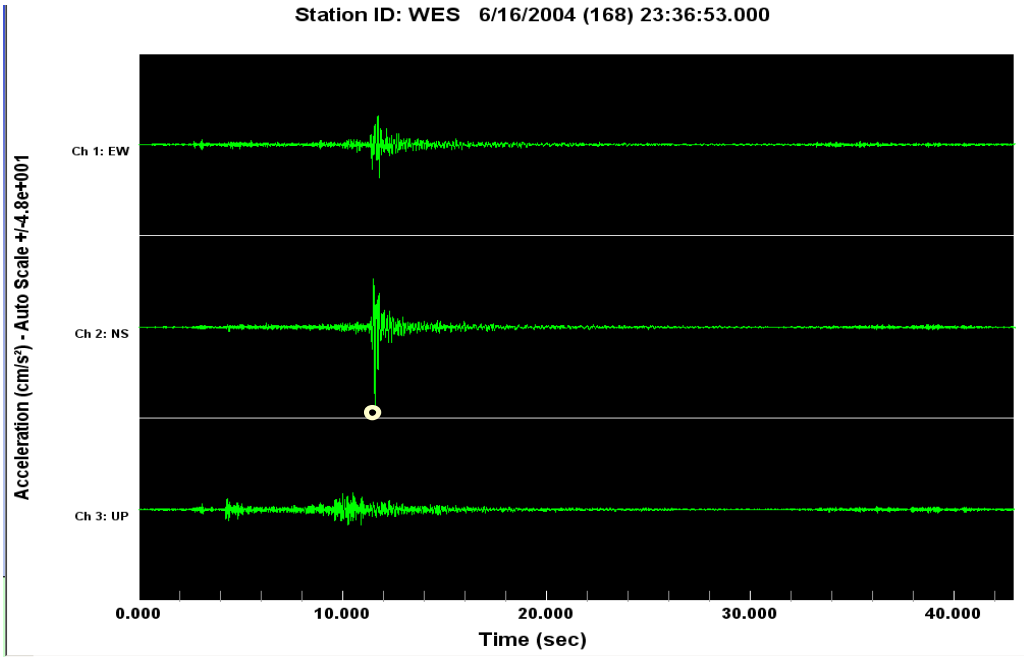

Figure 4.3 Acceleration –time history recorded at West end of Jamuna Bridge, Sirajganj.

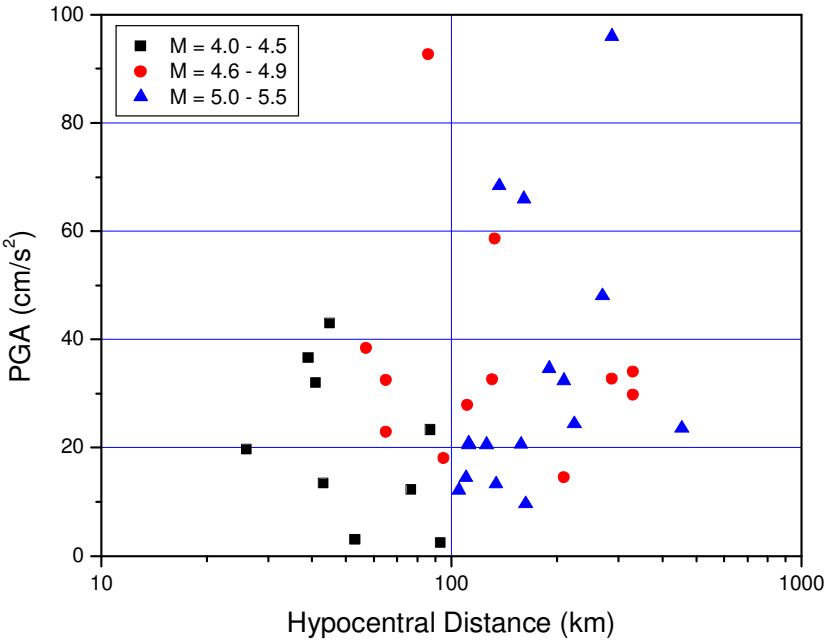

Fig 4.4 Observed earthquake data from SMA

4.4 Development of attenuation relation for Bangladesh

The study of attenuation of earthquake ground motions with respect to distance has been an important part of earthquake engineering. Its application to seismic hazard and/or seismic risk analysis is of great importance. Although the collection of recorded ground motion spurred various studies, most are for shallow earthquakes, especially the data from the Bangladesh and surrounding region. However, there are many earthquakes that have larger focal depths especially for subduction zones like those in Japan, the Philippines, etc.

The attenuation of ground motion from intermediate-depth earthquakes may be quite different from shallow earthquakes given the difference in fault mechanisms and path characteristics. Ground motions from deeper earthquakes have been observed to be stronger than shallow earthquakes for the same magnitude and distance. This chapter presents the results of the attenuation of earthquake ground motion based on events with focal depths of up to 70 km.

The data used in this part of the study are taken from recording stations of SMA described in Section 4.3.1.

Since the recording stations of this data set are fixed and there are many stations with several recordings, it is possible to consider the local site effect for each station. Usually,

the amplification effect of the soil layer is taken into account. But the amplification effect also depends on the local geography and site peculiarities. By considering the effect of each recording station, the "true" local site effect in included is the analysis.

The main objective is to determine the characteristics of the attenuation of seismic ground motion for intermediate-depth events and to develop attenuation equations that can be used for shallow to intermediate-depth earthquakes.

4.4.1 Attenuation model

Several regression models for the empirical determination of the attenuation of ground motion have been proposed. Examples of these are reviewed by Boore and Joyner (1982), Campbell (1985), and Joyner and Boore (1988). In this study, the initial model is based on the attenuation of body waves in an elastic medium from a point source (Joyner and Boore, 1981; Ohno, et al., 1993) and given as

$$\log y = b_0 + b_1 M + b_2 R + b_3 \log R \qquad (4.1)$$

where y is the ground motion index under consideration; in this study, y is the larger of the two horizontal components; M is the magnitude, R is the slant distance between the source and the recording station, and b_i's are the coefficients to be determined. The term $b_2 R$ represents an elastic attenuation and the term $b_3 \log R$ represents geometric spreading. The location of the source is generally assumed to be the center of energy release, which could be estimated by the size of the ruptured fault or by the centroid of the aftershock cluster, if aftershocks are recorded. In the near-field, the definition of distance becomes critical (Joyner and Boore, 1982) especially for earthquakes with a large fault extent. Ohno et al. (1993) showed that by redefining the distance with respect to the fault extent, the attenuation in the near-field becomes consistent with the attenuation of the far-field. In this study, R is defined as the shortest distance from the recording site to the fault extent. Since the effect of the change in distance definition regression is small in the far-field and for small events, the use of hypocentral distance is practical and justified.

Ground motion of deep earthquakes is generally stronger than that of shallow earthquakes with the same magnitude and source-distance. Figure 4.4 shows the recorded PGAs for the Bangladesh-India (2006), Haluaghat (2008) and Bhutan (2009) earthquakes, with

magnitudes 5.0, 4.8 and 5.5 respectively in blue triangles. The focal depths 33 km, 44 km and 60 km respectively. It can be seen clearly that the ground motion for the Bhutan (2009) earthquake is significantly stronger for the same distance. An additional regressor variable for the depth to account for this effect can improve the regression fitting (Crouse, et al., 1988; Annaka and Nozawa, 1988).

Effect of local ground condition is another important condition is another important factor. Usually attenuation equations are defined separately for rock and soil sites. Some use three or four soil type classifications. A common technique to consider ground condition is using a dummy variable for each ground type (Mc Guire, 1978; Kawashima et al., 1986). Since the recording stations in this case are fixed and many records come from a given site, it is possible to consider the local site effect for each station. This effect can be verified by examining the residuals with respect to the recording station. Regression is then performed by assigning a dummy variable for each site (Draper and Smith, 1981). The regression model is then given by

$$\log y = b_0 + b_1 M + b_2 R + b_3 \log R + b_4 h + \sum_{i=1}^{N} c_i S_i \tag{4.2}$$

where h is the depth in kilometers of the point in the fault plane that is closest to the recording site, c_i's are the station coefficients and $s_i = 1$ for station i, $S_i = 0$ otherwise.
A preliminary analysis was performed to verify the significance of the depth term and station coefficient to the regression (Molas and Yamazaki 1994). Equation 4.2 can be expanded in matrix form as:

$$\begin{Bmatrix} \log y_1 \\ \log y_2 \\ . \\ . \\ \log y_n \end{Bmatrix} = \begin{bmatrix} 1 & M_1 & R_1 & \log R_1 & h_1 . S_{1.1} & \ldots & S_{N-1,1} \\ 1 & M_2 & R_2 & \log R_2 & h_2 . S_{1.2} & \ldots & S_{N-1,2} \\ . & . & . & . & . \; . \; . & \ldots & . \\ . & . & . & . & . \; . \; . & \ldots & . \\ 1 & M_n & R_n & \log R_n & h_n . S_{1.n} & \ldots & S_{N-1,n} \end{bmatrix} \begin{Bmatrix} b_0 \\ . \\ b_4 \\ ..... \\ c_1 \\ . \\ c_{N-1} \end{Bmatrix} + \begin{Bmatrix} \varepsilon_1 \\ \varepsilon_2 \\ . \\ . \\ \varepsilon_n \end{Bmatrix} \tag{4.3}$$

where n is the number of records, N is the number of recording stations, and ε_i associated with residual. If the jth data recorded in the Nth station, the S_{ij} is taken as –1.0 for i = 1 to N –1. In notation form:

$$Y = X\beta + \varepsilon \tag{4.4}$$

and the least square solution is

$$b = (X^T X)^{-1} X^T Y \tag{4.5}$$

where b is the estimator of β and the expected value of E(b) is β.

The coefficient of the Nth station is

$$C_N = -\sum_{i=1}^{N-1} c_i \tag{4.6}$$

These preliminary analyses justify the inclusion of the depth term and the station coefficients in the attenuation model.

4.5 Results and discussion

In this study, the model is based on the attenuation of body waves in an elastic medium from a point source (Joyner and Boore, 1981; Ohno, et al., 1993). Equations 4.1 were used to regress the 37 acceleration data from 12 events (Table 4.2). But for a specific earthquake, number of recorded acceleration value is few. Using these limited data the output will not be satisfactory. More data is needed to regress and formulate a reliable attenuation relation. The number of intensity based observed data (Table 4.3 and Table 4.4) are more than acceleration based observed data. Intensity of these events was converted to acceleration. These converted 40 acceleration data from 8 events (which includes larger magnitude) were regressed. The results of the regressions are given below:

$$Y = 100.49 + 104.44M - 0.075r - 221.05 \log r \tag{4.7}$$

$$Y = 196.16 + 57.34M + 0.11r - 242.2 \log r, M < 8 \tag{4.8}$$

$$Y = 337.21 + 54M + 0.208r - 305.73 \log r, 5.5 < M < 8 \tag{4.9}$$

where Y is PGA in cm/s^2, M is magnitude of earthquake and r is the hypocentral distance in km. For different values of M (eg. 5, 6 and 7) acceleration against distance were plotted using equation (4.8) and shown in Figure 4.5. Some observed data obtained from digital system mentioned earlier are plotted and shown in Figure 4.5. Although, the higher PGAs were obtained for higher magnitudes but due to lack of enough data, no proper attenuation relationship can be developed.

Due to the large number of records for each station, it is possible to determine the station coefficient which is a kind of correction term for the amplification / deamplification of the ground motions relative to other recording stations. It is generally accepted that softer soils tend to amplify the earthquake ground motion relative to rock and stiff soils. However, other local site conditions such as geology and topography may also affect amplification. By considering recording stations individually, these effects are automatically included.

Since from the recorded data it can be seen that the earthquakes are shallow-focus earthquakes that is why depth effect has not been considered. Some recorded stations are analogue and some are digital system. Data collected from the digital system obviously be better than the data collected from SMA (analogue system). Therefore after obtaining more data from digital system the attenuation relation (equation 4.7 to 4.9) can be updated and improved.

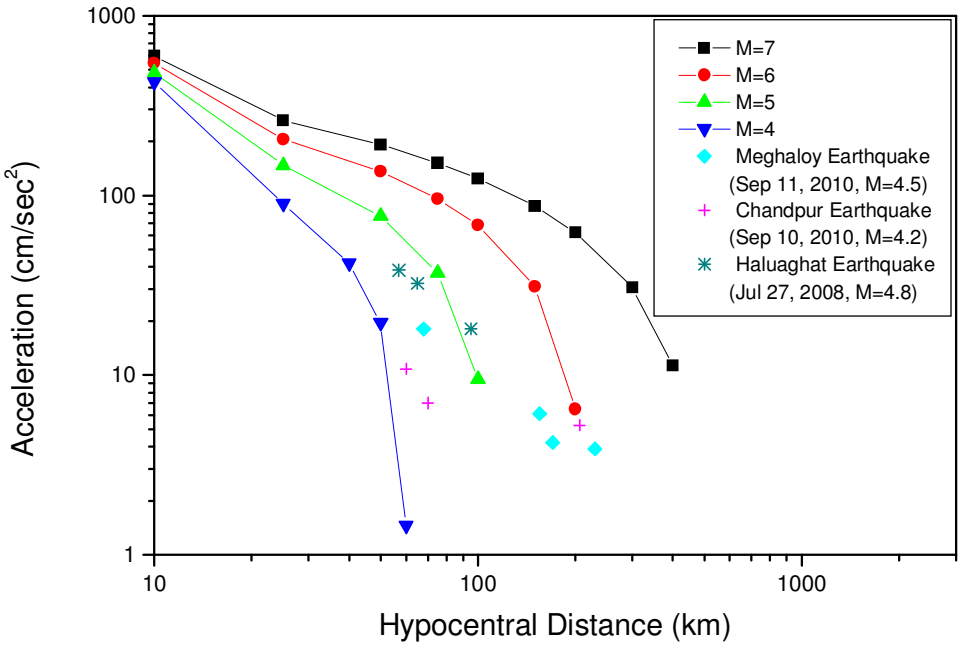

Figure 4.5 Acceleration against hypocentral distance relationship

Table 4.1 Summary of recorded earthquake events at different locations

Name of the earthquake	CODE	Occurrence date	Latitude (deg.)	Longitude (deg.)	Magnitude	Depth (km)	Maximum recorded acceleration (cm/sec^2)	Recorded site
Bay of Bengal	BAY MAY30 2006	30.05.2006	20.60°N	91.94°E	4.7	29	16.0	Agrabad, Rahamatganj and Coxbazar
Jessore	JES AUG 05 2006	05.08.2006	23.10°N	89.20°E	4.0	15	24.0	Meherpur and Sathkhira
Mynmar-India	MID NOV 03 2006	03.11.2006	22°N	93.30°E	5.2	33	34.0	Rahamatganj, Coxbazar, Bandanbhan, Khagrachari and Rangamati
Bangladesh-India	BDI NOV 10 2006	10.11.2006	24.60°N	92.60°E	5.0	33	34.0	Sylhet, Sunamganj, Moulovibazar and Hobiganj
India-Mynmar	IDM JUL 28 2007	28.07.2007	22.80°N	93.30°E	4.8	15	32.0	Rahamatganj, Bandarbhan, Khagrachari and Rangamati
Bangladesh-Myanmar	BDM NOV 07 2007	07.11.2007	22.80°N	92.60°E	5.3	15	96.0	Rahamatganj, Bandarbhan, Khagrachari,Cox'sbazar and Rangamati
Modhupur	MOD MAR 20 2008	20.03.2008	23.60°N	89.75°E	4.2	25	32.0	Airport Hazicamp ,jamalpur and Serajganj Jamuna Bridge east and west end.
Rajshahi	RAJ JUL 05 2008	05.07.2008	24.4°N	88.5°E	4.1	29	42.9893	Chapai-nawabganj
Haluaghat	HAL JUL 27 2008	27.07.2008	23.60°N	91.20°E	4.8	44	54.3198	Sherpur, Jamalpur, Netrokona, Kishoreganj, Hobiganj, Rangpur and
Bangladesh-Myanmar	BDM AUG 23 2008	22.08.2008	22.80°N	92.60°E	4.9	25	58.5964	Rangamati, Bandarban and Chittagong(Rahmatganj)
Tangail	TAN JAN 06 2009	06.01.2009	24.39°N	89.75°E	4.0	10	19.72705	Jamuna-bridge East site, West site, Bogra and Natore
Bhutan	BHU SEP 21 2009	22.09.2009	24.50°N	88.75°E	5.5	60	48.0967	Panchagarh,Dinajpur,Lalmonirhat,Rangpur and Airport Hazi-camp.
Chandpur	CHAND SEP 10 2010	10.09.2010	23.50°N	90.50°E	4.2	-	10.8200	Brahmanbaria, Sherpur, Hazicamp (Dhaka) and GSB(Dhaka)
Assam	MEGHA SEP 11 2010	11.09.2010	26.00°N	90.20°E	4.5	-	18.07	Panchgarh, Kurigram, Natore and Bogra.

Table 4.2 Summary of recorded earthquake events at different locations with specific value of acceleration and distances from the sources

Name of earthquake	Occurance date	M	Depth, h (km)	Distance, d (km)	$R=\sqrt{(d^2+h^2)}$	Acceleration (cm/s^2)	Recorded stations
Bay of Bengal	30.05.2006	4.7	29	330	331	34.0	Agrabad
				330	331	22.82	Rahmatganj
				200	209	14.5	Cox's Bazar
Jessore	05.08.2006	4.0	15	75	76.5	12.2	Meherpur
				40	43	13.47	Satkhira
Mynmar-India	03.11.2006	5.2	33	130	134	13.3	Rahmatganj
				150	154	-	Cox's Bazar
				100	105	12.15	Bandarban
				160	164	9.62	Khagrachari
				105	110	14.5	Rangamati
Bangladesh-India	10.11.2006	5.0	33	107	112	20.8	Sylhet
				155	158	20.6	Sunamganj
				122	126	20.58	Molovibazar
				155	112	20.55	Hobiganj
India-Mynmar	28.07.2007	4.8	15	130	131	32.6	Rahmatganj
				110	111	27.8	Bandarban
				85	86	92.6	Khagrachari
				80	287	32.66	Rangamati
Bangladesh-Myanmar	07.11.2007	5.3	15	160	161	66.02	Rahmatganj
				136	137	68.4	Bandarban
				122	123	-	Khagrachari
				206	207	-	Cox's bazar
				112	287	96	Rangamati
Modhupur	20.03.2008	4.2	25	88	87	23.33	Airport Hazicamp
				30	39	36.6	Jamalpur
				38	41	32	Sirajganj JBE
				37	45	-	Sirajganj JBW
Rajshahi	05.07.2008	4.1	29	35	45	42.98	C Nawabganj
Haluaghat	27.07.2008	4.8	44	34	57	38.43	Sherpur
				48	65	32.41	Jamalpur
				47	65	22.84	Netrokona
				84	95	18.09	Kishoregonj
Bangladesh-Myanmar	22.08.2008	4.9	25	122	125		Rangamati
				130	133	58.59	Bandarban
				166	168		Rahmatganj
Tangail	06.01.2009	4.0	10	20	23	-	Sirajganj JBE
				24	26	19.72	Sirajganj JBW
				52	53	3.03	Bogra
				92	93	2.43	Natore
Bhutan	22.09.2009	5.5	60	200	209	32.37	Panchagarh
				260	270	48.07	Dinajpur
				180	190	34.60	Lalmonirhat
				215	224	24.44	Rangpur
				450	455	23.56	Airport azicamp
Chandpur	10.09.2010	4.2	-			6.98	Brahmanbaria
						5.273	Sherpur
						10.82	Hazicamp
						6.74	GSB
Meghaloy	11.09.2010	4.5	-			6.10	Panchgarh
						18.07	Kurigram
						3.88	Natore
						4.22	Bogra

Table 4.3 Selected earthquakes in Bangladesh and neighboring region considered in the study

Event no.	Date	Macroseismic Epicentre		M_s	M_b	Depth (km)	Mean radius (km) of isoseismals (EMS)								Site
		Latitude	Longitude				D_3	D_4	D_5	D_6	D_7	D_8	D_9	D_{10}	
1	24 August 1858	18.72^0 N	95.27^0 E	6.5	-	-	-	-	-	-	186	112	65	-	Sandoway.MR
2	10 January 1869	24.79^0 N	93.17^0 E	7.5	-	48	543	-	342	247	-	115	44	-	Cachar.ID (NE)
3	14 July 1885	24.70^0 N	89.55^0 E	7.0	-	72	467	-	244	-	-	47	-	-	Sirajganj.BD (NE)
4	12 June 1897	25.84^0 N	90.38^0 E	8.7*	8.0	60	-	-	-	467	342	266	138	69	Assam.ID (NE)
5	29 September 1906	23.19^0 N	88.59^0 E	5.5	-	-	185	132	-	66	-	-	-	-	Calcutta.ID (PI)
6	23 May 1912	21.75^0 N	96.38^0 E	7.9	-	25	497	386	-	285	195	-	-	-	Mandalay.MR
7	8 July 1918	24.16^0 N	91.75^0 E	7.6	-	14	-	401	190	130	65	28	-	-	Srimangal.BD (NE)
8	2 July 1930	25.95^0 N	90.04^0 E	7.1	7.0	60	637	449	318	212	121	67	23	-	Dhubri.ID (NE)
9	15 January 1934	26.47^0 N	85.92^0 E	8.3	7.7	33	1274	-	933	562	340	-	190	113	Bihar.ID-NP (GB)
10	16 August 1938	23.05^0 N	94.75^0 E	7.2	7.0	60	-	-	-	-	115	58	-	-	Mawlaik.MR
11	15 August 1950	28.79^0 N	95.62^0 E	8.6	8.5	25	-	966	690	530	315	275	225	150	Assam.ID (NE)
12	21 March 1954	25.86^0 N	94^0 E	7.4	-	180	805	606	459	316	-	-	-	-	Manipur.ID (NE)
13	8 July 1975	25.58^0 N	92.60^0 E	6.7	6.5	112	434	226	101	28	-	-	-	-	Assam.ID (NE)
14	30 December 1984	24.72^0 N	92.90^0 E	5.7	5.5	4	-	-	-	10	6	-	-	-	Cachar.ID (NE)
15	20 August 1988	26.59^0 N	86.65^0 E	6.6	6.4	65	-	-	-	154	121	72	-	-	Bihar.ID-NP (GB)
16	8 May 1997	24.90^0 N	92.31^0 E	5.6	5.6	35	330	-	185	49	21	-	-	-	Sylhet.BD-ID (NE)
17	21 November 1997	22.07^0 N	92.75^0 E	5.3	6.0	56	-	230	136	65	29	-	-	-	BD-MR
18	22 July 1999	21.61^0 N	91.96^0 E	4.2	5.1	10	-	-	12	8	3	-	-	-	Moheshkhali.BD

Note: BD: Bangladesh; ID: India; MR: Myanmar; NP: Nepal; GB: Ganga Basin; NE: Northeast India; PI: Peninsular India.

*According to Bilham and England (2001), this is 8.1

Table 4.4 Conversion of intensity to peak ground acceleration using Trifunac and Brady (1975) relation.

Name of EQ	Intensity	Mean distance	logPGA	PGA
	3	543	0.914	8.203515
	4		1.214	16.36817
	5	342	1.514	32.65878
	6	247	1.814	65.16284
	7		2.114	130.017
	8	115	2.414	259.4179
	9		2.714	517.6068
, 1869,Ms=7.5, Cacha	10		3.014	1032.761
	3	467	0.914	8.203515
	4		1.214	16.36817
	5	244	1.514	32.65878
	6		1.814	65.16284
	7	*120	2.114	130.017
	8	47	2.414	259.4179
	9		2.714	517.6068
uly, 1885, Ms=7, Siraj	10		3.014	1032.761
	3		0.914	8.203515
	4		1.214	16.36817
	5		1.514	32.65878
	6	467	1.814	65.16284
	7	342	2.114	130.017
	8	266	2.414	259.4179
	9	138	2.714	517.6068
897, Ms= 8.7(8.1), As	10	69	3.014	1032.761
	3	637	0.914	8.203515
	4	449	1.214	16.36817
	5	318	1.514	32.65878
	6	212	1.814	65.16284
	7	121	2.114	130.017
	8	67	2.414	259.4179
	9	23	2.714	517.6068
2 July, 1930, Ms= 7.1	10		3.014	1032.761
	3	740	0.914	8.203515
	4	401	1.214	16.36817
	5	190	1.514	32.65878
	6	130	1.814	65.16284
	7	65	2.114	130.017
	8	28	2.414	259.4179
	9		2.714	517.6068
,1918, Ms= 7.6, Srim	10		3.014	1032.761
	3	434	0.914	8.203515
	4	226	1.214	16.36817
	5	101	1.514	32.65878
	6	26	1.814	65.16284
	7		2.114	130.017
	8		2.414	259.4179
	9		2.714	517.6068
975, Ms = 6.7, Assan	10		3.014	1032.761
	3	330	0.914	8.203515
	4		1.214	16.36817
	5	185	1.514	32.65878
	6	49	1.814	65.16284
	7	21	2.114	130.017
	8		2.414	259.4179
	9		2.714	517.6068
ay 1997, Ms= 5.6, Sy	10		3.014	1032.761
	3	535	0.914	8.203515
	4	230	1.214	16.36817
	5	136	1.514	32.65878
	6	65	1.814	65.16284

CHAPTER 5

APPLICATION OF DEVELOPED METHOD

5.1 General

At 10 h 22 m 7s (GMT) on 8 July 1918, one of the largest known earthquakes (Srimangal earthquake, magnitude 7.6) has occurred in the north-east region of Bangladesh. It damaged or destroyed the large majority of brick buildings, bridges, hospitals, water tanks, factories in the tea garden estates and killed 2 people (Sabri, 2002). Structural damage was widespread, extending as far as the whole area encompassing Sylhet, Moulavi Bazar, Habiganj, Brahmanbaria, Kishoreganj and Agartala (India). The shock was felt in a fairly large area as far east at Aijal (Monipur, India), west at Calcutta (West Bengal, India), south at Rangoon (Myanmar) and north at Katmundu (Nepal), an area of about 74000 sq. km (Stuart, 1920). Large cracks and fissures, land slide was extensive in the epicentral area. One of the fissures were 150 mm length and 300 mm deep. Sand boils were observed in many places. The maximum Modified Mercalli (MM) intensity was VIII-IX (Sabri, 2001). Sylhet, which is now a rapidly growing urban area of Bangladesh, was subjected to strong ground shaking that resulted in many houses either being displaced off their foundations, settled differentially, or destroyed.

Obviously a repeat of the 1918 Srimangal Earthquake or even a smaller, moderate-sized event could be catastrophic to Bangladesh, particularly to the Sylhet city and surrounding areas. Based on seismic zoning map of Bangladesh (Figure5.1) and seismic hazards for Bangladesh (Sharfuddin, 2001), the Sylhet city is situated in the highest seismic zone. A recent study by OIC (2009), identified five earthquake sources for Bangladesh as shown in Figure 1.2.

In this chapter a comprehensive earthquake loss assessment of Sylhet City is presented. Sylhet City which is situated in the north-eastern part of Bangladesh is shown in Figure 5.2 and Figure 5.3, has a high potential for earthquake damage and losses with a population of nearly 311050 people and a large percentage of structures that have not been designed to resist earthquake forces. Therefore, a

detailed seismic hazard and risk analysis is being conducted for Sylhet City. The results will be extrapolated to the adjoining areas.

Sylhet City has an area greater than 42.8 km ^{2} with about 51831 households in the city and a total population of about 311050 people. Major portion of the buildings are associated with residential housing. A building inventory methodology for the town of Sylhet was developed. 3040 buildings (12%) of the total were surveyed in the study area. On the other hand for the vulnerability and potential loss assessment of water pipelines and gas pipelines system, the construction and proposed blue prints of water and gas delivery pipelines of the city were digitized into a GIS. The population data, building inventory data and life line data with results presented as summaries will be used this chapter to illustrate the GIS-bases regional seismic hazard and risk analysis. The results and microzone maps presented here are preliminary and intended only for illustrative purposes.

The purpose of this study was to evaluate the potential losses from 1918 Srimangal earthquake (M =7.6) scenarios with the help of Mapinfo Professional software. These results have provided a basis for the city to effectively plan and prepare for future damaging earthquakes, and also a means to raise public awareness of the city's earthquake risk. A specific objective of the study was to estimate as accurately as possible the potential earthquake losses by (1) characterizing the earthquake hazard input geologic, geotechnical, and seismological data, and (2) improving the inventory data. These efforts resulted in one of the most comprehensive estimations ever performed in Bangladesh.

The evaluation was carried out in six tasks:

1. calculation of scenario earthquake ground motions
2. evaluation of liquefaction and earthquake-induced landslide potential
3. compilation and evaluation of building inventory
4. compilation and evaluation of lifeline and essential facility data
5. risk assessment

The case study presented in this chapter follows the GIS-based regional analysis methodology illustrated in Figure 3.5. Section 5.3 covers the GIS-based seismic hazard analysis for the region. Surface ground shaking and local site effects are

treated, including an illustration of the hazard integration methodology presented in Chapter 3. Section 5.4 details the regional earthquake damage and loss estimation. The current development of the structural inventory for this region is slightly different from the inventory methodology presented in Chapter 2. In Section 5.3.4 inventory development methodology will be discussed. A subset of the inventory is used to compute preliminary estimates of earthquake damage and losses in the region. A summary of the procedures and results of the GIS-based regional analysis is presented in Section 5.4.

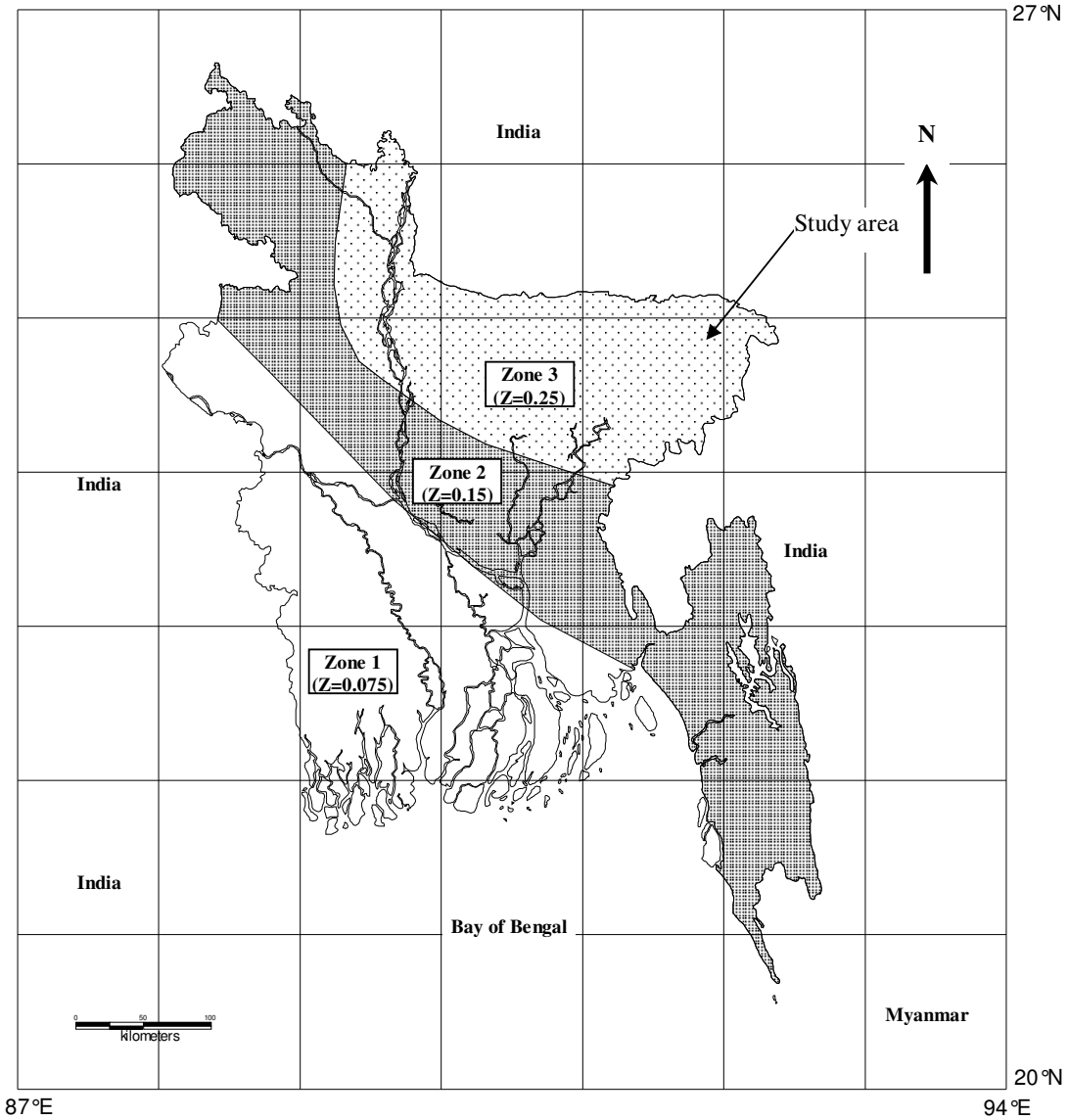

Figure 5.1 Seismic Zoning Map of Bangladesh (BNBC, 1993)

5.2 Geology of the study area

The Sylhet Trough of northeastern Bangladesh is a tectonically complex province of the Bengal Basin (Figure 2). It comprises 12 to 16 km thick sequence of Late Mesozoic and Cenozoic age sedimentary rocks (Johnson and Alam, 1991). The Dauki fault system with huge vertical displacements represents the transition between the Sylhet Trough and the Shillong Plateau (Hiller and Elahi,1988; Johnson and Alam,1991).

The Sylhet Trough was developed due to contemporaneous interaction of two major tectonic movements: (1) uplift of the Shillong Massif in the north and (2) westward propagation of the Indo-Burman mobile belt (Hiller and Elahi, 1988). Johnson and Alam (1991) argued that the Sylhet Trough had evolved from (i) a passive continental margin (pre-Oligocene) to (ii) a foreland basin linked to the Indo-Burman Ranges (Oligocene and Miocene) and (iii) a foreland basin linked to the south-directed overthrusting of the Shillong Plateau (Pliocene to Holocene).

The sedimentary sequence encountered in the formation of the structure is generally subdivided into the following lithostratigraphic units, from the oldest to the youngest: Bhuban (1194 m+) and Boka Bil (798 m) Formations of Surma Group (Miocene). Tipam Sandstone (646 m) and Girujan Clay (411m) Formations of Tipam Group (Mio-Pliocene) and Dupi Tila Formation (1095 m) (Plio-Pleistocene) (BAPEX 1989).

The Surma Grup consists of a deltaic diachronous sequence of alternating sandstone, shale, sandy shale and siltstones (Brunschweiller, 1980). The fluvial Tipam Group is characterized predominantly by sandstones and sandy shale at the bottom and clay at the top. The major rock types of the Dupi Tila Formation are also fluviatile sandstone (Talukder et al. 2006).

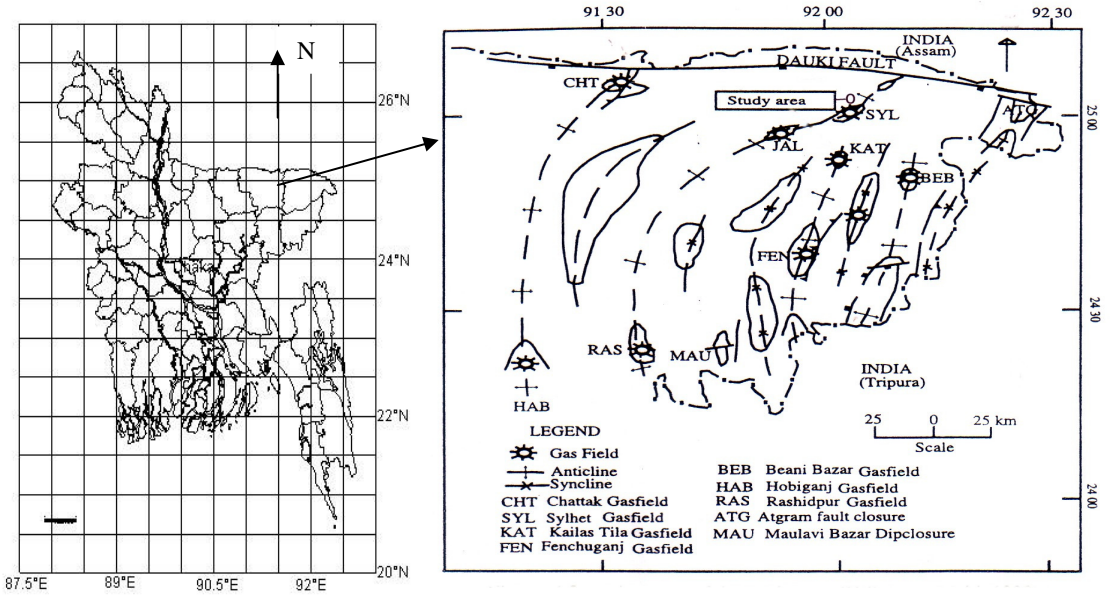

Figure 5.2 Study area

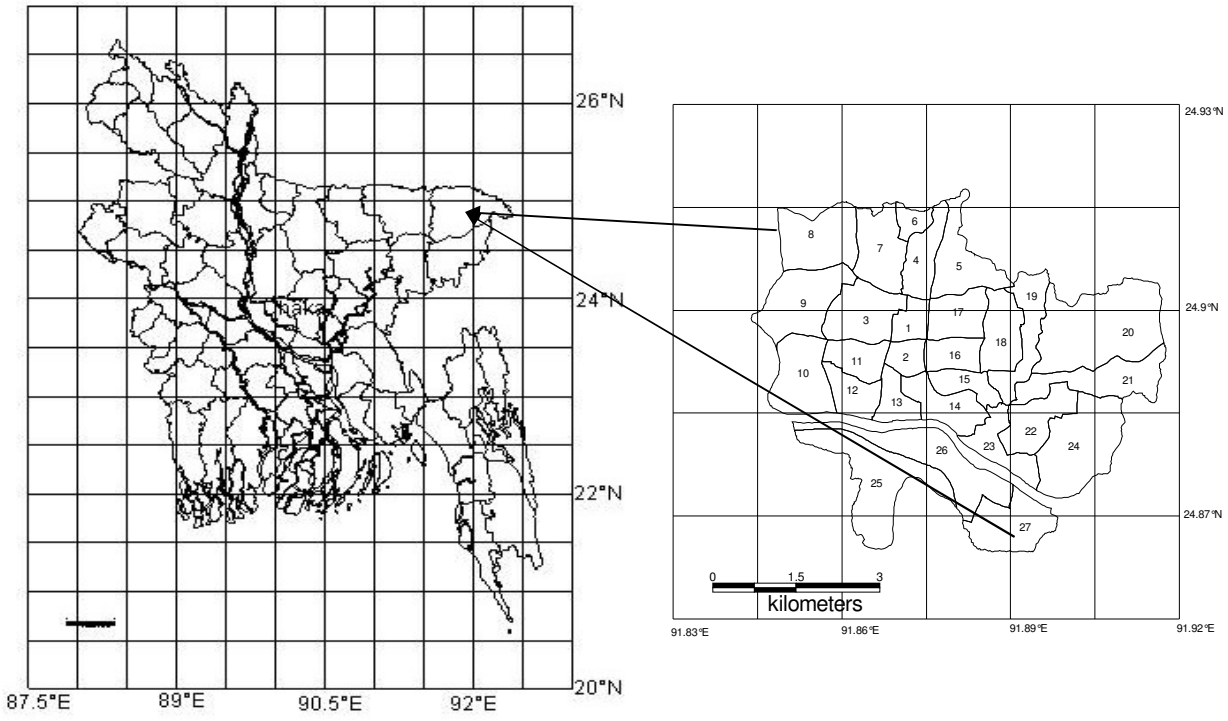

Figure 5.3 Map showing location of Sylhet and ward map of Sylhet city corporation

5.3 Seismic Hazard Assessment

Chapter 2 and Chapter 3 of this dissertation presented a discussion of regional seismic hazard analysis. The background of the various steps in the process, as well as the application of GIS technology in a regional study were discussed. Chapter 2 and Chapter 3 involves a more detailed discussion of local site effects, including soil amplification, liquefaction, landslide, and fault rupture, and the integration of these effects in a GIS-based regional seismic hazard analysis. The case study presented here illustrates several of these concepts in a simplified analysis over a fairly small region. Microzone maps are shown to help describe the hazard estimation methodology which is illustrated in the left half of Figure 3.3.

5.3.1 Surface Ground Shaking

As discussed in Section 5.1, this case study presents a regional seismic hazard and risk analysis for a scenario event, a magnitude 7.6 on the Sylhet City, Bangladesh. Figure 1.2 and 1.3 shows a fault map of this region. with the assumed scenario break needed to generate a magnitude 7.6 event on this region. In order to estimate the surface ground shaking in the region, the attenuation relationship developed by Mc Guire (1978) for peak ground acceleration is used. This relationship is given in the form:

$$y=0.0306e^{0.89M}r^{-1.17}e^{-0.2S} \qquad (5.1)$$

where :

S=0 for rock and S=1 for alluvium

y = PGA;

M = surface magnitude (7.6 in this example) ;

r = hypocentral distance;

PGA values are determined using equation (5.1). PGA values are converted to Mercalli Intensity (MMI) values. The equation used to compute MMI from PGA is that of Trifunac and Brady (1975) given in Equation (3.5) from Table 3.2 as:

$$\log(PGA)= 0.014+0.3\ (MMI) \qquad (5.2)$$

A map of the local site geology is required to define the soil types in the study region. Figure 5.17 shows a map of borehole locations. Figure 5.4 shows bedrock level PGA calculated using equation (5.1). To estimate the final surface ground shaking in the region, the map of ground motion buffer zones is combined with the soil type map to produce the final map of surface ground shaking as illustrated in Figure 5.6 for PGA and Figure 5.7 for MMI values. High ground motion values are shown to occur almost throughout the Sylhet City.

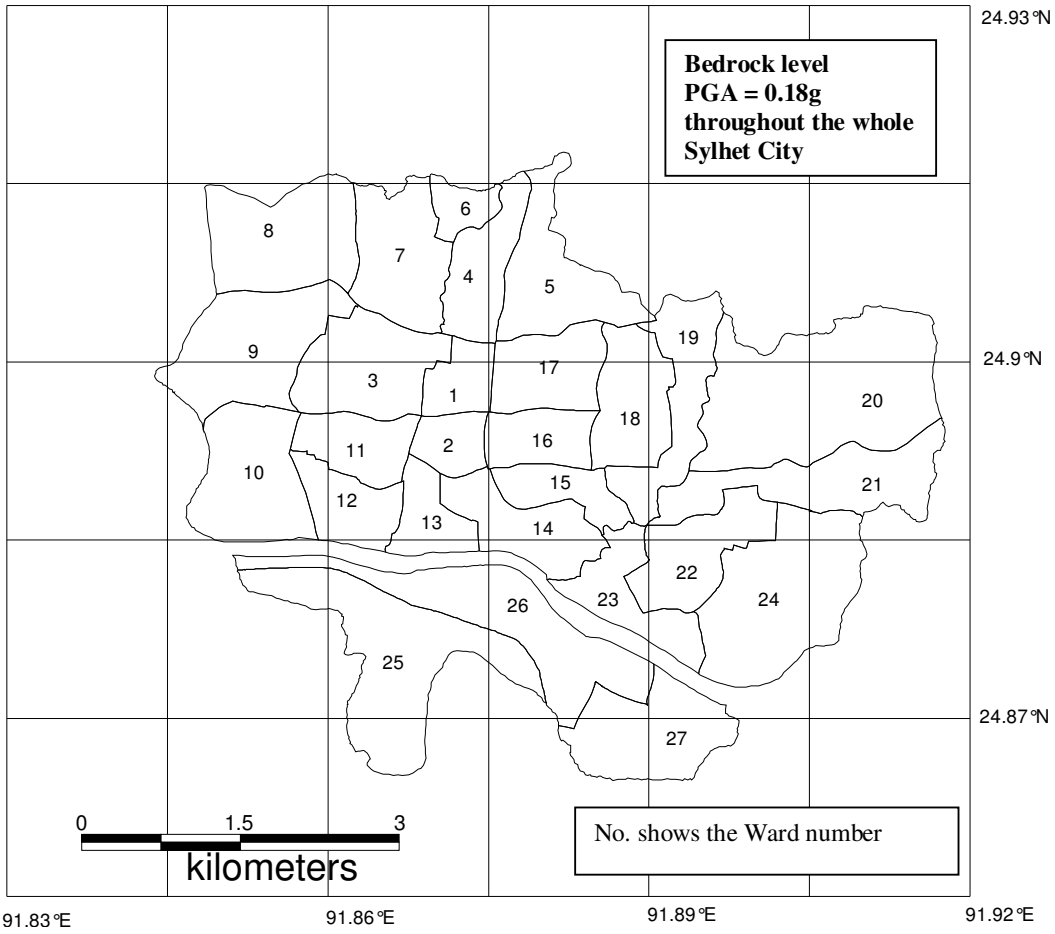

Figure 5.4 Distribution of bedrock level PGA of Sylhet city.

5.3.2 Potential hazards

Three potential hazards associated with earthquakes were evaluated: ground shaking, liquefaction, and landsliding.

5.3.2.1 Earthquake Ground Shaking

A fundamental limitation encountered in the estimation of ground shaking in Sylhet City is the lack of strong motion data in Bangladesh. The use of empirical attenuation relationships based on the recordings of strong motion is the traditional and most appropriate approach in estimating ground motions from future earthquakes. Such relationships are not available for the Bangladesh though we are using these available empirical relationships. An attempt has been made for the development of acceleration based attenuation law for Bangladesh. For this purpose Strong Motion Accelerograph (SMA) is being installed in several district PWD offices of Bangladesh. Record of an earthquake event from SMA is unavailable that is why an alternative attempt was made to develop an acceleration based attenuation law for Bangladesh using available intensity data. For the verification of this law some recent SMA data is needed. Hence, in this study, we have utilized available empirical attenuation law instead of what we have developed.

Ground motions were estimated using 1918 Srimangal Earthquake (M=7.6) as a scenario event. Maps for surficial ground shaking in terms of peak horizontal acceleration (PGA) and spectral acceleration were produced by multiplying the soil amplification factors. Soil amplification was determined using program SHAKE (Schnabel et al. 1972) and illustrated in Figure 5.5.

An extensive effort was made to characterize the subsurface geology of the city for the purposes of quantifying the effects of soil on ground motions, through the use of amplification factors, and assessing the liquefaction potential. The type of geologic material, thickness and shear-wave velocities. Characteristic profiles were developed for each bore hole response category using available subsurface and shear-wave velocity information, and considered a wide range of soil and rock conditions. Amplification factors were calculated as a function of site response category, spectral frequency, soil thickness, and input rock motion.

The resulting mapped peak horizontal accelerations for the M 7.6 scenario event varied between 0.35 to 0.45 g on soil in the Sylhet City (Islam, 2005) as illustrated in Figure 5.6. Figure 5.7 shows the MMI_{GS} and is calculated using equation (5.2).

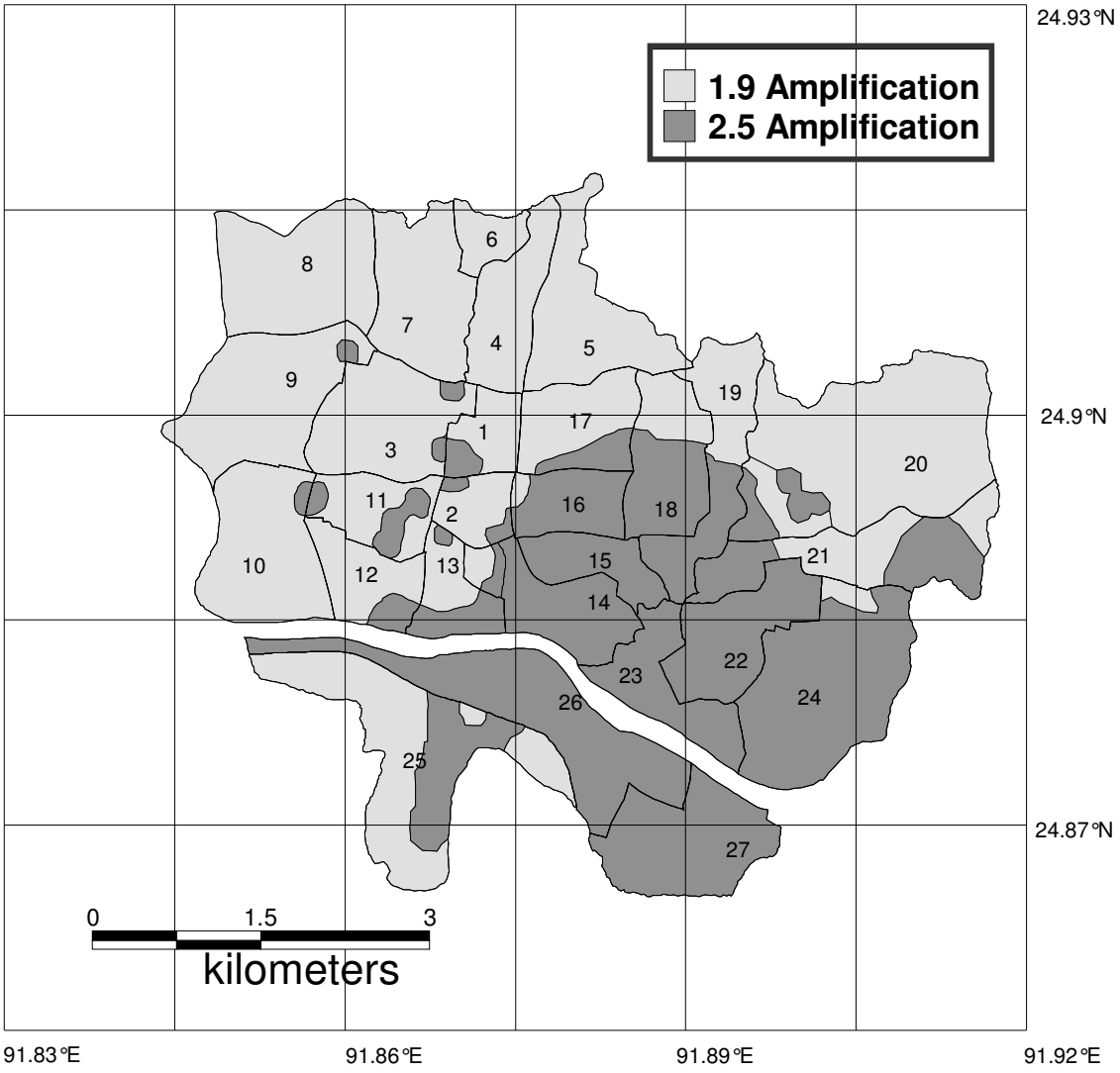

Figure 5.5 A Map showing regional distribution of amplification factor in Sylhet City Corporation

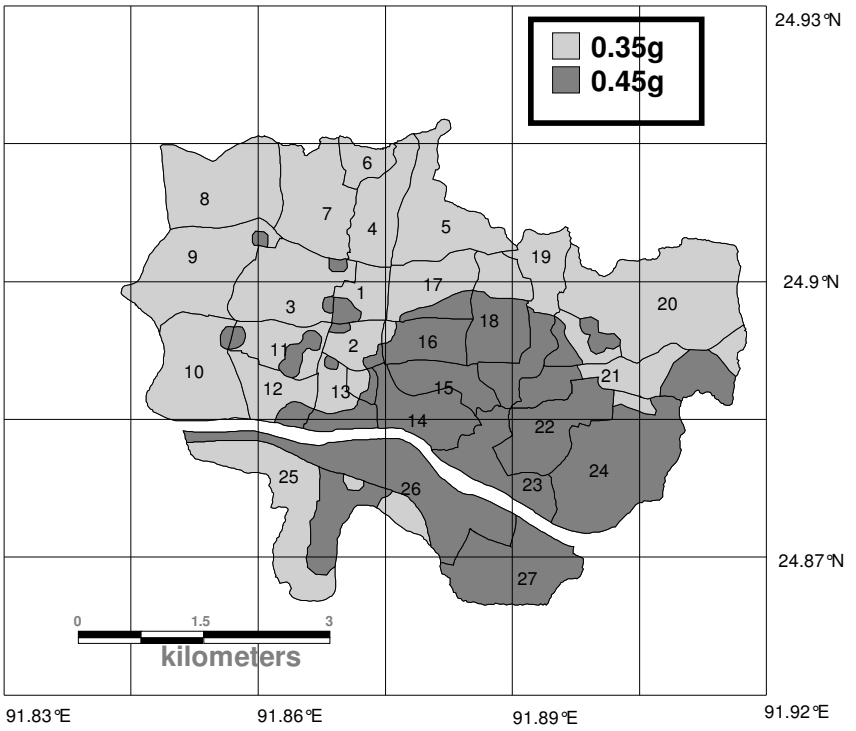

Figure 5.6 Map showing regional distribution of peak ground acceleration in Sylhet City Corporation

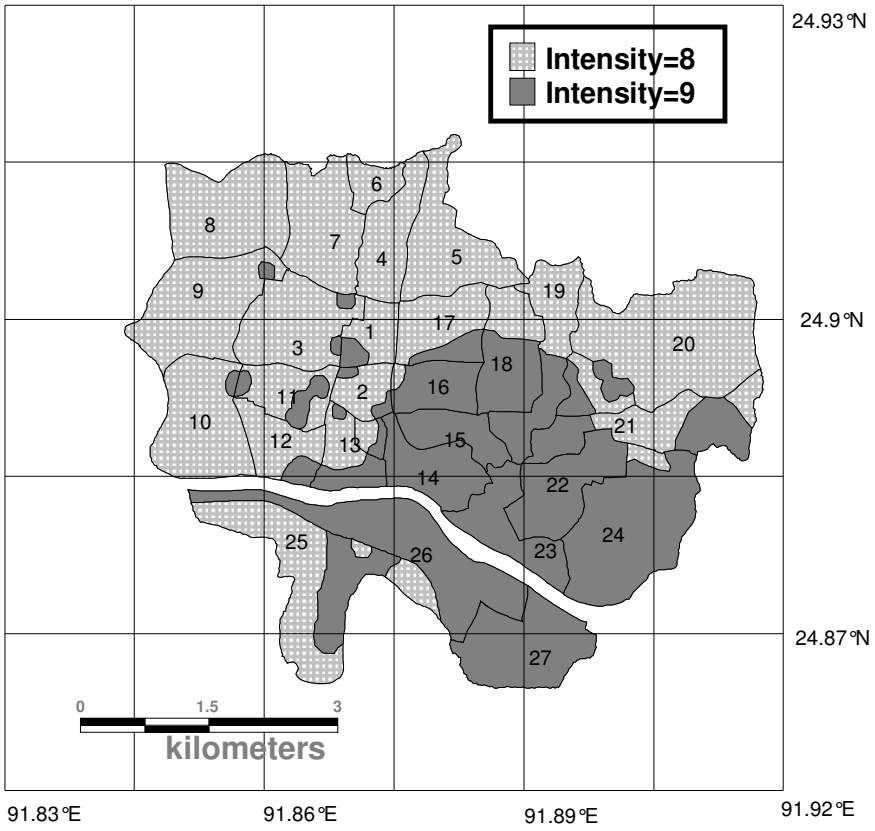

Figure 5.7 Map showing regional distribution of ground shaking hazard (MMI_{GS}) in Sylhet City Corporation

5.3.2.2 Liquefaction

The occurrence of liquefaction depends upon the susceptibility of the soil, the amplitude and duration of the ground shaking, and the depth of the water table. The evaluation of a soil's resistance to liquefaction involves the estimation of both the capacity to resist liquefaction and the demand placed on the soil by ground shaking.

We consider the potential for liquefaction (in terms of liquefaction-induced settlement and lateral flow) in assigning the potential for building and pipeline damage. For the earthquake scenario (M=7.6) and characteristic geologic profile, the liquefaction demand in terms of an average cyclic stress ratio (CSR) within potentially liquefiable soil was calculated across the city (Seed et al. 1983) The liquefaction resistance of soil, as expressed by the cyclic resistance ratio (CRR), in the representative profiles was determined based on shear-wave velocity and the clay/silt content of the soil. The ratio of capacity (CRR) to demand (CSR) is termed the factor of safety against liquefaction. Liquefaction is predicted to occur when the factor of safety is at or below 1 and not to occur when it exceeds 1.

The step in modeling the observed liquefaction was taken by some researcher using historical data and identifying the susceptible soils. Youd and Perkins (1978) categorized the susceptibility of soils according to age and depositional environment. In general, older soils have lower potential for liquefaction. In fact, essentially all documented liquefaction has occurred within soils of Pleistocene age or younger. Figure 5.8 illustrates the liquefaction potential in Sylhet city corporation area.

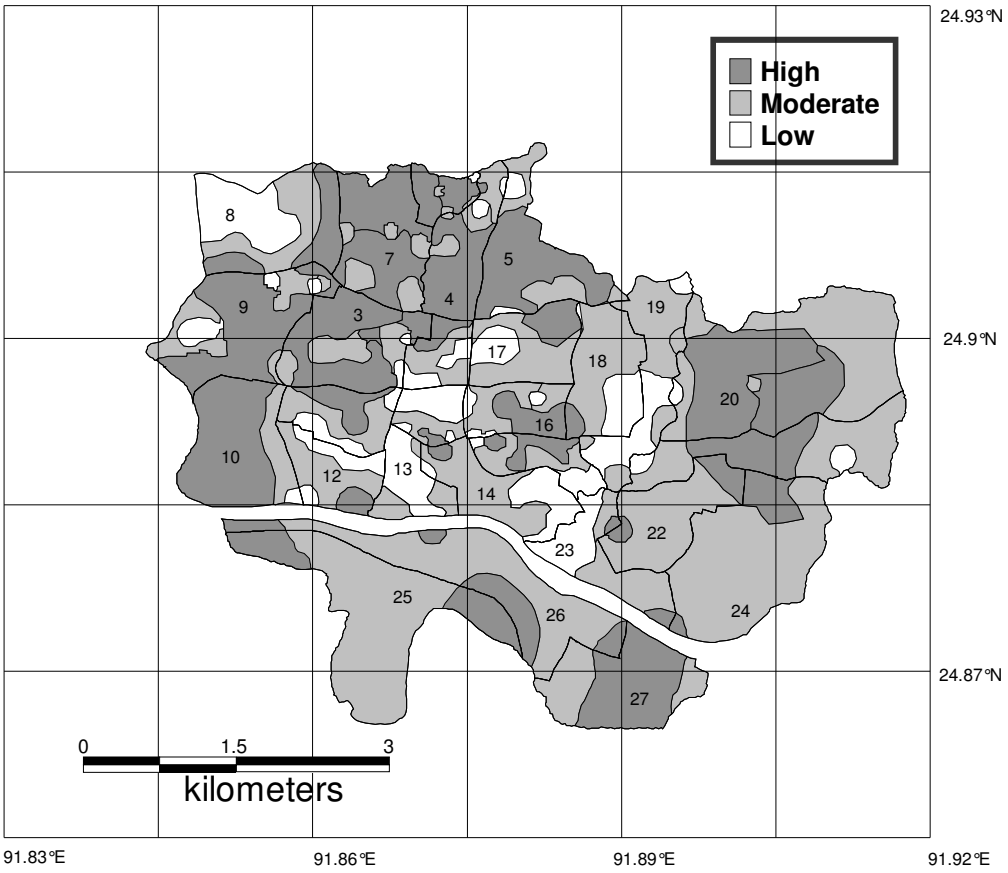

Figure 5.8 Map showing regional distribution of liquefaction potential in Sylhet City Corporation area

5.3.2.3 Earthquake-induced Landsliding

In addition to the movement associated with liquefaction-induced settlement and lateral flow, there is also a potential for landslides in sloping terrain, where the additional seismic forces may temporarily exceed the slope strength. Landslide hazard is typically very difficult to quantify because landslides come in many forms and are caused by a variety of processes. Specifically, the susceptibility of an area to earthquake-induced landslides is assigned based on the general steepness of slopes, the soil/rock type, hydrological conditions, the groundwater conditions, vegetation, land use and the severity of earthquake. Most of these factors are necessary for the investigation of an individual slope, but for seismically induced landslide analysis on a broad regional basis, the factors are typically limited to slope angle, geology, location of previous land slides,

magnitude of the seismic event, and distance from the seismic source (Hansen and Franks, 1991). Based on available information stability analysis was performed as per Wieczorek,et al.(1985) and using GIS a landslide hazard map (Figure 5.9) is developed.

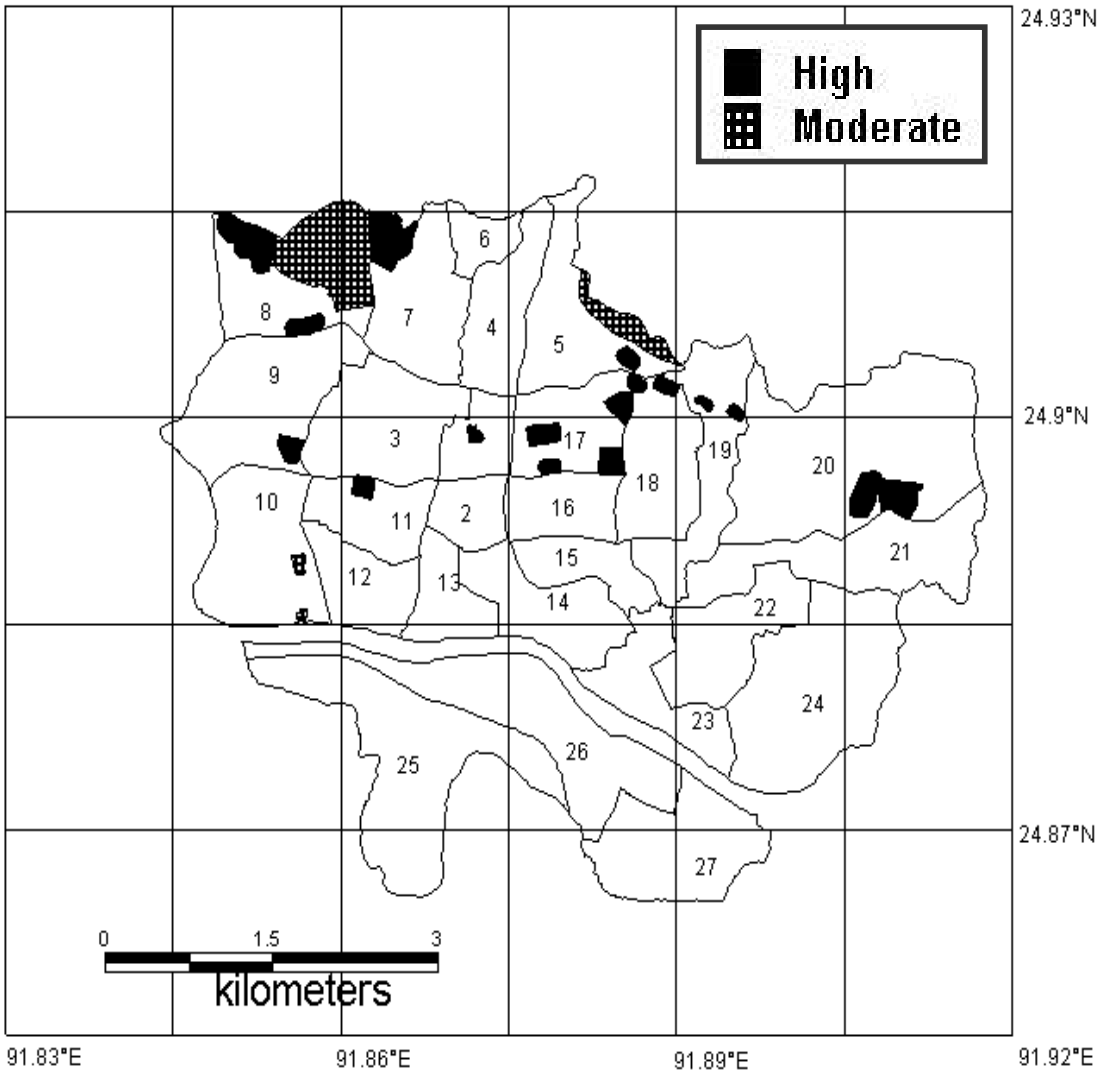

Figure 5.9 A map showing landslide potential

5.3.3 Hazard Integration

The previous section discussed about the potential hazards. The various seismic hazards leading to MMI_{GS} due to ground shaking, MMI_{LIQ} due to liquefaction and MMI_{LAN} due to landslide are quantified according to the sequence presented in section 3.4.3. The integration of these three hazards is assumed to follow the weighted average methodology described in Section 3.4. The heuristic hazard combination rules used for the region in this case study are those listed in Table 3.2a. Figure 5.10, Figure 5.11shows the final combined seismic hazard for the scenario event in the study region.

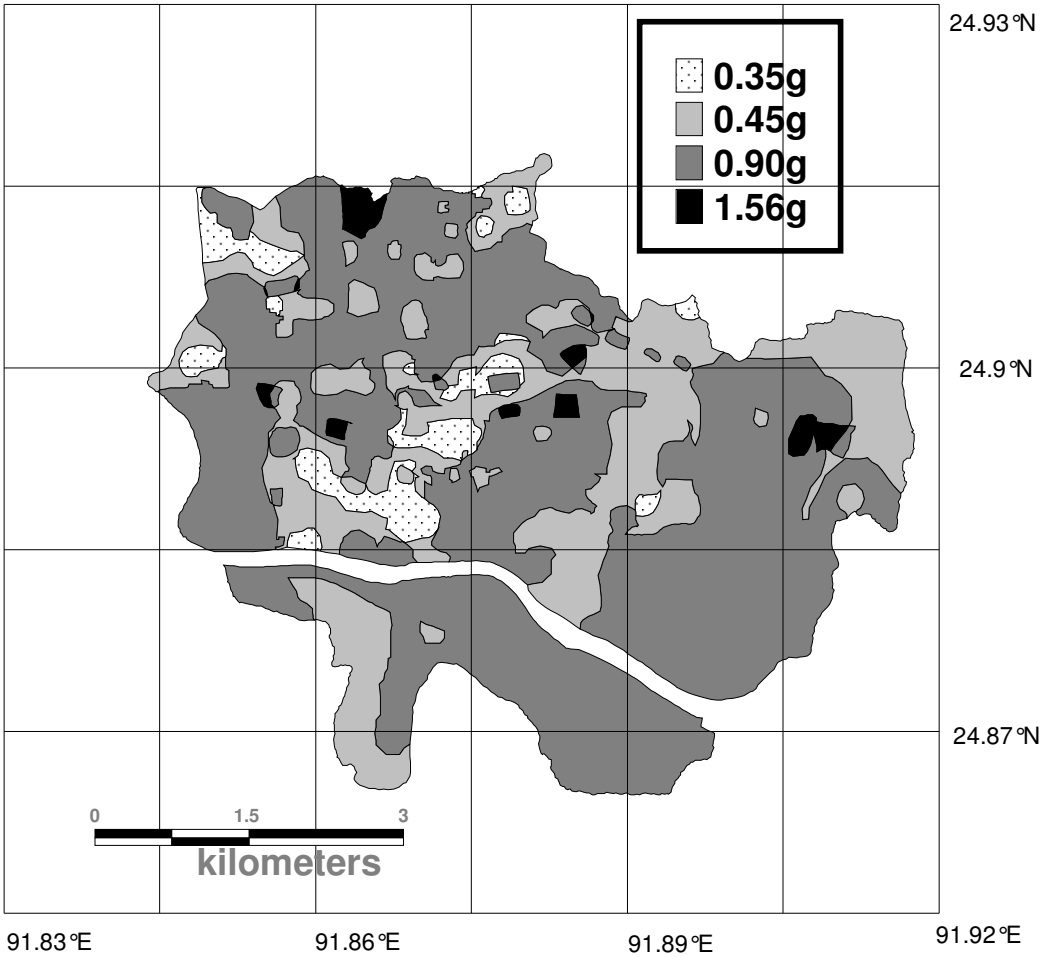

Figure 5.10 Map showing regional distribution of combined seismic peak ground acceleration in Sylhet City Corporation area

The results of the characterization and analyses indicate that greater amplification and liquefaction hazard are experienced in the ward 8 (Figure 5.12 and Figure 5.13). The greater liquefaction demand, as well as the presence of loose sand deposits, results in a greater risk of liquefaction in the city area.

Similar to the ground hazard map, high values of MMI are found to occur almost throughout the Sylhet City. This is due to the high ground shaking in this area, as well as the high hazards due to liquefaction and landslide. It is again emphasized that the results of this case study are only preliminary and are based on several simplifying assumptions. The analysis method and integration rules are chosen with the intent of illustrating the use of GIS technology in a regional seismic hazard analysis and can easily be modified as additional information becomes available. The rest of this case study deals with the estimation of damage and loss due to the scenario event.

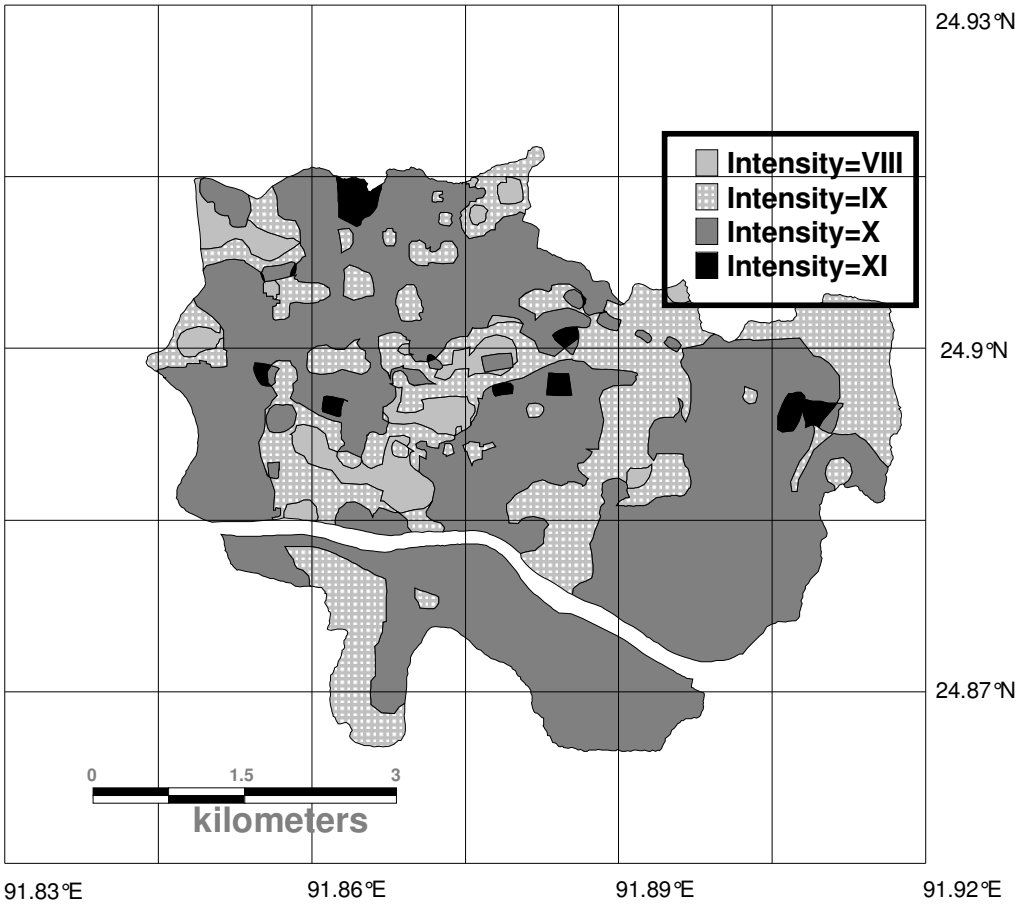

Figure 5.11 Map showing regional distribution of combined seismic hazard (MMT_F) in study area

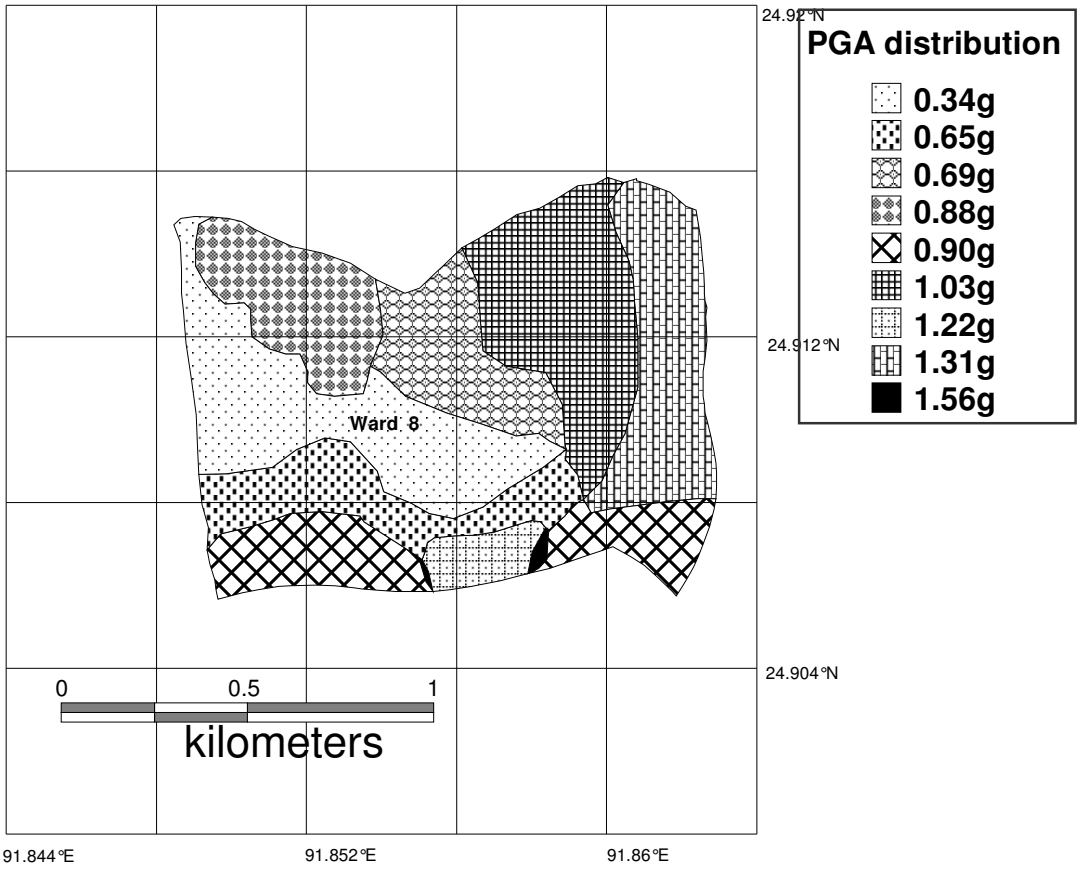

Figure 5.12 Map showing regional distribution of combined seismic peak ground acceleration in ward 8

5.3.4 Inventory data

In this study Microsoft Access and Excel software and GIS Map Info Professional have been used to develop a relational database to store and analyse soil data and building data. The format of the data collection questionnaire was used in the survey is similar to FEMA-154.

5.3.4.1 Preparation of updated digital ward map for Sylhet City Corporation

A ward map is collected from Sylhet City Corporation which was divided in to 13 wards (Figure 5.14). Recently Sylhet City Corporation office divided this municipality area into 27 wards on the basis of voter list. The Sylhet City Corporation authority did not prepare updated map containing 27 wards.

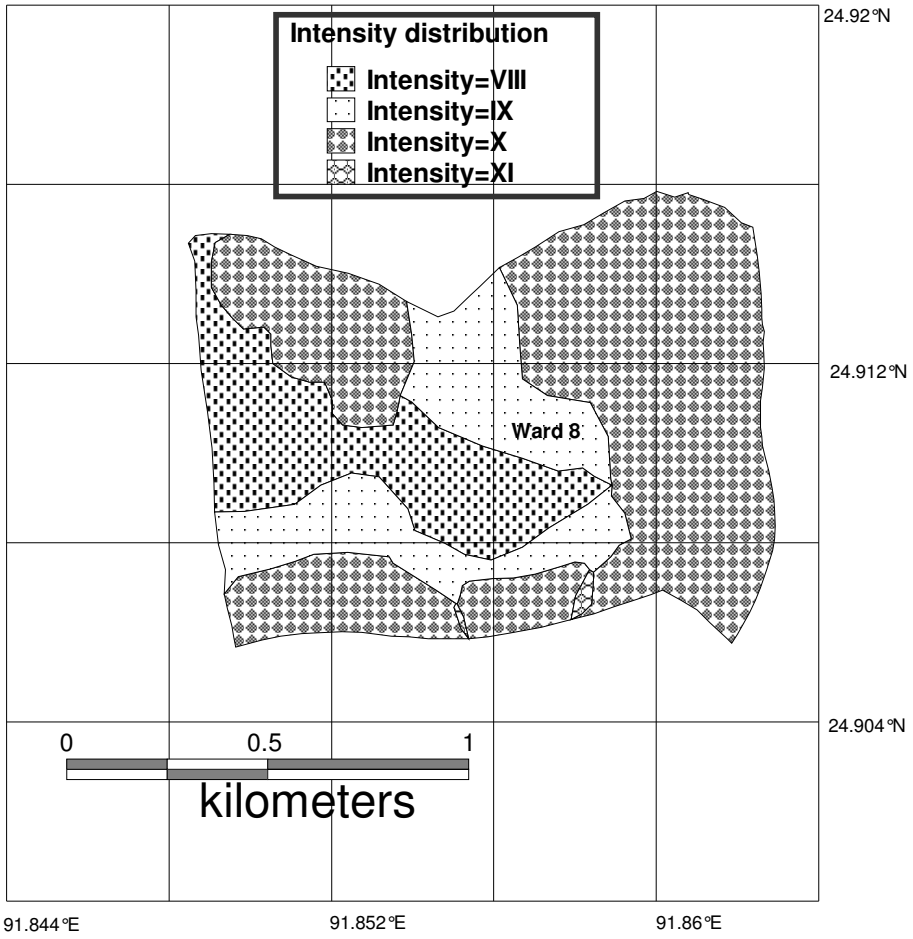

Figure 5.13 Map showing regional distribution of combined seismic hazard (mmt_f) in ward 8

Using GPS value of different fringes location as well as nucleus location, ward map containing 13 wards is split up into 27 wards after having a discussion with the concerned authority. The ward map is updated and digitized in GIS environment as per voter list and mouza map, collected from City Corporation office. Figure 5.15 shows the updated ward map of this study area.

5.3.4.2 Population of the study area

In census 1991 population was given according to local area so by investigating this scenario together with ward list containing individual area is given. Population distribution is also determined according to ward map where 27 wards

are distinguished. According to the 1991 census the population of the study area was 234355. Considering the growth rate since 1961 to 1991 (Table 5.1) and based on the 1991 base population for the municipal area, it is estimated that the 2003 population for the same area would be around 311050. During 1991 annual population growth was 3.36%. For interpolating the population of 2003 this annual growth rate is assumed for this study house hold size in the urban area was 6.4 in 1991 for this study house hold size for study area **6** is assumed

Table 5.1 Population Growth Trend of Sylhet Municipal Area

Year	Population	% Increase	Annual Rate of Growth (%)
1901	13893	-	-
1911	14457	4.0	0.39
1921	16912	16.9	1.58
1931	21435	26.7	2.4
1941	28128	31.2	2.75
1951	33124	17.7	1.65
1961	40644	22.7	2.07
1974	63417	35.9	3.5
1981	87922	27.9	4.8
1991	22554	15.6	15.6

Source: BBS, 1997

The increase of population in Sylhet city is largely due to in migration, which during 1974-81 was 56% of the total increase in the city. The increase has been higher in the rural-urban fringe areas than in the inner city areas.

Construction sub-sector has also expanded in recent years, with a boom in luxury residential housing and shopping centers. This is largely due to the remittances of Sylhetees living in the UK. Calculated ward wise population distribution, household, area and population distribution is shown in the Table 5.2 and population density map is shown in Figure 5.16.

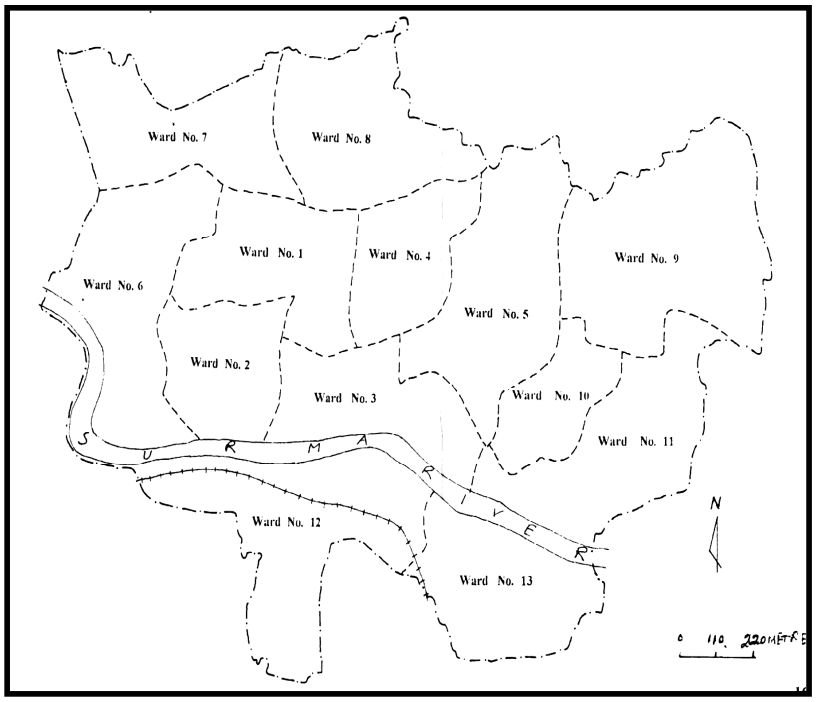

Figure 5.14 Map showing 13 wards in Sylhet City Corporation

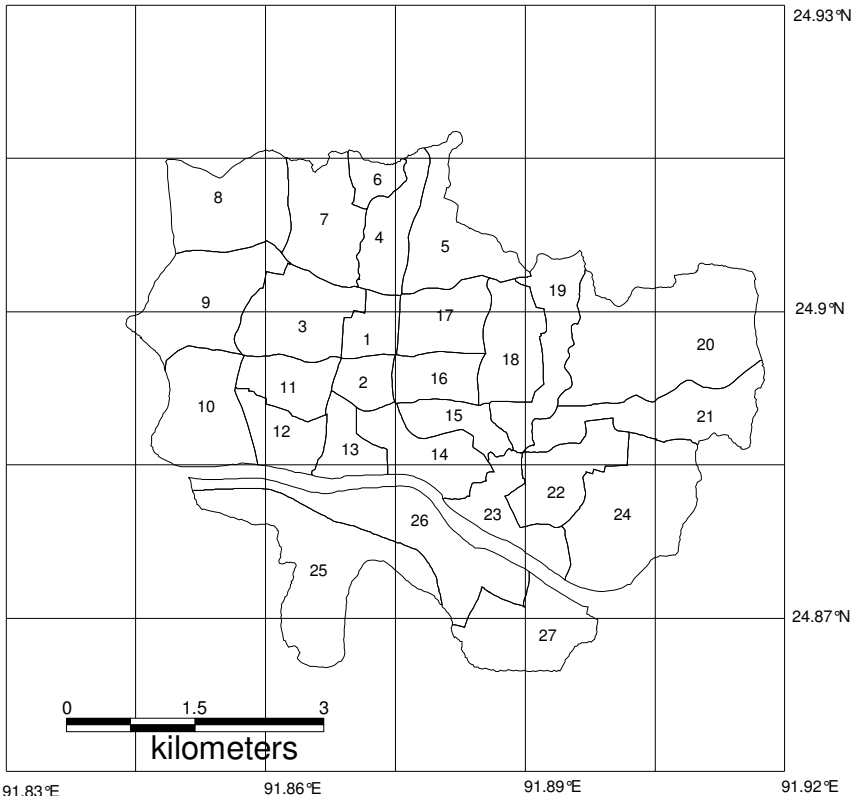

Figure 5.15 Ward map of Sylhet City Corporation

Table 5.2 Ward no, House hold, Ward areas, Population density, Housing units for Sylhet City Corporation.

Ward No	Population	House hold	Area (km^2)	Density
1	16721	2787	0.387768	43121
2	8364	1394	0.352439	23732
3	12227	2037	1.09469	11169
4	4008	668	0.719014	5574
5	11733	1955	1.05498	11122
6	8402	1400	0.261897	32081
7	14800	2466	1.04652	14142
8	13844	2307	1.84222	7515
9	9306	1551	1.5368	6055
10	11063	1843	1.19193	9282
11	8571	1428	0.595735	14387
12	14011	2335	0.576226	24315
13	12692	2115	0.461826	27482
14	12263	2043	1.02057	12016
15	6781	1130	0.471889	14370
16	13718	2286	0.522848	26237
17	16523	2753	0.754641	21895
18	15405	2567	0.858518	17944
19	10291	1715	0.919895	11187
20	8033	1338	2.61574	3071
21	7266	1211	1.20709	6019
22	3815	635	1.02446	3724
23	10988	1831	1.28589	8545
24	17329	2888	0.89411	19381
25	17066	2844	1.5015	11366
26	12656	2109	1.56068	8109
27	13174	2195	1.53369	8590

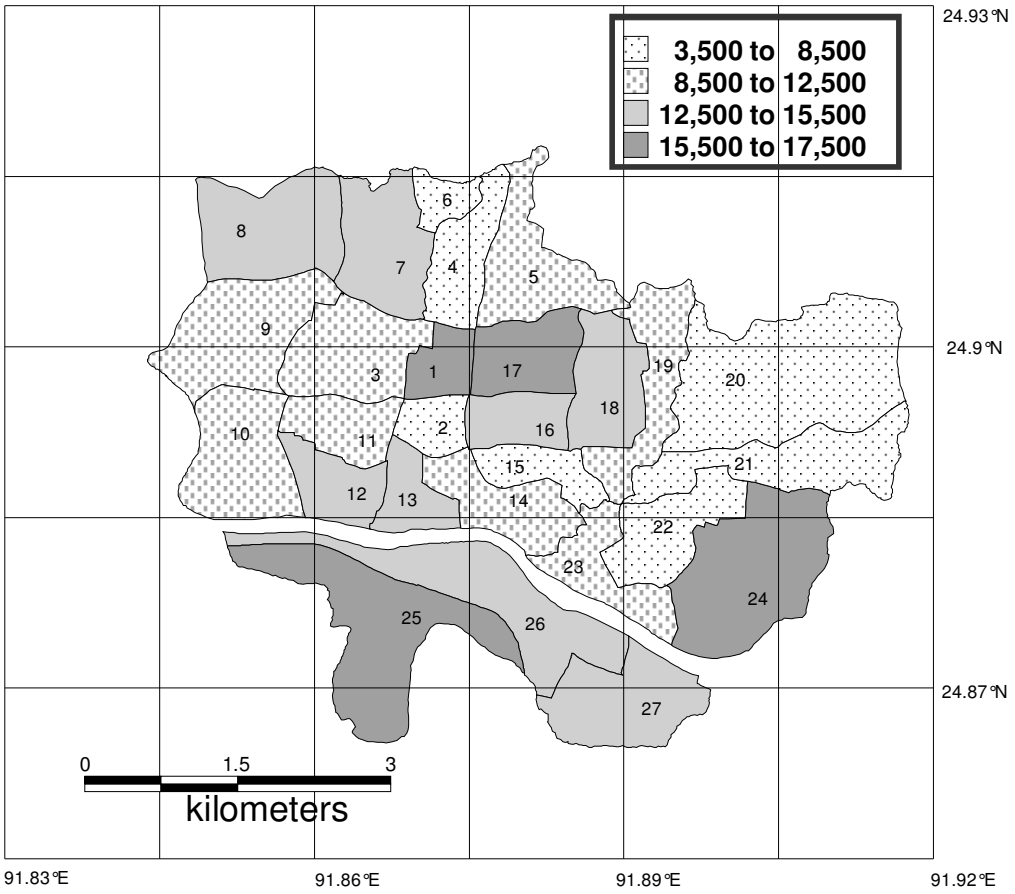

Figure 5.16 Map showing population density map of Sylhet City Corporation

5.3.4.3 Land use

Of the total area of municipality, about two thirds are built-up while agricultural land, vacant space and water bodies take up another one-third (Table5.3).

Residential use takes more than 50% of the land while commercial use takes about 5%, educational and health together about 5%, administration takes 2.5%, and industrial takes only over 1%. Other uses take small proportions of land. At present; the most conspicuous developments are taking place in the form of luxury and expensive residential buildings and shopping centers.

Building stock data from census reports was generally compiled at district level, but for big cities like Sylhet, ward level data exist (BBS, 2001). For this study, ward was adopted as the basic geographical reference (geo-code) for the loss model.

Table 5.3 Land uses in Sylhet 1985

Category of Use	Area in Acres	Percentage of Total Area
Residential	3759	51.5
Commercial	343	4.7
Educational	198	2.7
Health	184	2.5
Administrative	155	2.1
Industrial	86	1.2
Religious	25	0.3
Graveyard	23	0.3
Historic	16	0.2
Socio-Cultural	10	0.1
Agricultural	1568	21.5
Vacant space/open space/water bodies	931	12.8

5.3.4.4 Soil data used

A total of 167 boreholes SPT data were collected from different relevant organization and used to study site amplification as well as soil liquefaction potential characteristics of municipality area. Among these data, 9 boreholes with SPT-N data upto a depth of 30 m. were directly collected for checking the authenticity of other collected data as well as estimation of site amplification factor . The typical soil data are upto a depth of 15 m. Table 5.4 Presents locations and number of borehole data from different areas of Sylhet used for this study. Figure 5.17 shows borehole locations used.

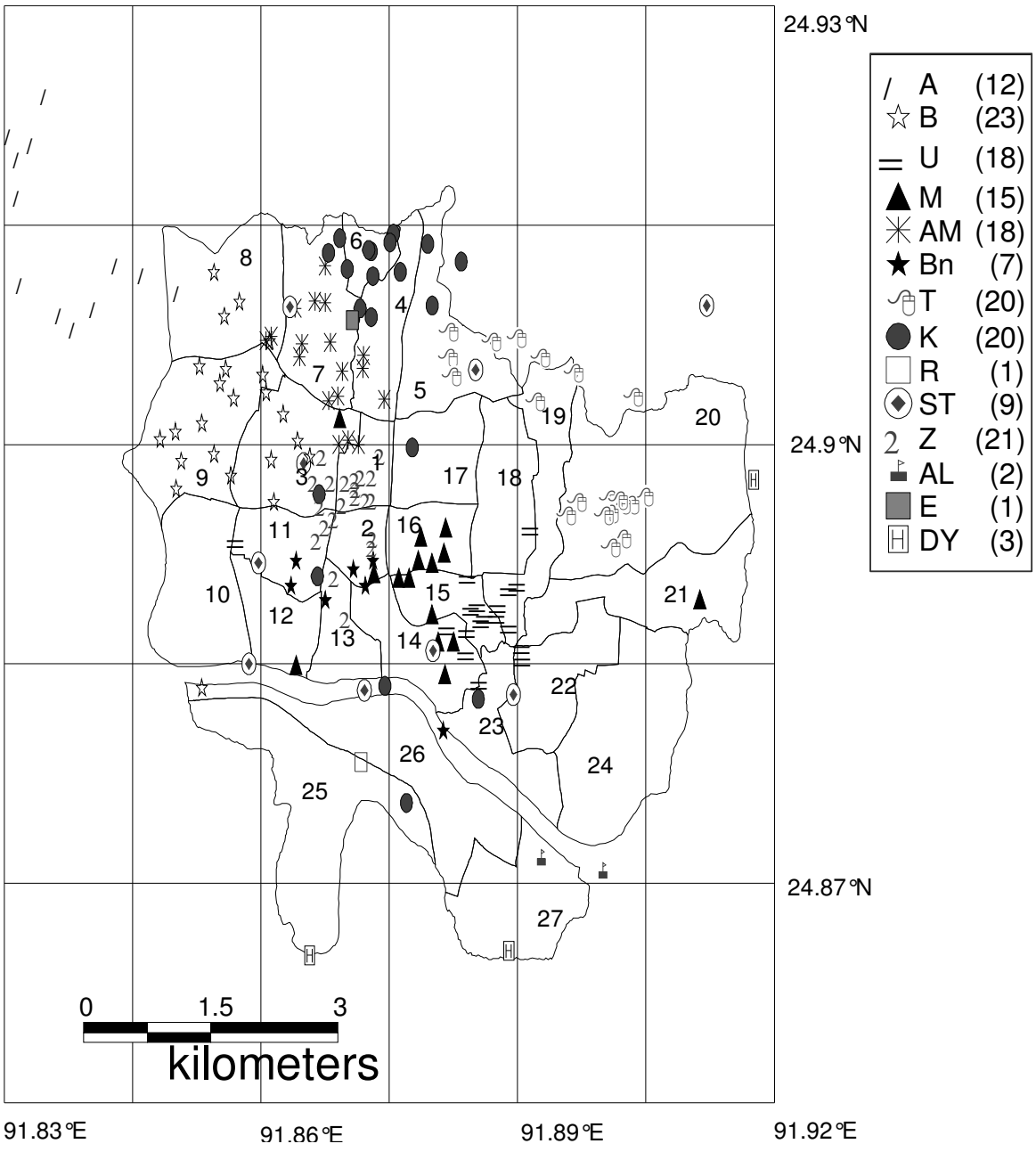

Figure 5.17 Map showing borehole locations considered for this study

Table 5.4 Location and Number of Borehole Data of study area

Area Code	Locations Included	Location Code	Number of Data
Akhalia	University Campus, Kumargoan	A	12
Bagbari	Modina Market, Pathantula, Sagardhigirpur, Subidbazar.	B	23
Amburkhana	Amburkhana Point, Housing Estate, Dargah, Jalalabad	Am	18
Zindabazar	Chouhatta, Tatipare, Zindabazar Point, Jallarpar, Jail Road, Nayasarak.	Z	26
Mendibag	Suphani Ghat.	M	17
Uposhahar	Block-A, B, C, D, E.	U	18
Tilagar	Tilagar Point, Majortila, Alutal, Shibgonj	T	20
Khasdabir	Mojumdari, Pirmahalla, Lichubagan, Choukidhighi.	K	20
Bondor	Taltala, Zero point of Sylhet, Station road, Kadamtali bus-stand.	Bn	07
Sylhet	Jalalabad, Law college, Bus-stand, Polytechnic	S	10

5.3.4.5 Hillocks data

The eroded hills are mainly formed by the hill ranges and hillocks (locally called tila) appearing in the north east and south of Greater Sylhet and also round about the Sylhet town. These hill ranges attain a low elevation and have a gentle slope. Hillocks are scattered in Sylhet City Corporation area . Among 27 wards some northern out fringe wards such as 5,7,8 have some hillocks and some core wards such as 1,9,10,11,17,18,19,20 have some hillocks. Figure 5.18 shows location of hillocks. Table 5.5 shows the present location together with height and slope of hillocks in City Corporation area.

Table 5. 5 Location of hillocks in Sylhet City Corporation

Ward No	Location	Height (Feet)	Slope angle (Degree)
1	Kajal sha	40	70
2	Kajal sha	25	45
3	Kajal sha	15	45
1	Naya sarak	40	45
2	Naya sarak	45	60
1	Manik pir	40	75
2	Manik pir	40	65
3	Manik pir	35	45
1	Mirboxtola	20	45
1	Ghor gobinda tila	30	85
2	Ghor gobinda tila	30	80
3	Ghor gobinda tila	25	75
1	Corer para	20	75
2	Corer para	30	90
1	Howladar para	30	90
2	Howladar para	30	90
3	Howladar para	25	90
4	Howladar para	25	90
1	Kazitula	25	45
2	Kazitula	30	45
3	Kazitula	30	45
4	Kazitula	40	75
5	Kazitula	30	90
6	Kazitula	20	45
7	Kazitula	30	60
8	Kazitula	30	60
1	Shai Eidgha	25	90
2	Shai Eidgha	40	80
3	Shai Eidgha	30	60
4	Shai Eidgha	30	90
5	Shai Eidgha	40	75
6	Shai Eidgha	45	60
1	Mitali R/A	30	75
1	Arambag	35	90
2	Arambag	35	90
1	Tilagar	20	60
2	Tilagar	25	60

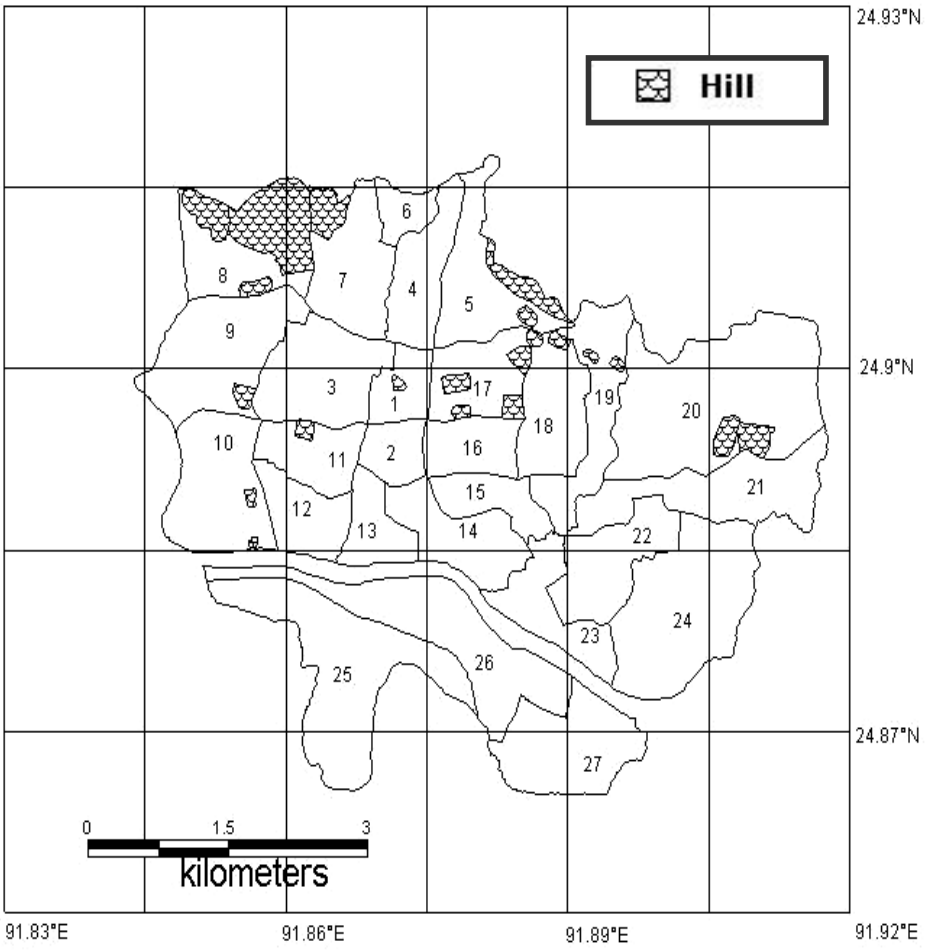

Figure 5.18 Map showing location of hill in Sylhet City Corporation

5.3.4.6 Building data

The building stock of Sylhet Municipality exhibits a mix of several different building technologies. The most commonly used building categories are

1) Reinforced-concrete frame building with partition wall;
2) Brick masonry buildings with reinforced concrete roofs and using cement mortar;
3) Informal brick masonry buildings (which may or may not use cement mortar)
4) Buildings made of other materials such as tin sheets, thatch, mud, wood and other lightweight elements.

The first two categories typically constitute engineered constructions in which the assistance of qualified engineers is usually taken at each stage. The last two categories are non-engineered constructions, wherein the services of skilled

engineers may not have been employed. In Sylhet, it has been observed that many reinforced concrete and brick masonry buildings have been constructed without the assistance of qualified engineers. Due to this reason, these buildings are also not engineered since they may be improperly designed or constructed resulting in lower strength.

A sample sites survey of the area is important for building damage estimation due to earthquakes, and also for earthquake disaster risk management. In the following paragraphs a pilot study undertaken for this survey was elaborated.
The methodology adopted for the sample site survey consisted of several tasks that are described briefly in below.

For survey purpose 27 wards have divided into four types. Group 1, which clustered 4,5,6,7,8,9,19. Ward 7 is comprehensively surveyed. Group 2 in which wards 1,2,3,11,15,16,17,18 among which all wards are partially surveyed. 10,12,13,14,23 wards are included in groups 3 where wards 12,13,14 are partially surveyed. Group 4, which are clustered with ward 20,21,24,25,26,27 where no survey is conducted but data is collected from BBS, 1991. Figure 5.19 shows location of these surveyed wards with respect to Sylhet.

A survey format was developed for the conduction of the pilot study survey. The format allowed for recording information from

i) A structured interview with the house owner,
ii) Visual observation of the condition of the buildings, and
iii) Measurement of the geometry of the sample building with tape.

For the pilot study, interview was adopted and questionnaire format was developed.

The questions for the interview consisted of about 40 to 50 queries to clarify in detail the characteristics of the buildings.

The survey format consisted of three parts, notably, A) General Information, B) Building Details, and C) Lifeline Details.

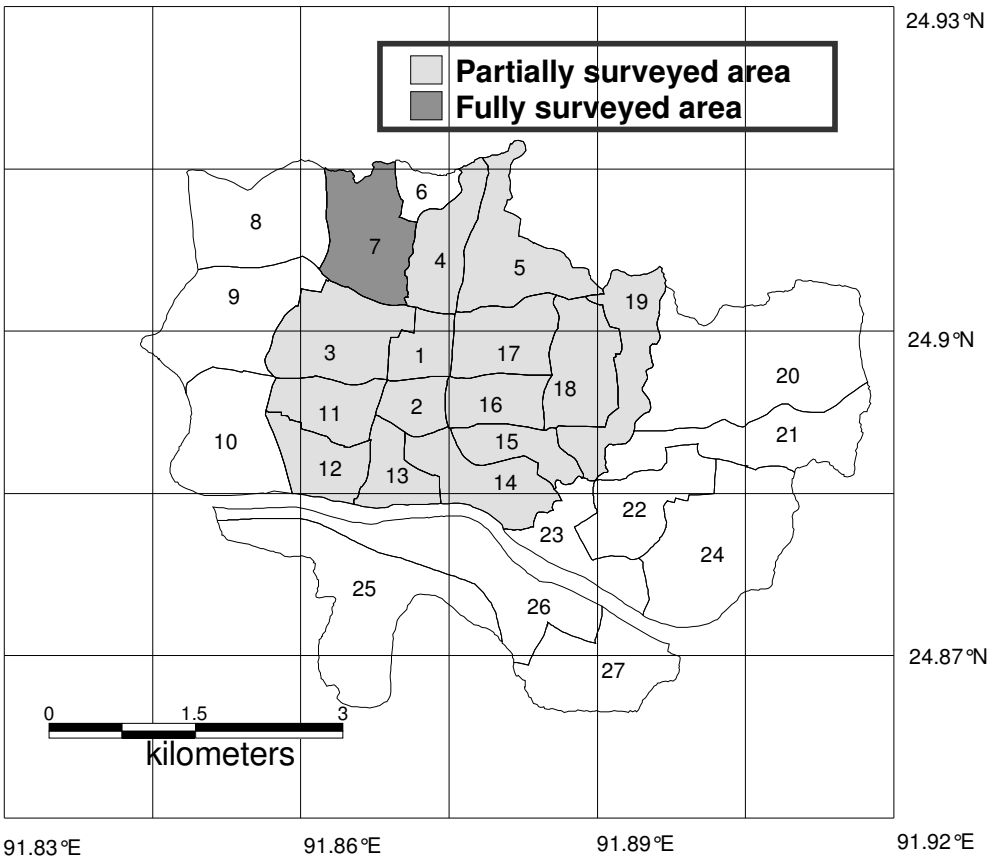

Figure 5.19 Map showing location of sample sites

5.3.4.7 Results of the site survey

Since Sylhet is an old city, several engineered constructions are also very old and were constructed decades ago. These buildings have already exceeded their useful service life and several of them have deteriorated badly. Most buildings that are found in Sylhet are non-engineered. These structures are typically designed and for constructed by people without appropriate technical qualifications. Most such buildings are designed without any detailed analysis and may also be a poor quality. Lifeline facilities distributed over the city area. But proper planning and design for earthquake resistance has not been considered.

The sample site survey results helped to classify all buildings in Sylhet into six types based on their definition in European Macroseismic Scale (Grunthal, 1998).

Table5. 6 Wall and Roof material used in Sylhet City Corporation (Source: BBS,1997)

Locality and wall material	Material of roof			
	Total house hold	Straw/bamboo /Polythene	Tiles/C.I/M etal sheet	Cement
Total House	16143	944	10912	4287
Straw /Bamboo	3495	787	2708	-
Mud/Unbrunt brick	1979	71	1908	-
C.I/ Metal Sheet	657	16	641	-
Wood	131	1	130	-
Cement/Brick	9881	69	5525	4287

3040 buildings (only 12% of the total) were surveyed from the above-mentioned wards. From the building survey results together with Wall and roof material are shown in Table5.6 is used to understand the building type distribution pattern. From the jurisprudence the building distribution of the study area is clustered in to four groups, such as gorup-1, group-2, group-3 and goup-4 shown in Table 5.7. The distribution pattern of building inventory is presented in Table 5.7.

Table 5.7 Building-distribution patterns in Sylhet City Corporation

Group 1		Group2		Group3		Group4	
Ward No: 4,5,6,7,8,9,19		Ward No: 1,2,3,11,15,16,17,18, 22		Ward No: 10,12,13,14,23		Ward No: 20,21,24,25,26,27	
Building Type	%	Building Type	%	Building Type	%	Building Type	%
A	0.51	A	0	A	12.26	A	12.26
B1	40.87	B1	36.62	B1	34.65	B1	34.65
B2	0.81	B2	6.58	B2	3.15	B2	0.42
C	50.57	C	48.22	C	23.14	C	26
D	0.24	D	0.58	D	0.27	D	0.14
F	7	F	8	F	26.53	F	26.53
Total	100%	Total	100%	Total	100%	Total	100%

The results of the survey are summarized in Table5.8.

Table 5.8 Building classification according to survey results and Bureau of Statistics (1991)

Ward No	Housing Unit	EMSA	EMSB1	EMSB2	EMSC	EMSD	EMSF
1	1399	0	512	92	675	9	111
2	700	0	256	46	338	4	56
3	1022	0	374	67	492	6	83
4	335	2	137	3	169	1	23
5	980	5	400	8	496	2	69
6	702	4	287	6	355	2	48
7	1238	6	506	10	626	3	87
8	1157	6	473	10	585	3	80
9	780	4	319	6	394	2	55
10	926	114	321	29	214	3	245
11	715	0	262	47	345	4	57
12	1170	143	405	37	271	3	311
13	1061	130	368	33	246	3	281
14	1024	126	355	32	237	3	271
15	567	0	208	37	273	3	46
16	1147	0	420	75	553	7	92
17	1380	0	505	91	665	8	111
18	1287	0	471	85	621	7	103
19	858	4	351	7	433	2	61
20	670	82	232	3	174	1	178
21	608	75	211	3	158	1	160
22	317	0	116	21	153	2	25
23	919	113	318	29	213	3	243
24	1448	178	502	6	376	2	384
25	1425	175	494	6	371	2	377
26	1058	130	367	4	275	2	280
27	1099	135	381	5	286	2	290

5.3.4.8 Construction age of Buildings

Of the 3040 building samples (Figure 5.20) it is appeared from the building survey that more than 62% of the building in Sylhet City Corporation area is less than 11 years old. However, about 4% of the buildings in Sylhet City Corporation area are more than 40 years old indicating to a higher vulnerability, especially if one considers that the predominant type of older buildings is of type EMSB. There are significant growths in EMSC constructions using RCC beam and column started only 20 or 30 years ago. Although some of these buildings are made of RCC, they are basically non-engineered and are extremely vulnerable.

A majority of building including ward number 4,5,6,7,8,9,10,20,21,24,25,26,27 posses more than 85% building is one storied building and the rest of building is 2-5 stories high and about 15% one the other hand ward number 1,2,3,11,12,13,14,15,16,17,18,19,22,23 posses more than 49% building is single-stories and the rest of building is 2-7 stories high and about 51%. Figure 5.21 show the distribution of buildings in the areas according to number of stories and floor space.

In the study area, for seismic loss estimation for building damage it is needed to know the average weighted house area as well as average weighted floor space. Table 5.9 shows the ward wise distribution of house area and floor space in the study area.

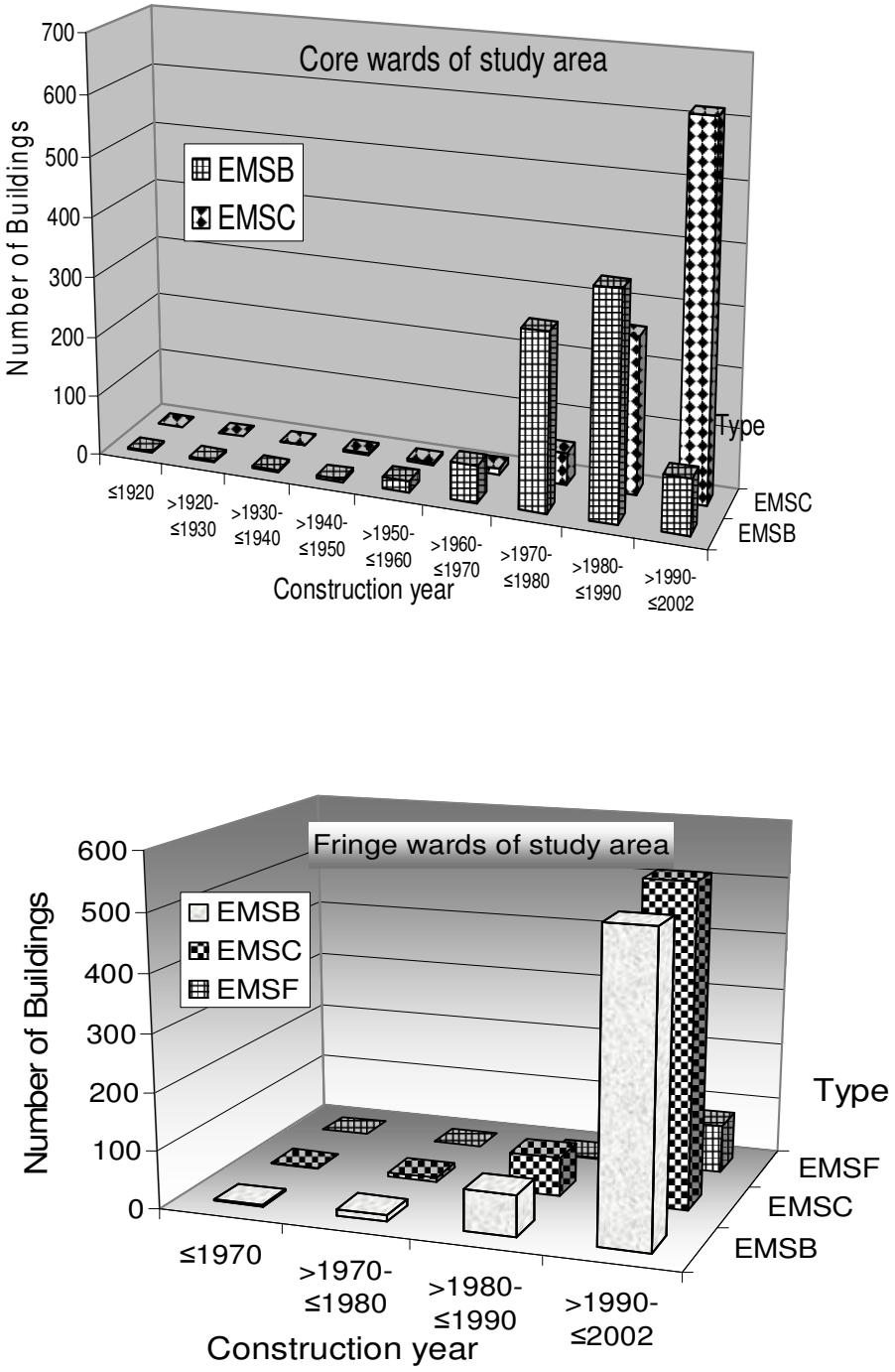

Figure 5.20 Distribution of buildings types with construction year for core and fringe ward in study area.

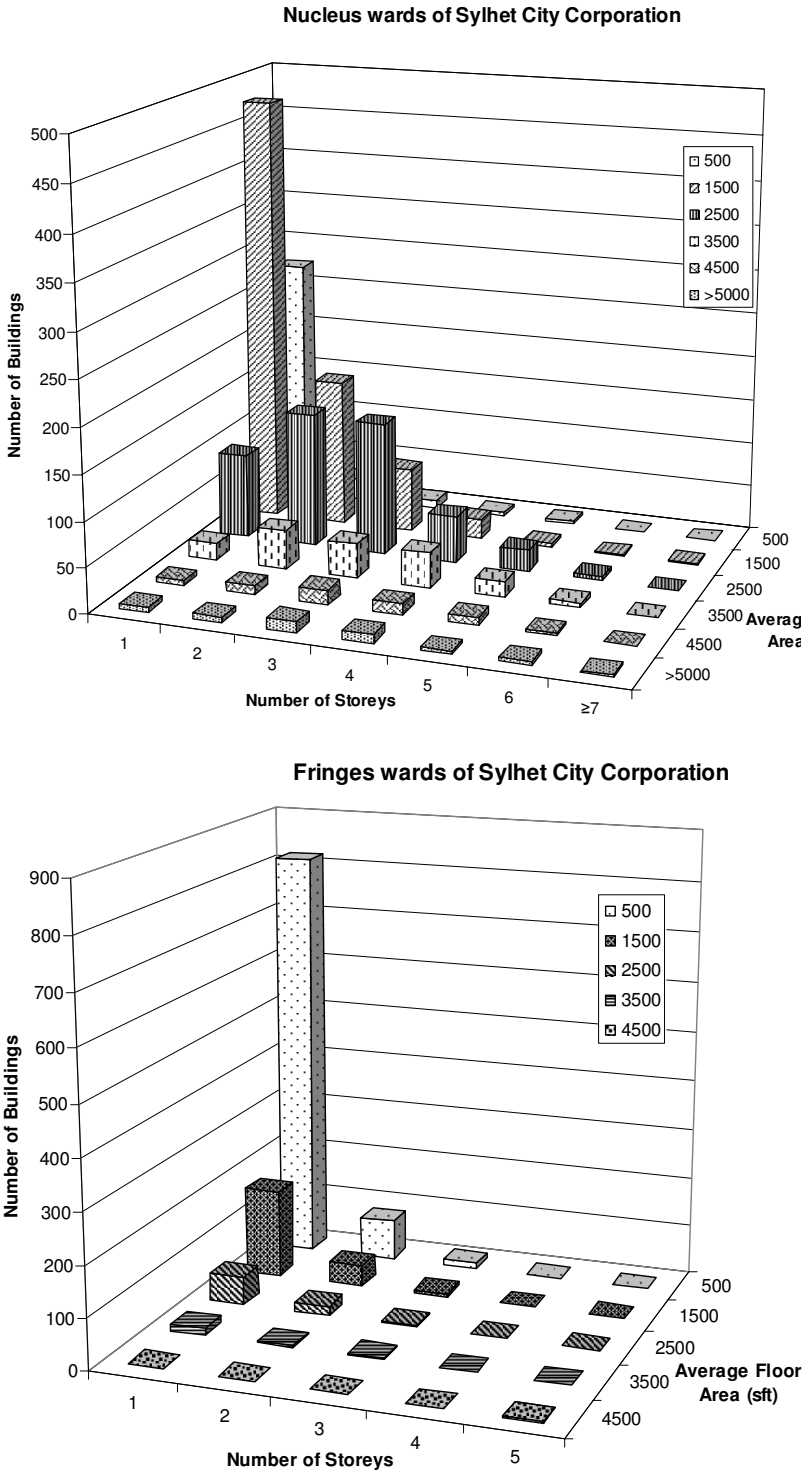

Figure 5.21 Distribution of building types according to their storey and floor area for core and fringe wards of study area.

Table 5.9 Weighted house area and floor space in study area

Ward No	Weighted House Area (sft)	Weighted House Area (m^2)	Weighted Floor Space (sft)	Weighted Floor Space (m^2)
1	1964	182.528	4568	424.535
2	1972	183.271	4695	436.338
3	1967	182.807	4648	431.97
4	908	84.3866	1206	112.082
5	879	81.6914	1113	103.439
6	878	81.5985	1114	103.532
7	871	80.948	1087	101.022
8	875	81.3197	1093	101.58
9	881	81.8773	1120	104.089
10	873	81.1338	1096	101.859
11	1965	182.621	4590	426.58
12	1959	182.063	4603	427.788
13	1967	182.807	4630	430.297
14	1967	182.807	4649	432.063
15	1977	183.736	4629	430.204
16	1957	181.877	4585	426.115
17	1967	182.807	4651	432.249
18	1974	183.457	4643	431.506
19	1969	182.993	4623	429.647
20	886	82.342	1127	104.74
21	884	82.1561	1138	105.762
22	1966	182.714	4658	432.9
23	1962	182.342	4568	424.535
24	871	80.948	1088	101.115
25	870	80.855	1083	100.651
26	878	81.5985	1109	103.067
27	877	81.5056	1102	102.416

5.3.4.9 Life lines data

Lifelines include water and sewage systems, electric power and communication systems, natural gas facilities (including pipelines), transportation systems, airports, and harbour facilities. In this study for the analysis of potential losses of lifelines only the most up-to-date site-specific data for water supply system and natural gas supply system were collected and analysed using Cheng et al.'s (2002) method.

The construction blueprints of water delivery pipelines (prepared by LGRD) of the study area were digitized into a Geographical Information System (GIS) for analysis and assessment. Informations of water supply system has been shown briefly in Table 5.10. Water pipe line and other features of the study area are shown in Figure 5.23. Pipeline distribution according material and diameter is also shown in Figure 5.23 and Figure 5.24. From the collected data it can be seen that only the municipality is well served by water mains where 28.8% of the households have access to piped water.

The construction blueprints of natural gas supply system (prepared by Jalalabad Gas Office, 2005, Sylhet) of the study area were digitized into a Geographical Information System (GIS) for analysis and assessment. In order to perform analysis, the pipelines were divided into two groups according to their diameters and the study area is divided into 1km × 1km grid with pipelines enclosed in the grid. Information's of natural gas supply system have been shown briefly in Table 5.12. Gas pipelines distribution of the study area are shown in Figure 5.25 to Figure 5.27. Pipeline distribution according material and diameter is also shown Table5.12

Table 5.10 Informations of water-supply system (source: Sylhet City Corporation, 2005, Sylhet)

Pipe network	A drawing prepared by LGRD collected from Sylhet City Corporation	
Capacity of supply system	Sylhet Municipal Water Supply System has capacity more than 36,37,000 litres per day.	
Source of water	Tube wells	
Tube wells	9 deep tube wells under Sylhet City Corporation	
	Privately operated tube wells 2789 nos. among which 2261nos. shallow tube wells, 20 nos. deep tube wells, 504 nos. DSP tube wells / Tara pump and 4 nos. rig wells.	
Treatment plant	Number of existing treatment plant is 1and Functioning well	
Storage tanks	3 overhead tanks (2 operational) and 1 under ground tank	
Water connections	3871 domestic and 156 commercial/industrial	
Length of pipeline installed	More than 118 km	
Material used	Material	Length (km)
	Polyvinyle Chloride(PVC)	44 (existing), 52(proposed)
	Asbestose Concrete(AC)	12.5
	Galvanised Iron(GI)	5.7
	Cast Iron(CI)	1.7
	Mild Steel(MS)	1
	Ductile Iron(DI)	1

Table 5.11 Water pipe line distribution according diameter and material in study area

Material	Diameter (mm)	Length (km)
AC	100	0.25
AC	150	4.59
AC	200	3.47
AC	250	2.33
AC	300	1.92
CI	100	0.49
CI	150	0.53
CI	200	0.67
DI	300	1.04
GI	100	3.52
GI	150	0.33
GI	50	0.06
GI	200	1.87
MS	100	0.32
MS	150	0.41
MS	250	0.25
PVC	100	17.5
PVC	150	17.72
PVC	200	4.09
PVC	50	1.18
PVC	75	3.46
Proposed	100	14.9
Proposed	200	15.20
Proposed	150	22.09

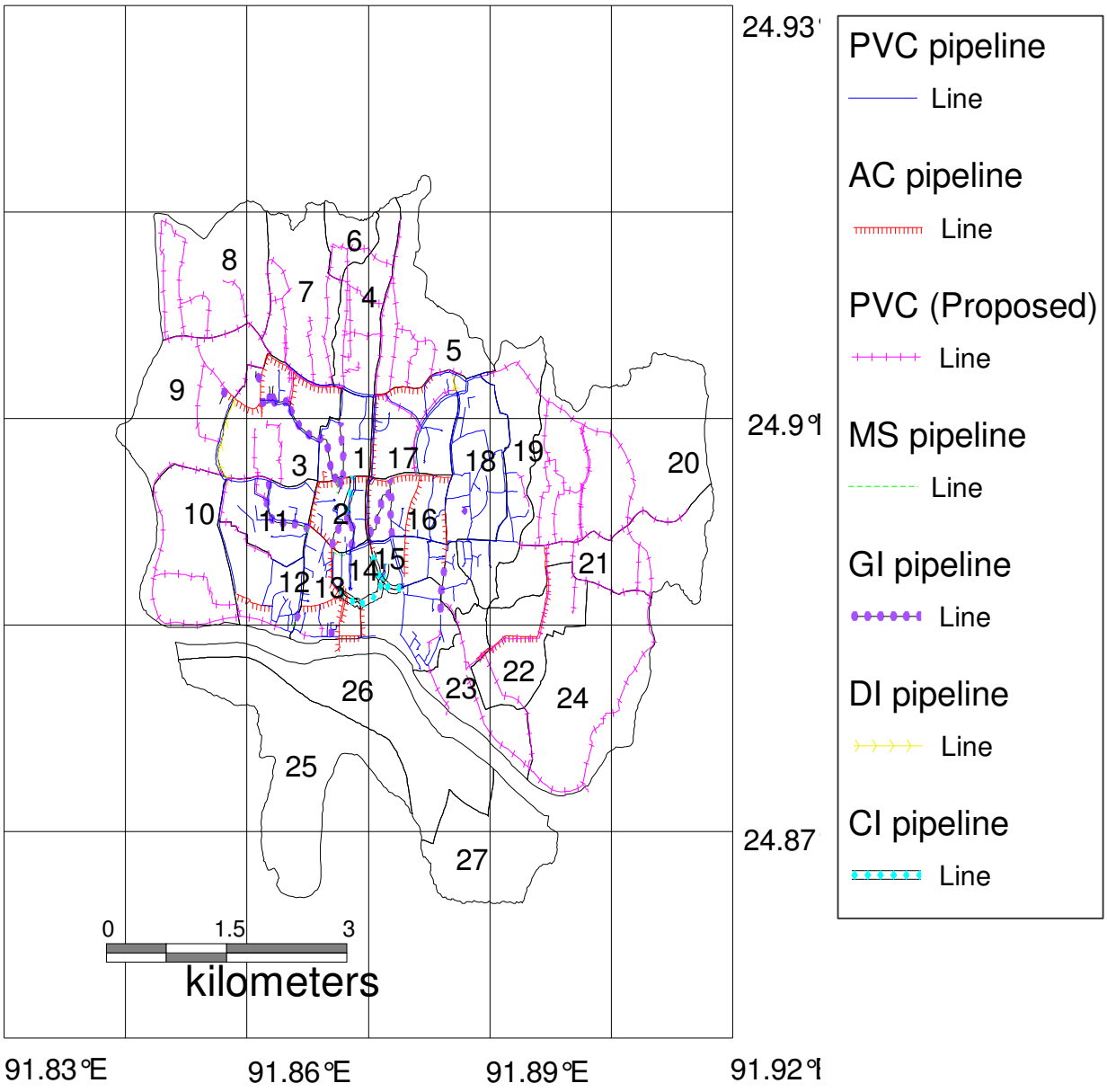

Figure5.22 Map showing distribution of water pipelines according material of Sylhet City

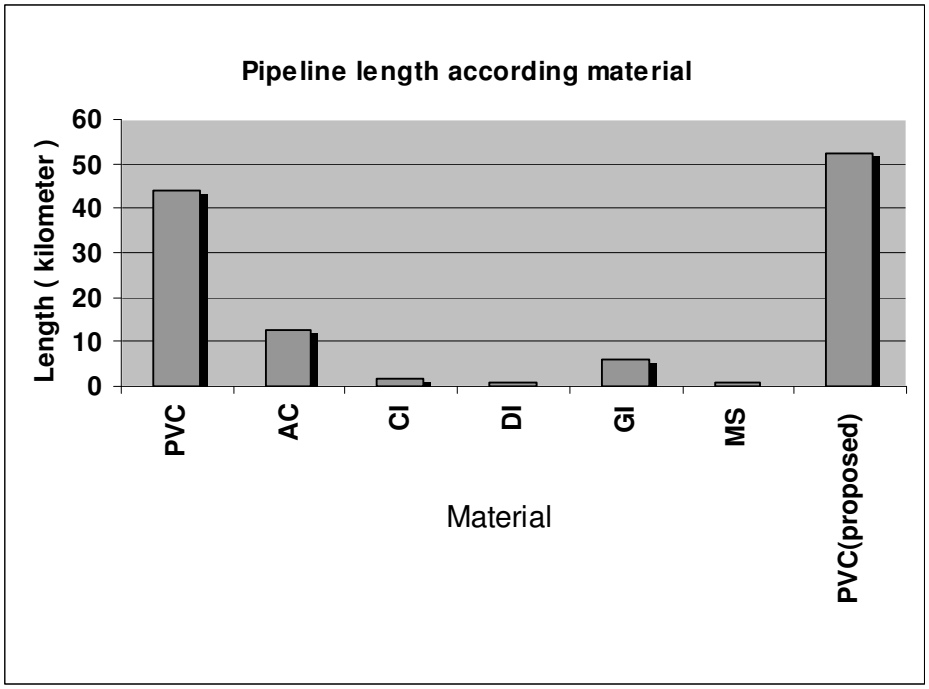

Figure 5.23 Distribution of lengths of water pipelines according to material in the study area

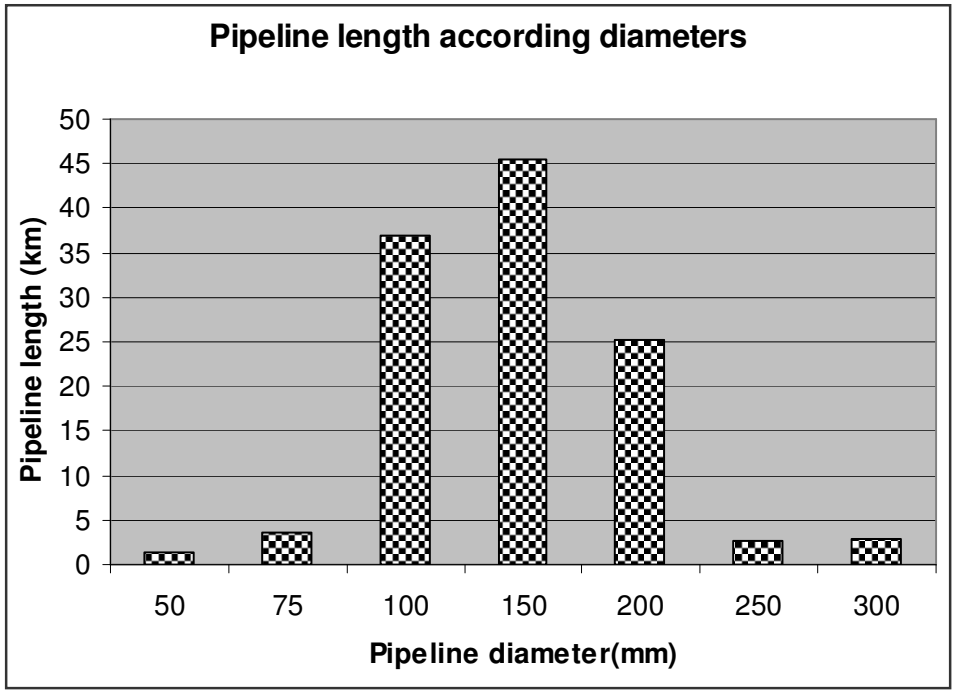

Figure 5.24 Distribution of lengths of water pipelines according to diameter in the study area

Table 5.12 Information of Gas-pipelines

Pipe network	A drawing from Jalalabad Gas Office						
Total capacity of the Jalalabad Gas Office	144.9 km						
Study area covered	106.4365 km						
Material used	Mild steel	Used for main flow					
		Distribution of 106.4365 km MS gas-pipe line					
		Pipe dia.(mm)	25	50	75	100	150
		Length (km)	42.8988	27.5269	22.1667	10.8925	2.9516
	PVC	Used for domestic and industrial purposes					
Gas valve stations		Total number of gas valve station used is 85					
		Distribution of 85 gas valve stions					
		Pipe dia.(mm)	25	50	75	100	150
		No. of valve stations	9	44	22	9	1

5.3.5 Inventory overview

Sylhet City has an area greater than 42.8 km^2 with about 51831 households in the city and a total population of about 311050 people. The 2003 population density distribution is shown in Table 5.2 and total number of building in the city is 25992. Major portion of the building are associated with residential housing.

The Sylhet municipal water supply system has a capacity of more than 36,37,000 litres per day. The length of pipeline installed exceeded 118 km.The piped water water system in Sylhet city serves about 3871 domestic connections and 156 commercial as well as industrial connections by Pourashava.(Sylhet City Corporation,1998) (Table 5.10 and Table 5.11). The Sylhet municipal Gas supply system has a capacity of more than 144.9 km but the length of pipeline installed

exceeded 106.4365 km. In the total pipelines there are a total number of 85 Gas Valve stations (Table 5.12).

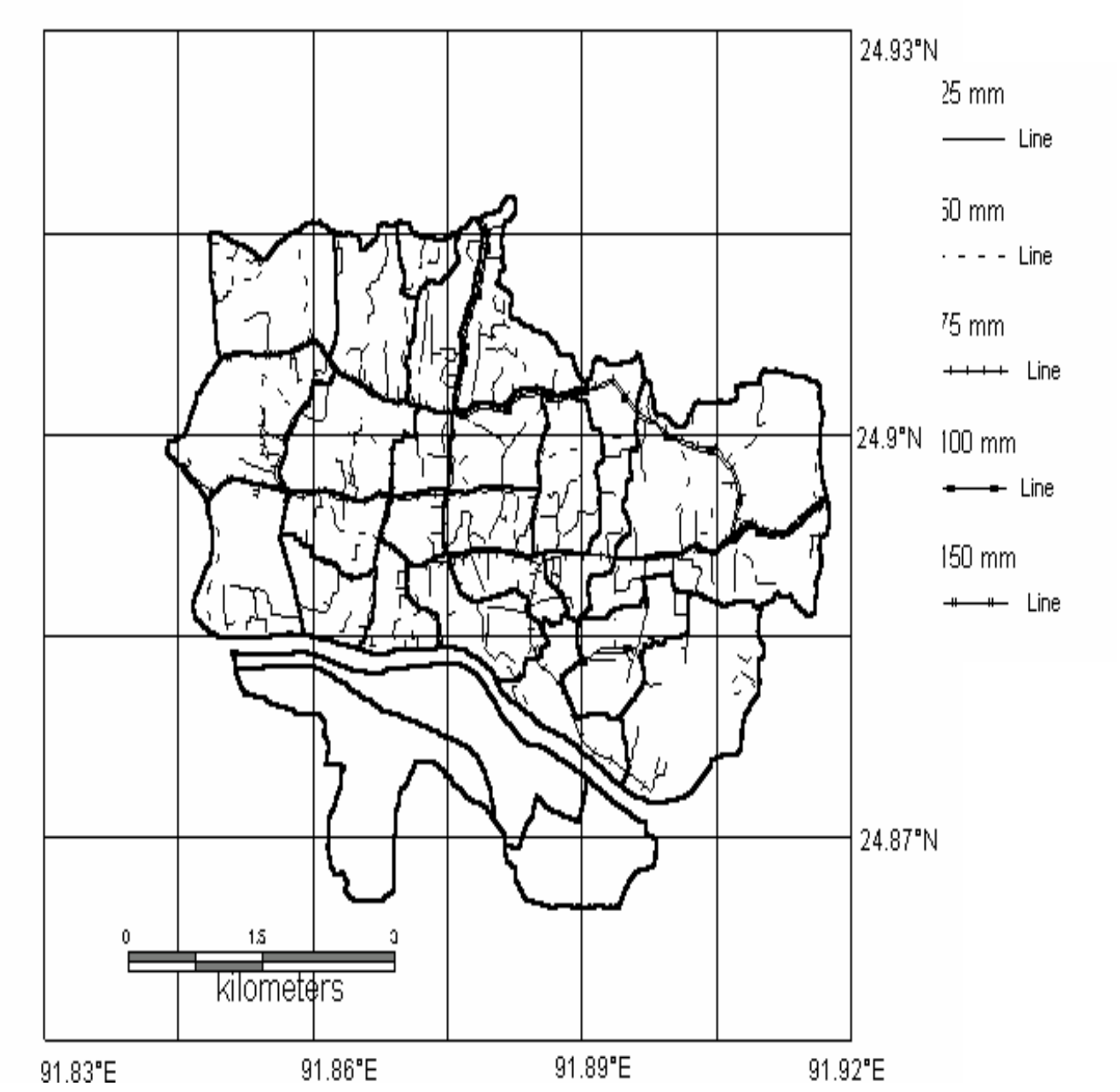

Figure 5.25 Gas pipeline distributions according to diameter.

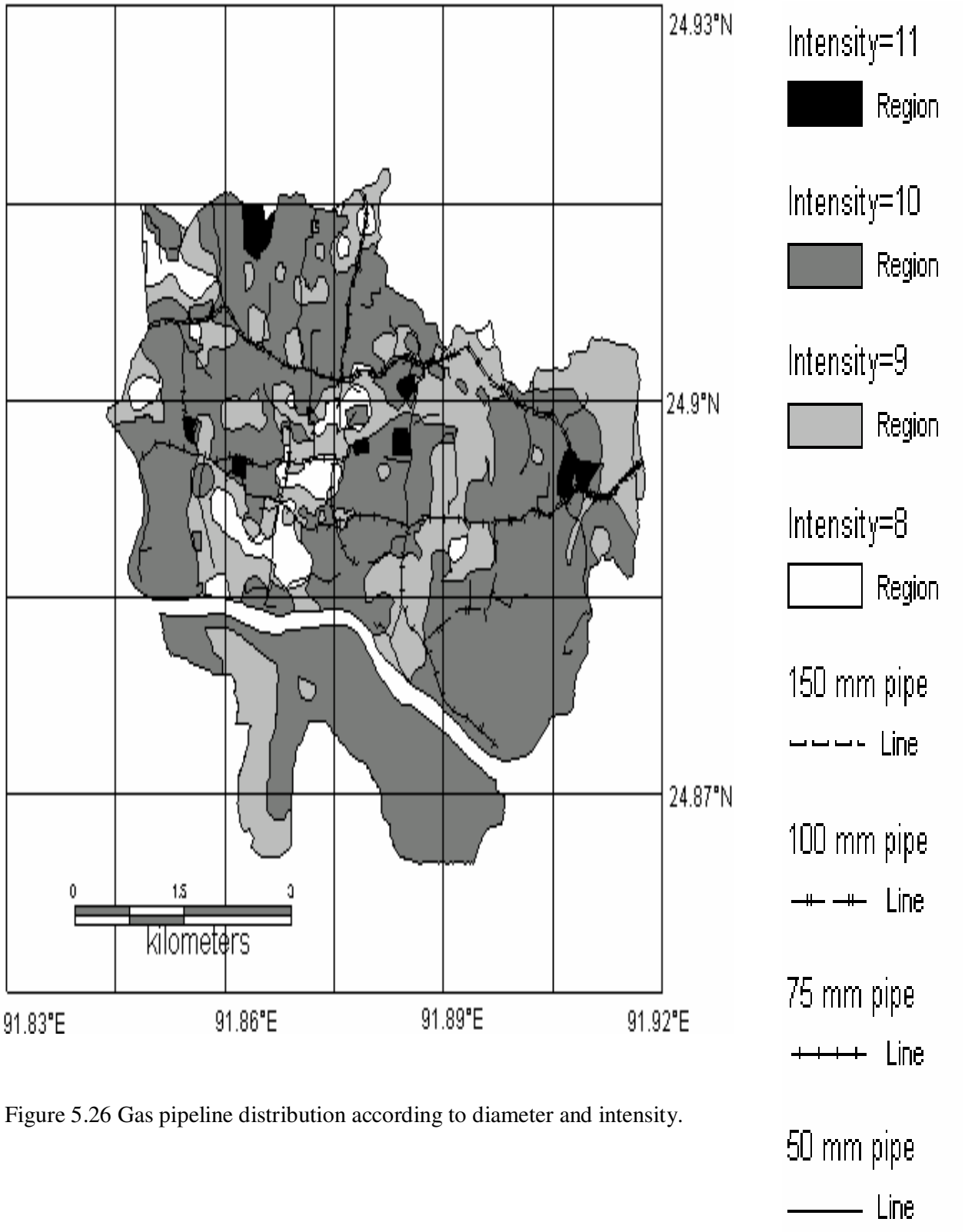

Figure 5.26 Gas pipeline distribution according to diameter and intensity.

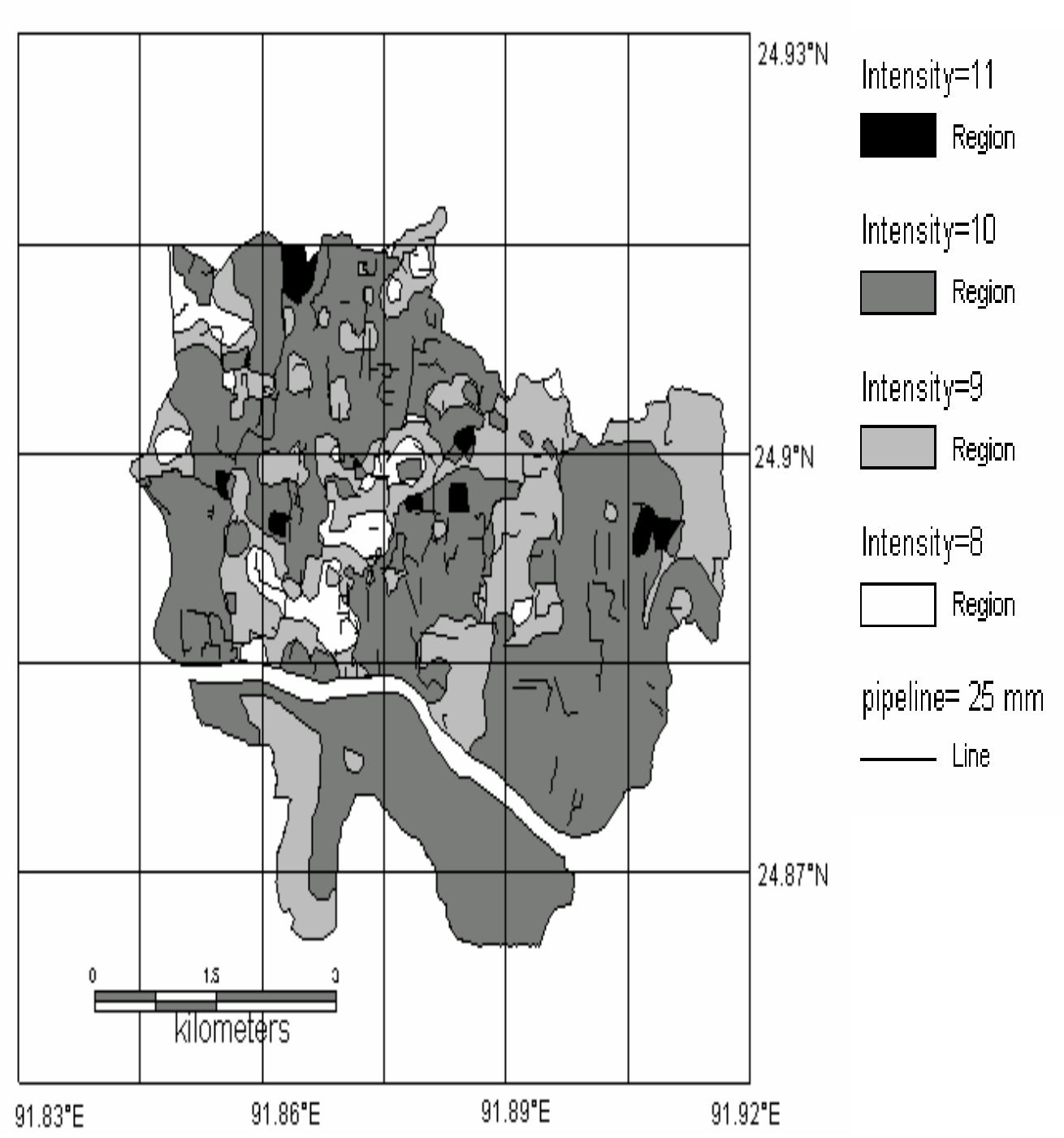

Figure 5.27 Gas pipeline distribution according to diameter and intensity.

5.4 Loss assessment

Table 5.13 provides an overview of the most significant losses that would be sustained in Sylhet if Srimangal earthquake (1918) scenario is considered in this study. Loss assessment has been done considering combined seismic hazard considering local site effects.

The findings highlight several critical factors that have important implications for earthquake risk reduction, planning, preparedness, emergency response, and disaster recovery. Results indicate, not surprisingly, that the **M** 7.6 Srimangal scenario would be the most destructive and disruptive to the Sylhet city. Results from the **M** 7.6 scenario include the following:

- 65% area will be affected with intensity X, 28%area will be affected with intensity IX, 5.5% area will be affected with intensity VIII and 1.5% area will be affected with intensity XI.

- Casualties at morning, noon and night time event assessed (Figure 5.28 to Figure 5.33). A nighttime event will cause the highest number of casualties. Of the estimated 47549 (approximately 15% of total population) casualties, close to 25875 or about 54 percent will be major injuries (injuries requiring hospitalization) or fatalities (about 21674).

- Nearly 15320 buildings buildings are expected to be damaged.

- There could be safety issues related to school children, teachers, and other persons in school buildings. The catastrophic failure or partial collapse of one or more school buildings during school periods could greatly increase the casualty estimates. Restoration of the schools for the emergency sheltering of the homeless and other contingency service will be demanding.

- Schools and fire stations are particularly vulnerable to damage. These losses are due to insufficient seismic building code standards and the vintage of the building stock, the majority of the structures in the city. This

situation may lead to issues with respect to providing reliable shelters for immediate use in emergency response and sheltering.

- Hospitals might suffer significant building damage. Due hospital damage the city may be faced with the serious issue of how to provide the needed care to existing patients and potentially thousands of earthquake victims from the affected communities.

- A good portion of the Sylhet city is susceptible to liquefaction. Ground failure effects, on the other hand, are more significant in the Charleston area for pipelines, roads and runways.

- Few million tons of debris will be generated, which includes concrete and steel—materials that require special treatment in "deconstruction" and disposal. Debris disposal, therefore, may pose a major challenge in the recovery phase. This total does not include biomass.

- In potable water pipes total number of damage points estimated 204 and total affected length 118.53 km. Widespread water failure may drain water within minutes or hours from the distribution system, thus preventing adequate water supply for fire suppression. In addition, rest of the urban households in the affected area will be deprived of water. It will take weeks, if not months, to restore the serviceability of the water systems. Therefore, significant external augmentation would be required to provide and sustain such a high repair level.

- Of all the utility systems, gas supply system is arguably the most critical for Bangladesh, as the natural gas is being used by the house holds as well as in many power plants. In natural gas supply system total number of damaged points estimated 981 and total affected length 436 km.

- This study is carried out only at Sylhet City Corporation area, which occupies 26.50 km^2 where as Sylhet Sadar Upazilla occupies 517.43 km^2. So only 5% area of Sylhet Sadar, which is with in the present study. It is believed that if potential earthquake trigger in northeastern part of Bangladesh, not only Sylhet City Corporation but also other part of this

upazilla might be severally affected. Consequently, if loss estimation is done according above mention issues it is very realistic that total loss due to this scenario event might exceeds several billion US dollars which is also be interpolated from past earthquake such as during 1999, September 21,Taiwan city affected this earthquake caused at least 2,297 people killed, 8700 injured, 600,000 people left homeless, and about 82,000 housing units damaged.

Table 5.13 Overview of results for key parameters in the case of 8 July 1918 Srimangal Earthquake (M = 7.6) scenarios

Category	Description of parameters	Results
Hazards	Peak ground acceleration (PGA)	Maximum 1.6g Minimum 0.45g
Critical	Schools with at least moderate damage	
Facilities	Hospitals with at least moderate damage	
	Fire stations with at least moderate damage	
Lifelines	Damage to potable water pipes	Total number of damaged points 204 (total affected length 118.53 km).
	Treatment plant with at least moderate damage	Has not been conducted separately
	Damage natural gas supply pipes	Total number of damaged points 981 (total affected length 436 km).
Building damage	Total number of buildings damaged A type B1 type B2 type C type D type F type	15320 59% 76% 76% 55% 12% 15%
Casualties	Morning event: Injuries Deaths	20569 (6.6% of total population) 17249 (5.5% of total population)
	Noon event: Injuries Deaths	13979 (4.5% of total population) 11713 (3.75% of total population)
	Night event: Injuries Deaths	25875 (8.3% of total population) 21674 (7% of total population)

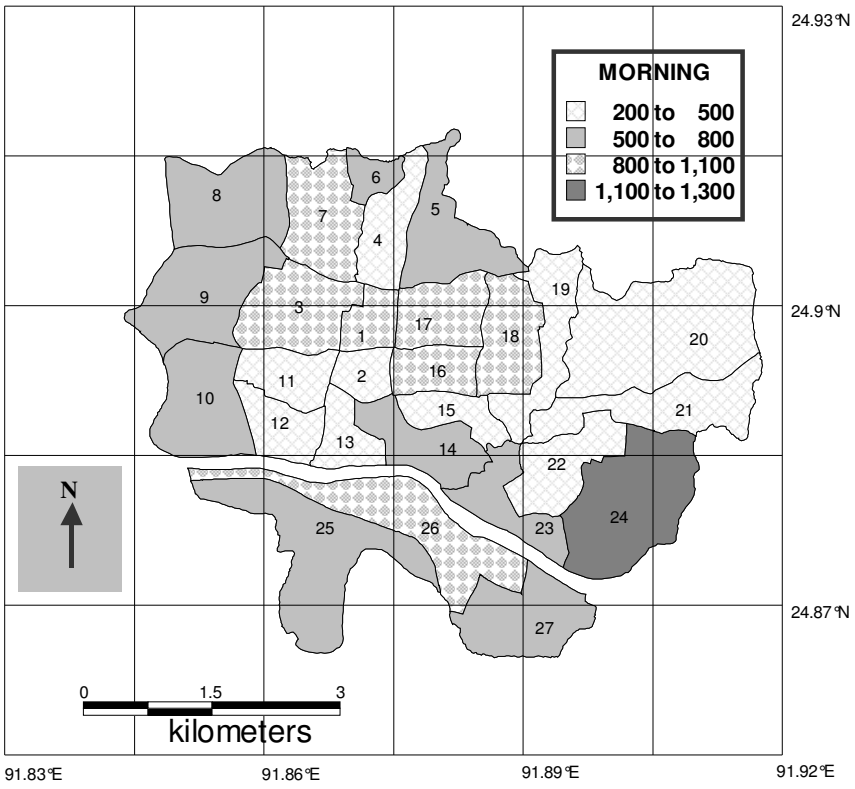

Figure 5.28 Map showing total number of deaths at Morning in Sylhet City

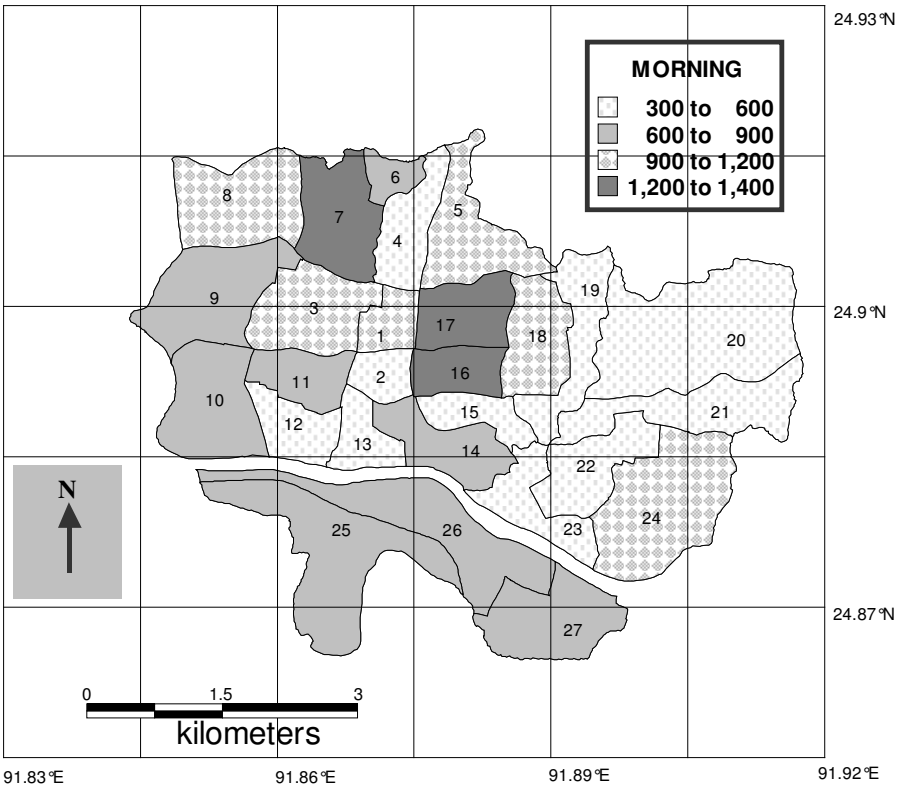

Figure 5.29 Map showing total number of injuries at morning in Sylhet City

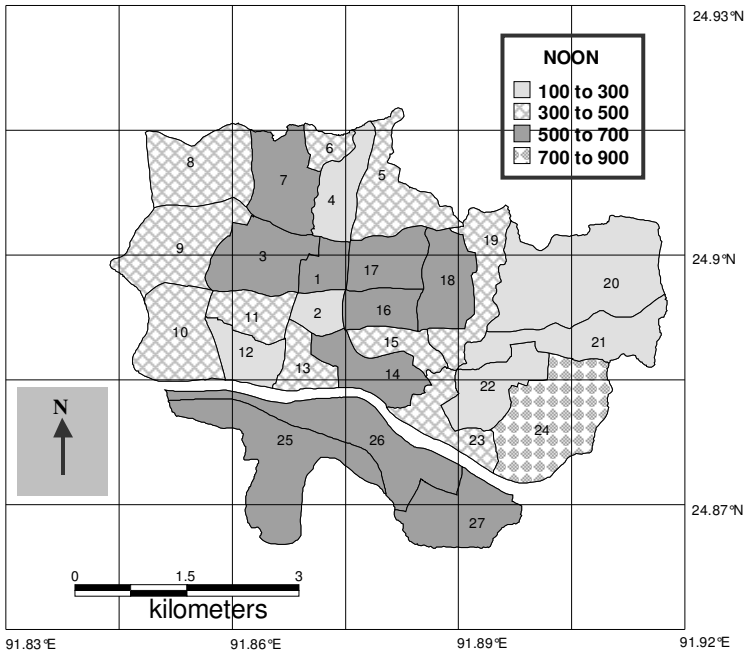

Figure 5.30 Map showing total number of deaths at noon in Sylhet City

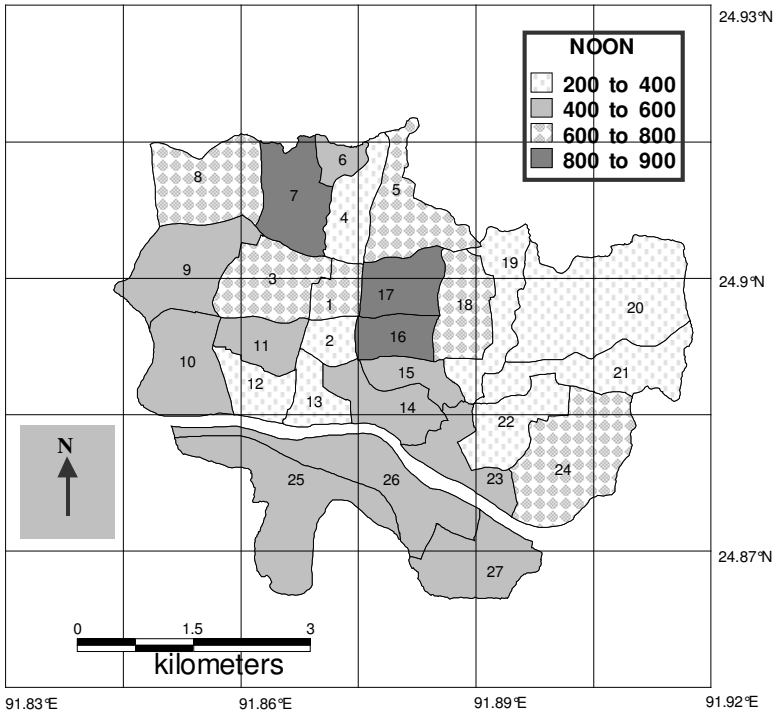

Figure 5.31 Map showing total number of injuries at noon in Sylhet City

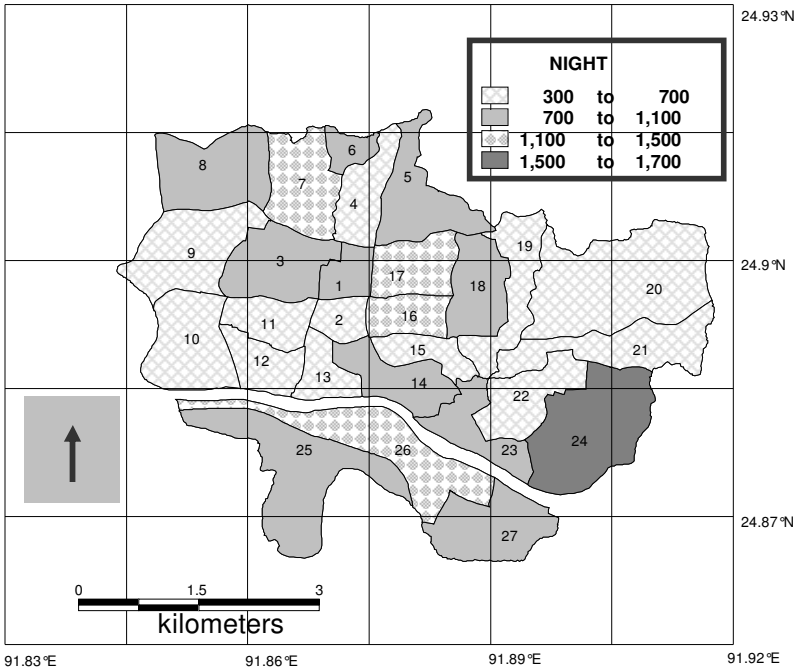

Figure 5.32 Map showing total number of deaths at night in Sylhet City

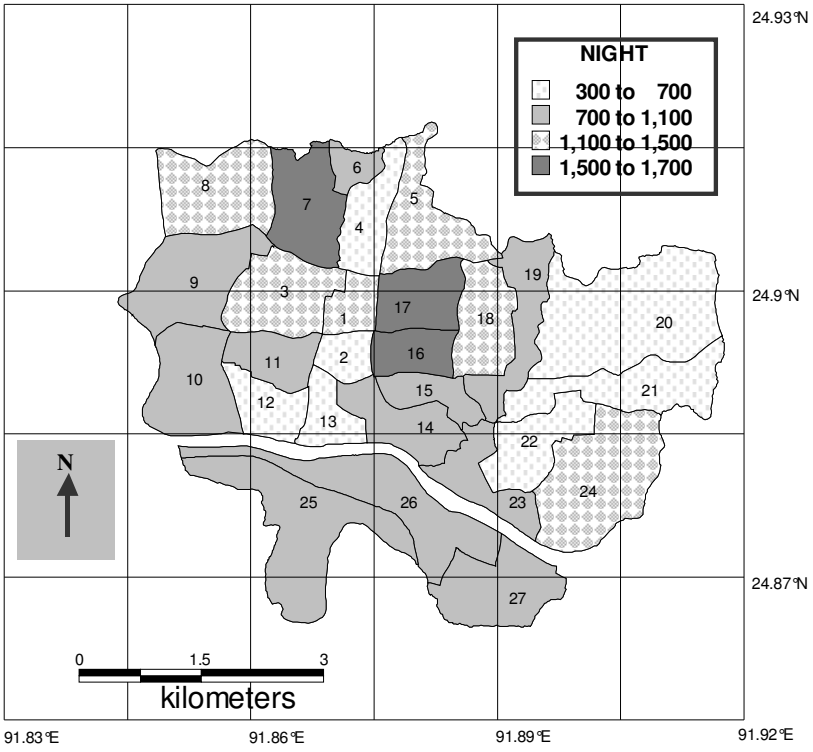

Figure 5.33 Map showing total number of deaths at night in Sylhet City

5.5 Summary

This chapter presents a case study to illustrate the GIS-based methodology for regional seismic hazard and risk analysis discussed in this dissertation. In this case study Srimangal earthquake (1918) of magnitude 7.6 was considered to develop a combined seismic hazard map and for estimating earthquake damage and losses of Sylhet City. This chapter contains a simplified version of the project, but serves to illustrate the role of geographic information systems in all aspects of the analysis, from identifying the potential seismic sources to computing the final loss estimates.

Maps and example database tables are shown at various stages in the analysis to illustrate the overlay procedure and the relationships among the various models and tables of data. The seismic hazard analysis details the estimation of ground shaking, the effects of the various collateral hazards, and the combination of all seismic hazards in the region. The next part of the analysis covers the development of structural inventory and the estimation of earthquake damage and losses. These results are shown in Table 5.13 for buildings and water/gas pipelines.

The number of deaths is estimated at over 21674 (at night) in this case study. This seems very high when compared to recent previous earthquakes in Bangladesh, indicating that the models used to estimate casualties need further investigation.

As discussed in Sections 3.3.5.1 and 3.3.6.1, the results of damage and loss in this case study are not intended to be used for site- specific analysis. They are based on simplified models and several assumptions, therefore they are meant to be used only for averages or summaries on a regional basis. Relative comparison of the results is intended to indicate areas that should be investigated in a more detailed analysis. The final results are also meant to help emergency managers and planners allocate resources and prepare hazard mitigation programs in a region.

CHAPTER 6

CONCLUSIONS AND RECOMMENDATIONS

6.1 Conclusions

The purpose of this research has been the development of methodology for using geographic information system (GIS) to integrate the various components of a regional multi-hazard seismic risk analysis. In this thesis, the seismic risk analysis includes consideration of primary hazards due to ground shaking and to local site effects such as soil amplification, liquefaction, landslide, and surface fault rupture. The model also incorporates structural inventories and motion-damage relationships. The hazard maps are then overlaid and combined with structural inventory maps to produce maps predicting regional damage distributions. Combining the maps of damage distributions with maps of population distributions for the area results in final estimates of direct loss, indirect loss, and casualties.

The integrated GIS-based methodology presented in this thesis has been designed for seismic hazard and risk analysis on the regional, not site-specific level. The results are intended to provide general estimates of damage and loss distributions. For this reason, the hazard and loss models that have been chosen for use in this thesis are fairly simplified and suitable for use with regional spatially-distributed data. The flexible framework of the GIS-based methodology allows the analysis system to be updated and expanded with new models and database information.

The major conclusions and findings of the study have been summarized below:

- The integrated GIS-based methodology presented in this thesis is designed for seismic hazard and risk analysis on the regional, not site-specific level. The results are intended to provide general estimates of damage and loss distributions.

- The behavior of the local soil conditions, as well as the accuracy of the geologic and geotechnical information, can vary greatly from region to region. For this reason, the regional hazard combination methodology developed in this thesis has been based on weighted average approach.

- An attempt has been made to investigate and distinguish the PGA/intensity values of a region due to liquefaction, land slide and fault rupture. By analyzing the data of ground motion obtained from locally built SHAKE Table for a particular soil, quantification of secondary site effects have been made.

- As a result of continuous monitoring in the last five years, twelve earthquakes (M<5) with 37 acceleration data have been recorded. More data is needed to develop a reliable attenuation model.

- The number of intensity based observed data are more than acceleration based data. Intensity of these events has been converted to acceleration. These converted 40 acceleration records from 8 events (Magnitudes between 6 and 9) have been regressed to develop an attenuation model.

- The developed method on seismic hazard analysis has been applied on Sylhet City. To estimate the damage and loss of Sylhet City due to a scenario event having the same magnitude and location of 1918 Srimangal earthquake with magnitude 7.6 has been considered. A detailed structural inventory of more than 3040 buildings, 106 km gas lines and about 118 km of water supply lines have been compiled.

- Economic loss estimation has been carried out using the damages expected to be suffered due to the scenario event. Among total buildings, 59% is expected to be damaged. In case of lifeline, total number of damage points is 204 for water pipes and total number of damage points is 981 for gas pipes.

6.2 Recommendations

This thesis has covered a broad topic; therefore several areas of future research may be identified. These areas can be divided into four general categories. The first category concerns the effects of local site conditions, including seismic hazard integration. The second area deals with the definitions and models for earthquake damage and loss estimation. The third category concerns the utility of a regional seismic hazard and risk analysis. The final category concerns the development of

acceleration based attenuation relation for Bangladesh. The specific recommendations have been summarised below:

- In this thesis, soil amplification has been modeled by a simple multiplication factor, liquefaction and landslide have been modeled with a qualitative description of 'high', 'moderate', 'low', potential and surface fault rupture has been characterized by a defined zone of rupture potential. More quantitative models for these site effects may be developed.

- In this thesis secondary site effects have been studied in the laboratory for a particular soil. By using different types of soil the simplifying assumption for the relation between the primary site effect and secondary effects may be improved.

- The motion-damage relationships used in this thesis have been based on expert opinion. Clearly, new relationships are needed that estimate damage as a function of an instrumented ground motion.

- Loss of functionality and other in-direct losses such as debris-removal and financing of repairs need to be considered.

- There are few models for non-monetary losses such as casualties, unemployment and homelessness. As with indirect loss models, improvements to the non-monetary loss models are best made by sociologists and socio-economists rather than structural engineers.

- Acceleration, velocity and displacement response spectra may be generated from accumulated strong motion data. Then response spectra can be used to develop attenuation models for different structural period.

REFERENCES

Agbabian, M and G.V. Chilingarian (1991). “Earthquakes of the Armenia Highlands (Seismic Setting).” University of Southern California Report. Los Angeles, California.

Aki, K (1988), “Local Site Effects on Strong Ground Motion.” Proceeding of the ASCE Conference on Earthquake Engineering and Soil Dynamics II. Rolla, Missouri, pages 103-155.

Alam, M. K., Hassan A.K.M.S., Khan M.R., Whitney J.W., (1990) “Geological Map of Bangladesh”, Government of the People’s Republic of Bangladesh. Geological Survey of Bangladesh.

Algermissen, S.T and K. Steinbrugge (1984). “Seismic Hazard and Risk Assessment: Some Case Studies.: The Geneva Papers on Risk and Insurance. Volume 9, Number 30.

Ambraseye, N.N.(1990). “Uniform magnitude reevaluation of European earthquakesassociated with strong ground motion.” Earthquake Engeering and Structural dynamics. Volume 19, pages 1-20.

Ambraseye, N.N and J.J. Bommer(1991). “ The attenuation of ground acceleration in Europe.” Earthquake Engeering and Structural dynamics. Volume 20, pages1179-1202.

Ambraseys N.N. (2000). Reappraisal of North-Indian earthquakes at the turn of the 20th Century, Current Science, Volume 79 (9-10), 1pp.237-1250.

Andrews, D.C.A. and G.R. Martin (2000). “Criteria for Liquefaction of Silty Soils”, in Proc. 12th World Conference on earthquake engineering, Aucland, New Zealand.

Anagons, T and A.S. Kiremidjian (1984). “Stochastic Time-Predictable Models for Earthquake Occurrences”. Bulletin of the Seismological Society of America. Volume 74, Number 6, pages 2593-2611.

Annaka, T and Y. Nozawa (1988). “A probabilistic model for seismic hazard estimation in the Kanto district.” Proc. 9th World Conf. Earthquake Engineering 2. Pages 107-112.

Ansary, M.A., F. Yamazaki, and T. Katayama (1994). “Peak values of ground motion indices based on two horizontal components.” Proc. 9th Japan Earthquake Engeeriong Symposium 3. E37- E42.

Antenucci, J.C, K. Brown P.L Croswell, M. J. Kevany, and H. Archer (1991). Geographic Information Systems: A Guide to the Technology. Van Nostrand Reinhold, New York.

Applied Technology Council (1985). Earthquake Losses Evaluation Methodology and Databases for Utah, ATC-36. Redwood City, California.

Applied Technology Council (1991). Seismic Vulnerability and Impact of Disruption of Lifelines in the Coterminous United States, ATC-25. Redwood City, California.

Arya, A. (2000). Non-Engineered Construction in Developing countries- An Approach toward earthquake Risk Prediction, Proc. Of 20th WCEE, No. 2824.

Association of Bay Area Government (ABAG) (1991). "Macroeconomic Effects of the Loma Prieta Earthquake". ABAG Report. Oakland, California.

Bangladesh Bureau of Statistics [BBS] (1996). Population Census Report, 1991, Dhaka

Bangladesh Bureau of Statistics [BBS] (2001). Population Census 2001: Preliminary report, August, 2001, Statistics Division, Ministry of Planning, GOB.

Bangladesh Petroleum Exploration and Production Company Limited [BAPEX] (1989). International Report on the Kailas Tila Structure.

Bilham, R., V.K.Gaur and P.Molnar (2001). Himalayan Seismic Hazard, SCIENCE. Volume 293.

BNBC (1993). Bangladesh National Building Code, HBRI-BSTI.

Bolt, B.A. (1987). Site specific study of seismic intensity and ground motion parameters for proposed Jamuna river bridge, Bangladesh, Report on Jamuna bridge study.

Bommer, J.R.Spance, M.Erdik, S.Tabuchi, N.Aydinoglu, E.Booth. D.del Re and O.Peterken (2002). Development of an earthquake loss model for Turkish Catastrophe Insurance Journal of Seismology, Volume 6.

Bonilla, M.G. et al.(1984). "Statistical Relations among Earthquake magnitude, Surface Rupture Length, and Surface Fault Displacement". Bulletin of the Seismological Society of America. 74, 2379-2411.

Boore, D. M., Joyner, W. B and T.E. Funnal (1993). "Estimation of Response Spectra and Peak Accelerations From Western North American Earthquake: An Interim Report." Open File Report 93-509. United States Geological Survey. Menlo Park, California.

Borcherdt, R.D. (1990). “Influence of Local Geology in the San Francisco Bay Region, California on Ground Motions Generated by the Loma Prieta Earthquake of October 17, 1989.” Proceedings of the International Symposium on Safety of Urban Life and Facilities Tokyo, Japan. November 1-2, 1990, pages 1-35.

Borcherdt, R., C. M. Wentworth, A Janssen, T. Fumal and J. Gibbs (1991). “Methodology for Predictive GIS Mapping of Special Study Zones for Strong Ground Shaking in the San Francisco Bay Region, CA.” Proceedings of the Forth International Conference on Seismic Zonation. Stanford, California. August 25-29, 1991. Volume III, pages 454-552.

Borcherdt, R.D. and G. Glassmoyer (1992). “On the Characteristics of Local Geology and Their Influence on Ground Motions Generated by the Loam Prieta Earthquake in the San Francisco By Region, California.” Bulletin of the Seismological Society of America. Volume 82. Number 2, pages 603-641.

Bothara, J.K., Y.K. Parajuli, A.S. Arya and R.D. Sharpe (2000). Seismic safety in owner-built buildings, Proc. of 12th WCEE, No. 2130.

Boyle R. and W. Dong (1991) “Using Geographic Information Systems with Embedded Expert Systems and a Coupled Dynamic Database to Perform Seismic Hazard Evaluation.” Proceedings of the Fourth International Conference on Seismic Zonation. Stanford, California. August 25-29, 1991. Volume III, pages 569-584.

Brillinger, D.R. and H.K Preisler (1985). “Further Analysis of Joyner-Boore Attenuation Data.” Bull. Seismological Society of America. Volume 75. pages 611-614.

Brunschweiller R O (1980). Lithographic monsters in modern oil exploration, Proc. Offshore South-East Asia Conf., Singapore.

Campbell, K. W. (1981). “Near-source attenuation of peak horizontal acceleration.” Bull. Seismological Society of America. Volume 71. Number 6. pages 2039-2070.

Cardona, C., R. Davidson and C. Villacis (1999). Understanding urban seismic risk around the World, Summary Report on the Comparative Study of the United Nations International Decade for Natural Disaster Reduction, RADIUS Initiative.

Chen, W.W., B. Shih, Y. Chen, J.H. Hung, H.H. Hwang (2002). Seismic Response of Natural Gas and Water Pipelines in the Ji-Ji Earthquake, Soil Dynamics and Earthquake Engineering, Volume 22, pp.1209-1214.

Chung, Y.S.,C Meyer and M. Shinozuka (1987). “Seismic Damage Assessment of Reinforced Concrete Members.” Technical Report NCEER-870022. State University of New York at Buffalo, New York.

Clough, G. W., K. R. Martin II, and J.L. Chameau (1993). “Lessons Learned from the 1989 Loam Prieta Earthquake: The Geotechnical Aspects.” Proceeding from the Symposium in Practical Lessons from yhe Loam Prieta Earthquake. San Francisco, California. March 22-23, 1993.

Coburn, A. W., R. J. S Spence, and A. Pomonis (1992). Factors Determining Human Casualty Levels in Earthquakes: Mortality Prediction in Building Collapse, Proceedings of the 10th World Conference on Earthquake Engineering, Madrid, Spain, Volume 10, pp. 5989-5994.

Crouse, C.B., Y.K. Vyas, and B.A. Schell (1988). “Ground motion from subduction-zone earthquakes.” Bull. Seismological Society of America. Volume78.Number 1. pages 1-25.

Dobry, R., I. Oweis, and A. Urzua (1976). “Simplified Procedures for Estimating the Fundamental Period of a soil Profile.” Bulletin of the Seismological Society of America. Volume 66, Number 4, pages 1293-1321.

Draper, N and H. Smith (1981). Applied regression anlysis (Second Edition). John Willey and Sons.

Dunbar, W.S and R.G. Charlwood (1991). “Empirical methods for prediction of response spectra.” Earthquake Spectra. Volume 7. Number 3. pages 333- 353.

Emmi, P.C. and C. A. Horton (1993). “ A GIS-Based Assessment of Earthquake Property Damage and Casualty Risk: Salt Lake County, Utah.” Earthquake Spectra. Volume 9, Number 1, pages 11-33.

Environmental Systems Research Institute (ESRI) (1992). Understanding GIS: The Arc/Info Method. Redlands, California.

Faccioli, E. (1976). “A Stochastic Approach to Soil Amplification.” Bulletin of the Seismological Society of America. Volume 66, Number 4, pages 1277-1277.

Fah, D., F. Kind, K. Lang, D. Giardini (2001). Earthquake scenarios for the city of Basel, Soil Dynamics and Earthquake Engineering, Volume 21, pp.405-413.

FICCDC Technology Working Group (1988.) “A Process For Evaluating Geographic Information Systems.” Technical Report 1, Open-File Report 88-105. United States Geological Survey. Washington, DC.

Finn,W.DlL., R.H. Ledbetter, et al.(1994). “Liquefaction in Silty Soils: Design and analysis, Geotechnical Publication No.44, American Society of Civil Engineers, New York, pp. 51-76

French, S.P., J. C. Castanon, and Hanson (1991). “A knowledge-Based Approach to Using Existing Data for Seismic Risk Assessment.” Department of City and Regional Planning Report. California Polytechnic State University, San Lusi Obispo, California. December, 1991.

Frost, J., J Chameau, and R. Luna (1992). “Geographic Information Systems in Earthquake Hazard Analysis.” Proceedings of the ASCE Specialty Conference on Computing in Civil Engineering. Dallas, Texas. June 1992. pages 452-459.

Fukushima, Y. and T. Tanaka (1990). “A new attenuation relation for peak horizontal acceleration of strong earthquake ground motion in Japan.” Bull. Seismological Society of America. Volume 80. Number 4. pages 757- 783.

Guzman, R.A. and P.C. Jennings(1976). “Design spectra for nuclear power plants.” Jour. Power Division, ASCE. Volume 102. pages 165- 178.

Hasen, A. and C.A.M Franks (1991). “Characteristic and Mapping of Earthquake Triggered Landslides for seismic Zonation. Stanfor, California. August 25-29, 1991. Volume I, pages 149-195.

Haskell. N.A.(1964). “ Total energy spectral density of elastic wave radiation from propagating faults.” Bull. Seismological Society of America. Volume 54. pages 1811-1844.

Hiller K and Elahi M (1988). Structural growth and hydrocarbon entrapment in the Surma Basin, Bangladesh, In Wagner et al., (Eds), Petroleum Resources of China and Related Subjects, Earth Sci. Series, Vol. 10, pp 657-669.

Ho, C.L., K. Kornher and G. Tsiatas (1991). “Ground Motion Model for Puget Sound Cohesionless Soil Site.” Earthquake Spectra. Volume 7, Number 2, pages 237-266.

Hong, H.P. and E. Rosenblueth (1987). “Seismic Spectra on Soil with Uncertain Properties.” Earthquake Engineering and Structural Dynamics. Volume 15, pages 911-920.

Idriss, I.M. (1990). “Response of Soft Soil Sites During Earthquake.” Proceedings of the Memorial Symposium to Honor Professor H. Bolton Seed. Berkeley, California . May 10-11, 1990.

Ishira, K (1993). “Liquefaction and flow failure during earthquakes.” Geotechnique 43, Number 3, pages 349 – 415.

Ihhihara, K and I. Towhata (1980). “One-dimensional Soil response analysis during earthquakes based on effective stress method.” J. of the Faculty of Engg., University of Tokyo (B), XXXV(4), pages 655-212.

Ihhihara, K and Yasuda, S (1991). “Microzonation for Liquefaction Potential during Earthquakes in Japan.” Proceedings of 4th International Conference on Seismic Zonation, Stanford, California, USA.

Iwasaki, T, K. Tokida, F. Tatsuoka, S. Watanabe, S Yasuda, and H.Sato. (1982). “Microzonation for Soil Liquefaction Using Simplified Methods.” Proceedings of the Third International Earthquake Microzonation Conference. Seattle, Washington. Volume 3, pages 1319-1330.

Jensen, J. R. and E. J. Christensen (1986). “Solid and Hazardous Waste Disposal Site Selection Using Digital Geographic Information Techniques.” The Science of the otal Environment. Volume 56, pages 265-276.

Johnson S Y and Alam A M N (1991). Sedimentation and tectonics of the Sylhet Trough, Bangladesh, Bull. Geol. Soc. Am., Vol. 103, pp 1513-1522.

Joyner, W.B and D.M. Boore (1981). “Peak Horizontal Acceleration and Velocity from Strong-Motion Records Including Records from the 1979 Imperial Valley, California, Earthquake.” Bull. Seismological Society of America. Volume 71. pages2011-2038.

Joyner, W.B and D.M. Boore (1988). “Measurement, Characterization, and Predication of Strong ground Motion.” Proceedings of the ASCE Conference on Earthquake Engineering and Soil Dynamics II. Rolla, Missouri, pages 43-102.

Joyner, W.B and D.M. Boore (1993). Methods for regression analysisnof strong-motion data. Bull. Seis. Soc. Am. 83, pages 469-487.

Juang, C. H. and D.J Elton (1991). “Use of Fuzzy Sets for Liquefaction susceptibility Zonation.” Proceedings of the Fourth International Conference on Seismic Zonation. Stanford, California. August 25-29, 1991. Volume II, pages 629-636.

Kanai, K (1957). “Semi-Empirical Formula for the Seismic Characteristics of the Ground”. Bulletin of the Earthquake Research Institute, University of Tokyo. Volume 32. Number 2. pages 309-325.

Kanamori(1971). “Faulting of the Great Kanto Earthquake of 1923 as Revealed by Seismological data.” Bull. Earthquake Research Institute, University of tokyo. Volume 49. pages 13-18.

Kawashima, K. Aizawa and K. Takahashi (1983). “Effects of Composition of Two Horizontal Components on Attenuation of Maximum Earthquake Ground Motions and Response Spectra.” Proc. Japan Society of Civil Engineers (in Japanese). Volume number329. pages 49-56.

Kawashima, K. Aizawa and K. Takahashi (1986). “Attenuation of Peak Ground Acceleration, Velocity and Displacement Based on Multiple Regression Analysis of Japanese Strong Motion Records.” Earthquake Engeering and Structural Dynamics. Volume 14. pages 199-215.

Kim, S. H., M. O. Gaus, G. Lee, and K.C. Change (1992) “A GIS-Based Regional Risk Approach for Bridges Subjected to Earthquakes.” Proceeding of the ASCE Specialty Conference on Computing in Civil Engineering. Dallas, Texas. June, 1992. pages 460-467.

King, S. A. and A.S. Kiremidjian (1993a). “GIS for Regional Seismic Hazard and Risk Analysis.” Proceedings of the NSF workshop on Geographic Information Systems and their Application in Geotechnical Earthquake Engineering. Atlanta, Georgia. January 28-29, 1993, pages 56-60.

King, S. A. and A.S. Kiremidjian (1993b). “Uncertainties in the Dynamic Response of Soils in the San Francisco Bay Region.” Proceedings of the Sixth International Conference on Structural Safety and Reliability. Innsbruck, Austria. Austria. August 9-13, 1993.

Kircher, C.A. and M. W. McCann (1983). “Appendix A: Development of Seismic Fragility Curves For Sixteen Types of Structures Common to Cities of the Mississippi Valley Region.” Jack Benjamin and Associates Report. Mountain View, California.

Kircher, C.A, A.A.Nassar, O.Kustu and W.T.Holmes (1997). Development of building damage functions for earthquake estimation, Earthquake Spectra. Volume 13 (4).

Kiremidjian, A.S. (1984). “Reliability of Structures to Differential Fault Slip.” Earthquake Engineering and Structural Dynamics. Volume 12, pages 603-618.

Kiremidjian, A.S and T. Anagnos (1984). “Stochastic Slip-Predictable Model for c Occurrences.” Bulletin of the Seismological Society of American. Volume 74, Number 2, pages 739-755.

Kiremidjian, A.S. (1992).” Methods for Regional Damage Estimation.” Proceeding of the 10th World Conference on Earthquake Engineering. Madrid, Spain. July 19-24, 1992. Invited paper.

Kiremidjian, A.S., S. A. King, M. Sugito, and H.C. Shah (1991). “Simple Site-Dependent Ground Motion Parameters for the San Francisco Bay Region.” The John A. Blume Earthquake Engineering Center Report No. 97. Department of Civil Engineering, Stanford University. Stanford, California.

Koyama, J.(1985). “Earthquake Source Time Functions from Coherent and Incoherent Rupture.” Tecthnophysics. Volume 118. pages 227-242.

Kurt, C.E, K. Mohyuddin, and B. Guo (1992). “A Comparison of Geographical Information System.” Proceedings of the ASCE Specialty Conference in Computing in Civil Engineering. Dallas, Texas. June, 1992. pages 17-24.

Luna, R. (1993). “Liquefaction Analysis in a GIS Environment.” Proceeding of the NSF workshop on Geographic Information Systems and their Application in Geotechnical Earthquake Engineering. Atlanta, Georgia. January 28-29, 1993. pages 65-71.

Lutz, K. A. and A.S. Kiremidjian (1993). “A Generalized semi-Markov Process for Modeling Spatially and Temporally Department Earthquake.” The John A. Blume Earthquake Engineering Center Report No. 104. Department of Civil Engineering, Stanford University. Stanford, California.

Martel, R. R. (1964). “Earthquake Damage to type III Buildings inLong Beach, 1993,” Earthquake Investigations in the Western United Status, 1931-1964. Publication 41-2. U.S. Department of Commerce, Coast and Geodetic Survey. Washington, DC.

Martin, P.P. and H.B. Seed (1978). “MASH-A Computer Program for the Non-Liner Analysis of Vertically Propagating Shear Waves in Horizontally Layered Deposits.” Earthquake Engineering Research Center Report 78-23 University of California, Berkeley.

Massachusetts Civil Defense Agency (1989). Metropolitan Boston Area Earthquake Loss Study. URS/Blume Report. San Francisco, California.

Masuda, T and M. Ohtake (1992). Comment on " A new Attenuation Relation for Peak Horizontal Acceleration of Strong Earthquake Ground Motionin in Japan " by Y. Fukushima and T. Tanaka. Bull. Seismological Society of America. Volume 82. pages 521-522.

McGuire, R. (1978). Seismic ground motion parameters relations, Journal of Geotechnical Division, ASCE, Volume 104, pp.461 – 490.

McLaren, M. (1992). "A Study of Earthquake Response Spectra for Different Geological Conditions." Bulletin of the Seismological Society of American. Volume 66, Number 3, pages 915-935.

Mohraz ,B (1976). "A Study of Earthquake Response Spectra for Different Geological Conditions". Bulletin of the Seismological Society of America. Volume 66, Number 3, pages 915-935.

Molas, G.L. and Yamazaki, F.(1994). Attenuation of ground motion of earthquakes with large focal depths. Proc. 49th Annual Conf. of Japan Society of Civil Engineers, Sapporo.

Murthy, V. N. S. (1991). Soil mechanics and foundation engineering, Volume 2, Revised and enlarged third edition, SAITECH, Bengalore, India.

NCEER(National Centre for Earthquake Engineering Research). 1997. Proceedings of the NCEER Workshop on Evaluation of Liquefaction Resistance of soils,Summary Report, T.L. Youd and I. Idriss, Eds., National Centre for Earthquake Engineering Research, State University of Newyork, Buffalo.

Newmark, N. M. and E. Rosenblueth (1971). Fundamentals of Earthquake Engineering Prentice-Hall, Inc. Englewood Cliffs, New Jersey.

Newmark, N. M. and W.J. Hall (1982). "Earthquake Spectra and Design". Earthquake Engineering Research Institute, Universiyy of California Berkely, p.103.

Ohno, S., T. Otha, T. Ikeura, and M. Takemura (1993). " Revision of Attenuation formula Cosidering the effect of fault Size to Evaluate Strong Motion Spectra in Near field." Tectonophysics. Volume 218. pages 69-81.

Ohsaki, Y. (1982). "Dynamic Characteristics and One-Dimensional Liner Amplification Theories of Soil Deposits." Department of Architecture Research Report 82-01. University of Tokyo. Tokyo, Japan.

Oldham, R.D. (1899). Report on the great Indian earthquake of 12th June, 1897, Memoir of Geological Survey of India, Volume 29, pp.1-349.

OYO Corporation International [OIC] (2009). Unpublished report on Earthquake Sources within Bangladesh.

Papageorgiu, A.S. and K. Aki (1983). " A Specific Barrier Model for the Quantitative Description if Inhomogeneous faulting and the Prediction of Strong Ground Motion. Part 1, Bull. Seismological Society of America. Volume 73. pages 639-722.

Park, Y-J., and A. H-S Ang (1985) "Seismic Damage Analysis of Reinforced Concrete Buildings." ASCE Journal of Structural Engineering. Volume 111, Number 4, pages 740-757.

Pyke, R. M. (1979). "Nonlinear Soil Models for Irregular Cyclic Loadings." ASCE Journal of the Geotechnical Engineering Division. Volume 105, Number GT6, pages 715-726.

Rashid.A (2000). Seismic Microzonation of Dhaka City based on site amplification and liquefaction, M.Sc. Engg Thesis, BUET.

Reitherma, R. (1985). "A Review of Earthquake Damage Estimation Methods." Earthquake Spectra. Volume 1, Number 4, pages 805-847.

Rentzis, D.N., A.S. Kiremidjian, and H.C Howard (1992). "Identification of High Risk Areas Through Integrated Building Inventories." The John A. Blume Earthquake Enginnering Center Report No. 98 Department of Civil Engineering, Stanford University. Stanford, California.

Ripple, W. K editor (1989). Fundamentals of Geographic Information System: A Compendium. American Society for Photogrammery and Remote Sensing and American Congress on Surveying and Mapping, Maryland.

Rojahn, Christopher (1993). Estimation of Earthquake Damage to Buildings and Other Structures in Large Urban Areas. Proceedings of the Geohazards International/Oyo Pacific Workshop. Istanbul, Turkey. October 8-11, 1993.

Sabri, S. A. (2001). Earthquake intensity-attenuation relationship for Bangladesh and its surrounding region, M.. Engg. Thesis, BUET, Dhaka

Schnabel, P. B., Lysmer, and H. B. Seed (1972). "SHAKE-A Computer Program for Earthquake Response Analysis of Horizontally Layered Site." Earthquake Engineering Research Center Report 72-12. University of California, Berkeley.

Seals, S. H. and R. J. Archuleta (1989). "Site Amplification and Attenuation of Strong Ground Motion." Bulletin of the Seismological Society of American. Volume 79. Number 6, pages 1673-1696.

Seed. H. B. and I. M. Idriss (1982). "Ground Motions and Soil Liquefaction during earthquakes, Mongor. 5, Earthquake Engineering Research Institute, University of California, Berkeley.

Seed, H. B., I. M. Idriss and I. Arango (1983). Evaluation of liquefaction potential using field performance data, Journal of Geotechnical Engineering, Volume 109, No. 3, pp. 458-482.

Seed, H. B., C Ugas, and J, Lysmer (1976). "Site-Depended Spectra for Earthquake Resistant Design." Bulletin of the Seismological Society of American. Volume 66, Number 1, pages 221-243.

Seed, R.B., K.O. Cetin., (2001). "Recent Advances in Soil Liquefaction Engineering and Seismic Site Response Evaluation" in Proc. Fourth International Conference on Recent Advances in Geotechnical Earthquake Engineering and Soil Dynamics, University of Missouri, Rolla.

Segawa, S., F. Kaneko, T. Ohsumi, H. Kagawa, and H. Fujitani (2002). Damage Estimation of Buildings in Kathmandu Valley and Proposals for Improvement of the Earthquake Resisting Capacity, Proc, 11th Japan Earthquake Engineering Symposium (Paper No. 410, CDROM).

Sharfuddin, M. (2001). Earthquake Hazard Analysis for Bangladesh. M.Sc. Engg. Thesis, BUET, Dhaka.

Slemmons, D.B. (1977). "State-of- the-Art for Assesing Earthquake Hazards in the United States." Report 6: Fault and Eaarthquake Magnitude, U.S. Army Corps Engineers, Waterways Experment station,Misc. Papers 73-1.

Smith, T. R., S. Menon, J. L. Star, and J. E Estes (1987). "Requirement and Principles for the Implementation and Construction of Large-scale Geographic Information System." International Journal of Geographic Information Systems. Volume 1, Number 1, pages 13-31.

Steinbrugge, K. V., S. T. Algermissen, H. J. Lagorio, L.S Cluff, and H. J. Degenkolb (1981). "Metropolitan San Francisco and Los Angeles Earthquake Loss Studies: 1980 Assessment." Open File Report 81-113. United States Geological Survey. Menlo Park, California.

Susuki, s. and A. s. Kiremidjian (1988). "A Stochastic Ground Motion Forecast Model with Geophysical Considerations." The John A. Blume Earthquake Engineering Center Report No. 88. Department of Civil Engineering, Stanford University. Stanford California.

Sylhet City Corporation, 1998: Sylhet Health City Plan.

Talukder S, Islam M S and Islam M A (2006) Seismic Stratigraphy of the Kailas Tila Structure, Sylhet Trough. Bangladesh, Bangladesh Journal of Geology, Vol. 25, pp. 31-47.

Tamura, I. And F. Yamazaki (2002). Estimation of S-wave velocity based on geological survey data for K-NET and Yokohama seismometer network. Journal of Structural Mechanics and Earthquake Engineering No. 696, Vol. I-58, 237-248 (in Japanese).

Thomson W. T. (1950) "Transmission of Elastic waves Through a Stratified Solid Medium." Journal of Applied Physis. Volume 21.

Topark,S. (1988). "Earthquake Effects on Buried Lifeline Systems". PhD Dissertation, Cornell University.

Trifunac, M.D. (1976). " Preliminary Analysis of the Peaks of Eathquake Strong Ground Motion-Dependence of Earthquake Peaks on Earthquake Magnitude, Epicentral Distance, and Recording Site Conditions." Bulletin of the Seismological Society of American. Volume 1, pages 139-162.

Trifunac, M.D. and Brady, A.G. (1975). "On the Correlation of Seismic Intensity with Peaks of Recorded Strong Ground Motion". Bulletin of the Seismological Society of America. Volume 65, number 1, pages 139-162.

Tsai, N. C. and G. W. Housner (1970). "Calculations of Surface Motions of a Layered Half-space." Bulletin of the Seismological Society of American. Volume 60, Number 5, pages 590-616.

Tsai, Y.B., F.W. Brady, and L.S. Cluff (1990). "An Integrated Approach for Characterization of Ground Motions in PG&E's Long Term Seismic Program Diablo Canyon." Proc. 4th U.S. National Conf. on Earthquake Engineering.

Usery, E. L., P. Altheide, R. R. P. Deister and D. J. Barr (1988). "Knowledge –Based GIS Techniques Applied to Geological Engineering." Photogrammetry Engineering and Remote Sensing Volume 54, Number 11, pages 1623-1628.

Vasudevan, R., A.S. Kiremidjian, and H. C. Howard (1992). "An Integrated Inventory Methodology for Seismic Damage Assessment." The John A. Blume Earthquake Engineering Center Report No. 102. Department of Civil Engineering, Stanford University. Stanford, California.

Wald, D.J. and P.G. Somerville (1994). “Rupture Model of the Great 1923Kanto Earthquake Inferred from Geodetic and Teleseismic Data.” Proc. 9th Japan Earthquake Engineering Symposium. Volume 3. E7-E12.

Wieczorek, G.F.R.C Wilson, and E. L. Harp (1985). “Map Showing Slope Stability During Earthquake in San Mateo Country California.” Map-I-1257-E. United States Geological Survey. Menlo Park, California.

Whitman, R. V., editor (1992). Proceeding from the Site Effects Workshop, October 24-25, 1991. Technical Report NCEER-92-0006. State University of New York at Buffalo, New York.

Whitman, R.V., T. Anagnos, C. Kircher, H.J. Lagorio, R.S. Lawson and P. Schneider (1997). Development of a Natural Earthquake Loss Methodology. Earthquake Spectra, 13 (4).

Wilson R.C. and D.K. Keefer (1985). “Predicting Areal Limits of Earthquake Induced Landsliding,” Evaluating Earthquake Hazards in the Los Angeles Region, Professional Paper 1360. United State Geological Survey. Passadena, California, pages 317-493.

Yamazaki, F. (1993). “Comparative Study on Attenuation Characteristics of Ground Acceleration in Europe, North America and Japan.” Bull. Earthquake Resistant Structures Research Center, IIs, University of Tokyo. Volume 26. pages 39-56.

Yamazaki, F. and O. Murao (2000). Vulnerability Functions for Japanese Buildings Based on Damage Data due to the 1995 Kobe earthquake, Proc. of 3rd Japan-UK Workshop on Implications of Recent Earthquakes on Seismic Risk, London: 10-27 to 10-38.

Yamaguchi, N. and F. Yamazaki (2001). Estimation of Strong Motion Distribution in the 1995 Kobe Earthquake Based on Building Damage Data, International Journal of Earthquake Engineering and Structural Dynamics, Volume 30, pp.787-801.

Youd, T.L. (1991). “Mapping of Earthquake-Induced Liquefaction for Seismic Zonation.” Proceeding of the Fourth International Conference on Seismic Zonation. Stanford, California. August 25-29, 1991. Volume I, pages 111-147.

Youd, T.L. and D.M. Perkins (1978). “Mapping of Liquefaction-Induced Ground Failure Potential,” J. Geotech. Eng. Div. ASCE, 104(GT4), 433-446.

Annexure

SEISMIC HAZARD AND RISK ASSESSMENT FOR MYMENSINGH, BANGLADESH

Introduction

Mymensingh town at 24°45′ north latitude and 90°25′ east longitude covers an area of about 21.72 sq. km. The municipality has a population of more than 365,000. The town lies in one of the earthquake prone areas of Bangladesh. **Figure A1** shows the seismic zoning map of Bangladesh. Mymensingh falls in zone 3 with a seismic coefficient of 0.25g. Recent earthquakes in and adjoining areas of Bangladesh is a wake up call for the Bangladeshi people to take adequate measures against earthquake. In this study for microzonation purpose bore holes with SPT data and historical large earthquakes were used as scenario events. From attenuation relations, peak ground acceleration in the bedrock level was estimated and was used to develop a regional combined seismic hazard map based on site amplification as well as liquefaction. The methods to combine the different hazards are based on weighted average approach.

Geology of the area

The study area lies in the northern outlier of the Madhupur Tract and is within Old Brahmaputra flood plain. On the regional context, the Old Brahmaputra flood plain is located in the northeastern part of the Indian Plate. This flood plain comprises low-lying alluvial plain of the latest Holocene time and is bordered by the Madhupur Tract in the south-west and the Sylhet Depression in the East. Madhupur tract is covered with Madhupur Clay Residuum of the Pleistocene period (Alam et al. 1990) and Sylhet Depression comprises low lying alluvial flood plain of the latest Holocene time. It is considered that the underlying Dupi Tila sandstones have undergone sub-aerial weathering since Plio-Pleistocene to form this clay residuum. The unit is further underlain at depth by the Neogene Tipam Sandstone and Boka Bil Formation, the Miocene Bhuban Formation and the Oligocene Barail Formation The Mottled Madhupur Clay is dark reddish-brown to brownish-red, moderately sticky, compact and contains abundant nodules and concretions. Its thickness is greater than 5m (Islam et al 2006).

Mymensingh town lies to the right bank of the Brahmaputra River. The alluvial deposits of this area range from flood sand to over bank silt and ponded clay. These are yellowish brown or grey to reddish-grey silt to clay. More consolidated than active flood plain

sediments. Upper 0.5m is generally oxidized and underlies the Tipera surface (Morgan and McIntire, 1959; Coleman, 1968). This geological unit includes highland alluvium (Alam, 1988) and some Holocene slopewash deposit adjacent to higher ground. The average elevation of the floodplain is less than 15 m (PWD) and average elevation of the study area is 15 m (PWD). This area is bounded by the Old Brahmaputra River in the north and the Madhupur Tract in the south-west.

Other than Old Brahmaputra River, numerous natural channels drain this flood plain. Among these channels Sutia and Khiro Rivers are the most prominent. These channels and the Old Brahmaputra River have formed a drainage network of this area. The study area lies in the north of the Sutia River, in the east of the Khiro River and in the south of the Old Brahmaputra River. The out fall of the Sutia and Khiro Rivers is the Banar River at the southern part i.e, outlier of Mymensingh. Flowing along the south and east of the outlier, the Banar is a major river that meets the River Lakhya at farther south.

Tectono-geomorphic features

Tectonic activities of an area impart some expressions to the geomorphology of that area. Hence, tectono-geomorphic evidences reflect the past and present tectonic activities in an area. To understand the tectonic history of the eastern part of the Jamuna valley, aerial photographs of 1983, LANDSAT and SPOT images were studied and were verified in the field. The Jamuna valley lies in the central part of the Bengal Basin. On the regional context, the Bengal Basin lies to the northeastern part of the Indian Plate.

This valley evolved in a complex tectonic environment. A few of the tectonic elements are still active and are creating numerous tectono-geomorphic features. These features often produce lineaments of interest like Madhupur lineament, Manikganj lineament, Nagarpur lineament, Mirzapur lineament and Kaliakair lineament. Combinedly these lineaments delineate four tectonic blocks, viz., Nagarpur block, Saturia block, Jamalpur block and Madhupur block. The Madhupur block is a raised block on the east of the Jamuna valley. Each block is characterized by certain tectonic geomorphic features

(Islam et al. 1995). Mymensingh is located in the northeastern part of the above four tectonic blocks.

Regional tectonics

According to Molnar and Tapponnier (1975), for the past 40 million years the Indian subcontinent has been pushing northward against the Eurasian plate at a rate of 5 cm/year, giving rise to the severest earthquakes and most diverse land forms known. Recently, Bilham et al. (2001) pointed out that there is high possibility that a large earthquake may occur around the Himalayan region based on the difference between energy accumulations in this region. There is a seismic gap that is accumulating stress, and a large earthquake may occur someday when the stress is relieved. The major past earthquakes and some recent earthquakes that affected Mymensingh is presented in Table A1.

Data collection

A total of 77 soil reports containing 271 boreholes with SPT data were collected from different relevant organizations and stored in Microsoft Excel. Majority of the borings were drilled up to a depth of 15 m to 18 m. Among these, 10 boreholes with SPT-N data up to a depth of 30 m were directly collected by BUET (Bangladesh University of Engineering and Technology) for checking the authenticity of other collected data. The typical available boring is up to a depth of 15 m.

The paper map was collected from Mymensingh municipal authority and was digitised based on GPS data collected from different locations of the town using MapInfo software. Collected boreholes from Mymensingh municipality area were located in the map also based on GPS data (Khan, 2004). Site amplification as well as soil liquefaction potential values obtained for each boring were located in the digitised map. Figure A2 and A3 shows borehole locations together with the ward map. Figure A4 shows a typical bore hole. Using bore holes, soil profiles (Figure A5a and Figure A5b) was drawn to demonstrate the overall soil condition. The detailed soil profile and site characterization were presented in Khan (2004).

Assessment of seismic hazard

The methodology provided in HAZUS is a post earthquake management model that can be applied in regions that are at risk for earthquake disaster. The methodology generates estimates of the consequences to a city or region due to a scenario earthquake. Scenario earthquake could be a specified earthquake with magnitude and location. The evaluation methodology consists of three basic steps (Schneider and Schauer, 2005).

1. Study region definition: definition of the region, selection of the application area, selection of the appropriate data from the earthquakes.
2. Hazard characterization: definition of the earthquake hazard, hazard type and source, fault type, earthquake location.
3. Damage and loss estimation: social and economic loss estimation, structural hazard estimation.

HAZUS, as a user friendly risk assessment model, can address the earthquake hazard in US. It was developed over 17 years in US. It is a state-of-art decision support tool for assessing disasters. It is the first PC-GIS based evaluation tool. Capabilities in HAZUS include earthquake, flood and hurricane hazard characterization, building, essential facilities damage analysis, computing direct economic losses and secondary hazard.

However, as it is, HAZUS is not ready for use in Bangladesh. National and district boundaries and characterization of the earthquake data used in HAZUS are currently only available for US. HAZUS can provide a starting point for the development of a disaster risk assessment tool which could be used in Bangladesh considering user requirements and data availability. Earthquake disaster risk assessment and evaluation for Turkey was done successfully by Korkmaz (2009).

In the regional seismic loss estimation analysis, it is needed to determine the bedrock motion in the region. The most common method involves the use of an empirical attenuation relationship. These relationships express a given ground motion parameter in a region as function of the size and location of an earthquake event. Applying statistical regression analyses to recorded data numerous relationships in the past was developed. Often these relationships were developed with different functional forms and with

different definitions of ground motion, magnitude, distance, and site conditions. To select the most suitable attenuation law for predicting rock motions, 1885 Bengal earthquake, 1897 Great Indian earthquake and 1918 Srimangal earthquake were considered. The requirements for selecting the attenuation law are as follows:

(i) Applicable to the ground condition of engineering bedrock in this study.

(ii) Able to explain the observed or analyzed earthquake motion of 1885 Bengal earthquake, 1897 Great Indian Earthquake and 1918 Srimangal earthquake.

In this study, the engineering bedrock was assumed to be the layer at which the shear wave velocity (V_s) exceeds 200 m/s, which exist almost 30 m deep from the surface of the study area. In this study, shear wave velocity was estimated by using equation of Tamura and Yamazaki (2002). Distance versus PGA values for earthquakes was plotted on log-log paper. From isoseismal maps, the epicentral distances of different locations and their intensities are found. These intensities were converted into PGA by following Trifunac and Brady (1975) equation (1) and are plotted on Figure A6.

$$\log (PGA) = 0.014 + 0.3 (MMI) \quad (A1)$$

From these plots (Figure A6), it was found that McGuire (1978) [$PGA=0.0306e^{0.89M}r^{-1.17}e^{-.2}$ cm/s^2 where M=Magnitude and r=hypocentral distance] as well as Boore et al. (1997) equations follows the PGA trend. Since, McGuire equation was already used for Bangladesh for seismic hazard analysis (Sharfuddin, 2001) and due to its simple form; it is selected for further use. Table A3 presents the PGA values at bedrock level from different attenuation laws for different scenario event. Finally, 1897 Great Indian Earthquake with the highest PGA value 0.18g (where g is the gravitational acceleration) at bedrock level for Mymensingh was selected.

Site Amplification Analysis

Site amplification of earthquake motion is one of the most difficult site effects to model. The difficulties result from (a) the lack of sufficient data on local soil parameters, (b) the lack of sufficient strong ground motion at locations with different surface soil types; (c) the lack of sufficient strong ground motion data from vertical array measurements; (d) the

inability to accurately quantify the non-linear characteristics of soil; and (e) the use of approximate models to represent the true non-linear behavior of soils when subjected to dynamic forces (Kiremidjian et al. 1991).

Numerous methodologies were proposed for estimating the surface ground motion from the motion at the bedrock level and the geologic characteristics of local soil conditions. Current methods for estimating ground motion site amplification can generally be divided into three types: (a) empirical multiplication factors; (b) theoretical transfer function models; and (c) dynamic nonlinear models. For estimating ground motion site amplification, a lot of researchers used different methods. The most commonly used transfer function model is included in the computer program SHAKE developed by Schnabel et al. (1972). Vibration characteristics at different points of the study area were estimated by employing one dimensional wave propagation program SHAKE. SHAKE discretizes the soil profile into several layers and uses an iterative technique to represent the non-linear behavior of the soil by adjusting the material properties at each iteration step. The required input information includes depth, shear wave velocity, damping factor and unit weight of each soil layer.

The computations were made in the frequency range of 0 to 20 Hz at frequencies of every 0.05 Hz interval. The loss of energy of seismic waves in the soil layers is also considered. An estimation of the fundamental frequency and the maximum value of the amplification were obtained at each site. Figure A7 shows a typical amplitude-frequency curve of the study area and Figure A8 shows the distribution of fundamental frequencies of the study area.

Figure A9 shows map of amplification at fundamental frequencies of Mymensingh. 84% of the total area may face 1.4-amplification and 16% of the total area may face 1.8-amplification. Within the 1.8-amplification area, ward 1 covers 48% area and remaining area is covered by wards 3, 4, 12, 15, 18, 20 and 21.

Liquefaction Analysis

Regional liquefaction hazard mapping is typically done using either a geologic or a geotechnical technique (Juang and Elton, 1991). During the past 25 years, several geotechnical techniques for analyzing soil liquefaction were proposed, resulting from the need for a more quantitative estimate of regional liquefaction hazard. Most of these techniques involve the comparison of the cyclic stress ratio generated by an earthquake with the cyclic stress ratio which would be required to liquefy the soil (Youd, 1991). The most commonly applied technique was developed by Seed and Idriss (1971). According to their method, the cyclic stress ratio generated by the earthquake (CSRE) at a particular depth below ground surface is computed as follows:

$$CSRE = \tau_{av}/\sigma'_o = 0.65(a_{max}/g)(\sigma_o/\sigma'_o)\, r_d \qquad (A2)$$

where, a_{max} = PGA at the ground surface (in % of g)

g = the acceleration due to gravity (in g)

σ_o= the total overburden stress in the soil at the depth in question

σ'_o = effective overburden pressure

r_d = the depth-dependent stress reduction factor

The cyclic stress ratio required to induce liquefaction of the soil (CSRL) is determined from empirical charts relating CSRL to corrected penetration resistance, $(N_1)_{60}$, calculated from standard penetration test (SPT) values as

$$(N_1)_{60} = C_n\,(ER_m / 60)N_m \qquad (A3)$$

where,

ER_m = the SPT measured potential energy value

C_n = the σ'_o – dependent correction factor

N_m = the measured SPT resistance value

The empirical charts estimate the CSRL needed to induce soil liquefaction for a given magnitude and $(N_1)_{60}$ value. The CSRE at the soil site due to the given magnitude earthquake was calculated by equation (2). If the computed CSRE is equal to or greater than the CSRL then liquefaction is assumed to occur at the site for the given earthquake.

A more recently developed geotechnical method for evaluating soil liquefaction was proposed by Iwasaki, et al. (1982). This method is similar to Seed and Idriss (1971) method described above in that it also involves the calculation of a stress ratio giving a "yes" or "no" answer for the occurrence of liquefaction, but the Iwasaki, et al. (1982) method goes one step further by attempting to quantify the severity of the liquefaction. The stress ratio or liquefaction resistance factor, F_L is defined as:

$$F_L = R/L \qquad \text{(A4)}$$

Where,

R = the soil liquefaction capacity factor

L = the dynamic load induced in the soil by the seismic motion

R is assumed to be a function of the SPT value and the effective overburden pressure in the soil and is calculated from equations for different ranges of mean grain size, D_{50}. The equation for calculating L is almost identical to that given for CSRE in equation (2). The severity of liquefaction is quantified with a liquefaction potential index, P_L, defined as:

$$P_L = \int_0^{20} F(z)\, w(z)\, dz \qquad (5)$$

Where

$F(z)$	=	$(1-F_L)$	for $F_L \leq 1.0$
$F(z)$	=	0	for $F_L > 1.0$
$W(z)$	=	$(10 - 0.5\,Z)$	for $z \leq 20$ m
$W(z)$	=	0	for $z > 20$ m

P_L	>	15	very high possibility of liquefaction
$15 > P_L >$		5	high possibility of liquefaction
$5 > P_L > 0$			low possibility of liquefaction
$P_L = 0$			very low possibility of liquefaction

The value of liquefaction potential, P_L indicates that a soil mass is susceptible to liquefaction if $P_L > 0$. If the value of P_L is large, the soil is very susceptible for liquefaction.

Using the above methods, the liquefaction resistance factor, F_L, for the top 20 m of soil, and the resulting liquefaction potential, P_L for the 87 sites were calculated. Result of Liquefaction potential has been presented in **Figure A10,** which shows 3% of total area suffered severe liquefaction, 29% of total area suffered moderate liquefaction and the rest area have low liquefaction potential. Total 32% area shows moderate to high liquefaction which matches the geologic feature of the study area where it was mentioned that the alluvial deposits of this area range from flood sand to over bank silt and ponded clay.

Combination of Ground Shaking Hazard and Liquefaction

Ground shaking hazard and hazards due to secondary site effects are combined on the basis of experts' opinion. Figure A11through Figure A13 shows the intermediate maps of hazard integration .The intensities of combined hazard map were estimated and distributed over the ward map. The intensities lie between VIII to X (0.26g to 0.53g). 57% of the total area may suffer intensity VIII (0.26g), 33% may suffer intensity IX (0.53g) and only 10% of the total area may suffer intensity X (1.05g). The combined intensity i.e., the combined hazard map is shown in Figure A14.

Estimations of building amage and human casualties

For this purpose, a building inventory (Rahman, 2006) for Mymensingh was made based on field survey as well as Bangladesh Statistical Bureau data. Mymensingh town has 21,000 building units. Earthquake damage of buildings of different typologies was estimated by using fragility curves proposed by Arya (2000). Based on combined seismic hazard, 28% buildings were estimated to be damaged. Among the total damaged buildings, unreinforced brick masonry consists of 16%.

Earthquake damage of buildings of different typologies was estimated by using fragility curves proposed by Arya. Human casualty (death and injury) was estimated by Morbidity model proposed by Coburn. The final results for damage in Mymensingh town can be used to check the overall reasonableness of the models and methodologies. The estimated average damage for building stock is 28%. As expected, the damage for EMSB type,

which comprises of single storey and two or more storied brick masonry structures was the highest (about 18% of the total damage) (Figure 19 to 21). Among different building types, A type suffered 22%, B1 type suffered 24%, B2 type suffered 45%, C type suffered 8%, D type suffered 0%, and F type suffered 1% damage. FigureA15 to Figure A19 shows the damage scenarios of Mymensingh town due to earthquake .

Combining all the effect, the total number of estimated fatalities and injuries in 21 wards of Mymensingh town according to different times of the day are presented through Figure A20 to Figure A25 shows the injuries for each ward during morning, night and noon.Total estimated number of fatalities for the scenario earthquake is 3,887 in the morning, 4,872 in the night and 2,625 in the noon. It is about 1.06%, 1.33% and 0.72% of the total population of Mymensingh town. Total estimated number of injuries for the scenario of earthquake is 5050 in the morning, 6,410 in the night and 3,605 in the noon. It is about 1.38%, 1.76% and 0.1% of the total population of Mymensingh town. So for the scenario earthquake with site effects, 2.44% of total population in the morning, 3.09 % in night and 1.71% at noon will be estimated to be dead and injured.

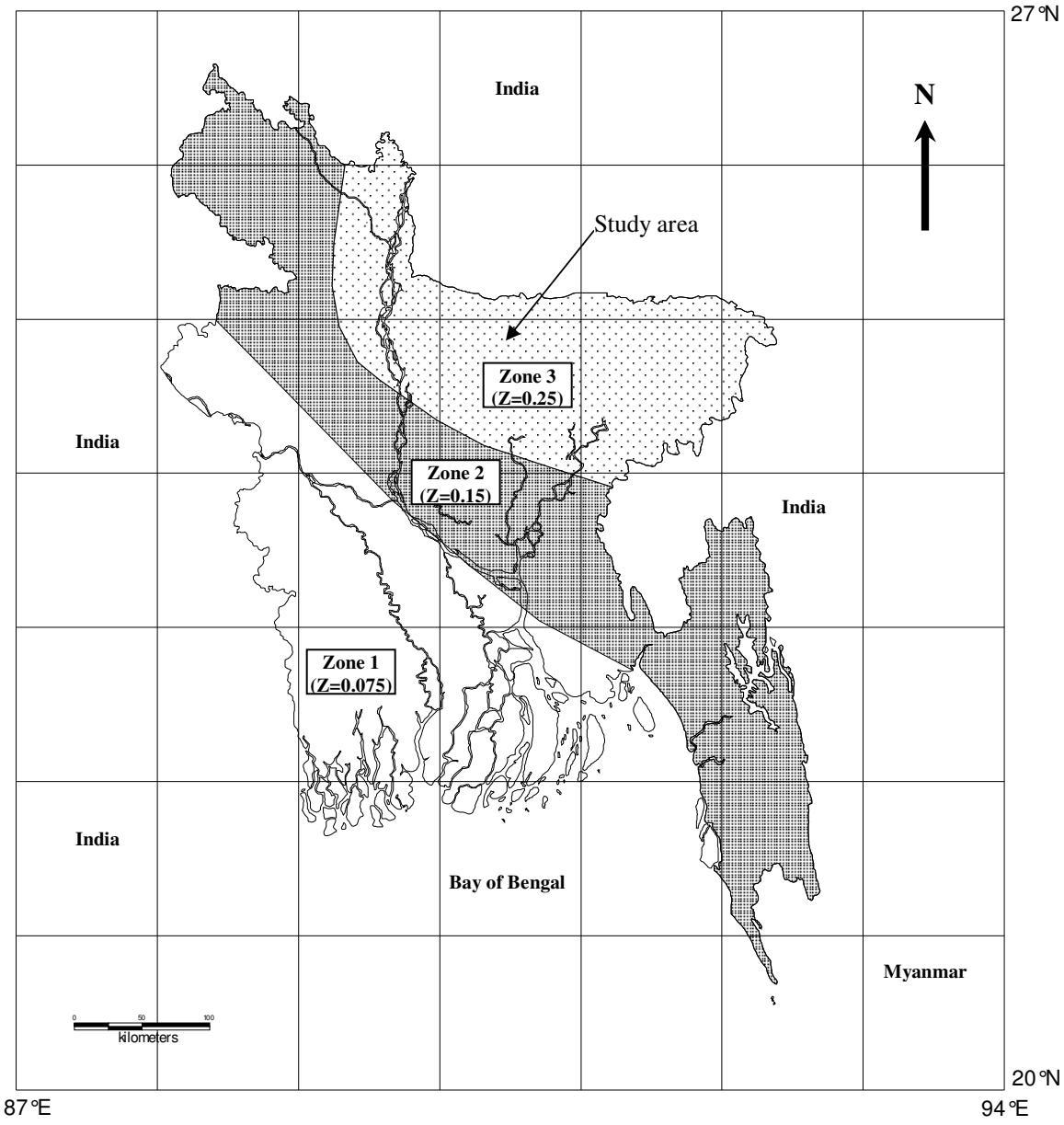

Figure A1 Seismic Zoning Map of Bangladesh (BNBC, 1993)

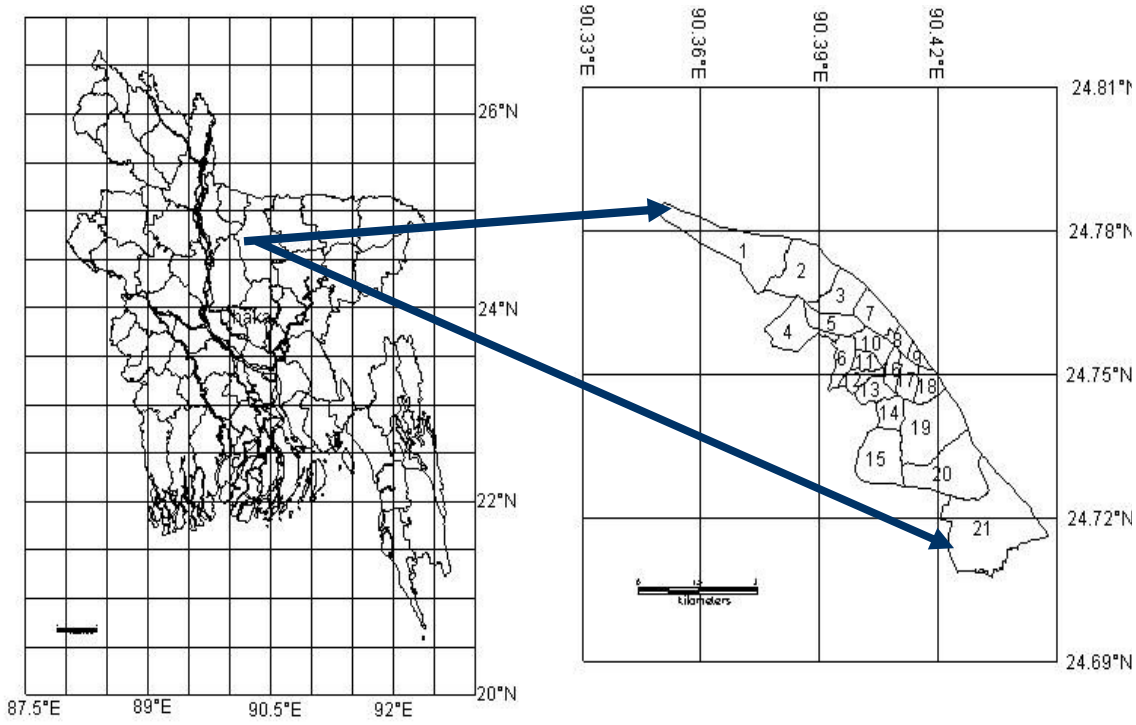

Figure A2 Location map of the study area

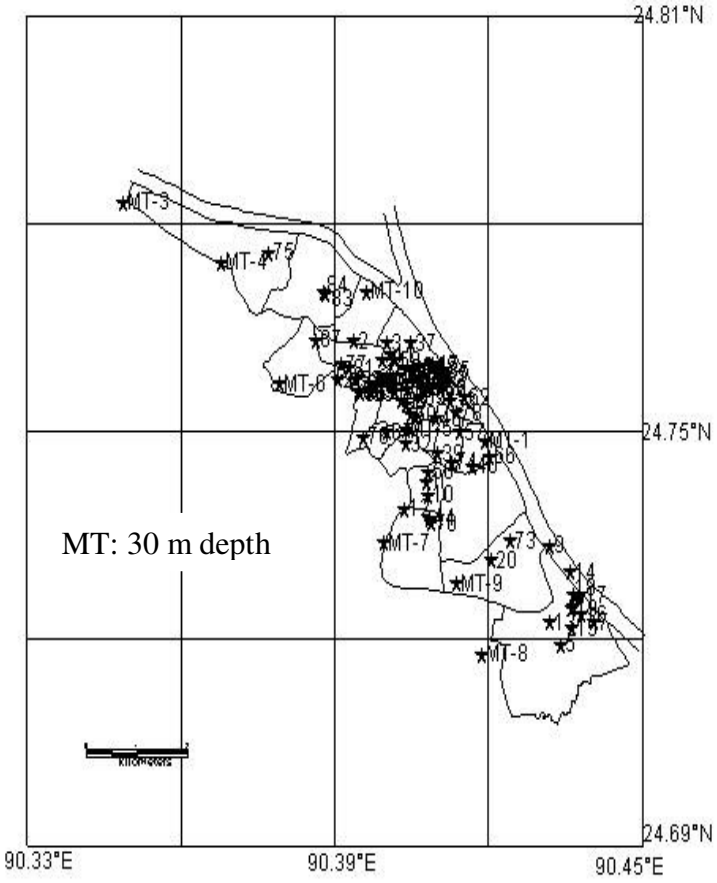

Figure A3 Bore hole location

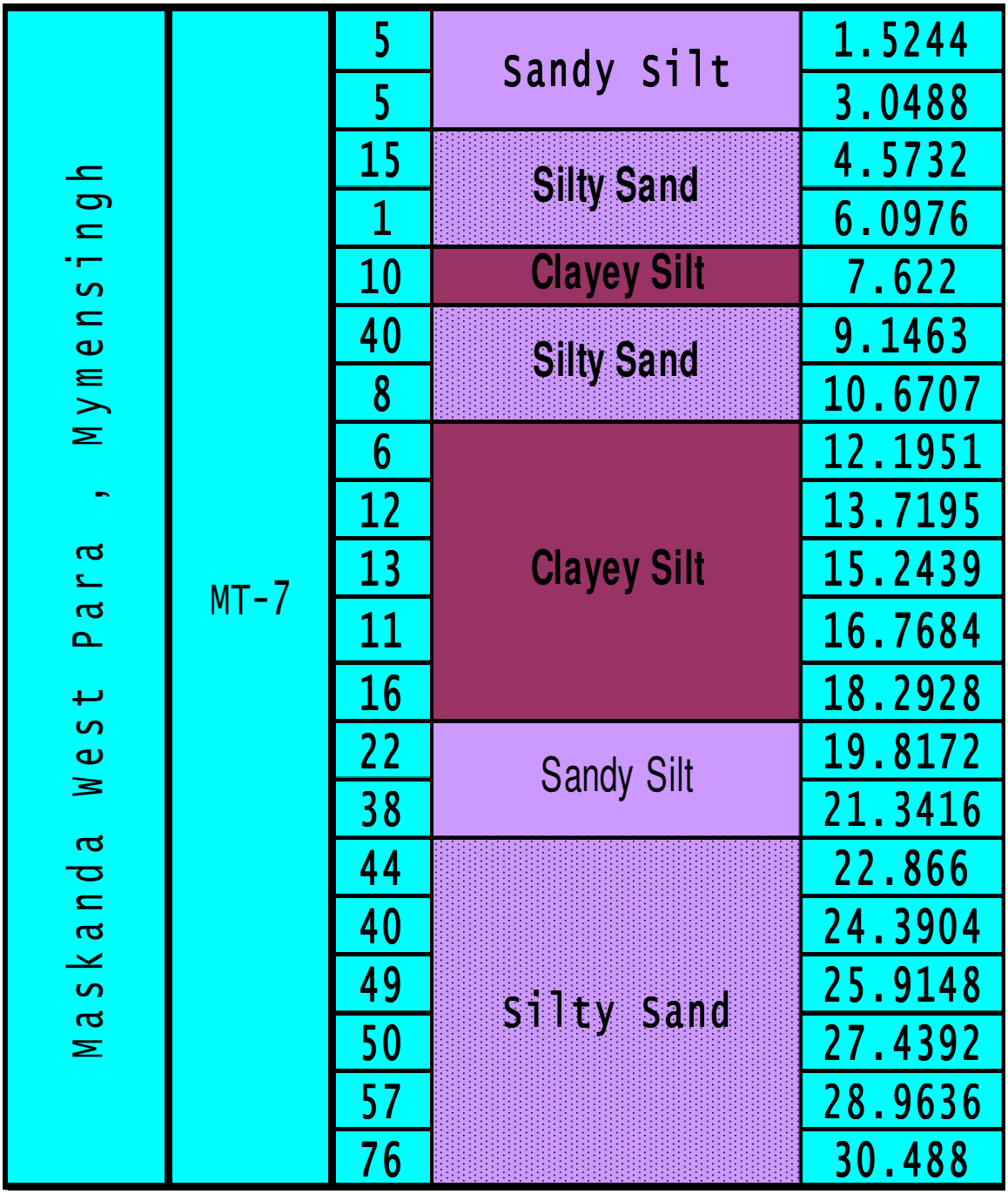

FigureA4 Typical bore log (MT-7)

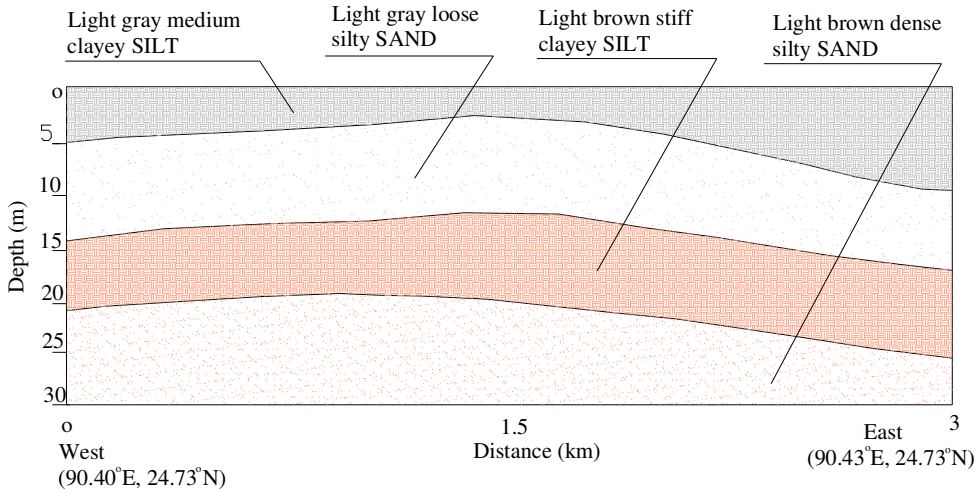

Figure A5a Soil profile along East-West direction

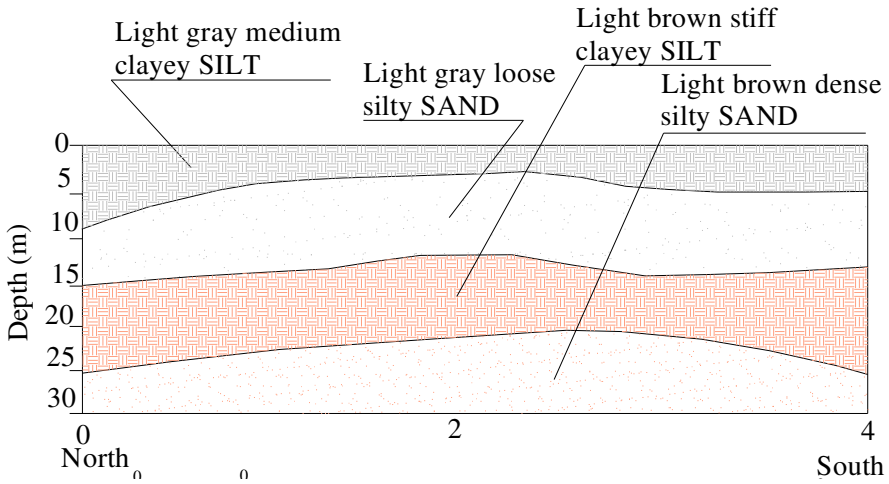

Figure A5b Soil profile along North-South direction

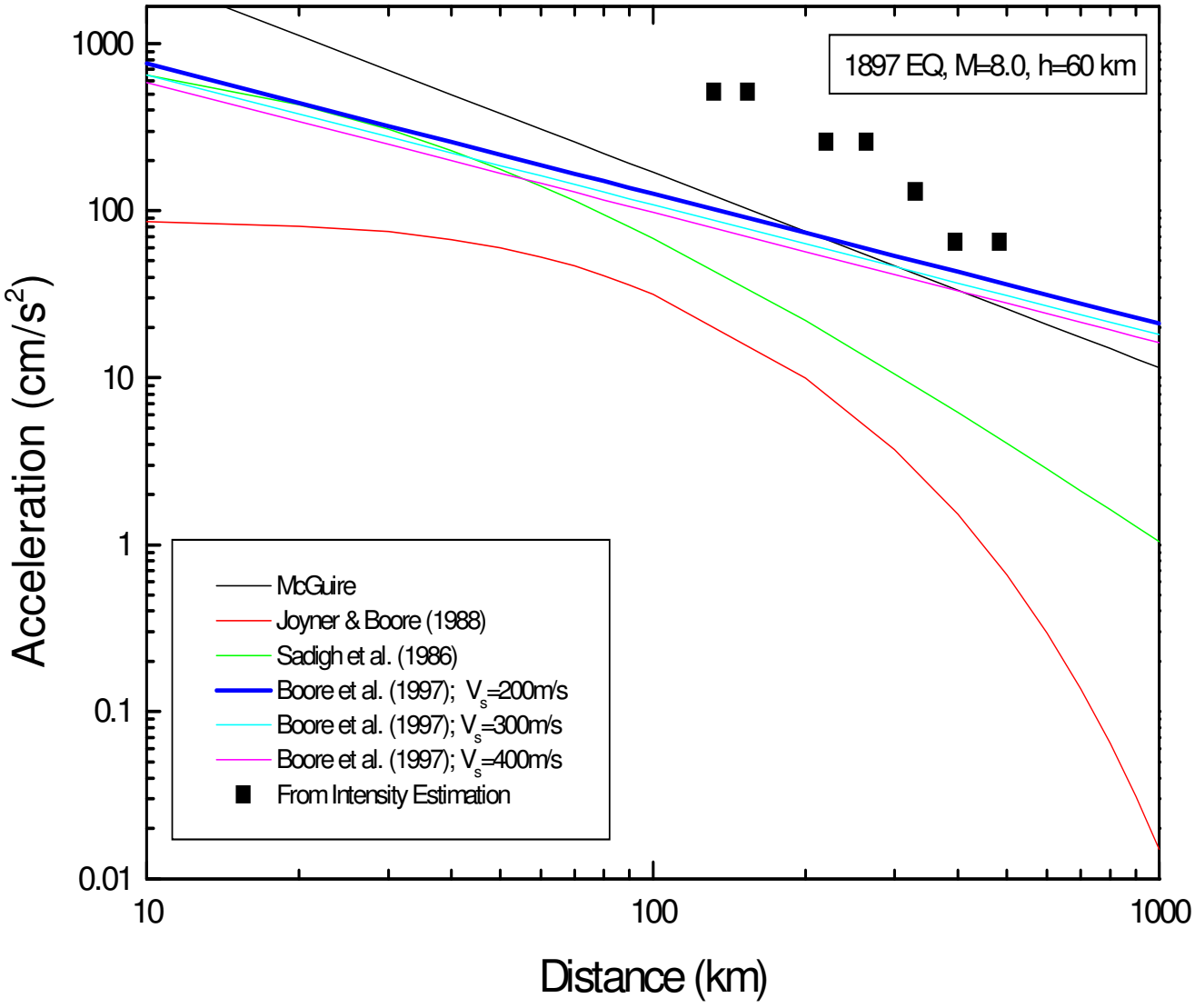

Figure A6 Distance versus PGA values for 1897 Great Indian Earthquake

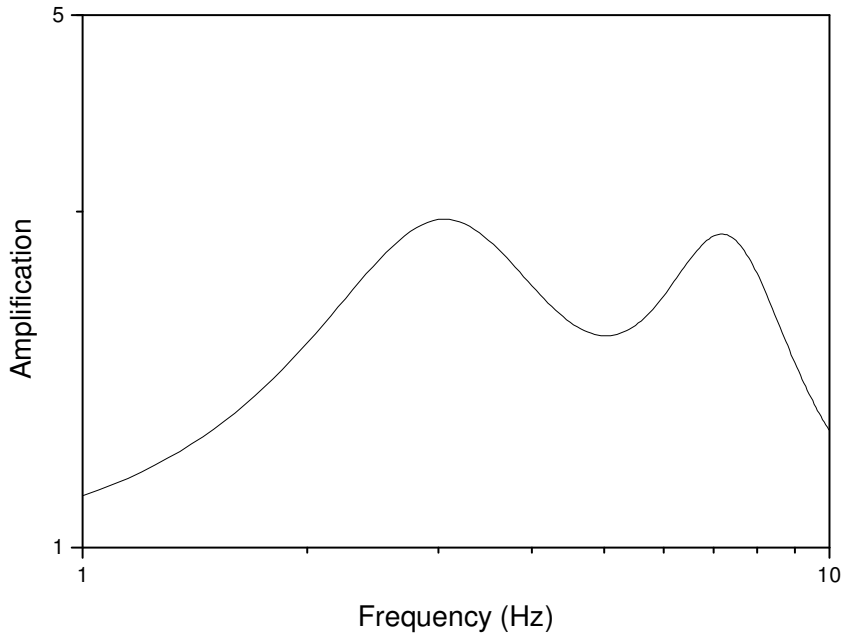

FigureA7 Typical amplitude-frequency relations at a site

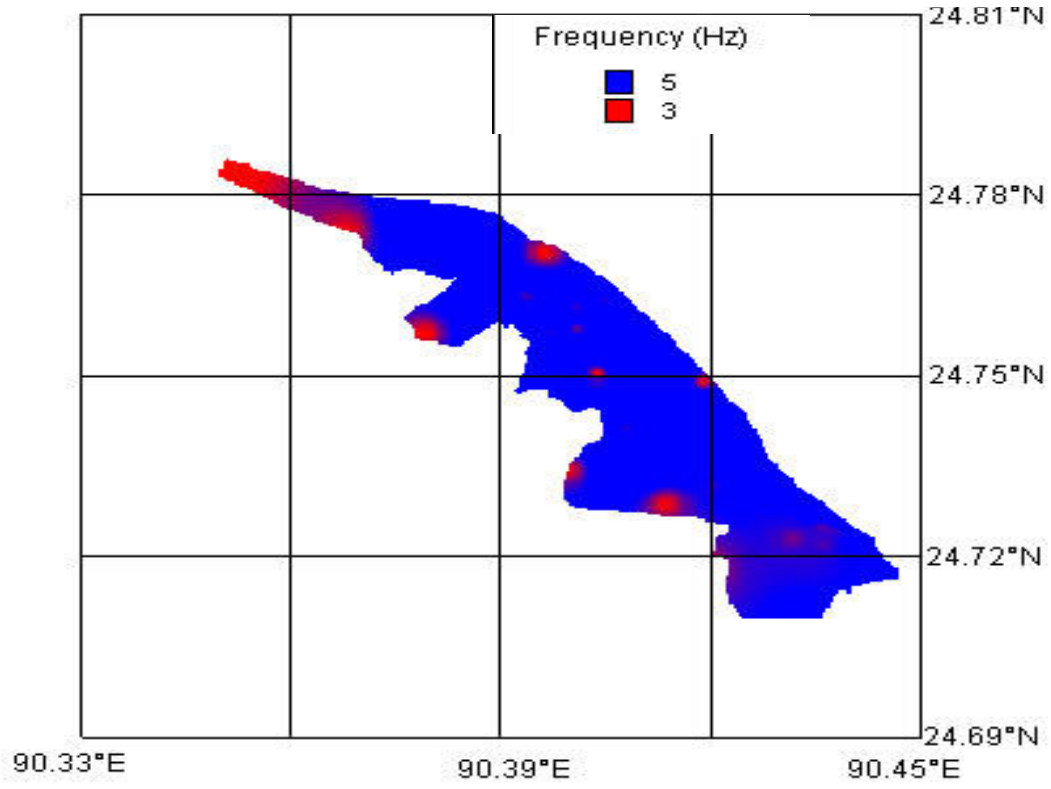

Figure A8 Fundamental frequencies

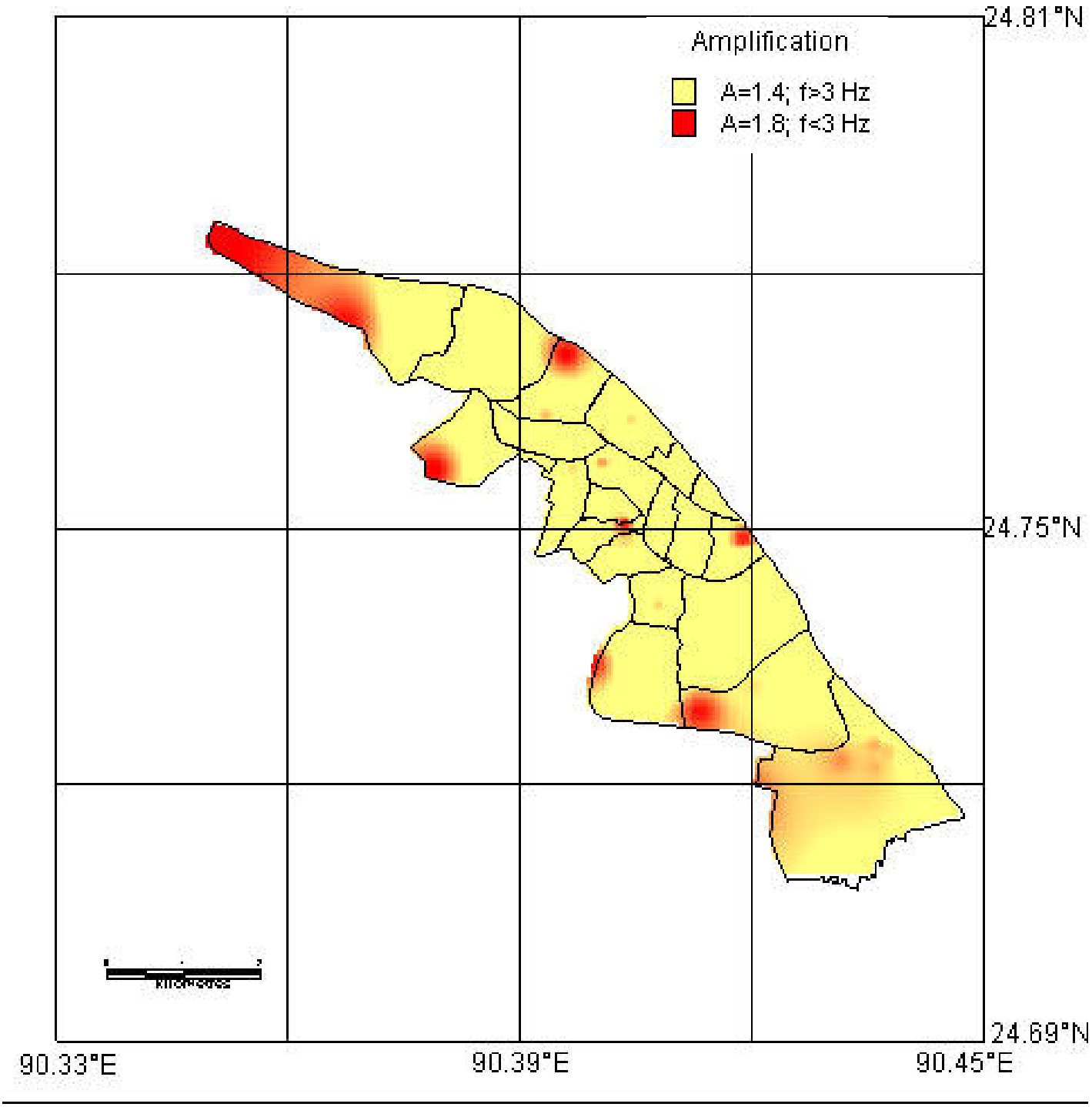

Figure A9 Amplification at fundamental frequencies

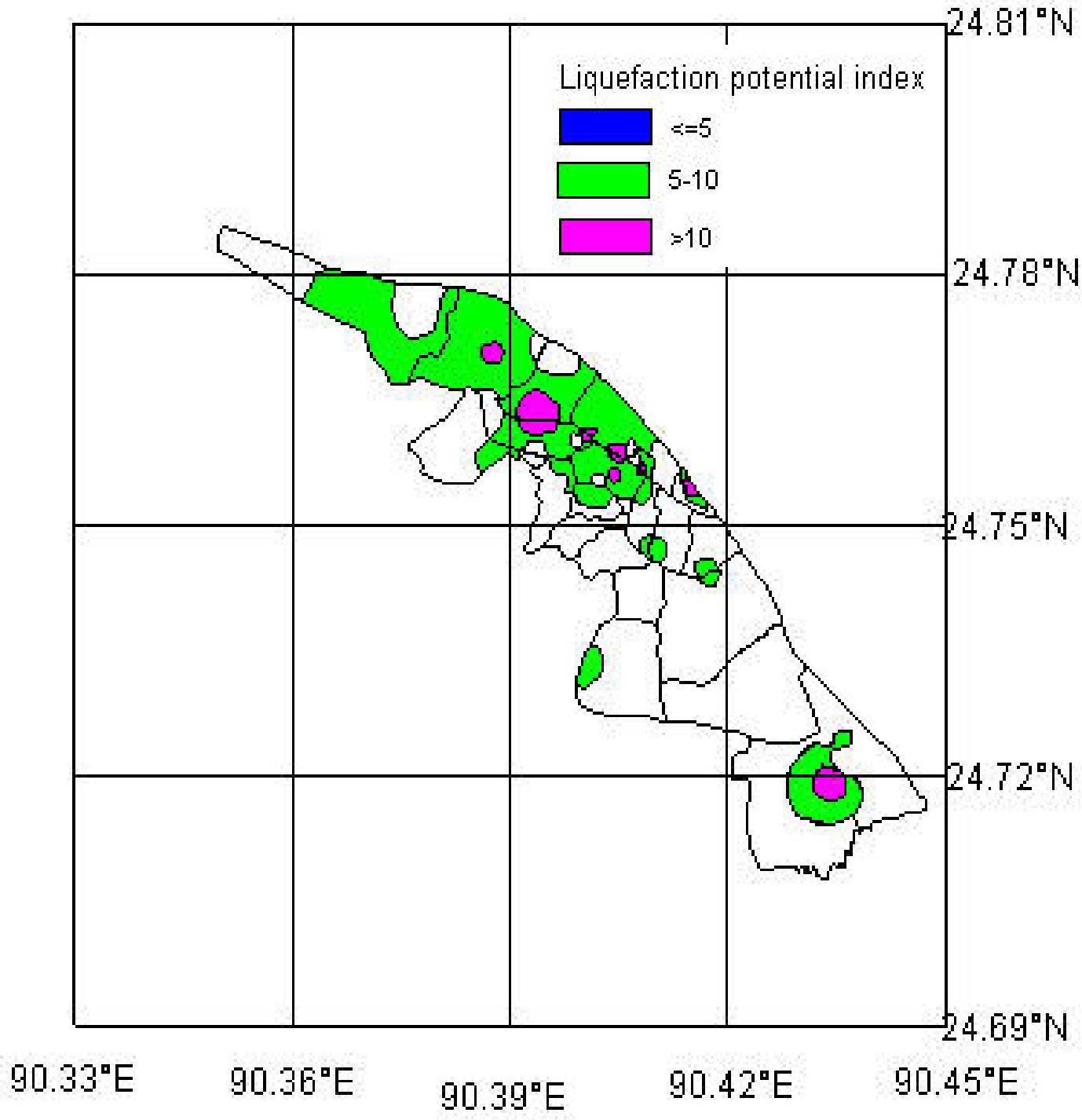

FigureA10 Seismic microzonation based on liquefaction potential index

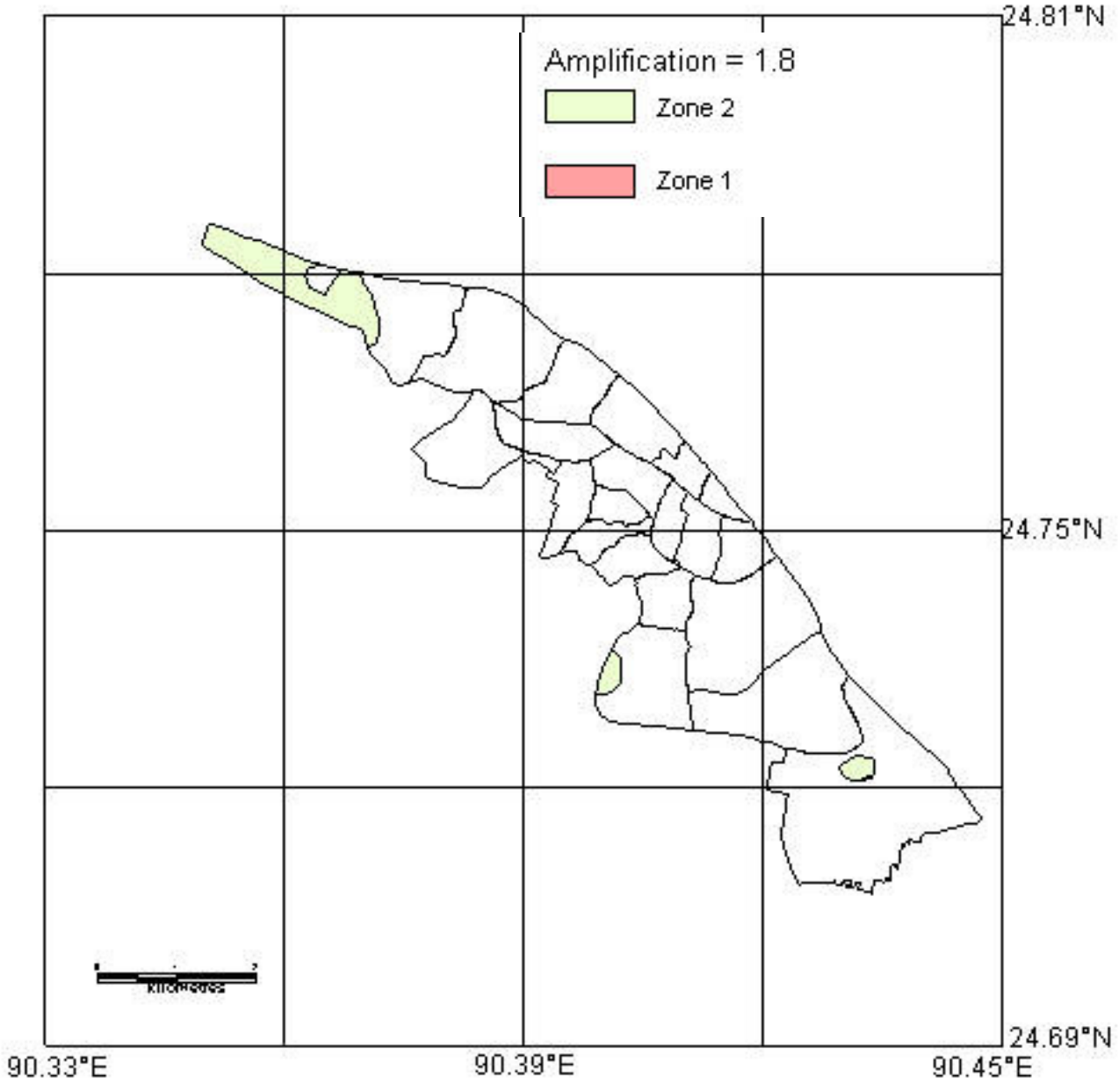

Figure A11 Map of 1.8 times amplification plus liquefaction areas

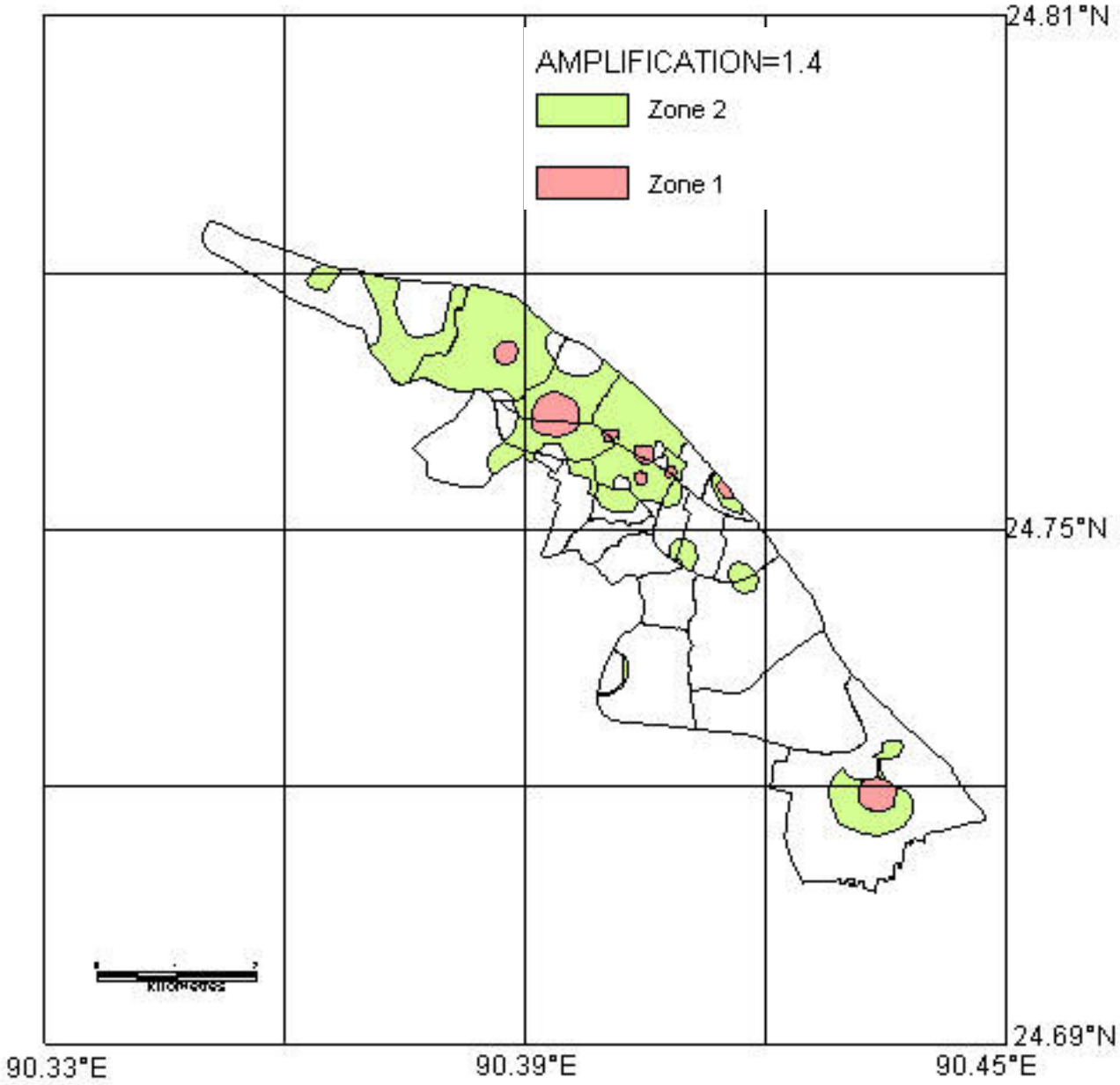

Figure A12 Map of 1.4 times amplification plus liquefaction areas

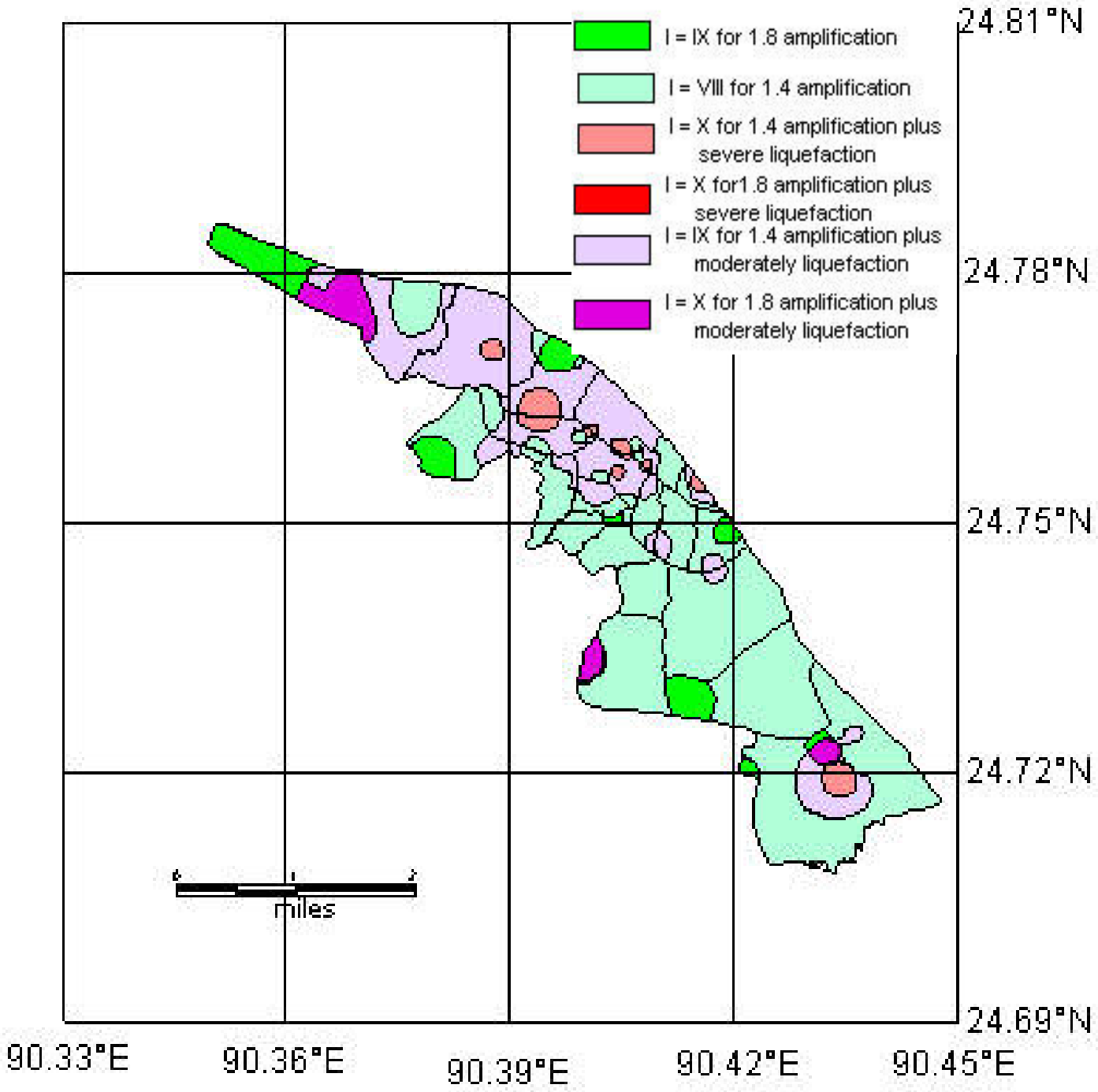

Figure A13 Combined intensity map considering liquefaction and amplification

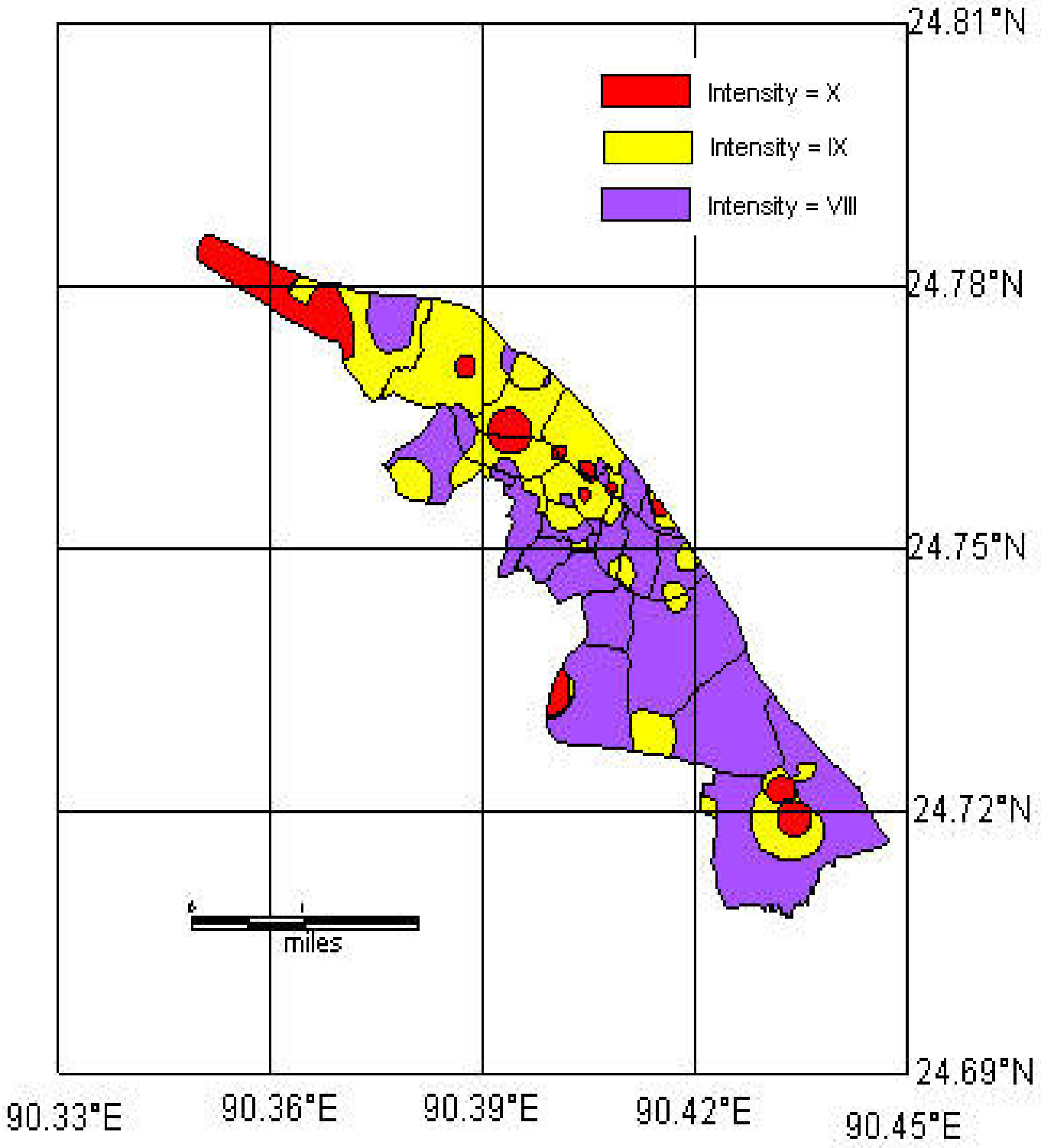

Figure A14 Combined hazard intensity map

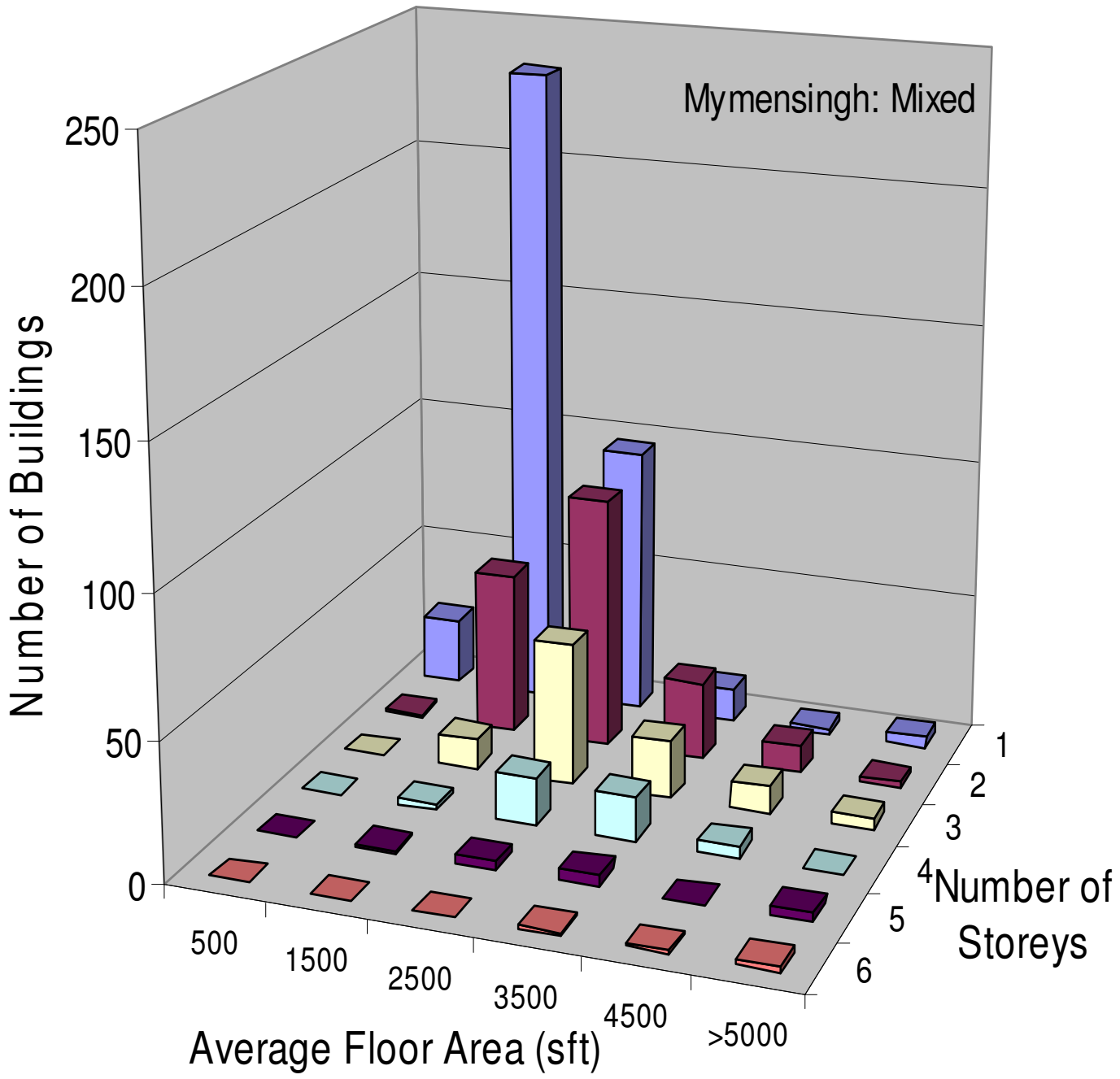

FigureA15 Storey and floor space distribution of buildings

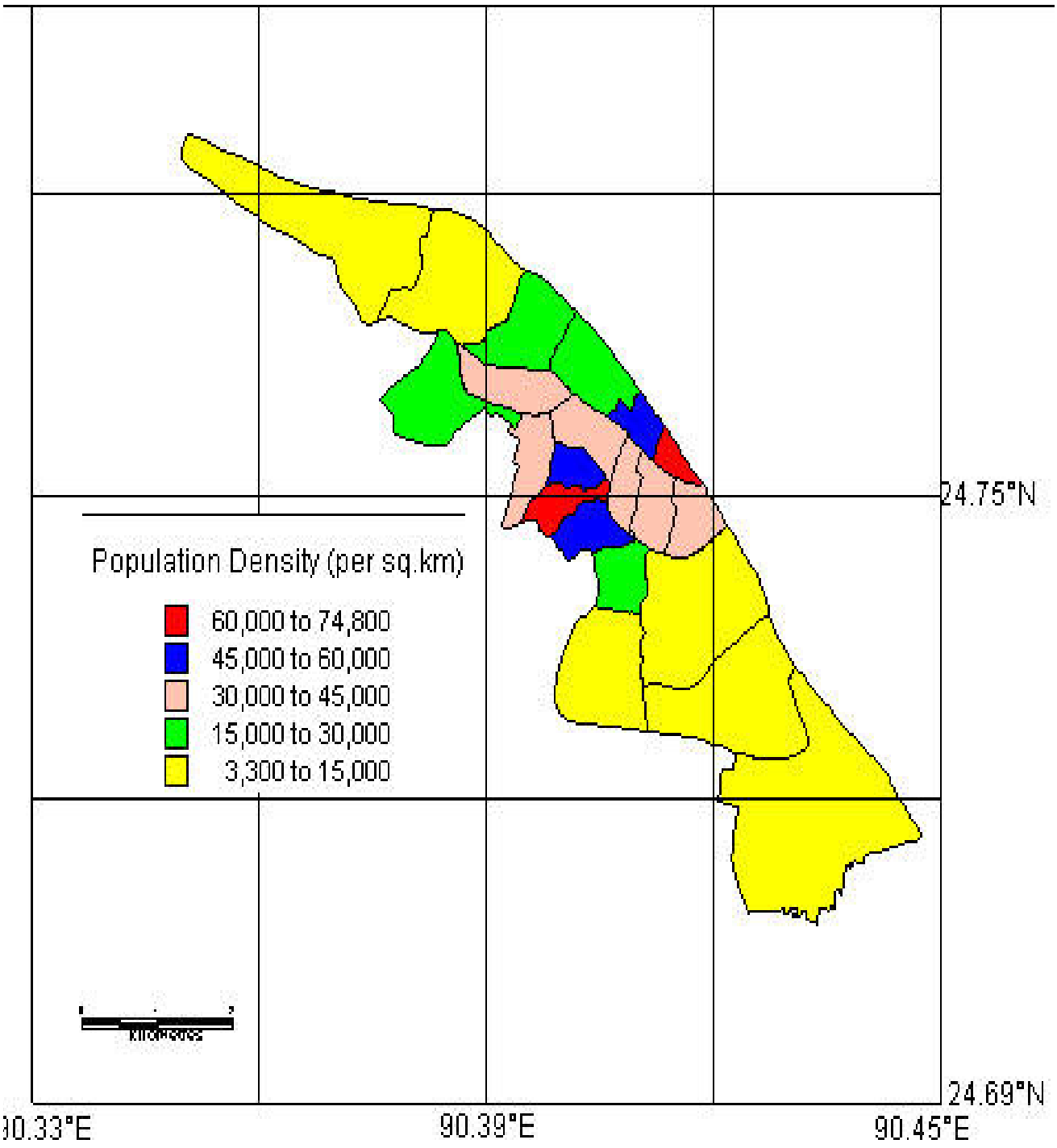

FigureA16 Population density map of Mymmensingh town

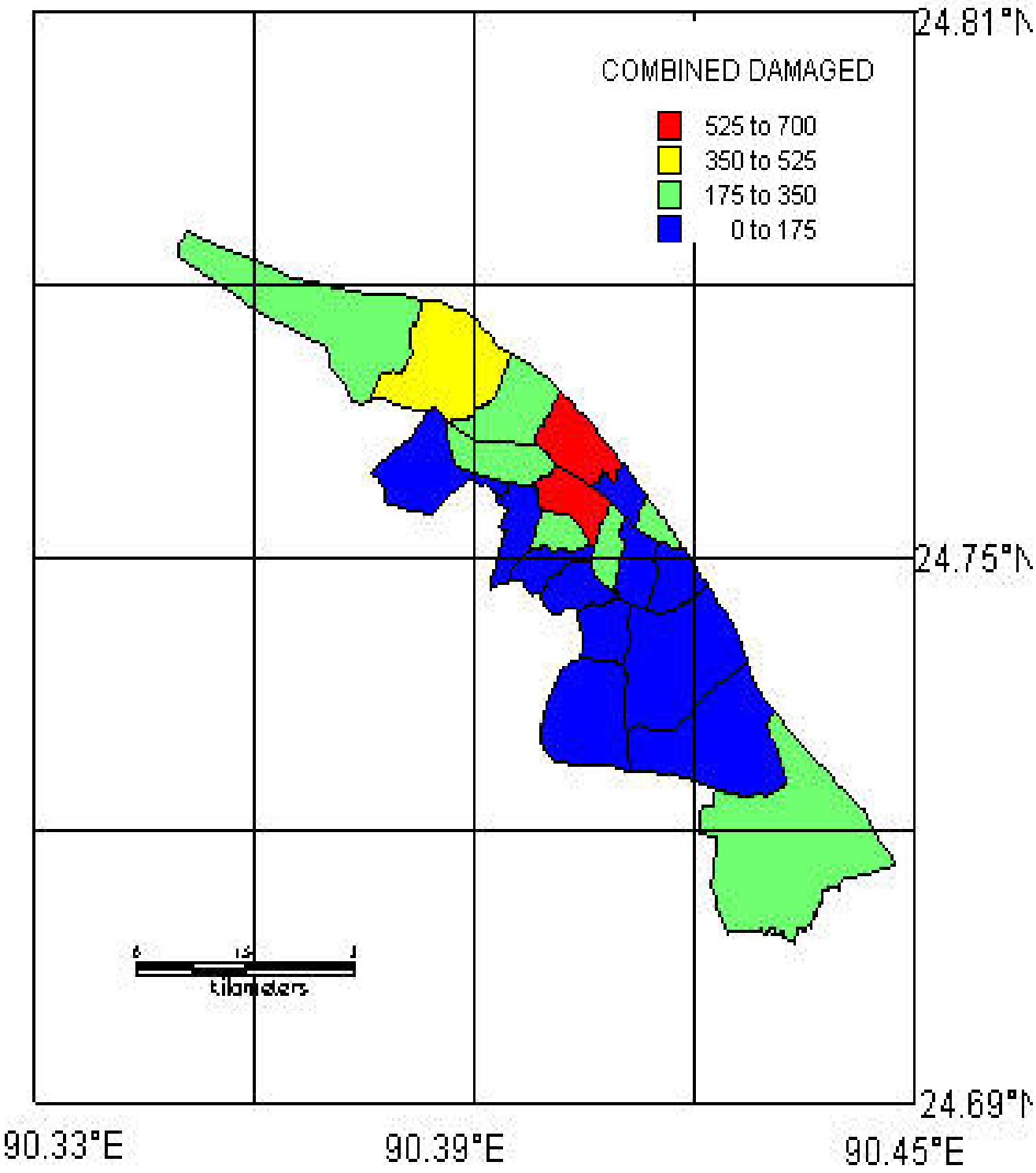

FigureA17 Building damage due to combined effects

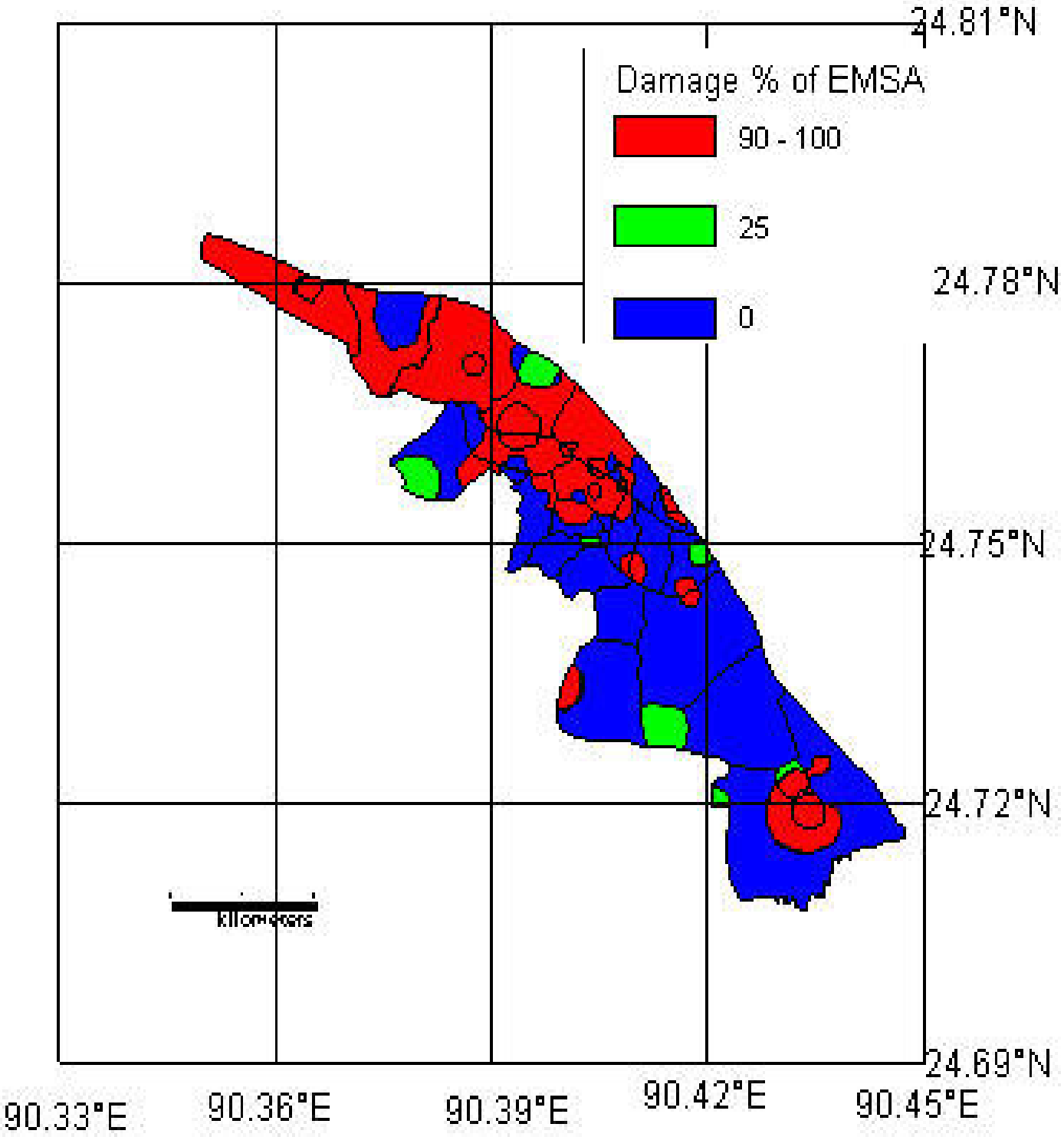

Figure A18 Percentage damage of EMSA type structure

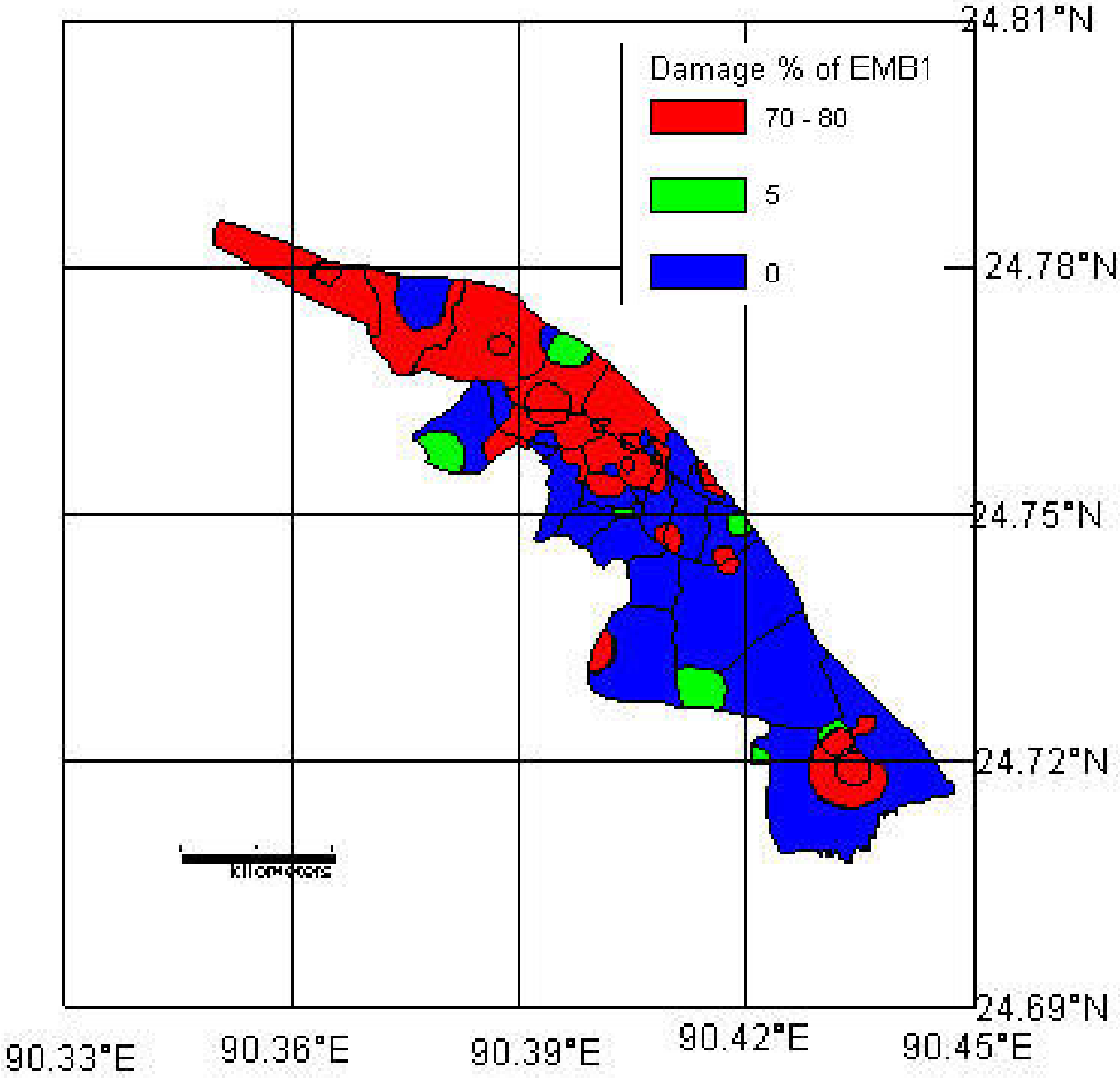

Figure A19 Percentage damage of EMSB1 type structure

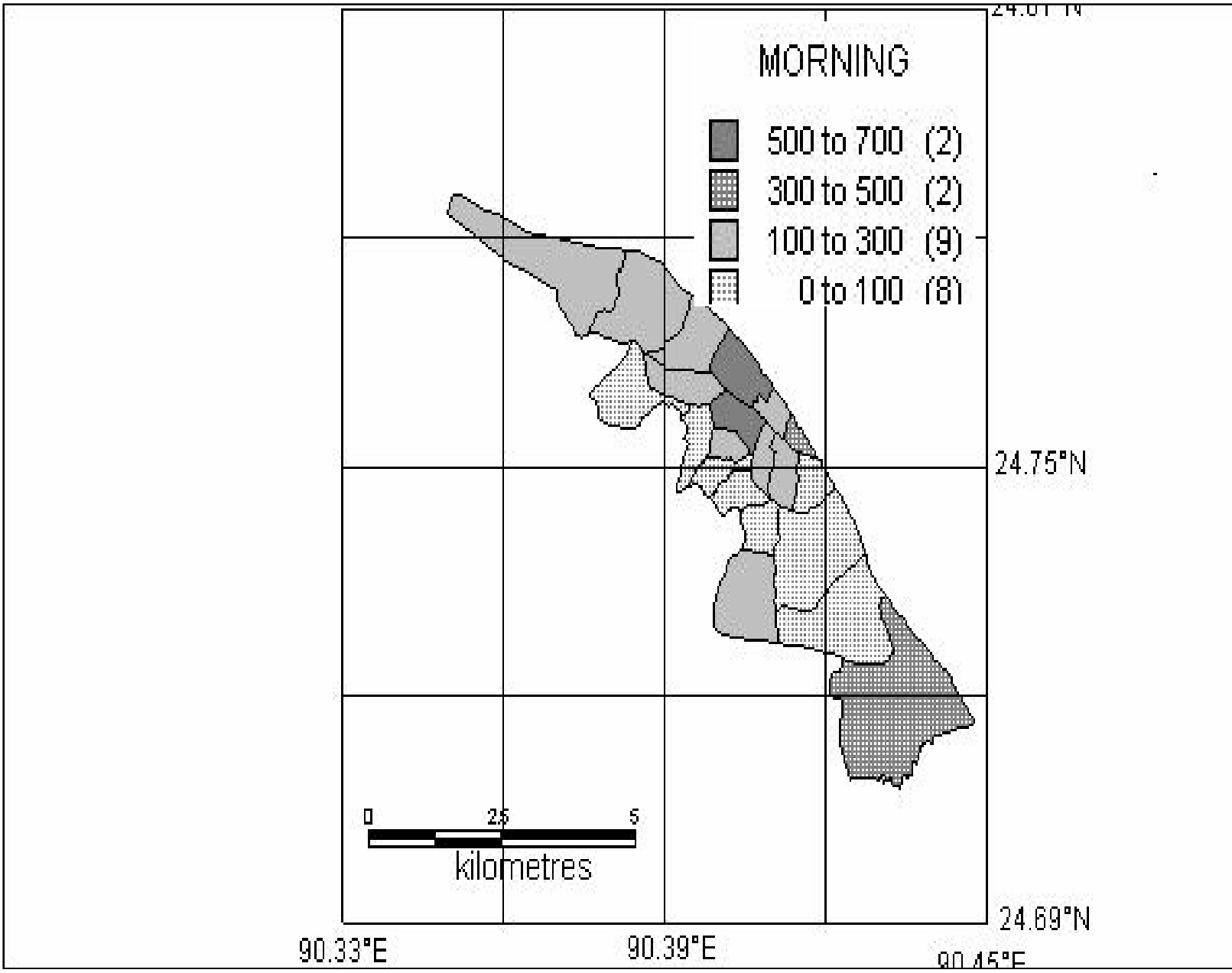

Figure A20 Estimated number of fatalities at morning due to combined effect

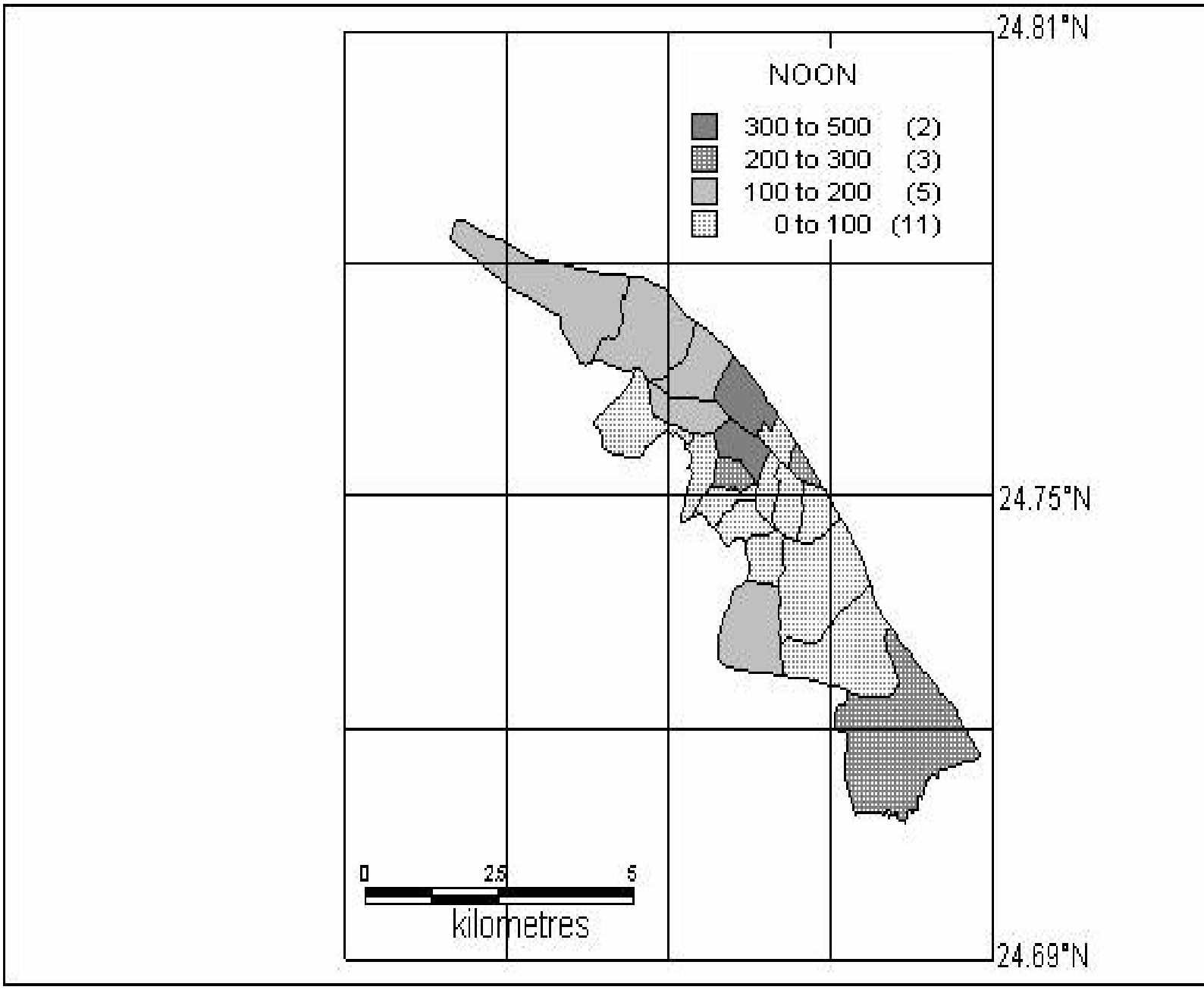

FigureA21 Estimated number of fatalities at noon due to combined effect

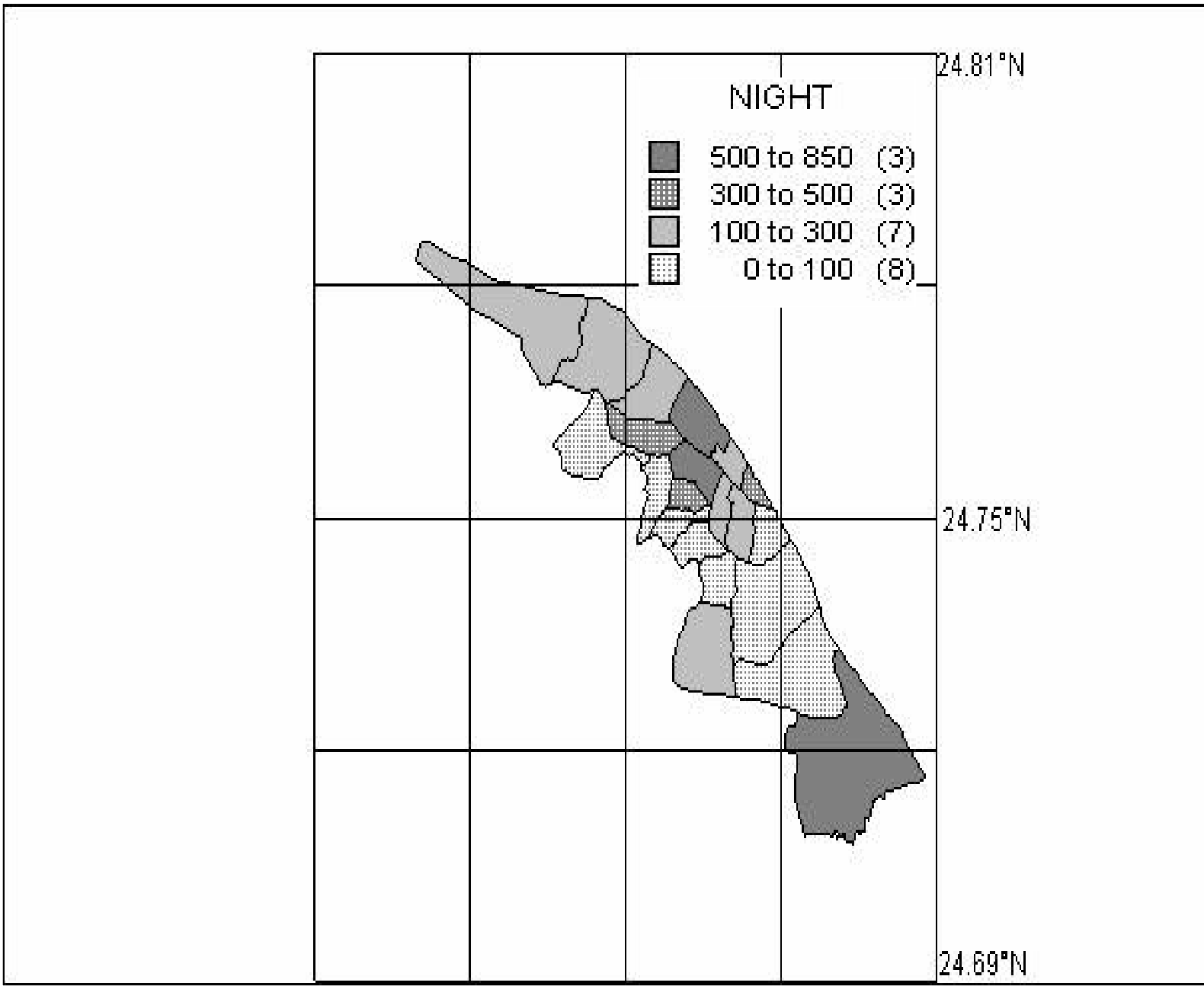

Figure A22 Estimated number of fatalities at night due to combined effect

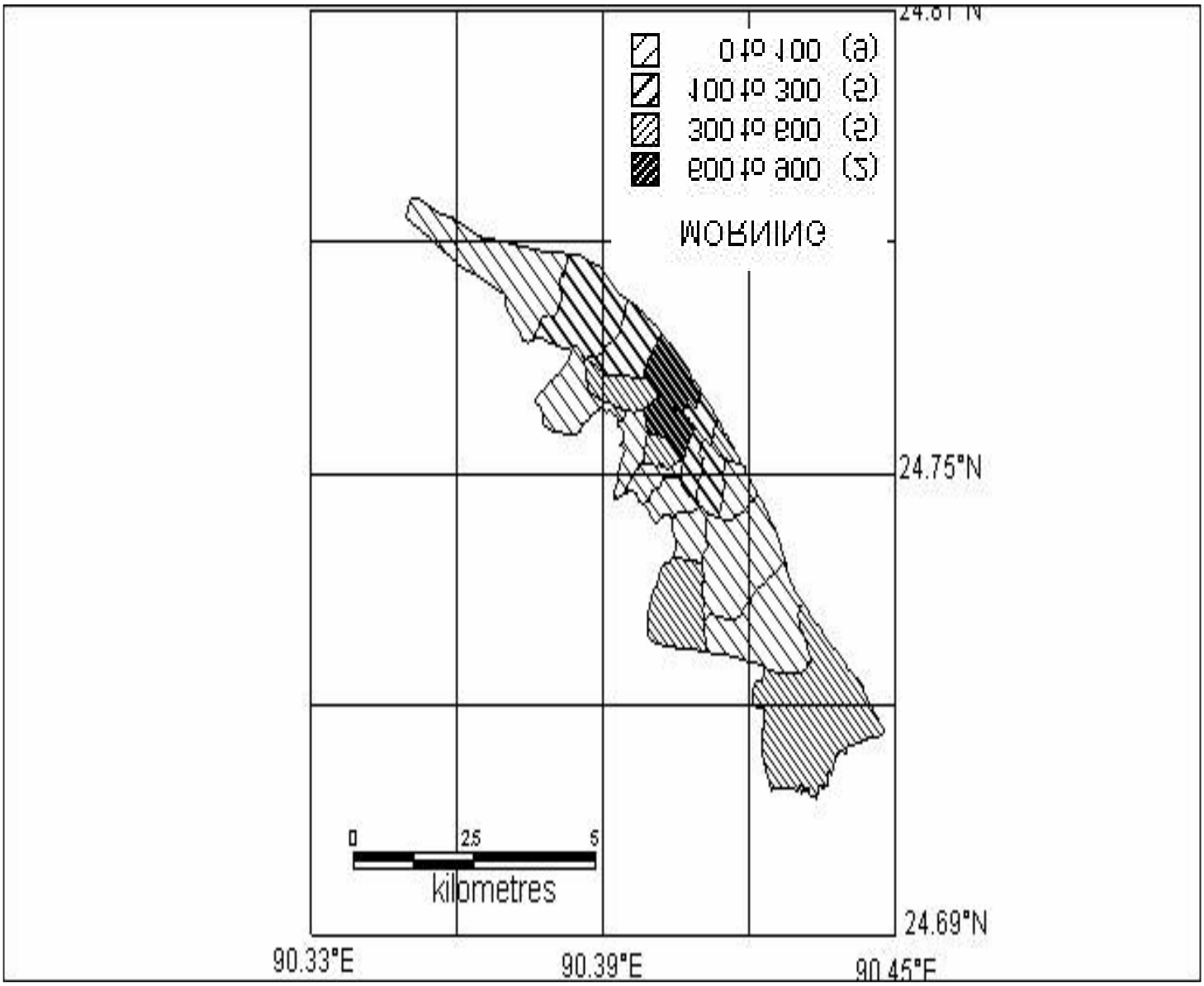

FigureA23 Estimated number of injuries at morning due to combined effect

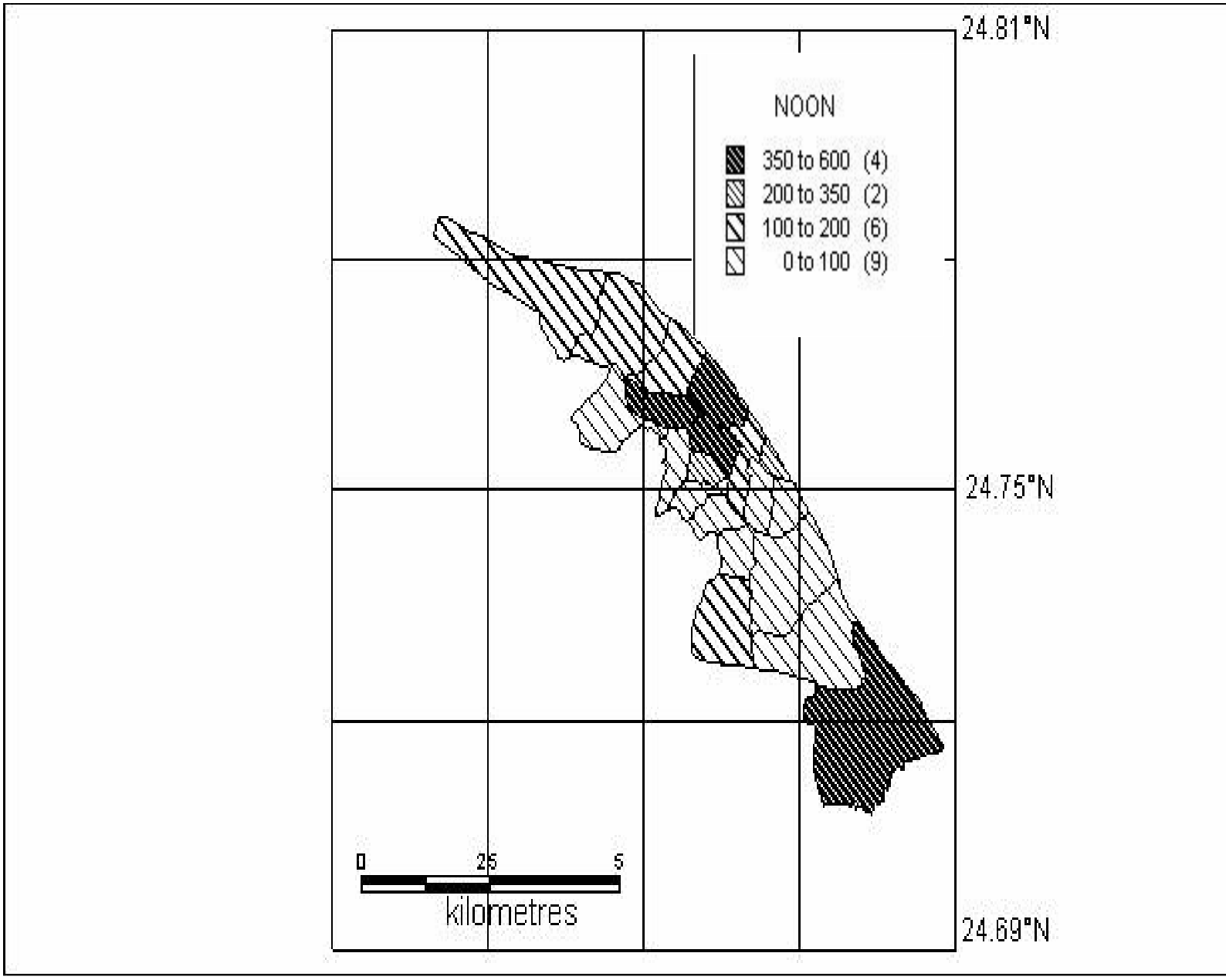

Figure A24 Estimated number of injuries at noon due to combined effect

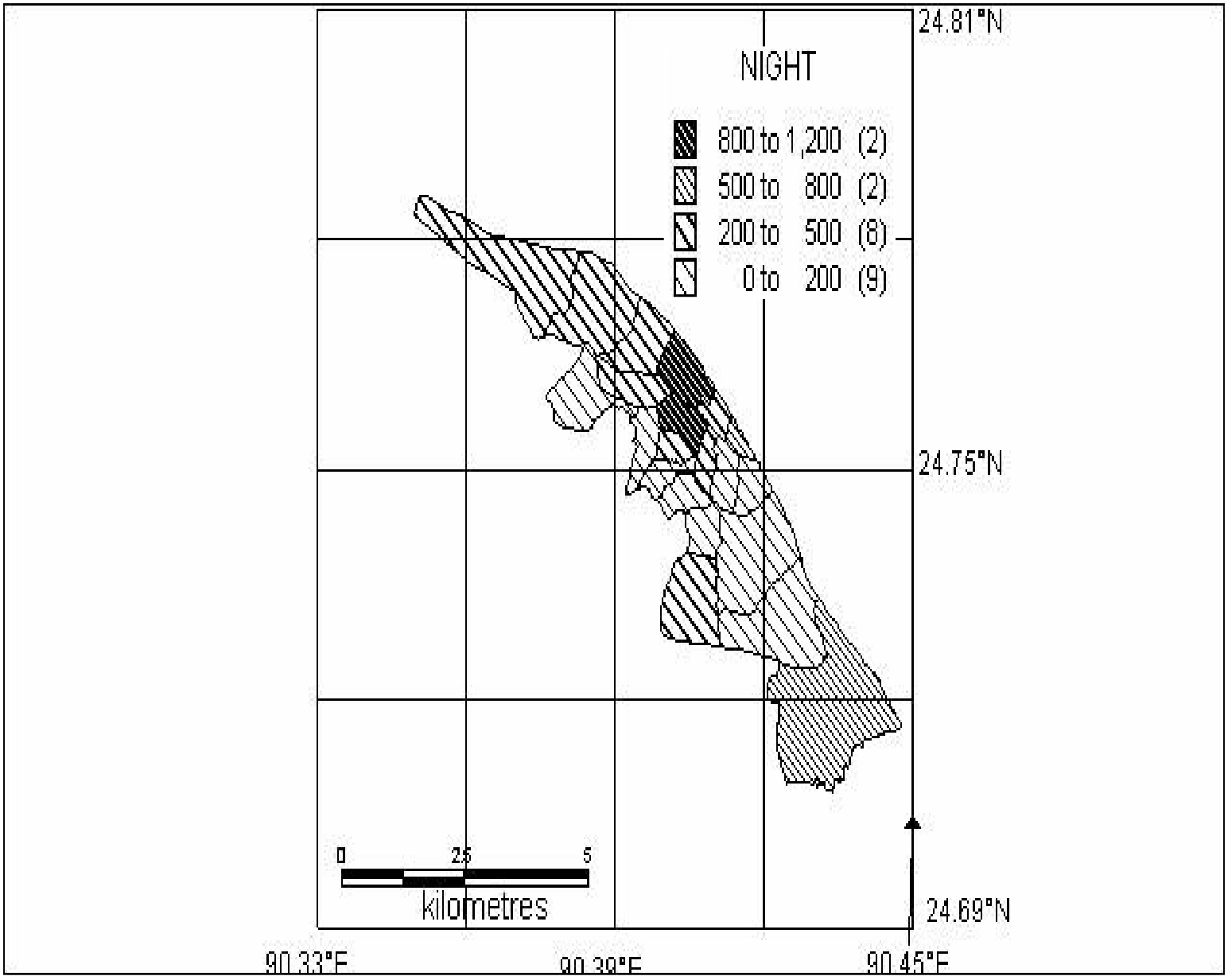

FigureA25 Estimated number of injuries at night due to combined effect

Table A1 Some historical and recent earthquakes with magnitude, intensities, epicentral distance and focal depth

Name of Earthquakes	Fault	Magnitude	EMS Intensity	Distance (Km)	Focal Depth (Km)
1885 Bengal Earthquake	Modhupur	7.0	VII	94	72
1897 Great Indian Earthquake	Assam	8.1	IX	151	60
1918 Srimangal Earthquake	Sub-Dauki	7.6	VI	146	14
1923 West Durgapur Earthquake	-	7.1	VI	81	33
1930 Dhubri Earthquake	Dhubri	7.1	VII	93	60
2008 Modhupur Earthquake	Modhupur	4.2	V	35	25
2008 Haluaghat Earthquake	Haluaghat	4.8	VI	10	40
2008 Mirzapur Earthquake	Modhupur	4.6	IV	45	20

Table A2 PGA values at bedrock level from different attenuation laws for different for scenario event

Attenuation Relations	PGA for Bengal Earthquake (1885)	PGA for Great Indian Earthquake (1897)	PGA for Srimangal Earthquake (1918)	PGA for west Durgapur Earthquake (1923)	PGA for Dhubri Earthquake (1930)
McGuire (1978)	0.0585g	0.183g	0.077g	0.0908g	0.0689g
Sadigh et al. (1986)	0.021g	0.0	0.0	0.0	0.0
Joyner and Boore (1988)	0.0185g	0.0252g	0.0172g	0.0320g	0.0219g
Boore et al. (1997)	0.0055g	0.0089g	0.0054g	0.0066g	0.0059g

TableA3 Attenuation relation for PGA

Author	Relation
Duggal (1989)	$y=227x10^{0.308M}(r+30)^{-1.2}$
McGuire (1978)	$y=0.0306e^{0.89M}r^{-1.17}e^{-0.2S}$ where S=0 for rock and S=1 for alluvium
Katayama (1974)	logy=2.308-1
Sadigh, et al. (1986)	$\ln y = - 1.406 + 1.1 M – 2.051 (r + 1.353 e^{0.406M})$ where M > 6.5
Joyner and Boore (1988)	$\log y = 0.43 + 0.23 (M – 6) – \log (r^2 + h^2)^{1/2} – 0.0027(r^2 + h^2)^{1/2}$; for rock
Ambraseys (1995)	logy=-l.43+0.245Ms-0.001r-0.786logr
Boore et al. (1997)	$\ln y = -.2424 + 0.527(M-6) – 0.778 \ln r – 0.371 \ln (V_s / 1.396)$ where, $r = (r_b^2 + 5.57^2)^{1/2}$